CRANFIELD UNIVERSITY

Evangelos Chrysochoidis

Rotorcraft Engine Maintenance Costs Analysis Based on Flight Profile and Usage

SCHOOL OF AEROSPACE, TRANSPORT, AND MANUFACTURING

Centre for Propulsion

PhD Thesis

Academic Year: Feb 2015 – May 2018

Supervisor: Professor V. Pachidis

May 2018

CRANFIELD UNIVERSITY

SCHOOL OF AEROSPACE, TRANSPORT AND MANUFACTURING

Centre for Propulsion

Full time PhD

Academic Year: Feb 2015 – May 2018

Evangelos Chrysochoidis

Rotorcraft Engine Maintenance Costs Analysis Based on Flight Profile and Usage

Supervisor: Professor V. Pachidis

May 2018

This report is submitted in partial fulfilment of the requirements for the degree of Doctor of Philosophy

Executive Summary

Rotorcraft cover all sectors of human activity, supporting military, civil and government needs. Their design allows them to: i) deploy at different operating environments, ii) support power-demanding flight profiles, and iii) be agile and highly maneuverable. Compared to a civil aircraft turbofan engine, which typically operates at 35,000 feet for several hours, turboshaft engines found on rotorcraft usually experience high-frequency power changes. This results in a decrease of the useful life of critical components, due to low cycle fatigue (LCF) considerations.

Methods developed so far, regarding the effects of engine degradation on engine performance and the estimation of the life of critical components, relate to aircraft turbofan engines, and therefore are not directly transferable to rotorcraft engines. Moreover, the current methods available to assess engine life cycle maintenance cost are also based on aircraft-related considerations and therefore are inapplicable to rotorcraft operations. Specifically, the current erroneous assessment premise is that the rotorcraft engine experiences two fatigue cycles per flight. This may be true for an aircraft due to its simple flight profile, but it does not apply to a rotorcraft due to the inherent diversity of the mission. After a thorough literature review, this work identified a gap in the existing knowledge regarding the life cycle cost assessment of rotorcraft, which may operate on a plethora of mission profiles within a given timeframe. In addition, the review did not reveal any evidence of a tool that could be deployed in these cases, particularly to assess the effect of different component designs on life.

To address the aforementioned limitations, this doctoral work established a new methodology to estimate turbine fatigue cycles according to the peculiarities of every mission profile. The method also assesses engine life cycle maintenance costs considering a mixture of several different flight profiles within a certain timeframe (instead of a single flight profile). The new toolset created can provide useful information to an operator, regarding turbine life limit estimations and incurred maintenance costs, also

considering factors such as: i) the fleet operating environment, ii) the flight profiles used, iii) fleet numbers and expected availability and, iv) pilot experience and flight attitude.

The proposed methodology regarding the turbine life estimation integrates: i) an in-house helicopter flight mechanics code, ii) an in-house tool, which calculates engine performance, and iii) a tool to assess the turbine life developed from the author. It creates a set of life-limits for three different flight profiles and then uses a newly developed method, named Weight Usage Flight Profile Method (WU-FPM). This estimates an 'equivalent' life-limit in flight hours based on the fatigue cycles limit, which was estimated from the three different flight profiles, over the duration of a year.

The life-limit data set is based on a Design Of Experiment (DOE) approach. The DOE estimates a representative turbine life for a reference flight profile, based on a design space which considers two operating (payload and climb rate) and one environmental parameter (ISA deviation). These are chosen within the rotrocraft Original Equipment Manufacturer (OEM) -defined capabilities. The parameters used for this life-limit are used to estimate the life limit for a Search and Rescue (SAR) and Oil and Gas (OAG) flight profile.

Regarding the maintenance cost assessment the methodology uses two scenarios to estimate the life cycle costs: i) the Minimum Shop Visit (MINSV), and ii) the maximum Life Limited Part (LLP) usage. The previously estimated 'equivalent' engine life due to turbine failure and the OEM-specified Time between Overhaul (TBO) are used to assess maintenance intervals, which support these scenarios.

The new method established was applied to selected test cases to demonstrate and assess its functionality. Results showed that regarding the operational and environmental parameters that affect Turbine Entry Temperature (TET), the payload and the ISA deviation are the most significant in hover and cruise, while the climb rate is the more influential parameter in the climb segment. Results also showed that the number of fatigue cycles per flight change according to the mission flight profile. For

example, for a passenger flight, the turbine experiences 4 fatigue cycles, while it experiences 10 on a Search and Rescue (SAR) and 12 on an Oil and Gas (OAG) flight.

Regarding maintenance cost prediction, the results show that the diversity of the missions influences the incurred cost significantly. For example, the costs incurred for a mission distribution of Passenger/OAG/SAR of 80/10/10% respectively, compared to a distribution of 50/40/10% can increase engine service life by 17.5%.

The developed methodology, combined with a surrogate model, can be a useful tool for a rotorcraft operator to support informed financial planning decisions, based on a short or longer-term analysis.

“There is nothing permanent except change”

Heraclitus

Acknowledgements

I would like to thank firstly Professor Pericles Pilidis for giving me the opportunity to join the Clean Sky Project team and my Supervisor Professor Vasilios Pachidis for his guidance and support during this 3-year effort.

Secondly, I would like to thank my wife Zoi and the small gang of the house George, Elena and Krysta for their support and for giving me the reason to proceed with this effort.

This research was based at the work of young but wise scientists that earned my admiration like Dr Ioannis Goulos who created HECTOR the flight dynamics simulator, which is the corner stone of the developed framework and Marvin Elter who generously shared his Matlab code, which was used as a basic element in the turbine life loads.

In addition, I would like to thank my colleagues at Cranfield team, Ezanee Girees,, Stavros Vouros and Hasani Azamar Aguirre, who helped me build my first lines of code in FORTRAN and Python. Special thanks to Dr. Mourouzidis Chris and his brother Thomas who were there anytime I needed a useful insight at engine simulations.

The list of friends continues with Dr. Ioannis Roumeliotis who reviewed my first draft, helped me shape the content in a more comprehensive way and add a scientific touch to the text.

Last but certainly not least, I would like to express my gratitude to my parents who always believed in me. I am sure that the first flight engineer I met in my life, my father Nikolaos Chrysochoidis, will be watching from up the sky and smile generously as he always did.

Contents

List of Appendices

List of Tables

List of Figures

Appendices List of Figures

Nomenclature

AD	Air Worthiness Directives
AUM	All Up Mass
CER	Cost Estimation Relationship
D	Depot Level -(OEM, MRO)
DMC	Direct Maintenance Costs
EFC	Equivalent Flight Cycles
EFH	Equivalent Flight Hours
EGT	Exhaust Gas Temperature
EVM	Earned Value Method
FEA	Finite Element Analysis
FH	Flight Hours
FPA	Flight Path Angle
HUMS	Health Usage Monitoring System
I	Intermediate Level,
LCC	Life Cycle Cost
LLP	Life Limited Parts
MMH	Maintenance Flight Hours
MTE	Mission Task Element
MRO	Maintenance Repair and Overhaul
O	Operator Level
OAT	Outside Air Temperature
OEM	Original Engine manufacturer
PE	Prediction Error

PBH	Price by the Hour
SB	Service Bulletins
SEL	single engine light
TBO	Time Between Overhaul
TEH	twin engine heavy
TEL	twin engine light
TEM	twin-engine medium
TMF	Thermal Mechanical Fatigue
TOGW	Take-off Gross Weight

1 Chapter 1: Introduction

1.1 Overview

The rotorcraft industry is experiencing a phenomenal growth in civil, government and military sectors. The rotorcraft's main distinguishing features of agility and versatility in-flight operation coverage correspond to a market growing need for versatile and economical transportation in terms of time and costs.

Fleet availability and engine reliability rely on different factors. The former relates to technician's availability, spare parts, or modules available and other administration issues. The latter relates to engine performance degradation and unscheduled maintenance actions.

Engine's performance degrades for many reasons but if the focus is on proposed scheduled maintenance intervals, the driver is the engine's hot section Exhaust Gas Temperature (EGT). The manufacturers' trend is to design and produce engines with high power to weight ratio. To achieve this, the EGT is increased which in turn enhances thermal fatigue, oxidation, corrosion and reduces components' creep life.

Maintenance strategies are developed to ensure: i) engine reliability, ii) operator fleet availability and iii) decreased incurred costs. The manufacturers propose scheduled maintenance intervals based on their own assumptions about operating profiles, engine usage, and flight environment which most of the times do not relate to the actual operating environment of the rotorcraft.

The other issue that relates to maintenance is the rotorcraft fleet diversity. The EU project for greener aircraft named Clean Sky classified the turboshaft engine fleets, based on Maximum Take-Off Weight (MTOW), to four categories which are: i) Single Engine Light (SEL) ii) Twin Engine Light (TEL) iii) Twin Engine Medium (TEM) and iv) Twin Engine Heavy (TEH). All these categories are using engines of different generations, which follow a different maintenance strategy during their life cycle. The main strategies used today are the preventive and on-condition maintenance. Preventive maintenance relates to predefined inspection intervals and component or module replacement at a certain time. On-condition maintenance seems to be the

preferred one for the latest engines in production. It relates to inspections that assess the condition of parts and defines their replacement according to their status.

The Life Cycle Costs (LCC) that relate to an engine's operation and maintenance is a complex issue. The LCC estimation encompasses different disciplines and depends on different points of view. The manufacturer estimates the cost from the design phase to the product retirement. The operator or engine owner, on the other hand, estimates the cost about: i) operating time ii) availability, maintenance costs and iii) maximise his revenue. The international fleet of helicopters has unique features and the Life Cycle Costs from the design phase to the platform retirement vary for reasons such as mission diversity, operating environment, engine configuration, and age.

The different missions that the helicopter needs to cover forced the industry to produce many different configurations of the platform, which relate to the fuselage, rotor head, avionics, monitoring systems or engine type and number installed. To make things more complicated there is times that the same helicopter type operates in different environments or performs different missions. This will further lead to a different engine selection. There are many times that the same helicopter type can use same engine type with different ratings or use an engine produced by a different manufacturer. The operating environment defines the engine exposure to high or low operating altitudes or temperatures and to corrosive or dusty environments.

Literature shows that there are many quantitative approaches [2], [3], [4], [5] to predict the rotorcraft operating cost, a big percentage of which is the cost associated with engine life cycle maintenance. These methods are trying to provide estimates based on a deterministic or a stochastic method and strive to provide figures through a quantitative approach. In addition, they base their analysis on assumptions, like the '2 fatigue cycles per flight' that, are not always applicable in all helicopter usage cases.

The author believes that while all the quantitative approaches used so far provide a metric of some accuracy, they have two major disadvantages. One is that the engine's life used to estimate the maintenance costs does not address the issue of the components remaining life with regard to the operating conditions and the rotorcraft actual flight profile. The other is that the engine acquisition price is very sensitive to market fluctuating demands. In addition, the spare parts cost, which represents a great

portion of the maintenance costs, may vary due to material availability or unstable production lines.

To mitigate the first disadvantage mentioned above a more accurate tool needs to be developed. To this end, this research develops an integrated framework. This framework correlates the engine components life with the rotorcraft's actual usage and operating conditions. It provides the capability to assess the incurred maintenance cost that relates to the specific operator's needs. This capability helps the operator make an informed decision taking into account the trade-off between i) minimum maintenance costs, ii) maximum engine availability and iii) available budget for maintenance.

The second part in Chapter 1, aims to provide the reader with the key differences between fixed wing and rotorcraft. It continues with an overview of rotorcraft classification, market analysis, flight profiles, flight envelopes and performance capabilities and constraints. The third part elaborates on the issues that arise from rotorcraft usage and presents this research scope, the research milestones, the available resources and the contribution to knowledge.

Chapter 2 continues with a literature review. The review addresses the engine degradation issue and presents the past and current research on engine components life estimation. Special reference is made to the component failure due to low cycle fatigue and a review is provided regarding the severity factor method and the methods used for the engine cycles counting. The review continues with a reference to the current methods with regard to operating, maintenance cost estimation, and the summary highlights the gaps found in the literature and the proposed methodology to address these gaps.

Chapter 3 introduces the proposed methodology to: i) assess the components life due to LCF ii) define a reference flight based on representative operating parameters iii) create a method which relates rotorcraft profiles to real life scenarios and iv) assess the maintenance costs with regard to the number of times that the engine is inducted for service.

Chapter 4 uses the proposed methodology to assess the turbine life due to LCF and the incurred maintenance costs with regard to: i) a mixture of different flight profiles ii)

a change in the operating temperature and iii) the stress concentration factor used in the components design phase.

Chapter 5 summarizes the work performed within the scope of this research. It presents the key findings with regard to life estimation and cost analysis, the contribution to an operator and, recommendations for future work.

For the reader's convenience, the thesis uses Appendices, which show details regarding:

a. Component sizing method.
b. Maintenance scenarios and formulas.
c. Lifing code Flowchart.
d. Results for: i) the operating parameters sensitivity analysis performed ii) turbine life and iii) incurred maintenance costs.
e. Unit Conversion tables.
f. The design of experiment (DOE) method set up.
g. The Leave One Out method (LOO) used for the experiment's results validation.

1.2 Fixed Wing vs Rotorcraft

This paragraph describes the major differences between fixed wing aircraft and rotorcraft and shows that non –obvious extensions are needed.

Wilbur Right quote [6] offers a useful insight for the differences between rotorcraft vs fixed wings: *"Like all novices, we began with the helicopter (in childhood) but soon saw that it had no future and dropped it. The helicopter does with great labour only what the balloon does without labour, and is no more fitted than the balloon for rapid horizontal flight. If its engine stops it must fall with deathly violence for it can neither float like the balloon nor glide like the aeroplane. The helicopter is much easier to design than the aeroplane but is worthless when done."*

While this may sound like a basic description literature provide numerous sources for their differences that can be categorized using the following criteria:

a. Flight Profile
b. Flight Envelope and Efficiency

c. Engines Type
d. Operating and Maintenance costs
e. Infrastructure for maintenance
f. Certification
g. Data Management and publication
h. Systems Complexity
i. Components replacement time limits

As the research scope relates to engine maintenance and the incurred costs, the analysis will focus to the most relevant criteria.

Flight Profile

As Harris quotes [7] "While **airplanes and gliders** can only fly vertically by *first* flying *horizontally*, then turning the entire aircraft upwards, the **helicopter** must be able to *start* and *finish* with vertical flight".

This major difference provides the rotorcraft the capability to perform six basic different flight profiles: i) Emergency Medical Services (EMS), ii) Civil Search & Rescue (SAR), iii) Law Enforcement/Police, iv) Passenger Transport/Air Taxi, v) Utility and, vi) Oil & Gas while the airplane can only perform a single flight profile.

Flight Envelope and Efficiency

Regarding the efficiency, fixed wing aircraft are generally much more efficient than rotary aircraft. This is because of the difference in how they generate lift. The rotorcraft low efficiency is understood, if we compare the efficiency of lift versus drag of the different platforms. For example, a Cessna 150 has an L/D (lift to drag ratio) of 7 in cruise, while a helicopter would only have around 4.5 in cruise. Other sources show that small aircraft can achieve an L/D of over 10.

Regarding the speed limit, helicopters limits prevents them from going as fast as most turboprop or jet aircraft. This is because the tips of the rotors should stay at subsonic speeds. Current helicopters like the UH 60 are limited to around 200 knots. Newer designs such as the Eurocopter X3 and Sikorsky X2 are capable of up to 250 knots, but are still in development. A good example is the difference between a small helicopter and a small fixed wing plane. Even though the PA-31 (fixed wing) is heavier

than the AB- 206 (helicopter) and can carry more passengers, it can fly faster and further than the helicopter. The "fuel economy" of nautical miles per gallon is based on the fuel capacity and max range, so it is not an exact figure of actual fuel burn.

Figure 1-1 shows a plot for the flight envelop of a generic helicopter and turboprop plane in comparison to the V-22 tilt rotor.

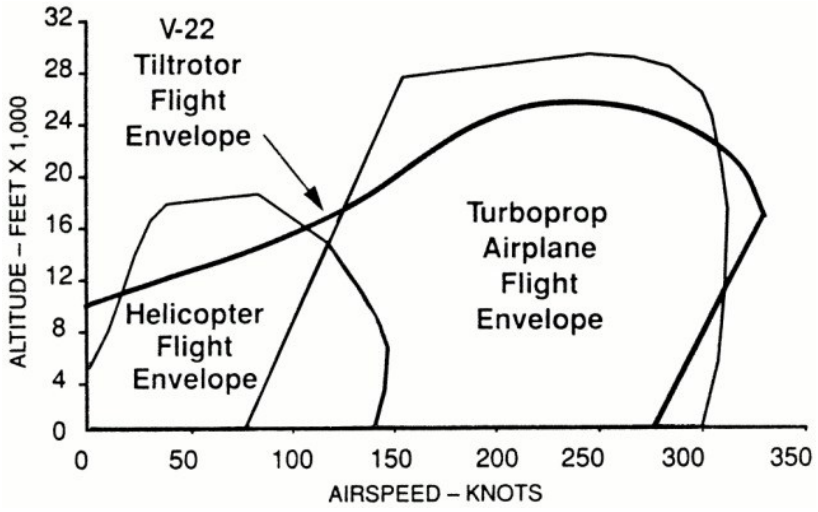

Figure 1-1 : Flight envelop of a generic helicopter and turboprop plane in comparison to the V-22 tilt rotor

Engines Type

One can assume that gas turbine engines are all share the same configuration while this is not so true. Flight profiles, mission length, payload, body length, operating costs, area of operation are some of the factors that dictate the engine configuration.

In fact, these engine types share a few basic qualities while being quite different. The turbo part in the name of each engine type indicates how both designs are similar. Essentially, both use a turbine that creates the energy needed for travel. With both designs, air is compressed to the point that adding a fuel results in the ignition needed to turn the turbine. Once ignition takes place, the compressor can sustain the thrust needed to become airborne and travel to any destination that you have in mind.

Regarding a turbofan engine, the turbine that is used to create the ignition causes a fan at the front side of the engine to turn. One of the benefits associated with a turbofan engine is that it can be more fuel efficient than other options.

Regarding a turboshaft engine, its mission is to provide power for the rotorcraft rotor

In that sense, it is optimized to produce shaft power rather than jet thrust. They are commonly used in applications that require a sustained high power output, high reliability, small size, and lightweight. Turboshaft engines usually drive a transmission, which is not structurally attached to the engine. The transmission is attached to the vehicle structure and, supports the loads created instead of the engine.

Infrastructure for maintenance

Fixed wing require large, expensive, infrastructure estate requirements with distance from urban centres. Rotorcraft require smaller, lower cost, infrastructure and real estate requirements, and proximity to urban centers, convenience, and unique, desirable, operational capabilities.

Data Management and publication

As Terra consulting [8] quotes “While most fixed wing manufacturers produce digital data for common maintenance manuals (AMM, IPC, FRM, TSM, etc.), it is uncommon for rotary aircraft manufacturers to provide similar digital data. Most helicopter manufactures use one or more of the common data standards internally, but generally produce unintelligent data for their customers. This presents a challenge for rotary operators to receive, review, and publish PDFs for internal use, especially if local changes need to be added or modified.

Helicopter operators by nature offer more dynamic flight services in more diverse operating conditions than their fixed wing counterparts. This creates challenges in maintaining digital content and records. Predicting due dates for maintenance events often requires complicated calculations that accommodate flight conditions (sandy, salty, icy, windy), flight payload, hoists used, etc.”

Components replacement time limits

Many turbine engine parts are also more sensitive to power cycles than to operating hours. A turboshaft turbine wheel that has gone from 70 degrees to 700, and from zero RPM to over 20,000, all in the space of about 30 seconds, has been tortured to a far greater degree than if it had been pulling the aircraft merrily along at 10,000 feet, for three hours. Therefore, the engine manufacturers are in on the act too, with many

rotating components having their useful life expressed in cycles. The Rolls-Royce 250 series engines are relatively simple to deal with – a start is one cycle, and most rotating parts have a life in cycles and hours. This brings up another issue that the fixed-wing do not usually have to face. Helicopters often land without shutting down the engine(s). If we want to get the maximum life out of the engine parts, we had better not count each landing as an engine cycle. This means you can add engine starts, or cycles, to the list of things an overworked pilot has to count. This is very different from the assumption of 2 cycles per flight used for aircraft engines. Paragraph 2.2.3 presents further analysis regarding cycles counting.

Operating and Maintenance costs

Paragraph 2.3.2 presents an analysis for this criterion.

From the above it is clear that the main feature that aircrafts and rotorcraft share is the open sky. The next paragraphs provide more details regarding the rotorcraft unique environment, classification, market, flight profiles, envelope and performance.

1.2.1 Helicopter Environment

A helicopter is far more complex than a fixed-wing aircraft. The existence of rotating parts, their aerodynamics and the interference with the airframe affect its stability and control and create problems with vibration and with the frame structure. The development of the helicopter is an interesting trip that started from the beginning of the 20th century. The first concept was to develop a direct lift aircraft that would be able to hover and to convert its flight from vertical to horizontal and be used for transportation at short distances. The evolution of technology in all aspects of the helicopter's platform made it possible to support different missions and serve both military and civil market needs.

The technological advances in powerplant, fuel and stability controls, navigation and safety aids gave to the helicopter the ability to fly higher and faster and perform operations in all operating environments that the fixed-wing aircraft could not support. This section will refer the helicopters categories and will discuss the engine performance and the factors that affect it. In addition, it will address: i) the flight envelope limitations ii) the flight profile and iii) the factors that relate to the most demanding flight segments that is hover and climb.

1.2.2 Helicopter Classification

The helicopter's classification can be based either on the operating agent that is civil, commercial or military or according to technical parameters like:

a. Rotor system (conventional tandem, NOTAR, coaxial, intermeshing).
b. Powerplant (piston or turboshaft).
c. Maximum Take-off Gross Weight.
d. A combination of the power plant.
e. A combination of the powerplant, gross weight and passenger's capability.

Agency	Category		
EASA	Single Engine Piston	Single Engine Turbine	Multi Engine Turbine
FAA	Category A	Category B	Category C
	MTOW >20000Pounds	MTOW >20000Pounds	MTOW < 20000Pounds
	10 passenger seats	9 or less	10 passenger seats

Table 1-1: Helicopter Classification [8]

Table 1-1 shows a classification according to FAA and EASA organizations. The number of helicopters in a fleet and the classification in the fleet varies mostly from the operator, the area of operation and the missions performed. An army that operates in different locations worldwide can maintain fleets of 10 to a few hundred helicopters. In the civil market the number per fleet is very limited and according to Filippone [9] it is estimated that 95% of the helicopters operating worldwide are light helicopters; Figure 1-2 presents the different types of rotor configurations while most of them use the conventional tail rotor configuration, shown in Figure 1-3.

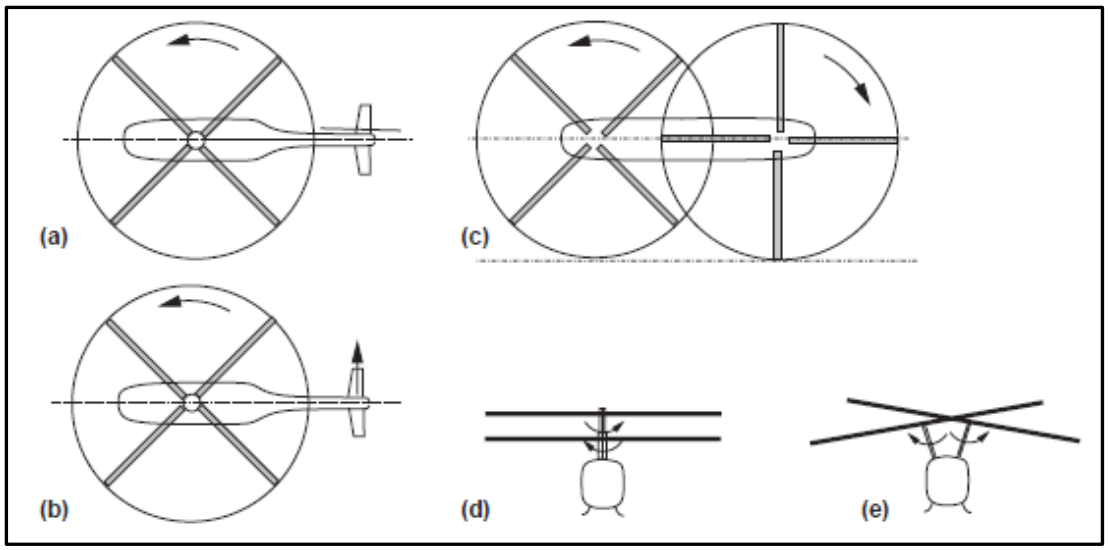

Figure 1-2: Different Rotor Configurations a. Conventional, b. NOTAR c. Tandem, d. Coaxial, e. Intermeshing [9][1]

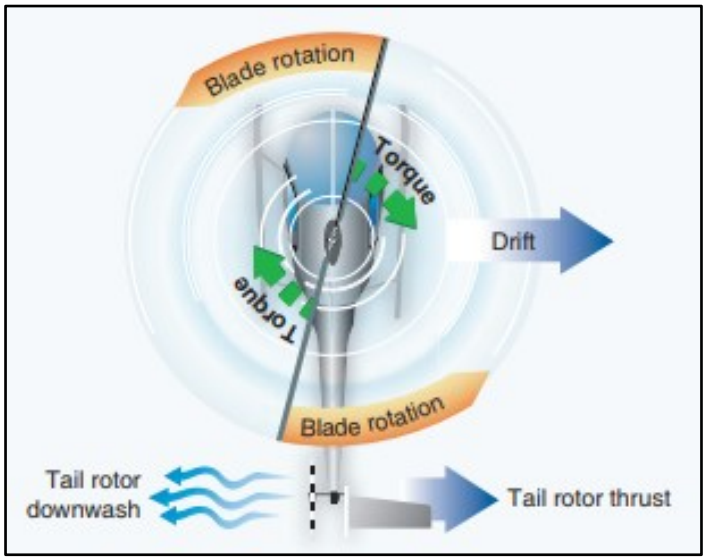

Figure 1-3 : Conventional Tail Rotor Configuration [10]

1.2.3 Helicopter Market

The helicopter market is growing fast and according to Frost and Sullivan Consulting [11], forecasts show that the international fleet will be almost tripled by the year 2033. The literature review showed that valuable information can be found with regard to the following categories:

a. Number of helicopters per country.
b. Number of helicopters per type of operation.
c. Operating costs.
d. Maintenance costs.
e. Accident and safety issues review.

While most of data are available for a certain fee from numerous consulting companies, some data can be found in the public domain.

	Period				
	1978-1988	1989-1999	2000-2010	2012-2022	2023-2033
New (Orders)	8018	5701	11733	13186	20711
Second-Hand Sales			23640		

Table 1-2: Helicopter Current Fleet & Forecast (Frost & Sullivan) [11]

The forecasted deliveries presented in Table 1-2, show that considerable market funds will be directed towards rotorcrafts. According to IBA Aviation Consultancy report [12] the reasons for this trend can be attributed to the following reasons:

a. Search and Rescue (SAR) operations will be privatized and the need for civil SAR helicopters will increase.
b. In the Oil & Gas market, the helicopter contracts are a very small proportion of the total oil rig production costs.
c. Smaller operators are struggling to finance new deliveries and a new market for helicopter leasing companies emerges
d. The lease market covers around 20% of the total market but this number will possibly grow in the next years.
e. Helicopter investment offers high liquidity and good returns, as the market is less volatile.
f. Helicopter fuselages have no life limits because the cabin is not pressurized as in aircraft. The fuselage life limit is based on inspections and can be extended accordingly. Other onboard equipment like avionics or HUMS systems can be updated and help the helicopter keep its initial value.
g. The estimated value for used helicopters can be around 70-80% of the purchase price even after 10 years of service.

h. The economic useful life of helicopters is about 5 years greater than the commercial passenger aircraft (25 years).

i. In the medium/heavy category, values of popular helicopters and helicopters depreciate at a much slower rate.

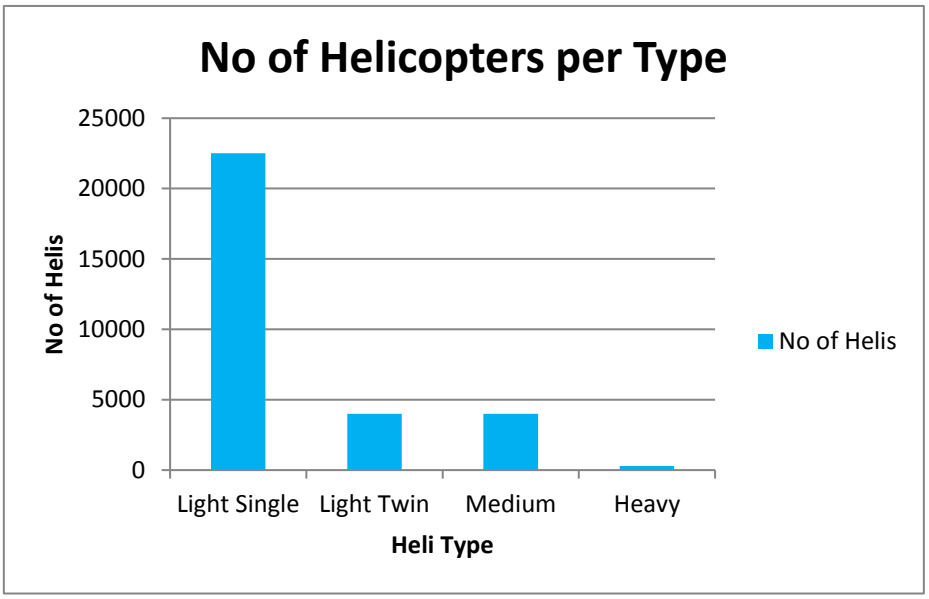

Figure 1-4: No of Helicopters per Type [12]

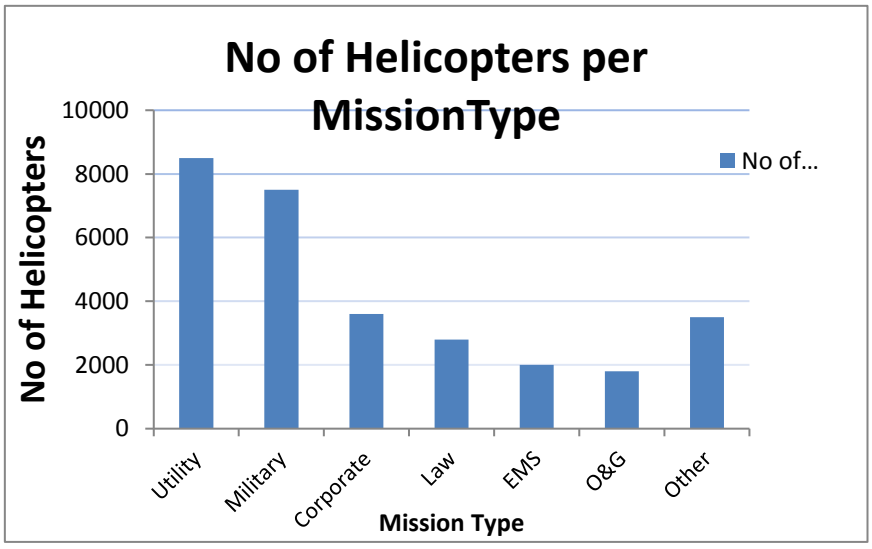

Figure 1-5: Drag/Airspeed Relationship [12]

1.2.4 Flight Profile

A rotorcraft flight profile is very different than an aircraft due to the capability to hover and perform steep turns. Flight profiles differ according to the mission. The following

table presents the basic flight profiles that relate to the categories showed in Table 1-1 and analyzes the OEM emphasis for each profile.

Emergency Medical Services (EMS).	1. Operational serviceability 2. All-weather day-night 3. Cabin space and accessibility 4. Cost of ownership
Civil Search & Rescue (SAR).	1. Operational serviceability 2. Payload range / endurance 3. All-weather day-night ops 4. Mission reliability 5. Sophistication of flight 6. automation (SAR modes) 7. Winching capability
Law Enforcement/Police.	1. Cost of ownership 2. External noise 3. Speed
Passenger Transport/Air Taxi.	1. Comfort – minimum cabin noise and vibration 2. Speed 3. Cabin space and layout
Utility	1. Cost of ownership 2. Versatility of cabin configuration 3. External cargo capability
Oil & Gas.	1. Payload range 2. Cost per passenger seat mile 3. All-weather operations 4. Marinisation features 5. Cat A performance from elevated heli-decks

Table 1-3 : Rotorcraft Missions and their Features

Most of the missions mentioned above can be served with a single or multi-engine helicopter. The limiting factor varies for every segment of the flight profile and the helicopter performance in each segment depends on the power output and the lift produced by the rotors. Any factor that affects engine and rotor efficiency affects performance. According to Litt and Chatterjee [10] , the three major factors that affect performance are: i) density altitude, ii) weight and iii) load and iv) wind.

Two representative profiles for SAR and Firefighting missions are shown in Figure 1-6.

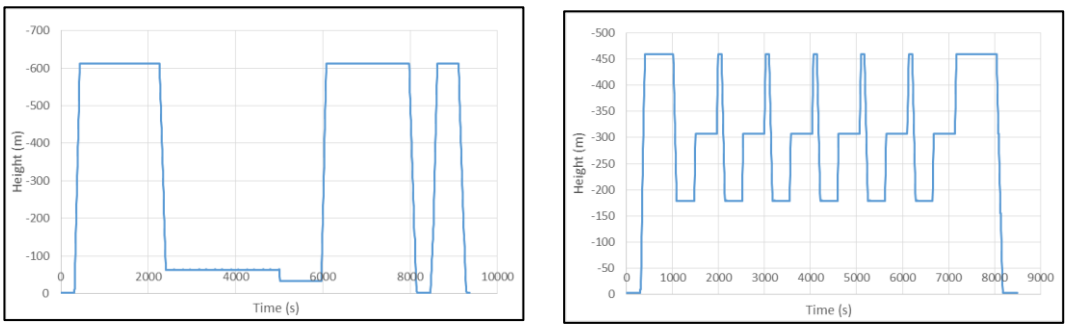

Figure 1-6: a. SAR Mission, b. Fire Fighting Mission [13]

1.2.5 Flight Envelopes

When we refer to the flight envelope, we mean the area that the helicopter can perform efficiently and with safety within the existing aerodynamic, environmental, engine performance and mechanical limits. Various factors affect the safe operation of the rotorcraft:

a. Helicopter performance (density altitude, weight, and wind).
b. Aerodynamic limitations (rotor limits, drag, IGE, OGE).
c. Structural limitations (engine over speed, transmission structural limits, rotor loading).
d. Airspeed limits.
e. Loading limits (maximum take-off weight, the centre of gravity).
f. Power limits (EGT limits).

The factors that relate to rotorcraft performance are discussed at the next paragraph. Regarding the other factors a usual way to demonstrates their limits is the velocity vs load factor diagram. A typical diagram is presented in the figure above. A brief explanation for the demonstrated areas is given below:

Load factors: Load factors refer to the acceleration forces affecting an aircraft in flight. If no acceleration is taking place, the load factor is equal to the force of gravity, 1 gravity (G):

a. When the rotor is producing more thrust than required for unaccelerated flight, the loadfactor will be greater than 1 G.
b. In hovering flight, load factor can be determined simply by dividing rotor thrust by weight.

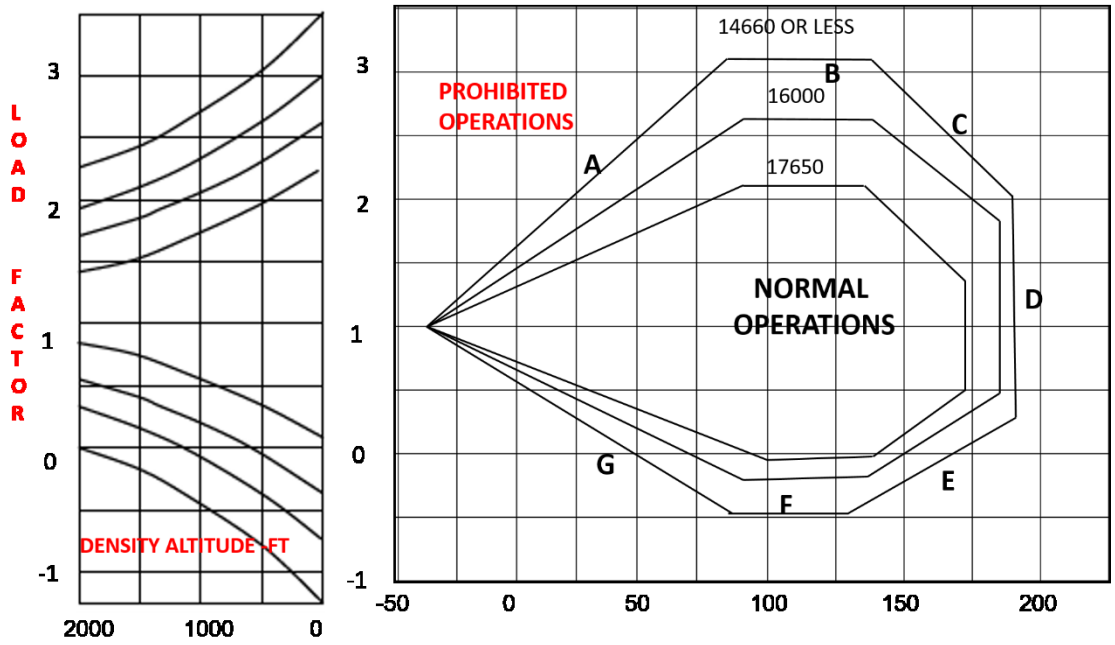

Figure 1-7: A typical Velocity vs. Load factor chart

Therefore, 20,000 lb of thrust applied to a 10,000 lb helicopter will result in a load factor of 2 Gs.

Areas A and G.

Low forward airspeed and insufficient excess power in these regions prevent the aircraft from reaching higher loads.

Area B.

The primary factors are structural and aerodynamic (static strength and blade stall). Blade stall onset begins to transition in this region and severity increases to become the primary factor for area C.

Area D.

This area is very dependent on rotor design and the operating weight. Primary limiters are blade stall and compressibility effects.

Area E.

Flapping angles are the primary culprit. In tandem seat aircraft, incursion into this area may result in the rotor blades coming dangerously close to the canopy or physically striking components on the nose of the aircraft.

Area F.

This is very rotor dependent. A teetering rotor loses cyclic control at zero G (i.e., mast bump), but designers of articulated, hinge less, rigid types tweak this area by the amount of flapping offset. In advanced rotors, negative G capability is achieved this way, but offset comes with penalties in other areas as well (phase lag angle, for example creates rigging problems throughout the envelope)

While the combination of the above factors determines a successful mission within safety and cost margins the life cycle costs of the helicopter and the powerplant degradation is affected by other factors that have little to do with the flight. These factors are: i) the crew attitude ii) the maintenance strategy followed by the operator iii) the maintenance personnel iii) the spare parts availability and iv) the components reliability.

1.2.6 Helicopter Performance

The rotorcraft performance during a mission relates to factors that affect the engine and the rotor efficiency. The ability to predict the performance is very important because it allows the pilot to determine the maximum weight before take-off, the capability to hover at a specific altitude and temperature, the maximum climb rate and the distance to climb over obstacles. To cover that need the helicopter mission simulation has been a research field for many years.

Padfield [14] approaches the simulation modelling with a 3 level model as a means of measuring the progress of attained simulation fidelity. His approach proposes that Level 1 and 2 are suited for constructing conceptual design within the limits of operating envelope The Level 3 model is utilized to address rotor stability and load prediction in addition to vibration analysis up to the limits defined by the safe flight envelope.

Goulos et al. [15] worked on an integrated methodology and tried to simulate a twin-engine light rotorcraft within a Category A take-off manoeuvre. CAT-A manoeuvre

means that the helicopter is flown, at a speed 90 knots or less, in such a way, that in case of a single engine failure during take-off or landing, the helicopter can either safely continue the flight or safely abort it. The proposed method is related to the Level 1 of Padfield's simulation model. In a later work for helicopter rotor blade flexibility simulation, Goulos [1] developed a more complicated model that utilizes the unsteady aeroelastic rotor model and managed to assess the helicopter's main rotor behaviour at the 3rd Level of Padfield's hierarchical model.

The rotorcraft powerplant needs to deliver power to overcome the drag and weight and allow the rotor to perform efficiently at a wide operating range and loads. In addition to weight, the load factor (actual load during steep turns divided by gross weight) plays a significant role in the performance too. It is worth mentioning that anytime the helicopter flies at a curved flight path, the load supported by the rotor blades is greater than the total weight of the helicopter. An analysis of the required drag relative to the forward speed is shown in Figure 1-8.

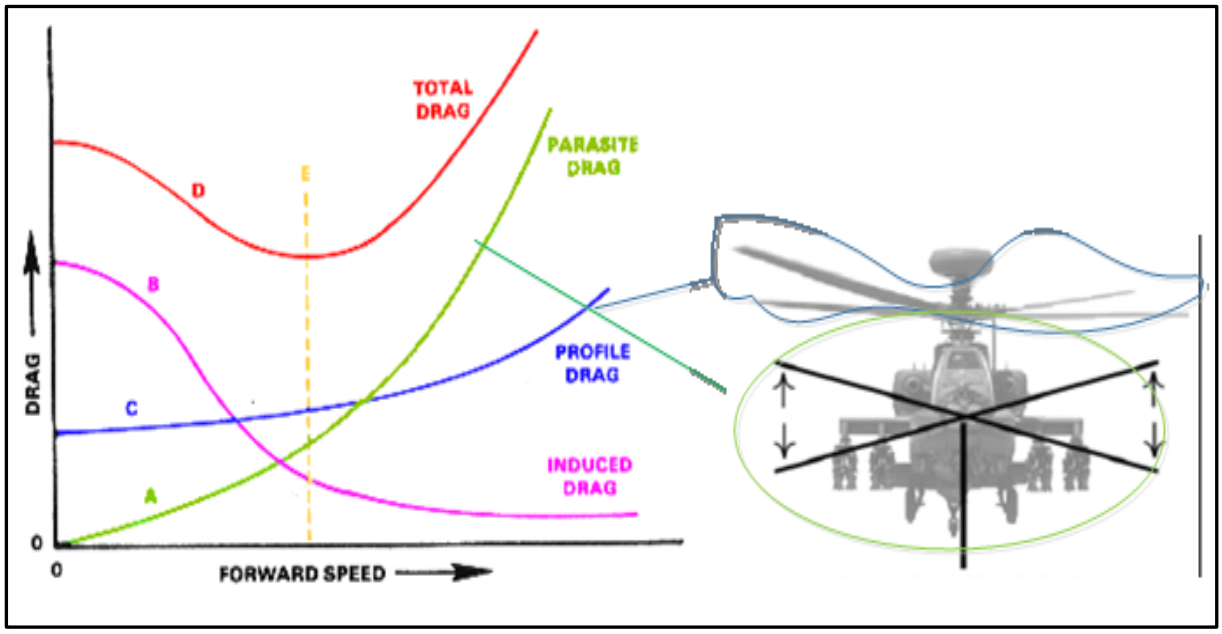

Figure 1-8: Drag/Airspeed Relationship [16]

Helicopter performance is related with parameters like the gross weight, density altitude, climb performance, life to drag ratios, engine fuel consumption, speed for minimum power or maximum range, power for maximum altitude – ceiling. The parameters affecting helicopter performance (FAA reference) are: i) air density, ii) atmospheric pressure, iii) altitude, iv) temperature, v) moisture, vi) weight (payload)

and vii) winds. The methodology section provides a detailed analysis of these parameters and the reasons for the ones selected for this research.

1.3 Project Scope and Objectives

1.3.1 Research Project Scope

Literature review reveals that there is a shortage in information relative to rotorcraft optimal trajectories, engine degradation, and the effect of those on direct costs and operator revenue while there is extensive reference to cost which relate to aircraft industry and commercial airlines. Regarding how the rotorcraft flight profile affects engine maintenance the ‘severity factor’ concept has been introduced. In addition, regarding the engine maintenance technology advancements have introduced new maintenance concepts.

Ackert [17] mentions the ‘severity factor’ concept derived from the Maintenance Repair and Overhaul (MRO) industry. The severity factor is used to compare the loads and stresses between actual usage and a reference flight profile which relate to engine de-rate and other operating parameters like: i) OAT ii) altitude iii) payload and iv) flight length. Hanumanthan [18] showed that the severity factor varies for short length vs long length cruising flight segments and is a tool used to address the engine’s degradation issue.

The literature review revealed that the method, which is based on the severity factor concept, has not been used for rotorcraft so far. Rotorcrafts by default operate over shorter ranges, their engines work under severe conditions and at altitudes that make them more sensitive to particles intrusion, oxidation and corrosion. The missions performed relate to many variables and the effort to evaluate engine degradation can be very challenging. The accuracy of the method relies on the chosen reference flight and its correlation with actual flights. The research papers, reviewed by the author in the context of this work, which are based on G.P.Sallee’s work on severity [19], defined the values for the operating condition variables as: i) ISA deviation ii) payload and iii) climb rate arbitrarily. Furthermore, the operating conditions used for the actual flights were not similar to the reference operating conditions. This approach decreased the method accuracy and revealed a gap that needs to be addressed.

With regard to maintenance concepts, according to Fraser [20], military fleet maintenance is based on the “standard school” preventive maintenance but the latest trend embraced by both military and civil operators is the ‘on-condition based’ maintenance. The technology advancements in build-in engine sensors that can predict engine performance and parts’ degradation are supporting this concept. The Health Usage Monitoring System (HUMS) combined with Helicopter Flight Data Monitoring (HFDM) and Condition Based Maintenance (CBM) support three important objectives: i) increased safety, ii) increased availability and iii) reduced operating costs. To realize the above objectives in an affordable manner, the onboard installed systems should be supported by wireless data transfer capability and trained personnel that would analyse the data. The high-numbered military fleets favour the idea to build this infrastructure but as the Hoffmann report [21] shows the civil operator’s fleet does not.

To that end, Cronkhite [22] mentions that the on-condition maintenance concept with the use of HUMS is difficult to implement and can be cost-effective after some time. To address this issue, engine manufacturers propose a method that keeps the maintenance out of the operator’s concern and transfers the maintenance work to the repair centres and the MRO industry. According to Desfor [23], PBH supporting contracts are used by operators worldwide and do keep the fleet availability high albeit only for those operators that can afford the price. PBH contracts offer different levels of services at different prices but the costs can be significant. The operators’ budget may restrict the commitment to a PBH contract.

Harris [24] mentions that the LCC estimation has been a field of research since the early years of rotorcraft life. The efforts leaned towards the development of Cost Estimation Relationships (CER) with the implementation of regression analysis. This analysis is taking advantage of historical data maintained at government databases or published from the OEMs’ in magazines that refer to Maintenance Repair and Overhaul (MRO). Research in that field shows that it is difficult to find cost data for turboshaft engines in the public domain and every effort to estimate the maintenance cost would use assumptions that would cause the estimation models to be unrealistic and difficult to verify.

From literature, it becomes evident that the operator needs a tool that will reveal the consequences of using specific trajectories and power settings in relation to engine performance and degradation. Such a tool would allow him to: i) maximize crew safety ii) increase expected revenue iii) choose the optimum method for engine induction for service and iv) increase fleet availability. This work suggests and discusses hereafter a qualitative approach that can be a solution to the problem.

The scope of this research is to answer questions from an operator's perspective such as:

a. What are the optimum flight trajectories that will have a minimal effect on engine lifing?

b. What are the costs associated with the variation of various flight trajectories in specific environments?

c. Is there an optimum strategy that an operator should follow so as to maximize the company's revenue, fleet availability and passenger's safety?

d. Therefore, three basic requirements can be identified:

e. A methodology to assess the engine performance and components life related to a representative reference flight, the actual flight trajectories, and similar operating parameters.

f. A methodology to estimate the maintenance costs incurred from the actual operating flight trajectories through a qualitative approach. This approach should combine the expected operating costs allocated to the annual budget with the incurred costs due to rotorcraft usage.

g. A methodology to combine the costs and engine life and help the operator make an informed decision, which will maximize the operator's revenue and fleet availability.

1.3.2 Objectives

The objectives that address the scope of this research project are presented in the next lines:

a. To perform an extensive literature review with regard to LCC, engine maintenance strategies and engine degradation assessment.

b. To develop a load and stress assessment module.

c. To develop a framework that will integrate the outputs from flight dynamics software with engine component stress/strain analysis and remaining life due to low cycle fatigue.

d. To develop a framework that will correlate the engine components' life with related maintenance cost.

1.3.3 Research Milestones

The milestones of this research are listed below:

a. Determine flight mission profiles and select engine configuration. The trajectories will simulate a reference flight and other profiles that will represent missions that assume severe engine usage. (D1)

b. Assess engine loads caused by the engine usage and environment for a reference flight segment and for various other actual scenarios. These scenarios are created while varying the parameters that affect engine behaviour and degradation. The parameters may be payload, power, OAT, and altitude. An in-house flight dynamics simulator, named HECTOR is used to provide the fuel and engine power data for a reference and actual flight profile segments. (D2)

c. Estimate the severity. The previously estimated data will provide information for the engine degradation about a baseline flight profile. (D3)

d. Carry out an operating and environmental parameters sensitivity analysis. (D4)

e. Assess engine maintenance life cycle cost. These costs will facilitate the costs incurred due to helicopter actual usage. (D5)

f. Apply the integrated simulation framework to a selected case study. (D6)

1.3.4 Knowledge Contribution

The main contribution arising from the successful completion of the milestones mentioned before is the development of a framework that can assist a rotorcraft fleet operator in:

a. Assessing the engine components life related to the actual flight profile and the operating environment

b. Estimating the approximate variable costs incurred and

c. Making an informed decision based on the trade-off between revenue maximization and fleet availability.

The framework uses a methodology, which addresses the gap in knowledge identified in G.P Sallee's work [19] and all other relevant research work and provides a unique capability to assess the engine's life in relation to the operator's flight profile.In addition, this framework of carefully selected tools can support an analysis of the component design effect in component life.

The unique feature of the methodology is that it is a hybrid model, which combines both the data driven, and model based methodologies as described in Bagul et al. review [25] of remaining useful life methodologies. The methodology is comprised of a DOE coupled with a cumulative damage model (WU-FPM). The DOE uses a simulation tool for flight dynamics and a theoretical method to assess the component remaining useful life (RUL). While initially the tool uses a DOE specific design space, when combined with a surrogate model, can assess the component life of any operator fleet. To achieve that the operator should define the design space for the fleet environmental and operational parameters.

1.3.5 Available Resources

The available resources for this research have been the following:

a. Conference Papers, Journal Papers.

b. PhD and MSc thesis.

c. Commercial software available online or provided by the Cranfield IT department. Microsoft office, Finite Element Software, (ANSYS, CAD, etc.).

d. In-house software or platforms (HECTOR, TURBOMATCH, HESTIA, etc.).

e. Internet and Course notes from either Cranfield or other Universities.

2 Chapter 2: Literature Review

A literature review is carried out in order to provide a background to the theory that was used in this research and the existing state-of- the-art methodologies and concepts that relate to engine degradation, maintenance strategies, life cycle costs incurred and methods to estimate them.

Within the first section, of the literature review chapter, issues that relate to engine life assessment and in particular the performance restoration and component life assessment will be discussed and the gaps in literature will be addressed. The part, which focuses on the component life assessment, will present: i) the practical methods developed like the severity factor and data analysis based on operator feedback and, ii) the theoretical approach regarding the component life assessment. This part refers to the methods used to assess the component failure due to low cycle fatigue and the methods used for the engine cycles counting.

The second section provides background information about the life cycle cost of the helicopter and the powerplant used to support it. In addition, a reference is made to the different approaches of the military and civil operators and to the latest methods proposed by the engine manufacturers regarding the maintenance cost estimation.

The last section summarizes the review findings, highlights the gaps identified in the literature regarding the turbine life assessment and the maintenance cost estimation and introduce the approach to address these gaps.

2.1 Engine Maintenance

This section aims to provide background but not detailed information with regard to engine maintenance, performance degradation and the methods to estimate it, the component failure and the mechanics involved.

The gas turbine operation is the result of a smooth cooperation of many different components, modules and accessories. All the contributing parts show wear and can affect the system operation. Gas turbines operate over a wide range of temperatures, speeds, power and environment. The components in the engine's main air path such as the compressor, seals and shaft, the combustor and the ones in the gas path such as the turbine disc, blades, and the stationary nozzles wear out for different reasons.

Kurz's and Brun's tutorial on component degradation [26] provides a comprehensive insight into the engine degradation mechanisms. The components wear can be either microscopic for example change in blade surface area, seal wear, invisible cracks, or macroscopic, like mass flow area change, vane bowing and component clearances with adjacent areas.

The engine maintenance is required for three principal reasons:

a. To keep the engine in service to generate revenue
b. To maintain the value of the engine by minimizing the physical deterioration and implementing the mandatory or optional OEM service letters
c. To meet the standards set by the regulating authorities.

The causes for removal can be for either scheduled or unscheduled maintenance:

a. Scheduled:
    1) Engine performance Restoration.
    2) Life limited parts (LLP) replacement.
b. Unscheduled:
    1) Foreign object damage (FOD)
    2) Hardware deterioration
    3) Accessories failure

This research focuses on the maintenance costs that relate to the scheduled maintenance events, which are the induction to a service station for: i) performance restoration, also named [27] as Time between Overhaul (TBO) and ii) a component replacement due to a part reaching its life limit. Therefore, the next paragraphs describe in more detail the engine performance degradation and the life-limited parts replacement.

2.1.1 Engine Performance Restoration

According to MacLeod, Taylor, and Laflamme [28], the engine deterioration does not follow a linear path with use but has a diminishing rate as shown in the following figure.

The first part occurs in the first few hundred flight hours after entry of the engine into service and is called short-term deterioration. The second part occurs gradually as service usage accumulates and is called long-term deterioration. Their work, on overall

engine performance decrease due to component deterioration, revealed that a 6% increase of the gas generator turbine nozzle through-flow caused from corrosion, cracking, bowing and erosion, resulted in an increase in heat rate by 3.55% but virtually no loss in power. Kurz and Brun [30] used a model which under these conditions showed a significant reduction in gas generator speed, with a significant 7% and 3% loss in power and efficiency respectively.

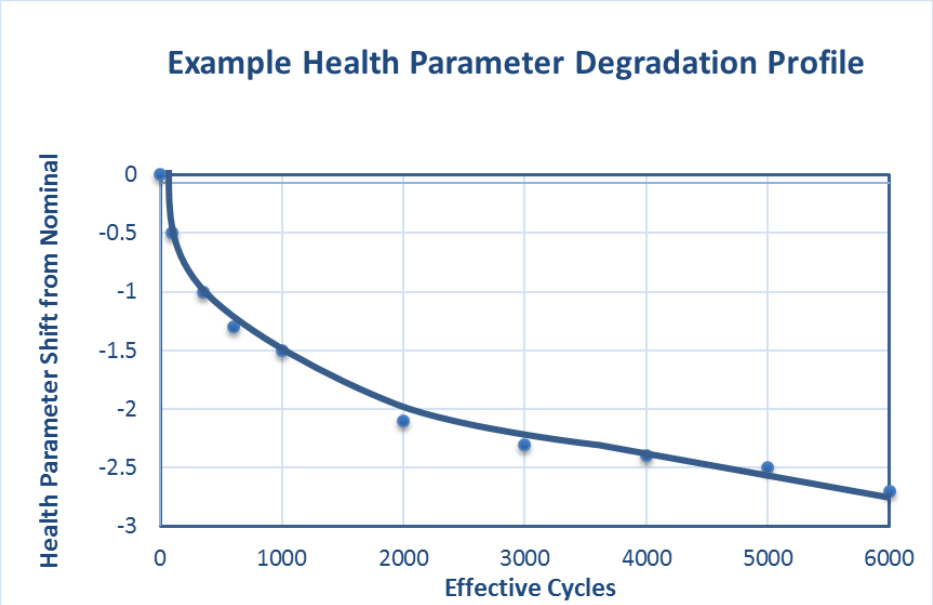

Figure 2-1 : Engine Health Parameter Degradation Profile [29]

To that end a NASA report [19] that was based on J79D engine historical records from five airlines, two airframe manufacturers and a P&W aircraft covering a period of 3 years from 1973 to 1976 showed interesting details on component degradation. It revealed that regarding short-term performance deterioration the Thrust Specific Fuel Consumption (TSFC) loses 1% in the first flight hour while an extra 0.5 % is added in the first 200 flight hours. Of these losses, 55% were attributed to low-pressure spool performance loss and 45% to the high-pressure spool loss. Regarding long-term performance deterioration the average performance loss was 4.4% in the 12000 hours and the causes for the loss was attributed 40% to flight loads, 40% to erosion and 20% to thermal distortion. These 4.4% losses can be recovered by 0.9 % due to repairs in high pressure turbine and by 2.8% due to refurbishment in low- and high-pressure compressor".

As mentioned in Cyrus.B.Meher at al. [31] “a further classification of performance deterioration can also be made in: i) recoverable, ii) non- recoverable and, iii) permanent. In more detail:

a. Recoverable Loss: The recoverable loss usually relates to compressor fouling. Compressor fouling can be reduced by physically cleaning the compressor blades and vanes or by water washing.

b. Non-recoverable loss: In general, the non-recoverable loss is mostly attributed to the following reasons:

- Hot corrosion that produces a material loss.
- High-temperature oxidation due to chemical reactions between components and the hot gaseous environment.
- Erosion due to particles impinging on flow surfaces which result in material removal from the flow path.
- Abrasion, which is the result of the rotating component surface rubbing on a stationary surface.

c. Permanent: Residual deterioration present even after a major overhaul.

Various methods determine the mechanical condition (health) of the gas turbines and ensure safe operation. One measure to understand the engine deterioration is the EGT margin decrease. The engine operating EGT is compared to the EGT red line limit which is estimated from the manufacturer. As the engine deteriorates, its performance decreases and that force the fuel controller to work on higher EGT temperatures to support the operating loads. The engine is removed when the EGT reaches the red line as shown in Figure 2-2, and inducted for overhaul.

Sing [32] reviews other available techniques such as i) oil condition and debris monitoring, ii) vibration monitoring iii) engine life usage and iv) visual inspection.

Hanumanthan [18] tried to assess the EGT margin consumption in his work. He used a Matlab code to run iterations with different levels of component degradation characteristics that resulted in EGT margin consumption. He thus estimated the degradation value that moved the EGT curve to intersect with the engine redline temperature.

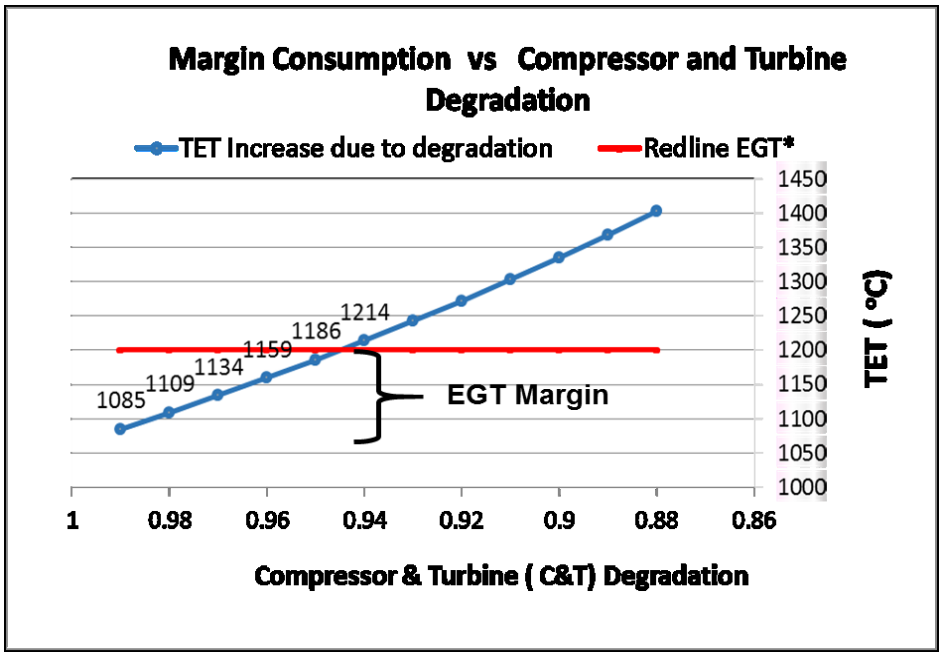

Figure 2-2 : EGT Margin Consumption

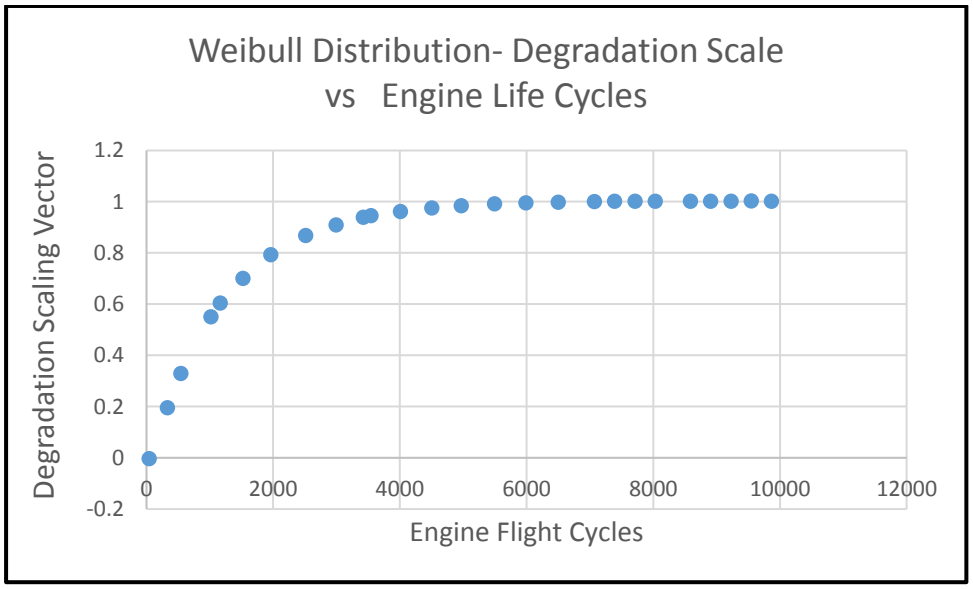

Figure 2-3: Weibull curve for degradation scale of engine E56 [18]

This degradation value was then used as an ordinal to a cumulative Weibull curve having slope value 1 and scale factor 0.7 as shown in Figure 2-3. The diagram abscissa of the intersection indicated the cycles to fail and thus the Shop Visit interval was estimated. Unfortunately, this method is not suitable to use in this research for the following reasons:

a. It is based on a degradation dataset taken estimated for rotating parts of JT9-d turbofan engines. The relation between degradation values versus engines flight cycles assumed that an engine uses 2 cycles per flight. The data set used and the 2 cycles/flight assumption is not applicable to the rotorcraft case for reasons that will be analysed at paragraph 2.2.4.

b. The methodology accuracy regarding the TBO limit was low due to the simplified assumptions taken at the Weibull cumulative distribution function. A selection of the factor values based on sensitivity analysis would provide higher accuracy but still would not solve the issue regarding the flight cycles assumption.

c. This research needs to base its methodology to as much as possible accurate time limits for performance restoration and rotating parts life. To that end, it is deemed safer to use the engine manufacturer TBO limit.

While the engine degradation may not be very useful to assess the TBO limit, it can support the fuel consumption estimation. Fuel consumption is a major contribution to engine costs and the effect on degradation in relation to the loads impose from different flight profiles could give a useful insight to the operator.

2.2 Component Life Estimation

Regarding component life estimation, it is worth arguing that even though the number of mechanical failures relative to the number of successful uses of components and structures is minimal, the cost of such failures is considerable as it relates not only to enormous costs but also to injuries and safety. Mechanical failures involve an extremely complex interaction of load, time, and environment, where environment includes both temperature and corrosion. They relate to a combination of the material properties and the appropriate design. Statistics based on in failure data reveal that at least half of the mechanical failures (50 to 90%) are due to fatigue.

As Fatemi [33] mentions designing for fatigue comprises synthesis, analysis and testing where one component is appropriate for product durability determination while the other for product development. While existing fatigue life models, including commercial and government computer aided engineering are used for analysis, they cannot consider all the synergistic aspects involved in fatigue (temperature, corrosion, residual stress and variable altitude loading). In that sense, the available methods to

address component life estimation can be categorised to theoretical and practical methods.

The theoretical approach is based on theories and experimental work developed since the word “fatigue” was first introduced back in the 1840s and 1850s and relate to material deformation, corrosion, thermal shock, brittle or ductile fracture and fatigue. The practical approach relates to methods like severity factor determination or model-based data analysis. This approach is estimating the components life based on data bases created either from actual flights flown to create a significant population for data analysis or from aircraft operators’ feedback. Paragraphs 2.2.4.1 and 2.2.4.2 presents detailed analysis for that approaches.

2.2.1 Theoretical Approach

The first part of this section addresses the three main reasons for the engine rotating component failure: i) low cycle fatigue ii) creep and iii) oxidation while the forth part continues with a review of the severity factor concept. The second part reviews the work done to show each reason effect on gas turbine engine for short or long haul flights. The third part refers to the engine cycle counting methods.

2.2.1.1 Rotating Component Failure

The rotating compressor and turbine hubs, shafts, or disks within the engine have a specifically defined operating life, at the end of which, the parts must be replaced and not used again. The operating life is based on the estimated life before component failure.

Component mechanical failure which, leads to an unsatisfactory performance in its intended function, is considered the change in size, shape, material properties of a structure. The failure happens according to Collins [34] through two fundamental behaviours such as plastic and elastic. The contributing factors are force, temperature, time and reactive environment.

The engine’s component that runs in extreme conditions is the HPT. While all the components in the engine operate at different loads, the HPT operates in a very hostile environment (the engine’s ‘hot section’), namely high temperature and pressure of the gas and elevated HP shaft speed. These two main aspects are the causes of the rising

of principal stresses (i.e. centrifugal and thermal stresses) acting on the turbine's blades and disc.

An accurate analysis of both short and long-range mission engines requires the identification of the most restrictive phenomena that limit the life of the component, determining its failure after a certain amount of time.

Literature review reveals that with regard to aircraft engine failures, the most commonly observed phenomena ([35][2], [36], [37], [38] , [39]) are low cycle fatigue, high cycle fatigue, creep and oxidation.

2.2.1.2 Fatigue

Fatigue is the sudden and catastrophic separation of an engine part into two or more pieces due to the fluctuating loads or deformation over a period. It is a surface phenomenon and it occurs in two phases. The first is the crack initiation and the second is the crack propagation. Fatigue failure can happen either at low or high stress and strain cycles and is mainly divided into Low Cycle Fatigue (LCF) and High Cycle Fatigue (HCF).

The low cycle is associated with high loads at the component's plastic region and with a frequency less than 10^5 cycles, while high cycle fatigue happens at the elastic region but at a high frequency of more than 10^5 cycles. It is important to understand that in Region I, in Figure 2-4, the material is always stressed in the vicinity or over the yield strength σ_y. It is the plastic strain that dominates and controls fatigue life. In Region II the material behaves elastically, and failure occurs under alternate stress whose amplitude σ_a is always lower than the yield strength σ_y. Region III is the region of unlimited life, at least in ferrous alloys and titanium, since the S-N curve flattens, and fatigue life becomes independent of stress cycles. The corresponding stress is called the endurance limit of the material.

Dieter [40] mentions that the mechanism of damage at High Cycle Fatigue (HCF) is in spending 90% of the life in the crack initiation, and 10% in crack propagation to failure, making them more catastrophic in nature due to abrupt failure.

Unlike HCF, the LCF involves 10% of the life consumed in crack initiation and 90% in crack propagation, giving a clear indication of the progress of failure, in terms of crack

detection. This is the reason that the critical components prone to failure by LCF are specified as life-limited parts, and are monitored on a cycle basis instead of flight hours [40].

A disk burst is potentially the most catastrophic failure in an engine. To avoid this, the disks design considers LCF and over-speed capability as primary objectives. The requirement for higher turbine stage work without additional stages has resulted in increased turbine blade tip speeds and higher turbine inlet temperatures. This trend has led to significant increases in turbine stage disk rim loading and the operation at the more severe thermal environment, thereby making it even more difficult to design turbine disks for a specific life requirement. According to Fatemi , to achieve higher turbine work levels both turbine blade tip speeds and turbine inlet temperatures will need to increase.

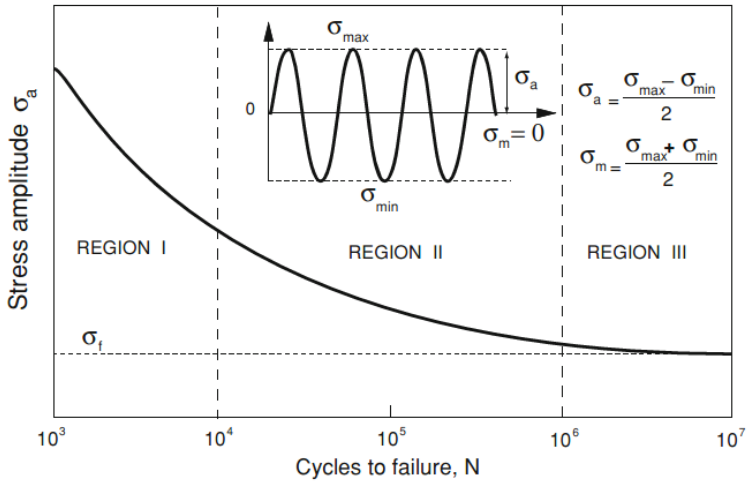

Figure 2-4: S-N curve, cyclic stress σ_α vs number of cycles to Failure N [40]

For the designer, the fatigue life prediction is critical. Currently, there are four models, which design engineers consider and the decision is based mostly on the component life expectancy. The models are the following [41]:

a. The nominal stress-life (S-N) model which, has been available for about 150 years, while the other models have been available only since the 1960s. The nominal S-N model uses nominal stresses and relates these to local fatigue strengths for notched and unnotched members

b. The local strain-life (E-N) model: The local E-N model deals directly with local strain at a notch, which, relates to smooth specimen strain-controlled fatigue behaviour.

c. The fatigue crack growth (N-AK) model: This model can be considered a total fatigue life model when it is used in conjunction with information on the existing initial crack size following manufacture.

d. The two-stage model, which consists of combining models 2 and 3 to incorporate both macroscopic fatigue crack formation (nucleation) and fatigue crack growth. This method uses the local E--N model that assess the time to the formation of a small macro crack, followed by integration of the fatigue crack growth rate equation for the remaining life. The two lives are added together to obtain the total fatigue life.

The criteria for a component fatigue design have evolved during time. They started from the infinite life design to damage tolerance and their usage is based on the component application. The criteria are:

a. Infinite-Life Design.
b. Safe-Life Design.
c. Fail-Safe Design.
d. Damage-Tolerant Design.

The criterion, which relatsd to the gas turbine rotating components, is the safe life design criterion. While the infinite life design addresses the variable amplitude, loading its implementation requires excessive material weight, which is not cost effective for the aviation sector. The safe life design considers the calculated life, computed from a combination of testing and statistical analysis, and estimates an allowable service life by using appropriate safety factors.

The failsafe and the damage tolerant designs relate to airframes and are based on the philosophy that if one part fails the system does not fail, thus, they could only be used if the rotorcraft used a multiengine configuration.

The fatigue analysis of the gas turbine components should take into account:

a. The operating temperatures of the engine (ISA deviation).
b. The range that the stress amplitude resides.

c. The cyclic nature of the stresses.

d. The operating environment (corrosive, altitude).

In the next lines, a further analysis of the 2 most used methods will be attempted. A more detailed analysis of the above methods and criteria can be found in Fatemi [41].

The nominal stress-life (S-N) model

The start point for every analysis is the stress loads history and its effect on crack nucleation. The very early method that has been developed to relate stresses with the crack nucleation is the S-N curve. 'S' stands for the cyclic stress range while 'N' represents the number of cycles to failure.

To develop the curve, as Boyer proposes [42][5] a series of samples are tested to failure at various stress ranges. The most common types of fatigue machines are small bending fatigue machines which can be i) cantilever beam, ii) rotating beam or iii) spin testing machines. The resulting life is plotted versus the corresponding stress range, as seen in Figure 2-5 and Figure 2-6. There are three key values, which separate the plastic, elastic and infinite life regions:

a. Ultimate Strength: Stress level required to fail with one cycle

b. Yield Strength: Dividing line between the elastic and plastic region

c. Endurance Limit: If all cycles are below this stress level amplitude, no failures occur.

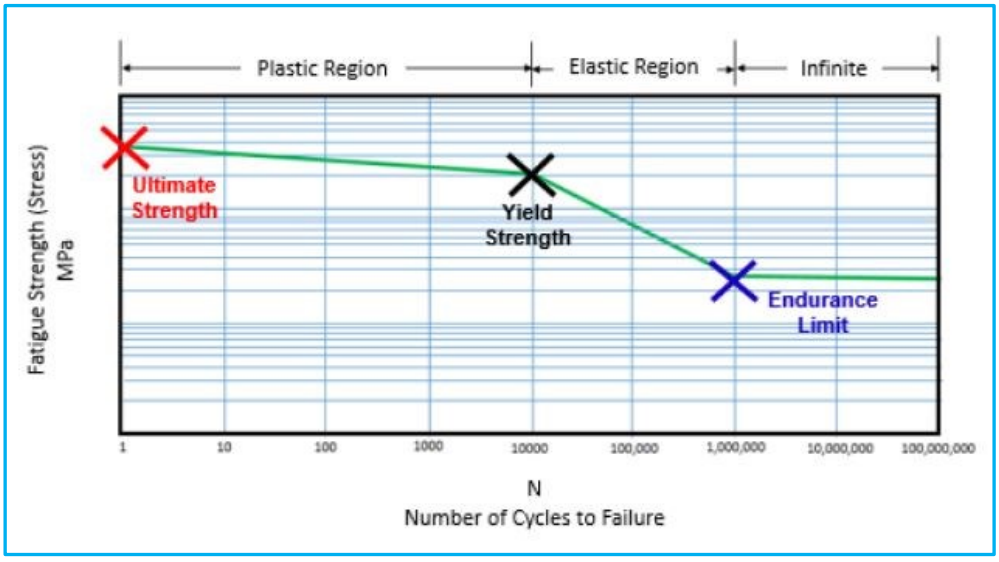

Figure 2-5: Typical S-N Diagram [43]

The S-N curve is the locus of these data points. In more thorough testing, multiple samples are tested at each stress range.

In the elastic region, as seen in Figure 2-6, the relationship between stress and strain remains linear. When a cycle is applied and removed, the material returns to its original shape and/or length. This region is also referred to as the “High Cycle Fatigue” region, because a high number of stress cycles, at low amplitude, can cause the part to fail. Typical factors that influence the performance of a material in the elastic region are residual stresses and geometric considerations. For example, a severe geometry change in the material may be more likely to have a crack initiate than a smooth geometry change.

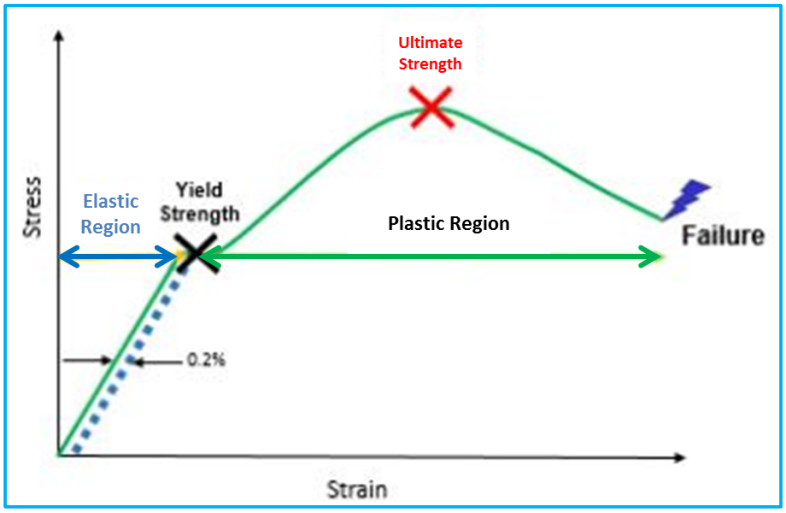

Figure 2-6: Typical Stress-Strain Curve [43]

In the plastic region, the material experiences high-stress levels, causing the shape and/or geometry to change due to the repeated application of stress cycles. This region is also referred to as the “Low Cycle Fatigue” region of the SN-Curve, where a low number of stress cycles, with high amplitude, result in failure. Material plasticity and geometry are big influences on the number of cycles to failure in the plastic region.

Calculating fatigue life or damage in the plastic region of a material with an SN-Curve is probably best avoided. If cyclic stress levels are in the plastic region, a strain-life approach would typically be recommended instead, which includes an E-N (Strain vs Number of cycles) as part of the analysis.

The local strain-life (E-N) model

An important aspect of the fatigue process is plastic deformation. Fatigue cracks usually nucleate from plastic straining in localized regions. Therefore, cyclic strain-controlled tests can better characterize the fatigue behaviour of a material than cyclic stress-controlled tests can, particularly in the low-cycle fatigue region and/or in notched members, where significant localized plastic deformation is often present. As a result, strain-controlled fatigue testing has become very common, even though the testing equipment and control are more complicated than in traditional load- or stress-controlled testing [44][6].

Strain can be measured and has been shown to be an excellent quantity for correlating with low-cycle fatigue. For example, gas turbines operate at steady stresses, but when they are started or stopped, they are subjected to a very high-stress range. The local strains can be well above the yield strain, and the stresses are more difficult to measure or estimate than the strains [44].

Strain-life also considers the order or sequence in which loads are applied. The metal exposure to repeating loads, which are close to the elastic limit, leads to a change of its softening and hardening characteristics, compared to steady loading. These result to the formation of a hysteresis loops as shown in Figure 2-8. The resulting strain is the sum of the elastic (ε_e) and a plastic (ε_p) strain as shown in equation 2-4.

$$\varepsilon_\alpha = \varepsilon_e + \varepsilon_p \qquad \textbf{2-1}$$

A power law expression for the elastic strain component, found by Basquin in 1910, links it directly to the number of cycles to failure (N_f) and the fatigue strength coefficient (σ'_f) and the fatigue strength exponent (b). These two parameters relate to material characteristics. Coffin and Manson, around 1950, found a similar expression for the plastic strain component which links directly the number of cycles to failure (N_f) with the fatigue ductility coefficient (ε_f) and the fatigue ductility exponent (c). The last two are also material characteristics

$$\varepsilon_e = \frac{\sigma_\alpha}{E} = \frac{\sigma'_f}{E} * \left(2 * N_f\right)^b \qquad 2\text{-}2$$

.

$$\varepsilon_p = \frac{\Delta\varepsilon_p}{2} = \varepsilon'_f \left(2 * N_f\right)^c \qquad 2\text{-}3$$

The total strain, as mentioned in Haslam [45][7], is obtained by substituting equations 2-2 and 2-3 in equation 2-1.

$$\varepsilon_\alpha = \varepsilon_e + \varepsilon_p = \frac{\sigma'_f}{E} * \left(2 * N_f\right)^b + \varepsilon'_f \left(2 * N_f\right)^c \qquad \textbf{2-4}$$

Where:

ε'_f	fatigue ductility coefficient	0.16 (0.35 to 1)
c	fatigue ductility exponent [41]	-0.04 to -0.7
σ'_f	fatigue strength coefficient	Values are taken from the ma
b	fatigue strength exponent	-0.05 to -0.12
E	modulus of elasticity	Depends on Temperature

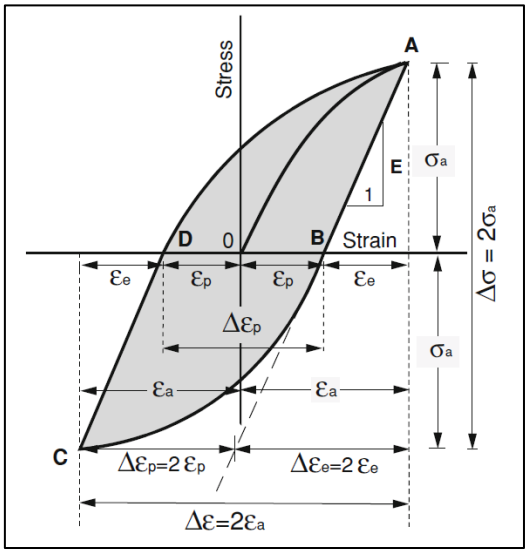

Figure 2-7: Stress-strain hysteresis loop [41]

The influence of the elastic and the plastic component on the total strain life curve is illustrated in Figure 2-8.

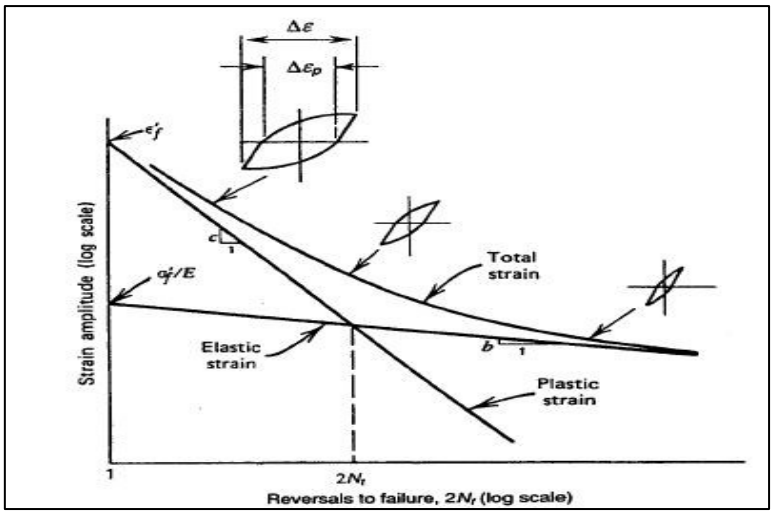

Figure 2-8: Hysteresis loops change with regard to Failure Cycles [41]

Figure 2-8 shows that the hysteresis loops are shrinking as the number of cycles to failure increases. Both elements of the fatigue equation are needed. For low cycle fatigue investigations only, the elastic term can be neglected and vice versa. The life where elastic and plastic components of strain are equal is called the “transition fatigue life,” 2N.

The equation for transition fatigue life can be derived by equating the elastic and plastic strains in equation 2-2 and 2-3 , respectively, resulting in the following equation:

$$2N_t = \left(\frac{E * \varepsilon_{f'}}{\sigma_{f'}}\right)^{\frac{1}{b-c}} \qquad \textbf{2-5}$$

For lives less than 2Nt the deformation is mainly plastic while for lives greater than 2Nt the deformation is mainly elastic. Figure 2-8 shows that even at relatively long lives significant plastic strain can be present; therefore, the strain based approach is an appropriate method to use.

To find the cycles to failure (N_f) from equation 2.4, the total strain (ε_t) has to be calculated. To achieve that, the Neuber’s approach to strain-life, where the stress and strain concentrations are related to one another, can be used. Neuber’s rule implies that the theoretical stress concentration factor (K_t) is equal with the geometric mean of the stress and strain concentration factors (K_σ) and (K_ε).

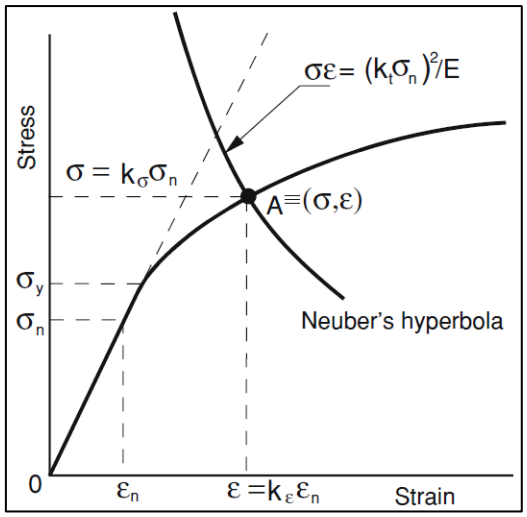

Figure 2-9: Neuber's Hyperbola [41]

The stress concentration factor is the ratio of stress (σ) near a crack, to the stress remote from the crack (σ_r). Similarly, the strain concentration factor is the ratio of strain near a crack (ε) to the strain remote from the crack (ε_r).

$$K_t = \sqrt{K_\sigma * K_\varepsilon} = \sqrt{\frac{\sigma}{\sigma_r} * \frac{\varepsilon}{\varepsilon_r}} \approx K_f \qquad \textbf{2-6}$$

$$\sigma * \varepsilon = \frac{(K_f * \sigma_r)^2}{E} = C \qquad \textbf{2-7}$$

The theoretical elastic stress concentration factor (Kt) approximately equals the notch factor (K_f). Though, the notch effects to the stress distribution are related not only to the elastic stress concentration factor, but to other factors such as i) notch radius, ii) material strength, and iii) mean and alternating stress levels. The elastic stress concentration factor (K_t) and the notch factor (K_f) are related through the notch sensitivity of the material which is estimated using equation 2-8.

$$q = \frac{K_f - 1}{K_t - 1} \qquad \textbf{2-8}$$

$$K_t = \frac{\sigma}{S} \qquad \textbf{2-9}$$

$$K_f = \frac{Fatigue\ Strentgh\ unotched}{Fatigue\ Strentgh\ with\ notch} \qquad 2\text{-}10$$

Where (σ) represents local stress at the notch, and (S) represents nominal stress. This relationship compares the theoretical stress-concentration factor, Kt, to the fatigue notch factor, Kf. In this relationship, a material that experiences no reduction in fatigue due to a notch will have a notch sensitivity factor of q = 0, while one that experiences a reduction in fatigue up to the full theoretical value will have a notch sensitivity factor of q = 1 [47].

Figure 2-10 shows the application of Neuber's rule on the stress-strain chart. If we substitute Hooke's law into equation 2-6, the Neuber's hyperbola is obtained. The hyperbola is perpendicular to the material's stress-strain curve. As mentioned in Haslam [45], the stress and strain at the top and bottom dead centre of a hysteresis loop are given at the intersection point of Neuber's hyperbola with the stress-strain curve.

It is expected that the cyclic load history will have variable amplitude and a way should be found to address that in order to estimate its effect on components life. Life estimates for such situations may be made by employing the Palmgren-Miner rule [48]along with a cycle counting procedure. Cycle counting permits an irregular time history to be broken down into individual events that may be evaluated from a constant amplitude S-N curve [49][8]. The method implementation will be further analyzed in the Methodology section.

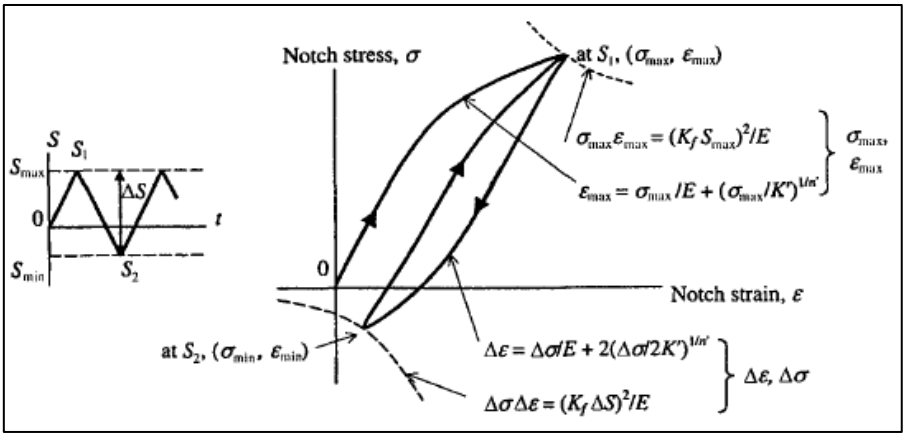

Figure 2-10: Illustration of notch stress/strain determination by Neuber's rule for constant Amplitude Loading [41]

2.2.1.3 Creep

Creep can be defined simply as a progressive deformation that takes place in the material at a constant temperature. The exposure time contributes to the phenomenon together with the whole range of temperature and loads acting during a mission.

Creep relates to the mobility of dislocations and discontinuities in the material, caused by the operating stresses and temperatures: at high temperatures, this process is emphasized, thus resulting in worse material's performances. This phenomenon is considered as a four-stage process:

a. The instantaneous elastic stage: That stage relates to a pure elastic deformation; and creates an initial strain to the metal.

b. Primary creep: This is a predominant stage and relates to low-stress levels and low temperature (i.e. room temperature);

c. Secondary creep: This stage is more constant and relates to a minimum creep rate phase, due to the balance between the competing processes of strain, hardening, and recovery.

d. Tertiary creep: At this stage, which, happens at high stress and temperature, there is an effective reduction in the cross-sectional area, together with metallurgical changes (e.g. recrystallization).

The following figure shows the generally accepted idealization of the creep processes. Creep damage can take several forms. As Viswanathan and Stringer [50][9] mentions, simple creep deformation can lead to dimensional changes that result in distortions, loss of clearance, wall thinning etc.

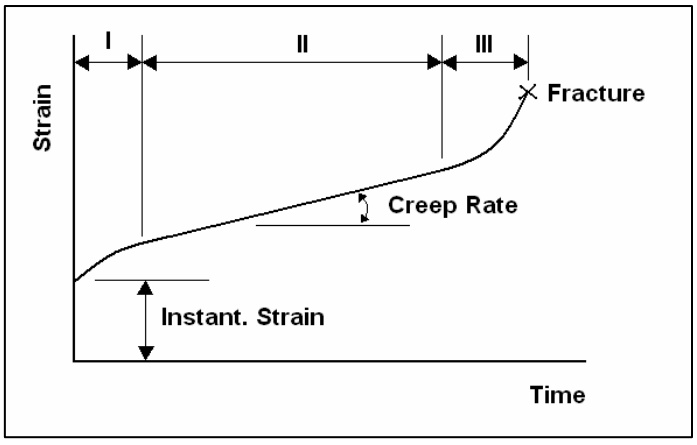

Figure 2-11: The General Creep Curve [51]

2.2.1.4 Oxidation

According to Fontana [52], the depletion of the oxide layer takes a considerable period to occur. This causes a material loss at a slower mode and results at a decreased hot gas path components exposure to stresses. The catastrophic oxidation occurs when the oxidation deviates from linear kinetics into a rapid, exothermic reaction at high temperatures. Suitable alloying and oxidation coatings reduce this phenomenon.

2.2.2 Fatigue-Creep-Oxidation effect on HPT Life

This paragraph reviews the work done regarding the three main reason for the rotating componetns remaining usel life assessment.

Charkous [53] worked on an in-house (Cranfield University) software tool named HESTIA that estimates TBO for the HPT module at the preliminary stage. HESTIA is cooperating with HECTOR and the interaction is shown in the next figure.

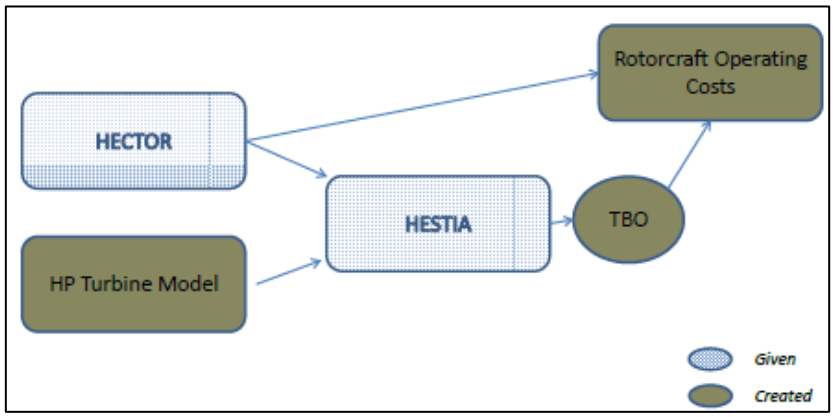

Figure 2-12: Flowchart with interconnection between the different modules [54]

The code used in HESTIA has a modular design and the life assessment relies on a physical model, which uses basic turbomachinery formulas [55] that relate to components preliminary design. This method's drawback is that the TBO definition refers to the HPT turbine life estimation instead of overall engine performance degradation, which is the main reason for a costly engine restoration. The HPT turbine is a life-limited part and once replaced, the engine enters a repair facility but there is no need for testing. The helicopter needs to perform a maintenance test flight. Apart from that, Charkous implemented his approach in two cases on an SA-330 and a BO-105 and, produced interesting results regarding the reasons that lead to a component replacement. The research showed that the turbine blade damage due to creep is

experienced only in in long-range missions. Rotorcraft missions are mainly short or medium range flights hence, it is relatively rare to see blade damage due to creep. Regarding oxidation, the effect is minimal due to the low operating temperatures. In this case, the main destructive phenomenon for the turbine is low cycle fatigue.

Elter [56] developed a code in Matlab based on the code initially used in HESTIA and reinforced it with the capability to assess the blade and disc cooling. In addition, the code allows for a probability analysis in which a prediction of life expectancy for a few engines has been pursued. This code used the strain method approach coupled with thermal fatigue where the strain relates to the thermal stresses amplitudes (ΔT) and the linear coefficient of thermal expansion.

$$\varepsilon_{max} = \Delta T * \alpha \qquad \textbf{2-11}$$

where a: linear coefficient of thermal expansion

This method assumes that the component is in the plastic region and performs a typical airliner flight with the basic segments (Taxi, take–off, climb, cruise, and descent, reverse thrust and idle). Elter's work on high-pressure turbine life prediction revealed that creep becomes important in long haul flights while low cycle fatigue is the dominant reason for the component failure in short haul flights with a range similar to the one of the rotorcraft.

To that end, Hanumanthan's work on aircraft HPT life estimation showed the low cycle fatigue-creep-oxidation effect on both long haul and short-haul flights for the areas on the HPT blade and the disc. The results showed that low cycle fatigue is the dominant reason both in long haul (> 4 hours) and short-haul flights (<4 hours). Creep contribution to life consumption increases with the flight duration and its limiting zone is the leading and trailing edge mid span. Oxidation is the least contributing reason and the limiting region is the leading edge for the blade and the disc rim region. Regarding rotorcrafts, although the relatively low flying altitude makes the ceramic-coated blades sensitive to airborne contaminants.

2.2.3 Engine Cycle Counting

Turbine engine inspection and component replacement intervals have been addresses by regulatory authorities like EASA [57] and FAA [58] for many years now. These intervals are based not only on flight hours but also on engine cycles.

While a “flight hour” is simply defined as the elapsed time from take-off to landing, engine cycles are a bit more complicated to establish and the method depends on the engine OEM.

The earlier days the definition of one complete cycle contained the following three events:

- An engine start,
- A take-off and landing and
- A shutdown.

In that sense, to count a cycle all these three events should take place. For example, if there is only an engine start and a shutdown no cycle must be accounted for. In addition, any number of take-offs and landings within only one engine start and one engine shutdown had not been considered, therefore, only one cycle was counted.

That relatively simple cycle counts however changed, and latest technology engines bear a cycle counter device that helps flight engineers monitor the engine's cycles.

The engine cycle, in general, relates to the stretching and relaxing of rotating components imposed by centrifugal forces and thermodynamic stresses. An engine logbook, which will include engine flight hours and engine cycles since new and since major inspections, is mandatory.

Any machinery has a finite life expectancy due to normal wear and tear. Historically, the number of flight hours had been the most common way used, from Engine OEM’s, to measure the engine performance restoration. The engineers determine a specific interval of flight hours, which they assume includes a safe margin of how long the specific engine type, will be able to operate within established performance specifications, based on certain assumptions and calculations.

In parallel, based on research spawned by major airplane accidents, it was discovered that the cycles contribute to what is termed LCF (Low Cycle Fatigue). Therefore, the maximum number of cycles must be limited to a point when LCF failure can be expected minus a predetermined safety margin. This service life limit is based on

engines that are being operated within approved operating limits and being maintained in accordance with published instructions.

Military engines like General Electric T700 series, for example, use 2 LCF counters that monitor major cycles and part cycles. The difference between the major and the part cycles lies on the gas generator Ng %. In general, the LCF1 counter counts the times that the engines Ng cycled through a predetermined width, for example, 95 to 40 Ng %. LCF2 counts a cycle when the engine cycled through a smaller width like 70-80 % Ng.

In general, engine OEM's are using different cycle counting methods and this raises an issue regarding the engine's maintenance. The maintenance complexity increases and poses a burden especially on mechanics that must maintain a fleet comprised of different helicopter types. It appears that a universal approach is needed that will consider the contemporary theoretical methods in cycle counting combined with the different flight profile used from rotorcrafts.

While OEM's uses practical methods to estimate the cycles ASTM standard E1049-85 [58] provided a very thorough review of the cycle counting methods used in research. The review separated the methods based on the use of the mean value of each cycle into: i) one or ii) two parameters method recognizing the latter as superior. The standard compares Rainflow to similar methods like the: i) range pair counting and, ii) repeated histories counting and finds it superior considering that the other two can estimate cycles in very simple time history scenarios. The rainflow method is very popular in turbine components life estimation due to its capability to work on many different time history-loading scenarios (force, stress, strain, torque, acceleration etc.).

2.2.4 Practical Methods for Component Life Prediction

The component life prediction relates strongly to the gas turbine performance degradation (addressed in paragraph 2.1.1), which occur prior to failure. The component failure due to degradation is the result of an underlying mechanism that acts and evolves over time. The accurate prediction of the components life requires identifying and understanding the potential failure mechanisms present in a gas turbine. This need has spawned extensive research in both the academic and private sector due to its profound effect on flight safety and Life Cycle Cost.

Numerous techniques addressed the issue with different points of view. Many of the techniques approach the issue either by developing models based on prior experience or knowledge or on failure data parsed from gas turbine operators. Another approach is to create a severity factor based on failure data parsed form different flight patterns. To estimate the severity factor, a set of failure data that relate to a flight pattern used as a reference compares to another set of failure data, which relates to flights with other profiles. The following paragraphs present both approaches.

2.2.4.1 Model Based Methods for Remaining Useful Life Assessment

Regarding the model-based methods classification the following criteria may be used:

a. Distinct characteristics of the different models
b. Model input type (e.g. type of data) representing the system in the study
c. Associated degradation mechanism,
d. Operating environment, and finally
e. Usage conditions

To that end, Bagul et al. [25] proposed the classification presented in Figure 2-13: Life prediction approaches and techniques. Figure 2-13, while Thurston [59] proposed a hierarchy of prognostic methods that have been categorized according to increasing cost and accuracy. The proposed methods are: i) experience-based prognostics, ii) evolutionary methods and iii) model-based prognostics. Tinga [60] reviewed these methods and concluded that the most sophisticated prognostic approach is the physical model-based approach.

Regarding the data driven methods, a Pratt and Whitney's engineer [62] published a paper, at 1981, for a cost prediction method able to forecast such factors as engine's shop visit rates, maintenance material cost, and spare engine and module requirements. The system fflexibility permitted tailoring to an individual airline's operating procedures, route structure, and maintenance philosophy. The component life prediction used Weibull analysis with data parsed from operator's failure data.

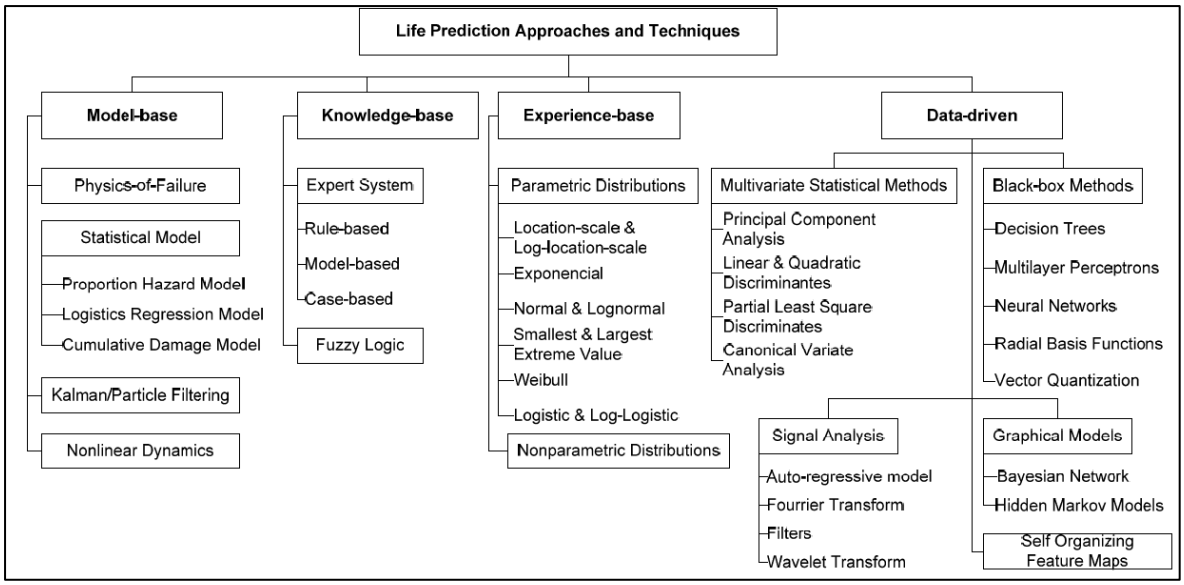

Figure 2-13: Life prediction approaches and techniques. [59]

2.2.4.2 Severity Factor Method Review

It was in 1980 when Stabrylla [63] published a paper describing the results of a study conducted to address the issue of unacceptable durability of fighter aircraft engines that have resulted in reduced system operating readiness and high operation and support costs.

Stabrylla evaluated the differences between actual flight usage and engine design usage and examined how these differences affect the relative durability/life of engine turbine components. Using existing analytical methods developed and validated for the CF6-50 commercial engine and the J79 military engine, the study evaluated the effects of engine application and mission content on the relative cyclic and steady-state durability of these components. He used OPSEV, software developed by General Electric to derive predictions for possible engine removals which have been compared to actual component removal data taken from a large flight data pool comprised of 3.5 million hours for CF6-50 engines and 25 million flight hours for the J79 engine. More specifically the large database provided data for Unscheduled Engine Removals (UER) as well as Total Shop Visits (TSV). The comparison showed that magnitude and trend predictions were in good agreement with experience. In addition to the information from real flights, the other source of data was from hours spent at the Accelerated Mission Test (AMT).

The severity factor according to Stabrylla is based on the summation of the damage rate fractions due to steady and cyclic loads. He proposed the estimation of the damages induced in a reference flight and an actual flight. Mathematically this is expressed by the following equations:

$$(\boldsymbol{\lambda_t})_r = (\boldsymbol{\lambda_c})_r + (\boldsymbol{\lambda_s})_r \quad \textbf{(2-12)}$$

$$(\boldsymbol{\lambda_t})_n = (\boldsymbol{\lambda_c})_n + (\boldsymbol{\lambda_s})_n \quad \textbf{(2-13)}$$

λ_τ Total damage fraction

λ_c Cyclic damage fraction

λ_s Steady-state damage fraction

$(\lambda_t)_r$ Total damage for the reference mission

$(\lambda_t)_n$ Total damage for the new mission

He then normalized the equation 2-3 by dividing both sides by $(\lambda_t)_r$

$$(\mathbf{S_t})_r = (\mathbf{S_c})_r + (\mathbf{S_s})_r \quad \textbf{(2-14)}$$

$$(\mathbf{S_t})_n = (\mathbf{S_c})_n + (\mathbf{S_s})_n \quad \textbf{(2-15)}$$

The cyclic part of the severity relates to the LCF and the steady part to creep and oxidation. The software OPSEV that Stabrylla used derived load and stress data based on basic failure equations and experience. The analysis used logged data from about 3.5 million flight hours. These data relate to full or “derate” thrust. The “derate” (reduced) thrust is the thrust used when the aircraft flies at reduced Take-Off Gross Weight (TOGW). This power setting may be used in both takeoffs and climb to extend engine life and reduce maintenance cost [64].

The study used three different cases to investigate the effect of mission profile on engine removals:

a. GE CF6-50 Engine Commercial Versus Military Transport Usage

The reference mission used in every case in the study was customized accordingly. For the CF6-50 engine, the reference mission of 4.4 hours’ duration with an average take-off thrust derate of 7.5 percent was used while the range of flight duration varied

from 2.5 hours to over 6 hours for most of the available data. The result showed that military transport aircraft engine usage is more severe than commercial aircraft usage. In addition, the major contributor to increased severity is the cyclic content.

b. GE F101 Engine - Bomber Vs Fighter Usage. For the GE F101 engine, the mission length was 4.43 hours in duration, with a mix of 90 % normal-day and 10 % hot-day usage. The results showed that severity is not only affected by the terrain differences but from the pilot's attitude in flying.

c. An F-14 with two F101 engine.

The results showed that mission content, not sortie length, is the major factor in severity. In addition, the flight carrier landing practice (FCLP) mission is almost as severe as the combat manoeuvres, thus practice flights can use up a significant amount of engine life. The steady-state severities of all the fighter missions are lower than the steady-state severity of the bomber missions, thus the increase in total severity is due to increased cyclic severity. The ratios of cyclic-to-steady-state severities for all the military usages studies are significantly greater than that of the commercial usages.

Overall, the results showed the following with regard to the severity factor:

a. It is very sensitive to the mission profiles.

b. It is misleading to simplify the procedure by averaging the results.

c. Every engine component is affected differently by mission usages.

d. It is important to consider the ratio of cyclic vs steady in the severity factor. The cumulative nature of the index may be misleading.

e. The military mission's usage was dominated by cyclic severity; the commercial was dominated by steady-state severity.

f. The results are macroscopic, and they indicate trends that identify the complex interactions of engines cycles, missions and relative damage calculation.

g. The actual flight usage of the engines is significantly more severe than the original design mission mix. The increase in severity was attributed to the higher cyclic content of the usage during tactical legs of the missions.

The study concluded that the methods used were macroscopic; they indicated trends in cause and effect that identify the complex interactions of engine cycles, missions, and relative damage accumulation. The mission's severity factor range showed an exceedingly wide range of severities above and below the unity value (0.480 to 3.509).

Academic research at Cranfield University adopted the Strabylla's severity factor approach but instead of using failure data from real flights, based the research on flight run on simulators software. Hanumanthan [18] work results show that the severity factor sensitivity is affected apart from the mission profile and the crew attitude, by operating and technological factors. The operating factors are OAT, Altitude, Mach number and the technological, related to the HPT module, are cooling effectiveness and thermal barrier coatings. In general, the severity factor for short flight segments is high, compared to the longer flights and apart from the flight segment power demands, the environmental conditions, OAT specifically, contribute significantly to engine degradation.

To this end, Pascovici [54] used a lifing module in his work that showed the cyclic and steady-state contribution to short, medium and long-range flights. It is evident that the cyclic vs steady ratios vary with the mission length and a detailed study could prove useful to understand the contribution to the engine degradation.

In addition to Hanumanthan's, Nalianda's [65] work on severity estimation using a model-based approach has shown that oxidation estimated life is the one affecting less the life limit on both the disc and blade of the HPT. The results of their work revealed that creep is the limiting factor in the blade life while LCF has a greater effect on the disc life.

Zuazo [66] reviewed three different life estimation models and provided the pros and cons of each method for each failure mode. The models utilized for the comparison were the following:

a. TMF model (Neu-Sehitoglu formulation) conducted by Lejona [67] using FEA
b. A strain-based model that estimated LCF in the plasticity region conducted by Maqueda [68]
c. A stress-based model that estimated LCF in the elastic region conducted by the Zuazo [66].

The important outcome of this comparison was that their severity estimates were very close in the region of 5%-20% derate. Nowadays the manufacturing companies follow the severity factor concept and produce charts that show the relation between the

severity factor and the power derate used by the pilots during all flight segments and the related restoration rates. A sample of a chart is shown in Figure 2-14.

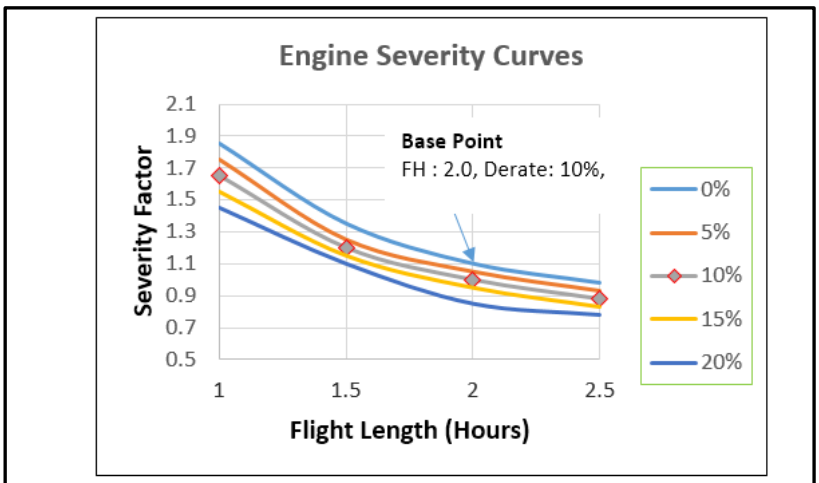

Engine Severity Factor → Restoration Rates -$/FH

FL (Hr)		1	1.5	2	2.5	1	1.5	2	2.5
Derate	0%	1.85	1.35	1.1	0.98	148	108	88	78.4
	5%	1.75	1.25	1.05	0.93	140	100	84	74
	10%	1.65	1.2	1	0.88	132	98	80	70.4
	15%	1.55	1.15	0.95	0.83	124	92	78	66.4
	20%	1.45	1.1	0.85	0.78	110	88	68	62.4

Figure 2-14: Engine Severity Curves vs Restoration Costs [17]

Ackert [17] in his article provided examples of how the severity factor affects the engine recurring costs at overhaul and provided examples of two different approaches for the engine overhaul and LLP replacement.

Overall, the literature review regarding the severity factor showed that:

a. The reference flight profile and the operating parameters used in the parametric study have a great impact on the estimated severities.

b. The accuracy of the estimated severity factor is sensitive to the physical model used for the components under consideration.

c. The payload for each mission or the OAT and the altitude can be used to investigate the effect in component lifing. All of them can have an effect on the load and stress contribution in each different flight profile [68].

d. The “derate” concept used for the turbofan engines is not an option for the turboshaft counterparts.

e. The design space of the operating environment with regard to: i) OAT, payload, ii) climb rates, and iii) derate between the reference and the actual or simulated flights should be selected very carefully. Any attempt to simplify the procedure can result in misleading results.

2.3 Cost Estimation

This section starts with some background information about the life cycle cost of the helicopter and the powerplant used to support it. The approach to value the costs around a helicopter and its powerplant is complex and a clear understanding of the parameters that are associated with the life cycle from design to disposal is of great importance. A reference is made to the Life Cycle Concept and the most used methods to predict the associated costs.

The next section refers to the direct operating costs that the potential buyer (operator, lessor, government and agency) needs to consider after the helicopter and engine considering the above. An effort is made to distinguish the parameters that affect the variable and fixed costs. A reference is made to the different approaches of the military and civil operators. Finally, with regard to the engine maintenance costs estimation during the life cycle of the engine, a reference is made to both the traditional and the latest methods proposed by the engine manufacturers.

2.3.1 Life Cycle Cost Analysis

Life Cycle Cost analysis is a really complex issue that has been initially identified in 1965 when a report was prepared by the logistics management institute, Washington Dc. [69]. Since then, the complexities of systems production, the involvement of marketing and the need for after-sales support of the product made it almost mandatory for the industry to base their thinking about costs in a life cycle concept. In 1989, Dhillon presented a list of over 500 publications on various aspects of life cycle costing [70].

The LCC concept, as Figure 2-15 shows, involves many disciplines that contribute to the different phases of a product life from conception to retirement. Apart from economics, the product design, its quality, reliability, availability, maintainability and logistics support are also factors under consideration.

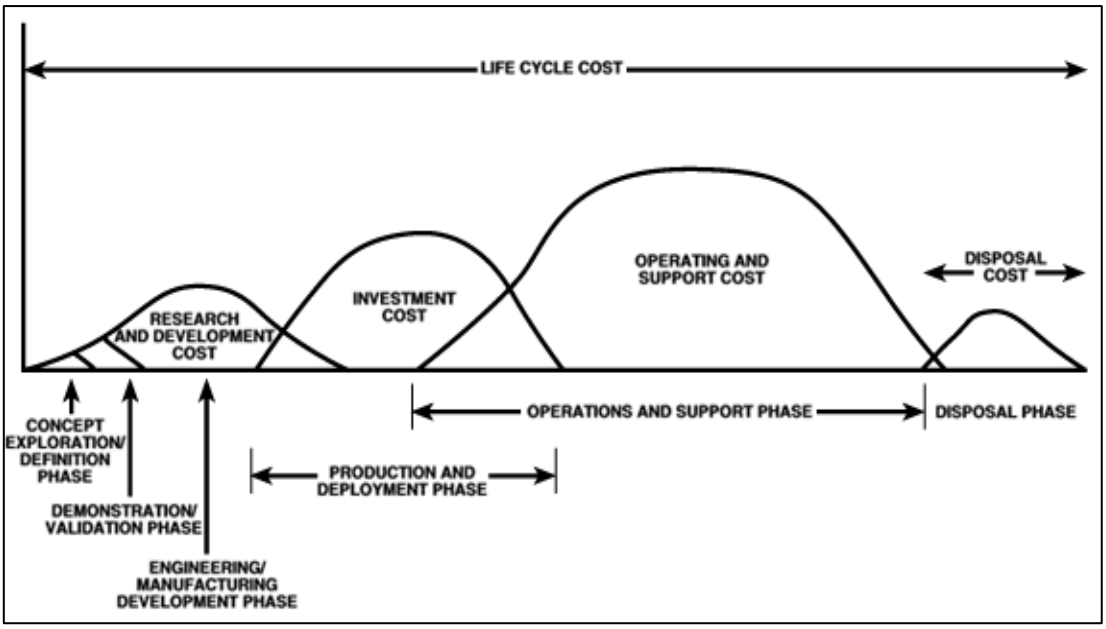

Figure 2-15: Life Cycle Cost Chart [71]

The manufacturers, agencies, operators, maintainers and all the people involved in the life cycle of a product apparently have a different point of view to assess the costs involved in the product life. Life cycle cost estimation is attempted from the early design and it takes place continuously with the accuracy of the model refined more as the aircraft is in operation and the first cost data become available. Zhao [72] provides a comprehensive review for the different cost LCC estimation techniques and concluded that there are two main estimates i) the first-sight estimate early on in the design process, and ii) a detailed estimate that is associated with precision costing. One major user of these 2 concepts is NASA [73]. Figure 2-16 shows the methods used for cost estimation by phase into the life cycle.

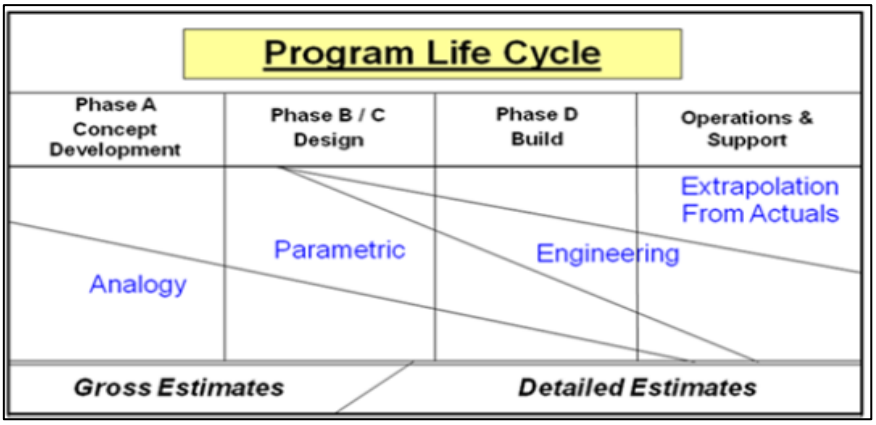

Figure 2-16: Use of Cost Estimating methodologies by Phase [73]

To this end, the US Department of Energy [74] provided a classification for the accuracy that different estimate classification and the applicable methodologies. The classification is presented in Figure 2-17.

Literature review shows that there are different standardized methods available to estimate the costs of owning and operating an aircraft or rotorcraft. Roskam [75] and Jenkinson [2] proposed methods to estimate LCC costs for aircraft while the Helicopter Association International (HAI) provided a guide for rotorcraft cost estimation [5].

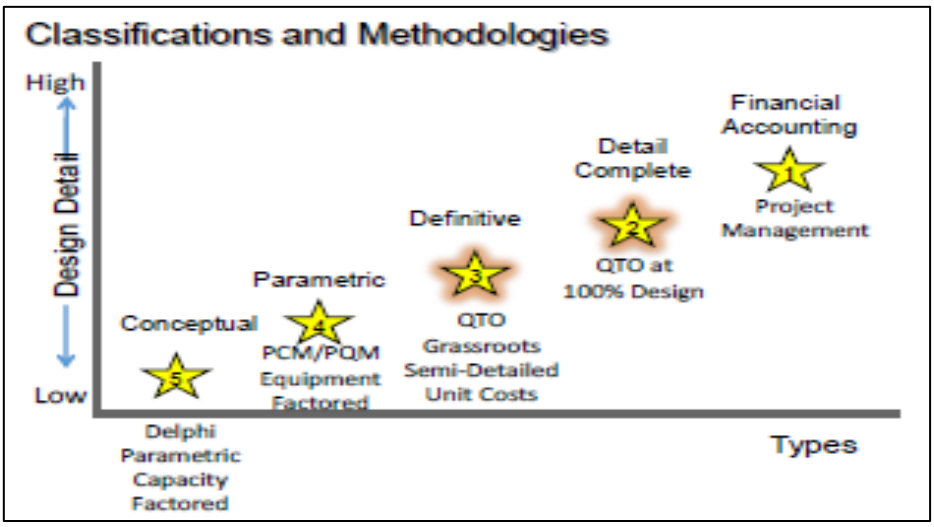

Figure 2-17: LCC Methods and Classification [74]

Roskam's developed a cost model based on methods presented by NASA and other associations during the 60's and 70's. Those methods were adapted and generalized to be used for any type of commercial planes. The developed cost estimation relationships (CER) were built by using used regression analysis and addressed all the possible type of costs since the design phase. He categorized the costs into the following categories:

- Research, development, test and evaluation cost
- Acquisition cost
- Operating cost
- Disposal cost.

  Jenkinson [2] offered a simplified model of Roskam, considering the trade-off between the different cost methods available. Jenkinson referred only to operating costs and used two categories:

- Indirect Operating costs (IOC): The costs not directly attributable to a particular aircraft type or the flying costs of a particular operation.
- Direct Operating costs (DOC): The costs associated with flying and direct maintenance. These costs are further categorized into 3 subcategories.
- Standing Charges
- Flight costs
- Maintenance costs: These are worth mentioning as they are linked to the HAI guide that is referred in the next paragraph that is worth mentioning

Helicopter Association International (HAI) [5] proposed a guide for the presentation of civil and commercial rotorcraft operating cost estimates. The guide was compiled to help the new and more mature operators in addition to airframe and engine manufacturers to realize the parameters affecting the operating costs. The surveys that the committee conducted with rotorcraft operators' help, have led to the categories shown in Table 2-1.

In addition, the committee addressed the issue of cost characteristics which appears to follow two distinct approaches that help operators understand costs. One approach is the categorization according to the behaviour of costs and the other to the assignments of costs.

The behaviour of costs:

This includes fixed and variable costs:

- Fixed costs: These costs remain constant as the level of activity changes. In essence, it refers to the costs that the operator will incur whether the helicopter flies 1 hour or 500 hours.
- Variable costs: These costs increase as the level of activity increases. To make it simpler if a helicopter does not fly, then the total cost of a variable cost will be zero.

Assignment of costs:

This approach includes direct and indirect costs:

- Direct Cost: This cost can be traced directly to an activity, product, or department
- Indirect Cost: This cost requires some method of assigning it to an activity, product, or department.

Roskam , Jenkinson and HAI mentioned above have influenced the work of other researchers like Pascovici [54], Charkous [53], Nalianda [65] and Harris [24][10]. Pascovici [54] proposed an economic model encompassing three modules that is i) a lifing module, ii) an economic module and iii) a risk module. His economic model included standing charges, flight costs and maintenance costs.

	Main Categories	Subcategories	Type	
	A. Fuel & Lubricants	Fuel & Lubricants	Variable	$/FH
	B. Maintenance	1. Life-Limited Parts	Variable	$/FH
		2. Major Overhauls (airframe and engine)	Variable	$/FH
		3. Periodic Inspections	Variable	$/FH
		4. On-Condition Components	Variable	$/FH
		5. SB and AD	Fixed	$/Yr
		6. Unscheduled Maintenance	Variable	$/FH
		7. Optional Equipment	Fixed	$/Yr
		8. Sources of Maintenance Cost Estimates		
	C. Insurance	1. Hull	Fixed	$/Yr
		2. Aviation General Liability		
		3. Workers' Compensation		
	D. Personnel	1. Flight Crew	Fixed	$/Yr
		2. Mechanics and Technicians		
		3. Office Staff		
	E. Training	4. Management Salaries		
	F. Depreciation	5. Benefits		
	G. Taxes		Fixed	$/Yr
	H. Finance		Fixed	$/Yr
	I. Overhead	1. Rental or Lease Fees	Fixed	$/Yr
		2. Utilities		

Table 2-1: Costs Classification per HAI

For the maintenance cost, he used a combination of Roskam and Jenkinson CER's and the module included a lifing module that provided data for the rotor blades and the HPT disc. The outcomes of the economic module were: i) the direct operating cost, ii) the engine maintenance cost and iii) the net present cost.

Charkous [53] worked on a model that estimated Direct Operating Costs (DOC), Daily Operations Costs, Mission-specific Costs and Fixed Costs using Harris equations in the context of HAI [5] categories.

Nalianda [65] presented a model which is shown in Figure 2-18 that covers operating costs as described by Jenkinson and is influenced by the concept of a cost index. The 'cost index' method is essentially a trade-off between two key objectives. The fuel consumed in a mission and the time of the mission. It is a method proposed by major airline manufacturers [76], [77].

Harris [7] made an effort to address helicopter variable and fixed costs and used HAI guide as a backbone. Following Roskam's methodology, he used commercial sources to get data that helped him to produce CER's so as to estimate helicopters operating costs.

To complement his work, Harris with Scully [78] wrote an article named "Rotorcrafts cost too much" in which he claimed "The rotorcraft industry is pricing itself right out of the commercial transportation marketplace. This is illustrated by helicopter prices that have inflated significantly faster than consumer product prices and by helicopter productivity per dollar that decreases with the increased purchase price. Specifically, inflation in helicopter purchase price has significantly exceeded the U. S. consumer price index since 1980".

Scott [79] recently published his work in which he coupled a historical study with engineering analysis and provided a CER that relates the procurement cost to the engine's size, complexity, and level of technology.

Historical turboshaft engine prices were collected from multiple government-maintained cost databases. The data included the year of procurement, procurement quantity, and average unit price about the transaction year dollar value. A single data set for analysis was created. The engine characteristics needed for the explanatory

variables were collected from a variety of sources including maintenance manuals as well as public resources [79].

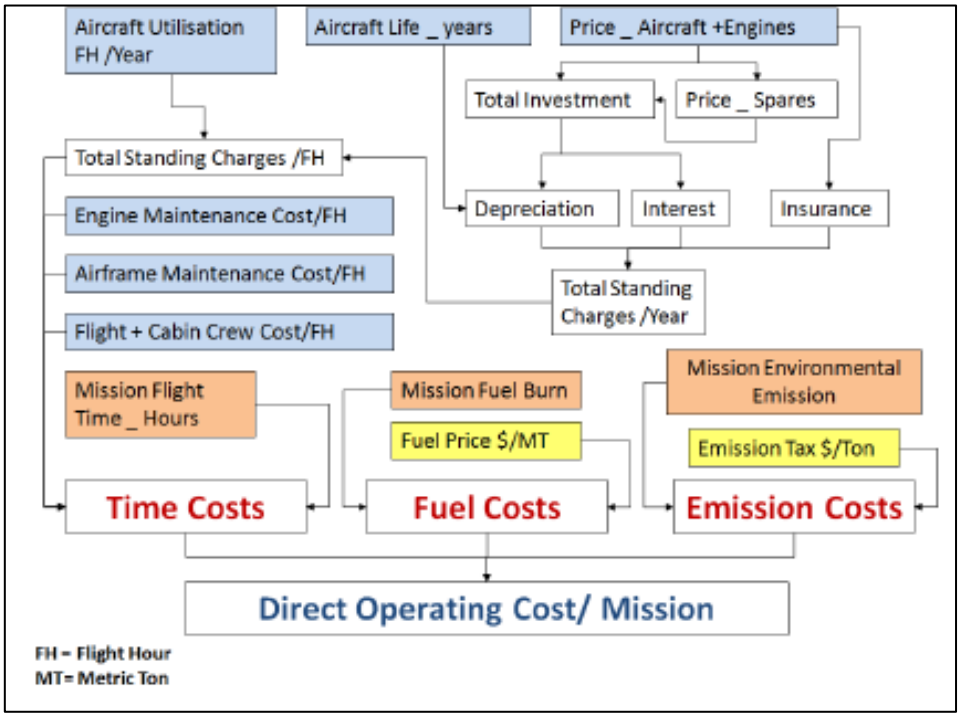

Figure 2-18: Costs flow in an operating model [65].

A formula was developed which showed that the maximum sea-level-rated horsepower is the best parameter to represent the cost-effectiveness of engine size. Apart from the size, the analysis also showed specific power and average pressure ratio, also drive procurement costs. This approach shows that a more powerful engine is substantially more expensive if the extra power is obtained by increasing the engine core's temperature and pressure. Historical trends in these design parameters reinforce the fact that power and efficiency requirements drive potentially costly engine design choices. The drawback is that in order to use the developed formula you need to have access to the database used at that time.

Pratt and Whitney published a research paper [62] with regard to maintenance policies and mission conditions describing an approach that uses Weibull analysis coupled with an in-house software. The software used Weibull frequency distributions to simulate the engine operation at the component level. The distributions have been adjusted for airline maintenance practices and mission conditions. When an accurate assessment of future engine shop visits has been determined, accurate projections of

logistics elements could be obtained. The projections included spare engines and modules, initial spare part inventory provisioning, overhaul shop facilities and engine tooling requirements. The Pratt and Whitney approach has been verified from data taken from operators that the company supports through the PBH contracts.

Academic researcher's, on the other hand, attempted to create different models using data from public sources and responses at questionnaires sent to operators. Seemann [80] proposed a parametric cost estimating the model by using available historic engine maintenance data. The proposed method was based on an alternative way of accounting for the Direct Maintenance Costs (DMC) at shop visits and on a model comprised of two sub-models namely i) CER and ii) effect module. His base of thinking was that the main reasons for engine removal are: i) EGT margin deterioration, ii) LLP expiration cycles and iii) unscheduled inductions due to FOD. Instead of using the material and labour cost at each shop visit he attributed the costs to restoration and LLP replacement cost. Using the data, he obtained through questionnaires he created CER's that estimated the shop visit interval and the shop visit cost. The CER module was complimented with an effect module that considered four factors and the EFC: EFH ratio. The four factors were: i) time and material, ii) the three-spool configuration iii) the severity and iv) the environmental factor. The model was verified for its plausibility by comparing the model results with available cost and interval estimations from Aero Strategy forecasts.

It is the author's view that Seemann's [80] approach is very flexible and can be very well adapted for a rotorcraft model. Special attention should be given to the severity factor estimation because the rotorcraft's missions are far more diverse than the aeroplanes and this factor can have the considerable effect on the final estimation.

2.3.2 Direct Operating Costs (DOC) Estimation

Jenkinson [2] and HAI [5] include Fuel & Oil and maintenance costs into the DOC estimation. The next three paragraphs refer to these costs and to their variation with time. Paragraph 2.3.2.4 refers to methods used to decrease the maintenance costs

2.3.2.1 Fuel Costs

The operating costs are highly influenced by the specific mission the helicopters perform. HAI recognized 28 different roles that a helicopter can play. The mission of

the helicopter dictates the manoeuvres performed and the crew choice between higher flight endurance vs higher range. Therefore, two approaches can be recognized as explained in the next paragraphs.

High endurance approach

The civil operator where the revenue is of great importance chooses to fly a helicopter at slightly slower speed than his military counterpart does. The importance of this case is to keep the helicopter airborne as much as possible. To achieve that, the fuel flow should be minimized (see the concave upward green line). Since the fuel flow is proportional to the power required the fuel flow will be minimized at the point where the power required is a minimum (The lower red dot, in Figure 2-19, where speed is 70 knots). This type of operations, in general, corresponds to flight mission like SAR and EMS.

High range approach

To maximize the range, the maximum distance for each pound of fuel burned is needed. The maximum range airspeed occurs where a line from the origin is tangent to the power required curve (concave downwards black line). This also corresponds to the minimum point of the thrust required curve (red dot, where speed is 98 knots). Harris [3] provides Figure 2-19 as a representative of the concept.

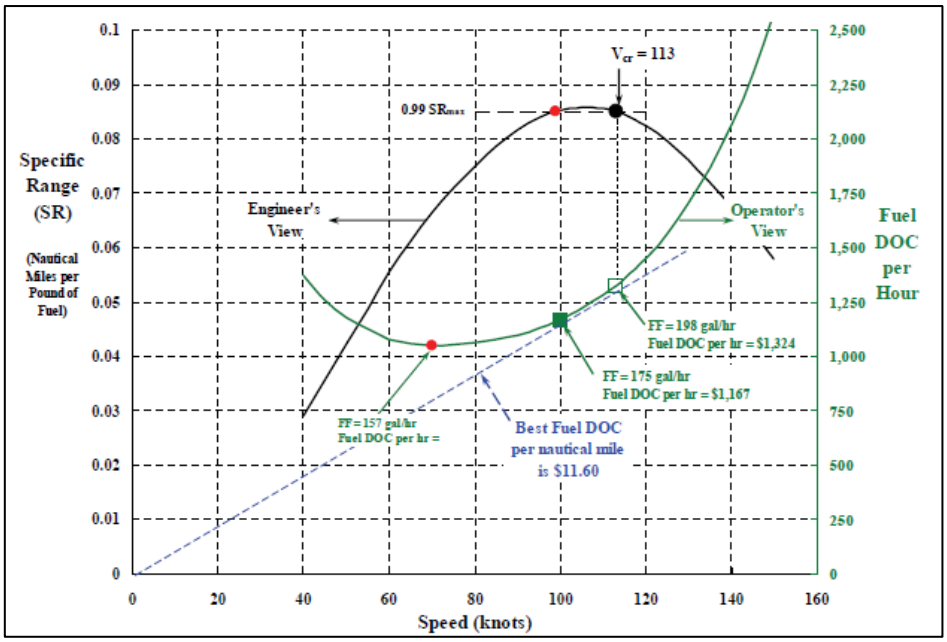

Figure 2-19: Speed vs Fuel Consumption Chart [3]

Marinai [81] mentions that while the engine costs for an aeroplane account for 26% of the DOC the fuel can be as much as 34% of engine related DOC.

2.3.2.2 Maintenance costs

Maintenance costs, in general, follow the same concept of the LCC estimation methods. A general classification is to estimate the costs of labour, spares, consumables, and repairs. The labour is counted in $/Hour or Euro/hr and the other metric used is MMH/FH.

In the early years, the accounting system based on the aircraft logistics and the accounting tree in the US were using [82] financial and economic reports to get the required data. At the early times, the costs were measured at $/ statute mile. Later on, the value was converted to $/FH. To this end, Harris [7] mentions that military operators forced the industry to provide a metric of MMH/FH needed for a helicopter maintenance. While this concept sounds very logical it is very difficult to implement because the MMH/FH metric is affected by various factors.

A helicopter's engine maintenance follows a system of 3 levels of maintenance and the MMH in every level is different. Maintenance activities are different at each level as shown in Table 2-2.

Ackert' article [17] provides a rough estimate of the costs involved in the maintenance of a turbofan engine whereas data for turboshaft engines are not available in the public domain. His article, illustrates two method, which show the cost trade off when adopting workshop management optimized for: i) Minimum number of shop visits and ii) Maximum usage of LLP hardware.

Although the activities mentioned in Table 2-2 make it easier to estimate the costs involved there are other factors that make things more complicated. The helicopter configuration that is closely related to the missions and the operating environment, the operator maintenance capabilities and the operator's fleet data also contribute to the cost estimation process.

As Harris [7] mentions: "Frankly, it is hard for me to imagine that all 622 operators (in 2009) have the same bookkeeping of operating cost line items". Airbus statistics for civil operators found in Hoffmann at al. article [21] show that 85% of the operators fleet has less than 4 helicopters. HAI provides approximately the same data for the Helicopter per fleet per operator.

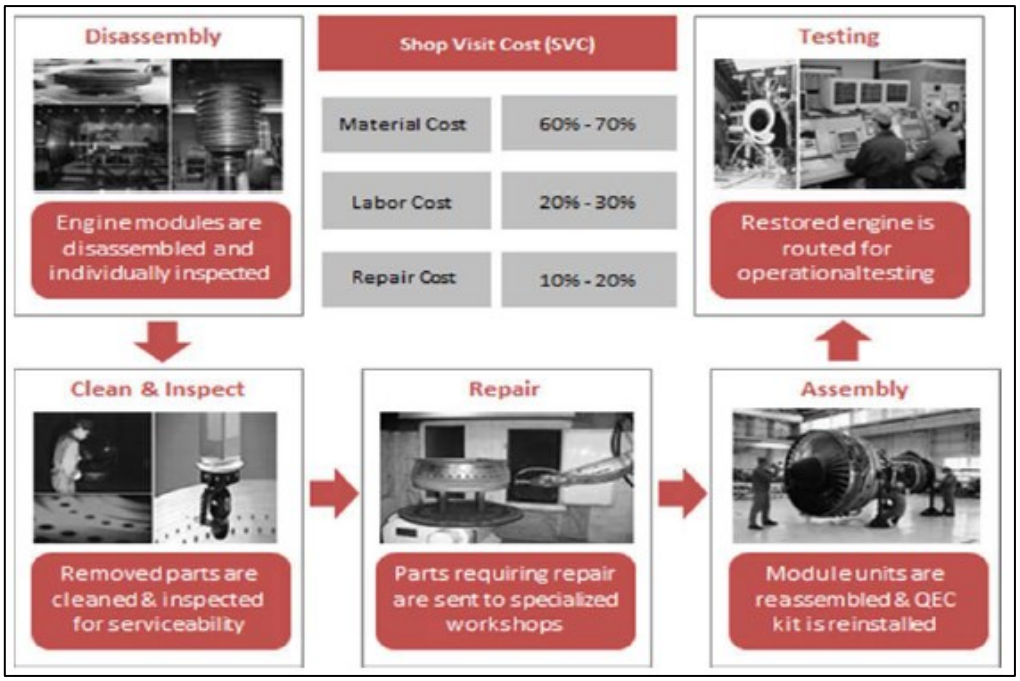

Figure 2-20: Maintenance Cost Analysis [17]

	1st level Operator Flight line	2nd level Repair station	3rd level Overhaul facilities
Maintenance Actions	Engine visual check	Periodic Inspection	Overhaul activities
	Health Check (Performance chart)	Unscheduled maintenance-minor repairs	SB implementation
	Periodic inspection	Repair	Repairs
	Engine Washing	SB implementation	
		Module Replacement	
		Flight Test	Test Bench

Table 2-2: Actions per Level of Maintenance

The engine restoration is the major contributor to the maintenance cost during its life cycle. MRO companies and OEM repair facilities may use a different approach to value the engine overhaul. In case of military fleets, a contract may be used for the induction of a number of engines in a number of years but in case of civil aviation two approaches are used nowadays.

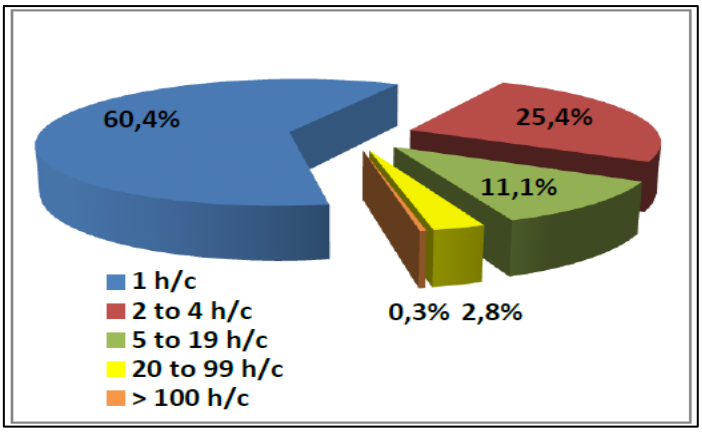

Figure 2-21: Airbus Helicopters Fleet Distribution – Helicopter No per Operator [21]

One approach assumes an induction cost, which relates to the engine configuration plus an extra cost for the extra spares used in every case. Another approach is a maintenance contract that uses the concept of Price by the Hour (PBH).

In the first approach, the company charges an induction cost for the administration fees and the average MMH derived from their experience. The company sets a reference standard that the engine performance should comply with. The engine status is checked and the work orders are produced. The final restoration value will include the spares used in case an LLP part is replaced and any additional work for any SB implementation. Once restored a new TBO may assign to the engine which returns to the customer with a warranty for some years ahead.

The second approach takes maintenance stress out of the operator's mind. The manufacturer sets a cost per FH charge to the operator and the engines maintenance is the responsibility of the manufacturer. Pratt and Whitney, Honeywell, Augusta Westland and MD helicopters are some of the companies that offer a 'Price by the Hour' contract. The services names vary in every contract and the payment options may be by the FH or monthly payments. Every company is offering different scenarios but in general, these contracts cover scheduled and unscheduled maintenance labour hours, SB implementation overhaul costs but they do not include the costs for LLP parts which is a major cost driver of maintenance costs.

2.3.2.3 Cost change with reference to time

Harris [7] made a reference to the costs changes for the S-61 helicopter within a period of 45 years. This approach is indicative of how the fuel price volatility affects the operating costs. The issue is addressed as an example to indicate that when designing for a helicopter that will be in the market for the next 25 years we need to think ahead and to consider the future trends and incorporate them into the design phase.

He compared the costs for an S-61 helicopter in 1967 and in 2011. The results are presented in Table 2-3 below.

DOC ($/85 Statute Mile trip)	S-61 in 1967	S-61 in 2011	% difference for Flying Operation
DOC total	359,73	3443,57	
Flying operation	116,57	1438,53	
Flight crew	71,87	315,77	From 62% to 22%
Fuel and oil	19,06	887,47	From 16.4% to 1.6%
Insurance	25,64	235,29	From 22% to 16.36%
Maintenance	117,62	1482,18	
Depreciation (including spares)	125,53	522,86	

Table 2-3: S-61 Helicopter Costs Comparison between 1967 and 2001 [7].

The table shows that the fuel price has changed dramatically affecting the operating costs accordingly. There are 2 points to address here; the engineering effort to improve turbine engine technology and attention to helicopter parasitic drag has improved fuel efficiency from a coefficient of 0.036 to 0.023. This is a 37% improvement. On the other hand, when the price of a gallon of Jet A fuel increases by a factor of two or three, all the progress that engineers can make in helicopter fuel efficiency (and thus lower fuel DOC) in a decade or two is eliminated.

This makes fuel efficiency even more important but also shows that a sensitivity analysis needs to be carried out in the design phase to build helicopters with this in mind in the future. Table 2-3 shows that fuel and oil and maintenance costs are major contributors to the direct operating costs. A reference to these costs is important to understand the way these contribute to the incurred costs. Regarding the fuel cost to

maintenance ratio the % increased from 16% (19.06/117.62) to 60% (887.47/1482.18)

2.3.2.4 Available Methods to Decrease Costs

While the industry and the operators strive to create a standard method of decreasing maintenance costs there are approaches that deviate from the everyday practice. Their contribution to maintenance depends on the operator and the engine generation with respect to technological advancement.

The first one is a process which is called cannibalization and relates to military units [83] or operators with a fleet that can support the concept. In cases that a helicopter is on the ground for service, its engine or some of its modules can be used to recover another engine in the fleet that experiences an unscheduled event. A US Army research on the effects of cannibalization of the T700-GE-401C engine in the US Navy revealed interesting results [83]. The results showed that cannibalization decreases the time between failures for cannibalized components considerably. This subsequently can have far-reaching effects on the size and costs of the Navy's inventory of spare parts. This concept may be used to increase short-term aircraft availability requirements. A drawback of the method is that the increased MMH, consumables and flight time required affected the budget and the availability of the operating squadron's workforce.

The second one is engine exchange. In this case, an MRO or an OEM can induct an engine for repair and exchange it with another of similar configuration and rating to the operator. In this case, the operator may be lucky enough and get an engine with lower flight hours or at a better price. Finally yet importantly other factors affecting engines maintenance cost are: i) the operator’s fleet, ii) the desired level of fleet availability, iii) the maintenance policy followed and iv) the spare engine or modules availability.

2.4 Summary

This literature review aimed to explore the current knowledge, reveal the gaps in the areas of: i) components’ life estimation and ii) maintenance costs assessment and consider appropriate methods to counteract these gaps.

The first part brought to attention the components degradation and its effect to the engine performance while the second part addressed the theoretical and practical approaches regarding the component remaining useful life assessment.

The theoretical approach elaborated on: i) the three main reasons for the engines' rotating component life consumption ii) their effect regarding the short and long haul flights and ii) the cycle counting methods.

The review showed that the main factor that affects the short flight profiles induced failures is low cycle fatigue (LCF) while creep and oxidation are not at a level that can make them an eligible candidate. Regarding the cycle count, it revealed that the regulatory guidelines to assess the rotating parts life limit are not mandatory and, they assume that the flight cycles are based on the aircraft flight profile. This assumption relates a regular aircraft flight profile (Comprised of a start, idle, taxi, take-off, climb, cruise, approach, landing, thrust reverse and shutdown segment) to one cycle while in rare cases where a profile might include touch and go segments, the cycles will be more than one.

While this assumption provides flexibility to the aircrafts' OEM's approach in cycle counting it cannot support the rotorcraft cycle assessment effectively. It is important that this research work will use a universal cycle counting method that will capture effectively the cycles due to the rotorcraft different flight profiles. The review showed that the 'rainflow' counting method is a very good candidate due to its capability to work on many different time history-loading scenarios (force, stress, strain, torque, acceleration etc.).

The practical methods review showed that these are based on: i) the severity factor concept, ii) statistical models based on failure data analysis parsed from operators and iii) on experienced or knowledge models. In addition, it considered the research work developed worldwide and adopted by Cranfield University researchers. The review revealed the following gaps:

a. The severity method is not applicable in the turboshaft engine as it is based on the following assumptions:

- The use of the turbofan engine derate feature, which is used in turbofan engines but is not applicable to the rotorcraft turbine engine.

- Relates the severity factor to the flight hours. The stresses that affect the turbine remaining life consumption of a rotorcraft relate mostly to different flight profiles and not on the shorty length. Rotorcraft flight length is similar to the short haul aeroplanes length; therefore, the cyclic part of the severity factor will be more profound and a different approach should be used to address the rotating parts remaining life.

b. The data driven methodologies relates to the data nature and the data resource availability. The issue regarding the data nature is not if they follow a statistical distribution but if the failure data relate to a realistic design space. In addition, an academic researcher bases his work on public data and has limited access to operator's failure databases.

The third part elaborated on the Life Cycle Costs and the literature review showed that public agencies, organizations, companies, operators, and researchers are using different guides to estimate the incurred costs. It would be rational to think that it would be sufficient to add the costs incurred at every phase of the cycle but in reality, the logistics around a product lifecycle are difficult to handle.

In addtion, the review found a shortage of information for rotorcraft costs and the available data related only to aeroplane turbofan engines. Harris work [3] on cost estimation provides an equation, formulated from regression analysis, using raw data from a United States based consulting company [84] and he based the calculation on the assumption that a helicopter's flight relates to two engine cycles. While this assumption may be useful for a qualitative approach, when for example, we need to compare costs for two different helicopters, it over simplifies the cost assessment.

Considering the above, this research proposes a methodology, which will attempt to address the gaps and employ the following features:

a. Estimate the engine performance data using a flight mechanics code to simulate flight profiles related to a representative design space. Use these data to create a set of remaining useful lives for a turbine based on a design space, which will consider both the operating capabilities of a specific rotorcraft regarding and the appropriate environmental parameters for a reference flight. The parameters selection will be based on the importance of various parameters to the engine performance.

b. Use the same operational parameters for actual flights and instead of using the severity factor approach create a mixture of flights, which relate to a realistic operator's scenario.

c. Implement the rainflow counting method to count the number of cycles for each different flight profile. The results of this method will be closer to reality regarding the rotorcraft missions.

d. Use a cumulative method that will provide more flexibility allowing for scenarios that are more realistic. The method will create a failure limit based on weight factors, which relate to the percentage of each flight profile in the mixture. This approach should take into account an accepted document like the HAI guide [5] and formulas that can assist a quantitative approach, like Harris CER's [7] can.

e. Replace the assumption used so far (two cycles/ flight) for engine maintenance costs with the cycles per mission estimated from the Rainflow analysis.

f. Use the Jenkinson [2] approach, regarding the cost estimation complexity, who believes that a choice has to be made and the chosen method should be able to show the difference between different designs or cases.

g. Use a method like the MaxLLP usage or MinSV, which supports a cost analysis on a short or long-time horizon.

h. Consider the degradation effect on fuel consumption. A comparison between the fuel costs due to degradation and the maintenance costs due to performance restoration and life limited parts replacement will provide a useful insight.

3 Chapter 3: Methodology and the Research Framework

3.1 Overview

The aim of the research is to create a tool that i) will consider the operator's rotorcraft usage and flight profile, ii) estimate the high-pressure turbine life and then iii) provide a cost analysis with regards to maintenance cost and degradation. This tool will further help the operator to make an informed decision based on the trade-off between maintenance cost and engine's availability.

Rotorcraft have been long criticized for high maintenance costs and while technology gets more sophisticated and provides solutions like HUMS usage, this is not considered a cost-effective solution for small fleet operators [12]. It is important therefore to provide a tool that will help the operator relate the rotorcraft usage with the related maintenance costs.

The methodology developed covers the following areas:

a. Latin hypercube sampling (LHS) and design of experiment (DOE),
b. Operating and Environmental Parameters selection,
c. Engine component life estimation model,
d. Operators usage scenarios definition,
e. Maintenance cost assessment,
f. Surrogate model development (Gaussian Process),
g. Surrogate model validation method (LOO).

The methodology follows a logical path. The starting point is the selection of three variables that can adequately represent the rotorcraft flight envelope. The two selected parameters, which capture the influence of the rotorcraft-operating environment to the engine performance, are: i) payload and ii) climb rate and the third one, which captures the effect of the environment, is the ISA deviation. These parameters define the design space that relates to the rotorcraft capabilities and supports a design of experiment. Considering the design space, the Latin Hypercube Sampling (LHS) method used due to its simplicity and high level of accuracy, estimates the parameter values for the experiment. Once we define the values of the parameters, we can use

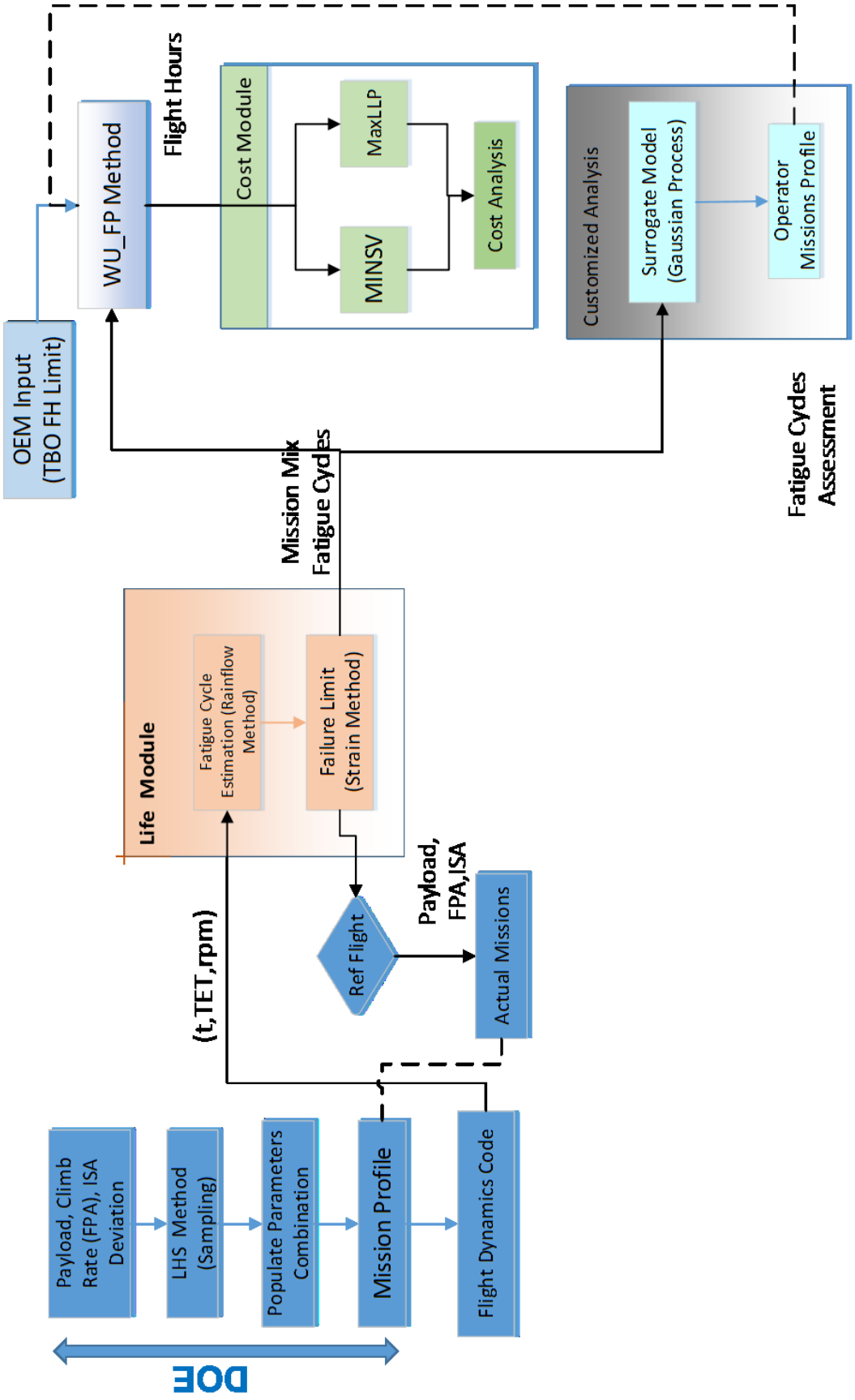

Figure 3-1 : Methodology Flow Diagram

a flight dynamics code to: i) simulate the rotorcraft flight and ii) provide data for the engine performance. The mission profile for a basic passenger flight scenario can be created and a set of simulations can be organized. The mission profile considers the covered length and the time spent at each flight segment. Appendix D show a typical mission profile with all the values used per segment. HECTOR uses Turbomatch to estimate the power demand and maximum temperature of all flight segments. Paragraph 3.1.2 describes briefly the simulator capabilities. Out of the numerus HECTOR outputs, this research will use the ones that relate to engine performance and flight conditions history: i) the flight time history, ii) the Turbine Entry Temperature (TET) and iii) the engine's RPM.

The life module uses these outputs to estimate the failure limit in cycles for the gas turbine module. The life module is a code developed from the author in Python and acts as a wrapper for three submodules. The first module written in MATLAB estimates the cyclic and steady stresses on the turbine blade and disc. The second module written in FORTRAN estimates the stress amplitude per flight segment and the cycles for the specific mission and, the third module written in Python uses the strain method to estimate the cycles to failure for the turbine blade or disc. The life module estimates the cycles to failure for: i) different flight profiles or, ii) for different component designs. The study case presented at the next chapter uses both capabilities. Paragraph 3.2.1 provides a detailed description of the code.

The outcome of the simulation loops is a range of values that represent the failure limit within the boundaries of the experiment design space. At this point, the median value of the data population is picked as a representative of the engine failure limits. The set of the parameter values (Payload, Flight path angle and ISA deviation) which relate to this life limit define the mission profile for other actual flights (SAR, Firefighting, OAG etc.) within the rotorcraft capabilities. This approach shows the effect of the mission profile on the component cycles to failure limit.

The selected type of the actual's missions can represent the actual flights of an operator flight profile. The output of the actual flights' simulation feed the life module and estimates the cycles to failure for the actual flights. At the end of this step, the methodology provides life data for a set of different flight profile.

At this point, we can consider that an operator flight profile comprises a combination of these flights and this combination can very well represent a real-life scenario. To estimate the equivalent failure limit for these flights' combination, the author developed a method named "Weighted Usage Flight Profile Method (WUFPM)". This method considers the failure limit in cycles for every mission type and the % that this mission is used for a 300-flight hour per year. The method uses the cumulative damage concept and the outcome is the gas turbine failure limit in flight hours. This outcome is an input to the cost model.

The cost module is written in Python and estimates the maintenance cost for the engine lifespan based on 2 different methods widely used for the aircraft's engine maintenance. The two methods are the Minimum Shop Visit Rate and the Maximum Life Limited Part Usage. Paragraph 3.5.2 presents the assumptions for the parameters used in this module. The two characteristic values used are failure limit in Flight hours as estimated from the WUFPM method and the time for between overhaul (TBO), which is a hard time limit given from the engine original manufacturer (OEM) or exist at the public domain. The TBO time limit influences the engine shop visit cost through the depreciation factor. Due to lack of data, suitable equations estimate the costs of the engine overhaul and LLP replacement.

The developed framework provide a customized analysis for an operator based on his flight profile. To facilitate that, the DOE output data helps to build a surrogate model, which will allow the cost analysis for an operator based on his unique flight profile. A cross validation method named leave-one-out method validates the model. Appendix I provides the method description.

As mentioned above the main effort of this research is to create a framework that will post-process HECTOR' output data that relate to engine performance and flight operating parameters. To develop the framework, initial work was conducted to develop the framework components and to ascertain that the data used in the modules were accurate and were based on proven theories. The work to accomplish this target includes the following:

a. Engine model development: The engine used for the mission simulation was trimmed to make sure it runs in the OEM standards and that operating limits were not

exceeded. A case scenario for an Alisson 250-C20 turboshaft engine and the file set up are analysed in Chapter 4.

b. Engine simulations for degradation: After the engine trimming, simulations assessed the impact of components degradation and its effect on performance and on TET margin consumption. Paragraph 4.3 discusses the results.

c. Life estimation module: A code was developed that post-processes the simulation output data and combined with Turbomatch and a MATLAB code estimates the turbine blade and disc life. The resulting component life together with the time for performance restoration (TBO) taken from the public domain is then entered at the cost model code mentioned above. The code uses the strain-based method together with ‘rainflow counting ’ method. Detailed analysis of the method used is provided in paragraph 3.2 and in the flowchart in Appendix C.

d. Design of experiment: Using the code mentioned, 4 sets of simulations were run for a passenger helicopter flight. The simulations were performed to assess the impact of operating parameters like payload, climb rate and ISA deviation on the engine operating temperature and compressor rotational speed. Details are given in paragraph 3.3.2.

e. Code development for experiment acceleration: To facilitate the experiment’s numerous simulations a code in Python have been developed that allows the full usage of the available computational power (8core processor) and minimizes the computational time. The code allows the user to enter the desired mission operating parameters to an input file. This file alters the HECTOR mission file and then the simulation can commence. Once the simulation finishes the code post processes the HECTOR output file and provides an excel file with the simulation results that relate to engine operating parameters (operating and cooling temperature or engine rotation for every flight segment). More details are given in paragraph 3.2.1 and Appendix H.

f. Data analysis: The simulations results provide data, which is used so that trends in life estimation could be found either, by using a simple technique like regression analysis or more advanced techniques like a spatial interpolation. The results are given in paragraph 4.3.

g. Cost module case scenario development: A code, which was initially developed in FORTRAN 95 and then converted to Python allows the calculations of maintenance data at all levels of maintenance. The code is a part of the developed

framework and detailed analysis of the formulas used in the code is provided in paragraph 3.5.

3.1.1 Gas turbine performance modelling

The engine is an integral part of the helicopter and its performance is based on environmental parameters and ambient conditions as well as: i) the pilots' input through the collective control ii) the total drag and iii) the weather conditions. An engine performance simulation model can predict the fuel consumption and provides the required power to sustain the helicopter loads.

As mentioned before the HECTOR framework is using a turbine performance simulation code-named TURBOMATCH. Turbomatch has been developed by MacMillan at Cranfield University [85] and is constantly upgraded to follow and meet the latest technological advancements in the industry. It can perform design, off design point and transient operation studies for different configurations for any existing engine in the market. It employs different component maps and the calculations performed are based on zero-dimensional aero-thermodynamic analysis in the sense that they do not contain any information on the fluid mechanics in them. They incorporate the rate processes occurring in the engine and are an aid in the analysis of the data produced from the thermodynamic analysis. The employed method essentially solves for the mass and energy balance between the various engine components.

3.1.2 HECTOR – Rotorcraft Simulation Framework

A framework that was developed at Cranfield University by Dr. Ioannis Goulos [13] named HECTOR was utilized in this work to assess the engine performance during all flight profile segments.

HECTOR can simulate the performance of a user-defined complete helicopter platform. It can analyse the overall performance of any designated helicopter-engine system, within complete and realistically defined three dimensional operations. Its capability expands to the areas of rotor blades natural vibration characteristics estimation and fuselage aerodynamic interference effects and in addition to the operations optimizing with respect to total mission fuel consumption and associated

environmental impact. The framework can generate rotorcraft performance charts and evaluate the required operating resource that is, fuel burn and mission time.

The overall process uses a predefined time-step Δt and breaks the mission into designated Mission Task Element (MTE). The underlying assumption is that, for every mission segment of duration Δt, the helicopter operates in trim and the engine is in steady-state off-design mode. This assumption is valid, considering that the primary focus of the structured numerical approach is the estimation of the total mission fuel consumption.

The mission operating conditions regarding altitude, flight speed, flight path angle and turn rate are determined from the user defined input file and the corresponding segment time-point (t).

The engine performance requirements are determined while the nonlinear rotorcraft trim model employed in the code tries to trim the helicopter at every time step in the mission. The power requirements and the corresponding inlet conditions like: i) altitude and ii) Mach number provide the data for the off-design calculations performed in Turbomatch. At this point, the engine fuel flow is determined among other off-design performance parameters.

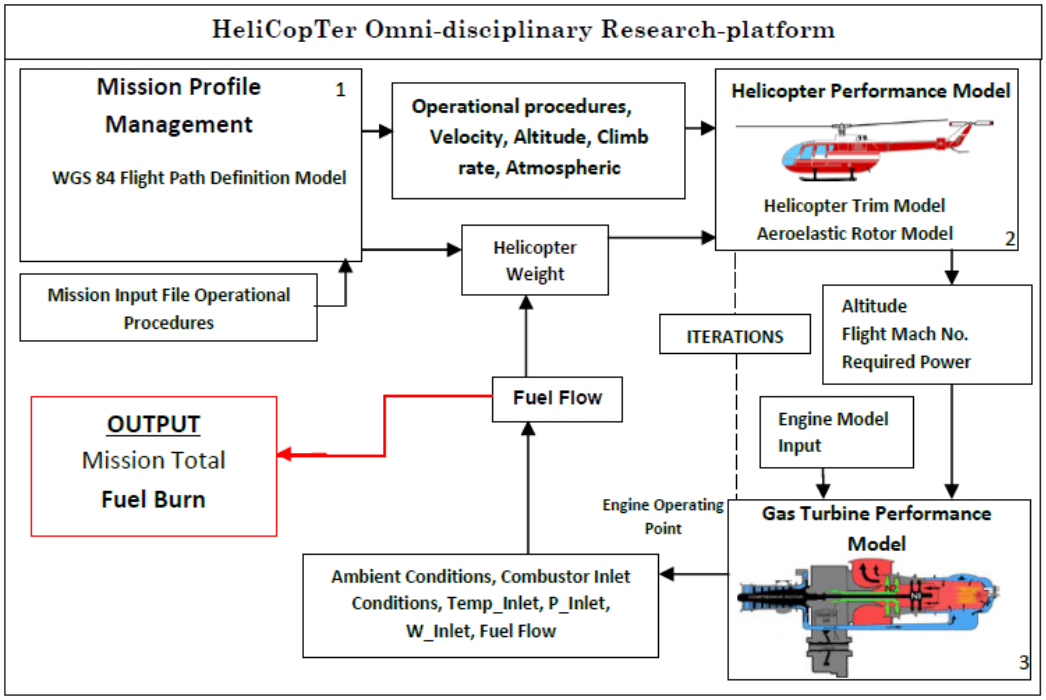

Figure 3-2: HECTOR Flow Diagram [13]

A numerical time integration method over the mission segments corresponding to $0<\tau<t$ is applied to calculate the fuel consumption which relates to the time-point (t). The fuel consumption calculated value is then subtracted from the initial AUM at the time (t) to simulate the helicopter's gradual weight reduction during the mission. The parameters that relate to the flight path provide the helicopters position in space. This process is repeated until the user defined convergence criterion is met.

Goulos [13] concluded that the accurate prediction of the aircraft's time-dependent AUM during flight is important for the identification of the most power-demanding conditions within a complete helicopter operation.

3.2 Operating and Environmental Parameters

Before we move on to the design of an experiment (DOE), a decision is needed for the adopted operational and environmental parameters, which will be used in the methodology. The selected parameters will be used to form the design space for the experiment and a sampling method will be used to find the parameters values, which will be used to run the set of experiments.

3.2.1 Parameters Selection

As mentioned in the overview section, the factors affecting helicopter performance are: i) air density, ii) atmospheric pressure, iii) altitude, iv) temperature, v) moisture, vi) weight (payload) and vii) winds. The above factors are dependant and interact with each other like for example in the case of air density. The atmosphere pressure, the temperature and the moisture content primarily influence the air density. While the pressure is proportional to the density, the temperature is inversely proportional, the pressure being by far the most influential parameter.

To make it easier to anticipate performance in any given atmospheric condition, the aviation community has agreed to use a set of average values as a reference. These average values are contained in the standard atmosphere also named as ISA which assumes that: i) Sea level pressure is 29.92 inches of mercury, ii) Sea level air temperature is 15 Celsius and iii) Temperature lapse rate is 1.98 Celsius per 1000 feet.

Based on that standard atmosphere the terms pressure altitude and density altitude has been created. The first makes allowance for actual sea level pressure being different form standard, while the second allows for temperature being less than equal to or greater than that at pressure altitude.

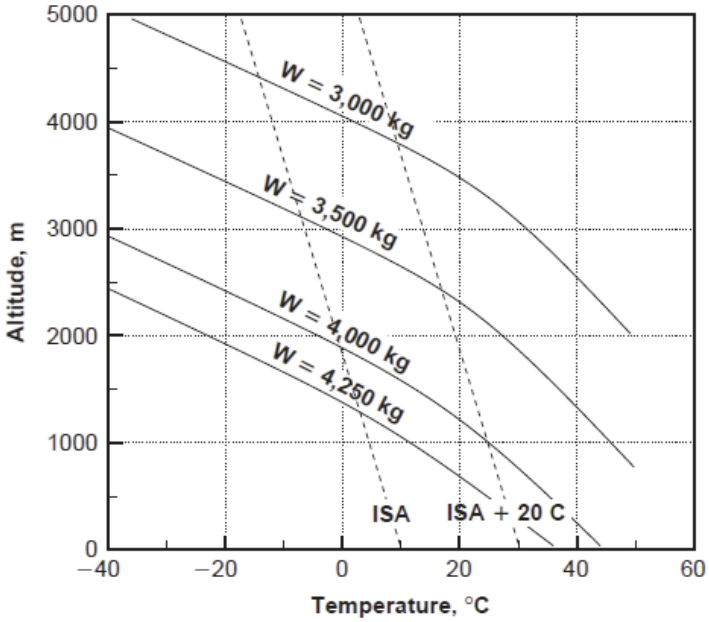

Figure 3-3 : EC-365, OGE hover performance, engines at maximum take-off power [Filippone]

The parameters named above play an important role at the two most demanding segments in a mission, which is the hover, and the climb segment. The next two paragraphs discuss their influence on these segments:

- Hovering Performance

During hover, more power is required than in any other flight segment. Obstructions aside, if a hover can be maintained, a take-off can be made especially with the additional benefit of a translational lift. The flight manuals provide various charts under various conditions of gross weight, altitude, ISA, and power. The density altitude affects the hover ceiling, where hover ceiling is considered the height where the power available is equal to the power required. The next figure shows the power required to power available curve. The excess power that can be used to allow the rotorcraft to hover is the vertical distance between the red line at point A and the green line above it. If the green line falls below the red the rotorcraft is not capable for hovering. Provide

that the pilot orients the rotorcraft into the wind, thus using the full potential of the engine and the induced flow, the 3 main parameters that influence the ability to hover is the weight, temperature and pressure.

An example for the weight influence is that for a Schweizer helicopter where for a gross mass of 725 kg the hover ceiling is 11,350 feet pressure altitude and with 910 Kg the ceiling decreases to almost half of that to 5400 Ft pressure altitude.

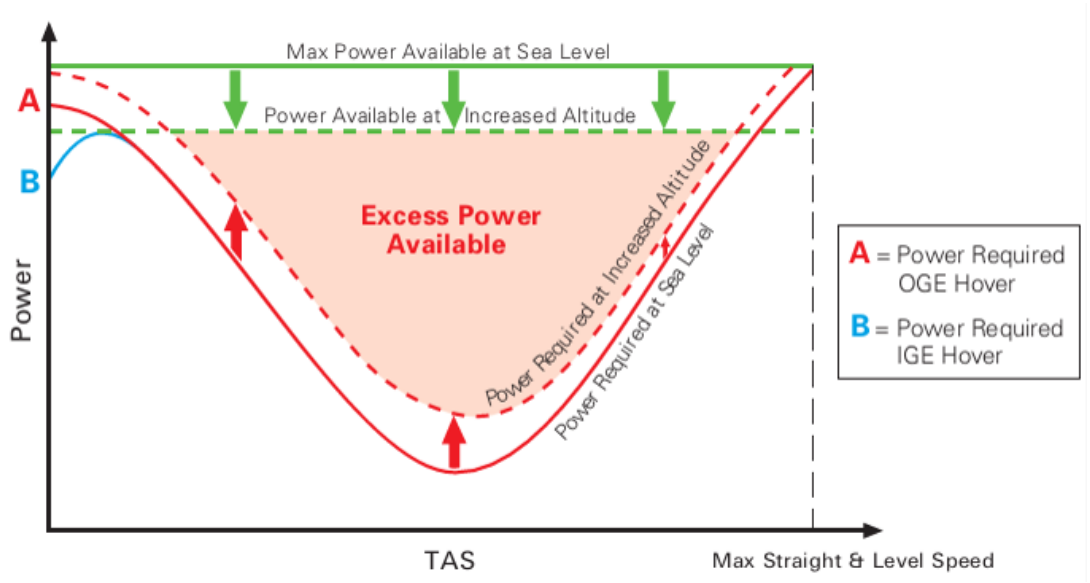

Figure 3-4: Power Available vs Power Required Curve

The differences in temperature in pressure as described before can be represented from the ISA deviation which means that the helicopter weight / payload (operational parameter) and the ISA deviation (environmental parameter) are two parameters that can adequately describe the helicopter performance and can therefore be used in this research.

- Climb Performance

The parameters that affect hover and take off also affect climb or decent performance. Performance may vary though due to weather, pilot techniques and overall condition of the helicopter. The normal procedure to determine the accepted climb rates starts by estimating the engine torque for a level flight under the specific conditions (weight, airspeed, pressure and temperature). Once this is established the limits for the climb rate mostly depends on the rotorcraft weight. The flight manual graphs show the limitations for the pilot's attitude for manoeuvres and the helicopter capability to

override obstacles. The pilot should always check the climb performance charts before attempting to climb. The ability to sustain a required rate of climb is crucial and that relates to the available torque that the combination of engine and powertrain system can offer. This is the reason that the rate of climb (operational parameter) is selected as the third parameter to use in this research.

3.2.2 Parameters Sensitivity Analysis

Once the parameters has been selected it is deemed necessary to find the correlation of the parameters and their effect on the engine behaviour. A simple method to achieve that is to perform a multiple regression analysis. Essentially, regression is the “best guess” at using a set of data to make some kind of prediction. It is fitting a set of points to a graph. Multiple regression analysis is used to see if there is a statistically significant relationship between sets of variables. It’s used to find trends in those sets of data. Multiple regression analysis is almost the same as simple linear regression. The only difference between simple linear regression and multiple regression is in the number of predictors (“x” variables) used in the regression.

Multiple regression models with 3 predictor variables can be expressed by the following equation:

$$Y = B_0 + B_1 * X_1 + B_2 * X_2 + B_3 * X_3 + e \qquad 3\text{-}1$$

The variables in this model are :

- Y, the response variable;
- X_1, X_2, and X_3, the 1st, 2nd, and 3rd predictor variables;
- e, the residual error, which is an unmeasured variable,

The B_I parameters are the regression analysis coefficients and show the impact of every operating variable to the response variable. In more detail, B parameters in the model represent:

- B_0, the Y-intercept;
- B_1, B_2, and B_3 the 1st, 2nd, and 3rd regression coefficients;

B_0, the Y-intercept, can be interpreted as the value you would predict for Y if both X_1, X_2, X_3 = 0. However, this is only a meaningful interpretation if it is reasonable that both X_1 and X_2 can be 0, and if the data set actually included values for X_1, X_2, and X_3 were

near 0. If neither of these conditions is true, then B_0 really has no meaningful interpretation. It just anchors the regression line in the right place.

Since X_1 is a continuous variable, B_1 represents the difference in the predicted value of Y for each one-unit difference in X_1, if X_2 remains constant. This means that if X_1 differed by one-unit (and X_2 did not differ) Y will differ by B1 units, on average.

To avoid overfitting in the regression analysis, an adequate number of missions should be selected for simulation. Austin's review [86] provides several rules of thumb for the numbers of observations per independent variable. A few 10 to15 simulations per variable, which means 45 simulations should be run, would suffice to perform the regression. To make sure that enough data are available for the regression it was decided to run 64 missions. The mission profile used is a simple mission comprised of 7 segments that allowed for a low computational time while making easier the results assessment. The 3 parameters used for the regression are: i) Payload, ii) Flight Path Angle (FPA) and iii) ISA deviation. The above variables and the design space for the experiment are shown in Table 3-1 as "Operating Variables".

Operational Variables			Results Variables	
Payload	FPA	ISA Deviation	TET	PCN
200	3,4,5,6	0/5/10/15	hover_max_tet	hover_max_pcn
350	3,4,5,6	0/5/10/15	climb_max_tet	climb_max_pcn
500	3,4,5,6	0/5/10/15	cruise_max_tet	cruise_max_pcn
650	3,4,5,6	0/5/10/15	descent_max_tet	descent_max_pcn

Table 3-1: Experiment Operating Variables

HECTOR mission files can be very lengthy and may contain from 10 to 25 bricks while each brick can contain from 3 to 13 parameters as shown in Table 3-2. The operating parameters that affect the engine performance and its lifetime are: i) the payload, ii) the altitude iii) the ISA deviation, iv) the climb/descent rate (or flight path angle-FAP), v) the speed, vi) turn rate velocity, vii) the wind speed, and viii) direction. The number of parameters varies for every brick, the reason being that every brick relates to a specific flight segment.

To accelerate the process a code was developed in Python. The code helps to enter the variable values to the mission input files for selected numbers of missions. The user enters the desired values to an input file which is connected to a template mission

file. The template file is used as a basis to create the HECTOR mission file for every run. While the code is not lengthy it is useful for the parameters “bookkeeping”, allows for the experiment execution in a more consistent, and controlled environment. Appendix H presents a code description.

	Cruise	Hover	Idle	Payload	Data Start
1	Brick No	Brick No	Brick No	Brick No	Static_Timestep
2	Brick_type	Brick_type	Brick_type	Brick_type	Dynamic_Timestep
3	End_Altitude	Duration	Duration	Delta_mass	Only_Plot_Mission
4	End_Speed	New_Orientation	Engine_Torque_fraction		Fuel_Burn_Initial_Guess
5	Climb_Rate	Isa_Deviation	New_Orientation		Fuel_Burn_Tolerance
6	Climb_Speed	Wind_Direction			Fuel_Reserves
7	Turn_Rate	Wind_Speed			
8	Sideslip_Angle				
9	End_Latitude				
10	End_Longitude				
11	Isa_Deviation				
12	Wind_Direction				
13	Wind_Speed				

Table 3-2: HECTOR brick data description

The predicted variables, the TET and the gas producer rotational speed, relate to the engine performance and affect the stresses and strains developed on the engine components. Table 3-3 depicts a sample of the operating values and the results for 4 flight segments. These are: i) hover, ii)climb, iii)cruise and iv) descent.

The resulted equations can then be used to estimate the predicted output for any combination of the independent “operating variables”. Fitting a regression model requires making several assumptions [87]. Estimating the model parameters requires that the errors are uncorrelated random variables with mean zero and constant variance. Tests of hypotheses and interval estimation require that the errors be normally distributed. In addition, we assume that the order of the model is correct; that is, if we fit a simple linear regression model, we are assuming that the phenomenon behaves in a linear or first-order manner. To make sure a regression describes a good fitting based on the available data we use the adjusted R squared and p-value parameters.

The adjusted R squared value shows the accuracy of the equation when it is used to perform an interpolation and derive a value for TET or PCN. It tells you how many points fall on the regression line. For example, 0.8 means that 80% of the variation of

y-values around the mean is explained by the x-values. In other words, 80% of the values fit the model. The adjusted R-square adjusts for the number of terms in a mode and it is used instead of the simple R squared if you have more than one x variable.

The p-value [88] for each independent variable tests the null hypothesis that the variable has no correlation with the dependent variable. If there is no correlation, there is no association between the changes in the independent variable and the shift is in the dependent variable. In other words, there is no effect.

Operating Parameters			TET			
Load	FPA	ISA	hover_max	climb_max	cruise_max	descent_max
200	3	0	1242.84	1132.77	1137.09	930.34
200	4	0	1242.84	1162.95	1137.27	930.36
200	5	0	1242.84	1197.8385	1137.27	930.36
200	6	0	1242.84	1220.49	1137.47	930.38
200	3	5	1262.96	1150.18	1152.32	943.88
200	4	5	1262.96	1180.58	1152.47	943.91
200	5	5	1262.96	1209.78	1152.53	943.93
200	6	5	1262.96	1237.95	1152.54	943.91
200	4	10	1283.06	1198.27	1167.67	958.18
200	6	10	1283.06	1255.44	1167.76	958.19
200	3	15	1303.19	1185.25	1182.62	972.67
200	4	15	1303.19	1215.66	1182.7	972.66
200	5	15	1303.19	1244.2	1183	972.71
200	6	15	1303.19	1272.99	1183.23	972.69

Table 3-3 Experiment value Sample for TET

If the p-value for a variable is less than the significance level, the sample data provide enough evidence to reject the null hypothesis for the entire population. The data favour the hypothesis that there *is* a non-zero correlation. Changes in the independent variable *are* associated with changes in the response at the population level. This variable is statistically significant and probably a worthwhile addition to the regression model. On the other hand, a p-value that is greater than the significance level indicates

that there is insufficient evidence in the sample to conclude that a non-zero correlation exists. Table 3-4 shows the regression polynomial coefficients, the P-value and the R squared value for the TET regression equation:

$$TET = B_0 + B_1 * X_1 + B_2 * X_2 + B_3 * X_3 + e \qquad 3\text{-}2$$

	Intercept B_0	Payload B_1	Climb Rate B_2	ISA B_3
hover_max_tet	1189.94	0.25	0.00	4.29
P-value	2.1E-130	3.23274E-85	0.996692676	7.09942E-71
Adjusted R Squared	0.999			
climb_max_tet	1009.74	0.17	29.68	3.53
P-value	8.63E-79	3.22673E-29	4.07894E-33	1.71225E-21
Adjusted R Squared	0.955			

Table 3-4: Regression coefficients for Hover and Climb Segments

The P-values at the intercept show a very strong correlation with TET, an argument that can be further supported by the residual values estimated at the regression.

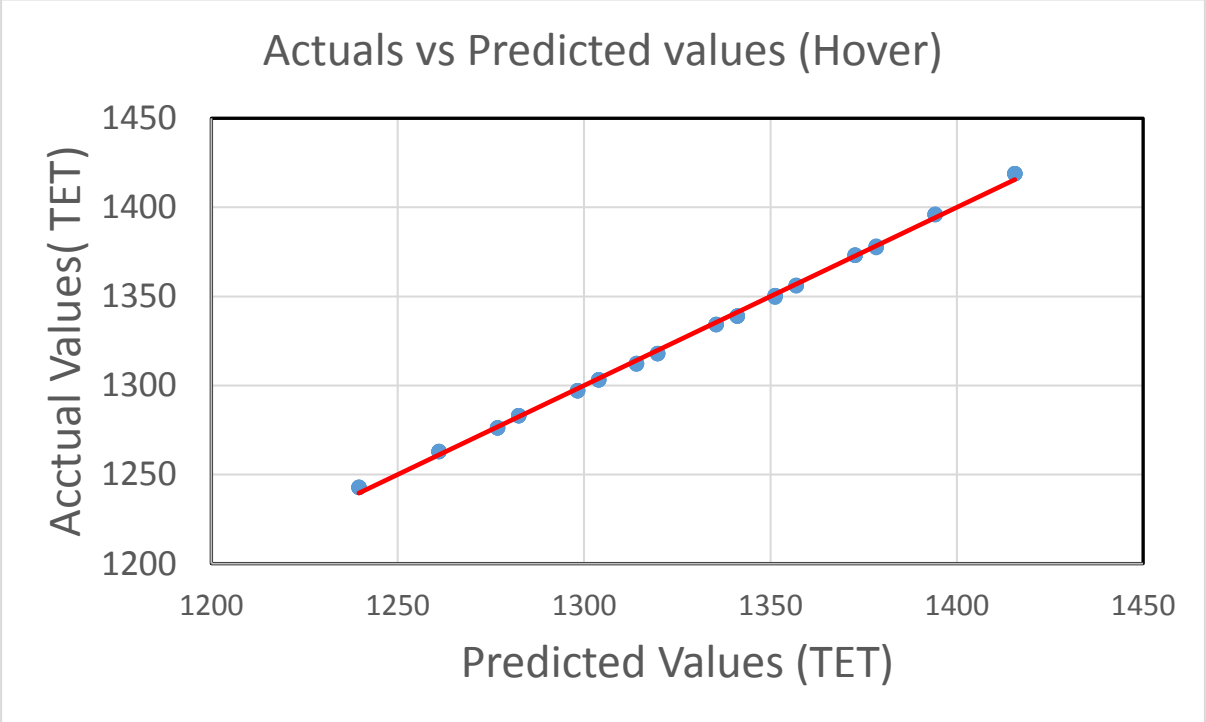

Figure 3-5 Actuals vs Predicted values for Hover Segment

Figure 3-5 and Figure 3-6 show that the predicted values are very close to the actual values for both the hover and climb segments. A small exception of 6 outliers at the climb segment does not alter the trend line and is not considered significant to question the regression fitness.

Table 3-5 shows the regression polynomial coefficients, the P-value and the R squared value for the TET regression equation for the Cruise and descent segment.

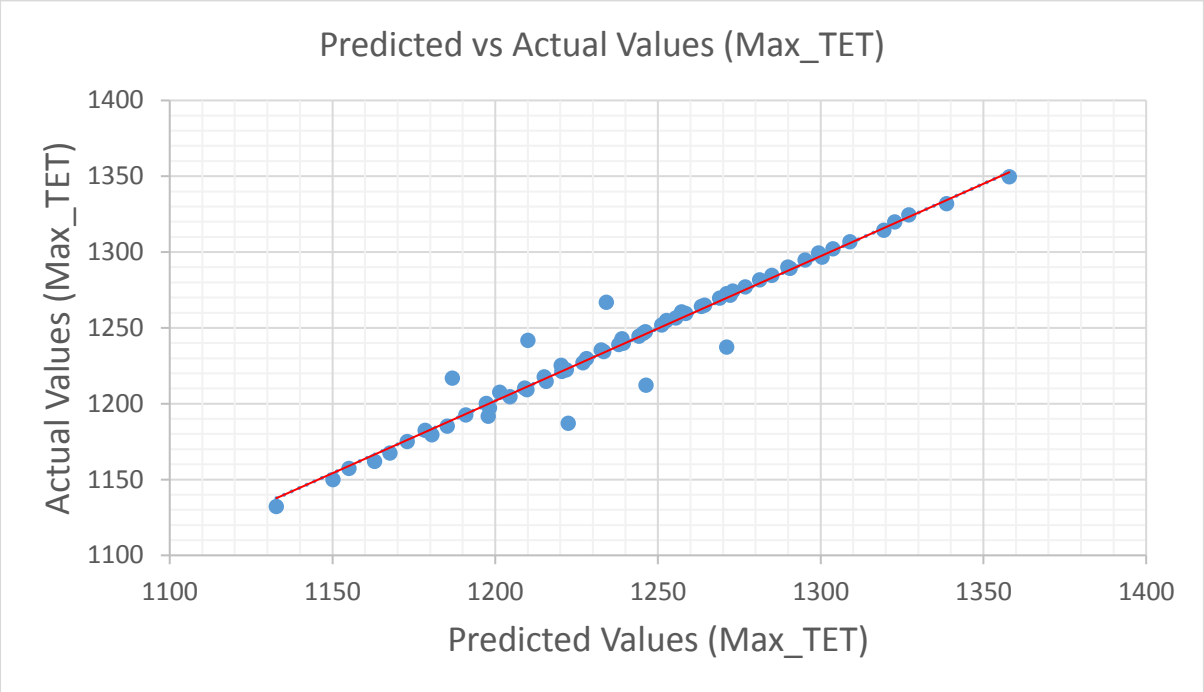

Figure 3-6: Actuals vs Predicted values for Climb Segment

	Intercept B_0	Payload B_1	Climb Rate B_2	ISA B_3
cruise_max_tet	1102.00	0.14	0.17	3.52
P-value	1.00453E-98	7.40786E-41	0.778403045	7.44722E-37
Adjusted R Squared	0.971			
descent_max_tet	906.90	0.10	0.02	3.10
P-value	9.1084E-129	2.39935E-67	0.920219061	6.8013E-68
Adjusted R Squared	0.997			

Table 3-5: Regression coefficients for Cruise and Descent Segments

The adjusted R-squared value shows that the regression equation has a good fit and can describe adequately the relationship between the 3 predictors and the TET. A review of the coefficients B_I shows the following:

a. The Bo values reveal that the TET values are higher at the hover and cruise segment while they decrease at the climb and take the lowest values at the descent segment

b. The B1, B2 and B3 values follow a decreasing trend starting from the hover segment all the way to the descent.

c. The B1 values that relate to payload are much lower than the B3 values that relate to ISA deviation. This event does not mean though that the ISA deviation is more significant than the ISA deviation. The value magnitude relates to the values that the variable can have from the data sample. The ISA deviation relates to the design space of 0, 5, 10, and 15 while the payload to the design space of 200,350,500,650 kg. It is worth reminding that B_1 represents the difference in the predicted value of Y for each one-unit difference in X_1 if X_3 remains constant. Higher values of B_1 would have a great effect on the predicted TET and this is the reason that the B_1 values magnitude is so low.

A review of the P-values for every segment reveals the following:

a. Intercept: The values for all 4 segments are very close to 0 which means that there is a very strong correlation with the predicted TET value.

b. Payload: The values, in general, show that the Payload has a stronger correlation to TET than the ISA deviation. Payload has a stronger effect than ISA at i) the hover and ii) the climb section while the correlation is less at the cruise and descent segment.

c. Climb Rate: The climb rate shows as expected a strong correlation at the climb segment while it is not significant at all the other segments and can even be excluded from the independent variables. It is interesting to realize that the climb rate effect at the climb segment is bigger than the effect of the payload or the ISA deviation.

d. ISA: The ISA deviation is the second more significant variable compared to Payload at the first 3 segments while in the descent segment is incrementally more significant.

3.2.3 Operating Parameters Sensitivity Analysis

The regression analysis performed in the previous section can prove very useful for two reasons:

a. The equation that describes the predictor's relation can be used as a surrogate model and help predict TET or PCN values without the need to run simulations.

b. The coefficients BI show the correlation of the independent variable with the response variable.

The analysis provided in the previous section about the P-value figures showed that these values are very close to 0. The parameters significance can be revealed from the number of decimals but still, the magnitude is low. To that end, it is deemed necessary to perform a sensitivity analysis that will provide figures of greater magnitude and hopefully we can come up with a better understanding of the variable's significance.

One simple approach to perform a sensitivity analysis is to change one-factor-at-a-time and to calculate the effect of this change on the output. This approach employs usually two steps:

a. Change the value of a selected input variable while keeping the others at their baseline (nominal) values, then,

b. Return the variable to its initial value and repeat the process for each of the other inputs.

The sensitivity is the measured by tracking the changes in the output.

Currently, there are many available tools [89] that can help a researcher perform a sensitivity analysis. Excel, which is a widely available spreadsheet application, is capable of different analysis: i) what-if analysis (Tornado charts), ii) base-case analysis, iii) breakeven analysis and iv) optimization analysis.

A Tornado chart shows how sensitive the output is to several different inputs. Consequently, it shows us which parameters have a major impact on the results and which have a minor impact. Tornado charts are created by changing input values one at a time and recording the variations in the output. To create a Tornado diagram for the TET a baseline value for every segment should be used. The baseline value was

calculated using the operating parameters baseline values considering the experiment design space. The baseline values for every segment can be seen in Table 3-6.

Operating Parameters Baseline Values	Labels	Low Values (-30%)	High Values (+30%)
350	Payload	245	455
4	FPA	2.8	5.2
7	ISA Deviation	4.9	9.1

Table 3-6: Sensitivity Analysis Baseline Values

The equation 4.2 was used to estimate the TET values where the coefficients were taken from Table 3-7 for every segment.

Parameter	Reg Coefficient	Hover	Climb	Cruise	Descent
Intercept	B_0	1189.941875	1009.743	1102.005	906.9003333
Load	B_1	0.24819875	0.167454	0.137987	0.101239583
FPA	B_2	0.0008	29.67637	0.172437	0.0159375
ISA Deviation	B_3	4.2873125	3.525157	3.517363	3.1020875

Table 3-7: Regression Analysis Coefficients

The low and high values for each operating parameter can be estimated by using the values that correspond to the ±30 percent, of every baseline value (Table 3-6). To assess the significance of TET for an operating variable, for example Payload, for the Hover segment the following steps are used:

a. The TET is estimated with the equation 4-2 where the baseline values are used for every parameter.

b. Then to estimate the low value for the payload I use the equation 4-2 while for the parameters I use the low value for the payload (245) and the baseline values for the climb rate and the ISA deviation.

c. To estimate the high value for the payload I use the equation 4-2 while for the parameters I use the high value for the payload (455) and the baseline values for the climb rate and the ISA deviation.

d. I repeat the steps 2 and 3 for the other two variables (climb rate and ISA deviation) and I plot the result using as reference the TET which I estimated at step 1.

e. Figure 3-7 to Figure 3-10 show the significance of the 3 independent variables to TET. The results derived from the analysis match with the ones from the P-values as shown in Table 3-4 and Table 3-5. The sensitivity analysis showed the following:

f. The payload firstly and the ISA deviation secondly is the most significant parameter that determines the engine TET.

g. The climb rate is more significant at the climb segment.

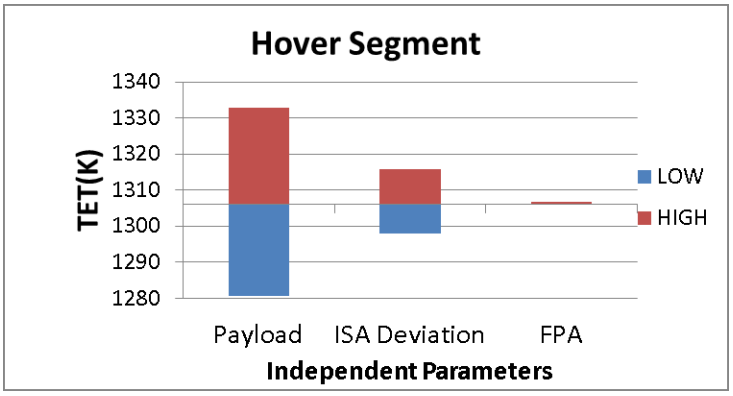

Figure 3-7: TET Sensitivity for a 30% change in Operating Parameters for the Hover Segment

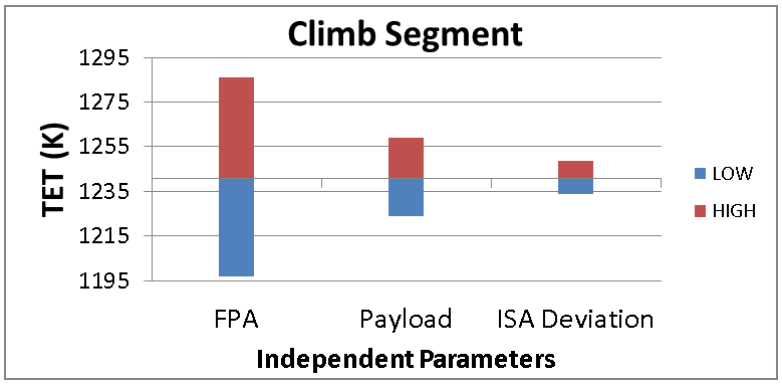

Figure 3-8: TET Sensitivity for a 30% change in Operating Parameters for the Climb Segment

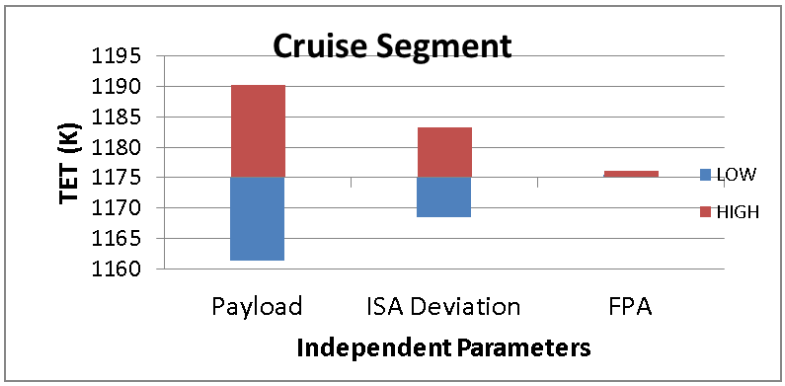

Figure 3-9: TET Sensitivity for a 30% change in Operating Parameters for the Cruise Segment

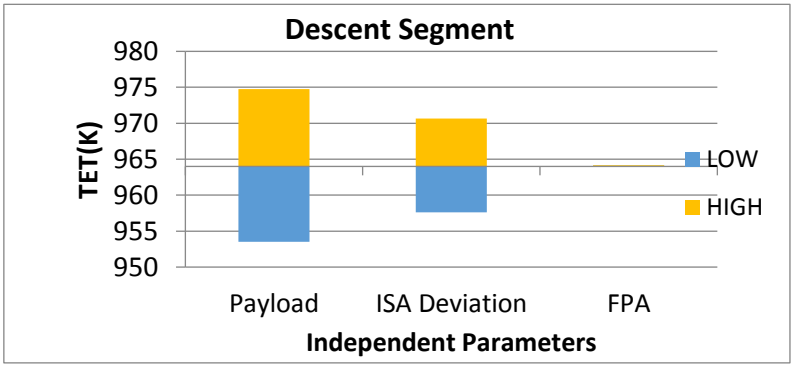

Figure 3-10: TET Sensitivity for a 30% change in Operating Parameters for the Descent Segment

3.3 Design of Experiment (DOE)

The previous paragraphs addressed the selection of the operational parameters that comprise the design space for the rotorcraft flight profile and a sensitivity analysis was used to provide a better understanding of the variable's significance.

The research scope, as initially defined, assumed that a simulation tool would be used, which would estimate the aerodynamic loads of the flight and sequentially provide the power requirements which would define the engine load and performance. It is obvious that the design space of the input variables that comprise the operating environment is very wide, and it is safe to consider that statistical methods can address the operating spectrum as well as the outcomes.

Data analysis is a process [90], which aims to discover useful information, suggest conclusions, and support decision-making. The approaches and techniques to

accomplish its target depend on the applied business or science domain. It relates to either descriptive or predictive analytics that can provide some insight to decision makers. Table 3-8 provides several methods that can be used in this research. The best candidate would be the one that makes use of the tools on hand and would provide the desired output.

Mathematical programming or optimization techniques	**Stochastic process techniques**	**Statistical methods**
Calculus methods	Statistical decision	Regression analysis
Calculus of variations	Markov processes	Cluster analysis- pattern
Nonlinear programming	Queueing theory	Design of experiments
Geometric programming	Renewal theory	Discriminate analysis
Quadratic programming	Simulation methods	
Linear programming	Reliability theory	**Modern or Non-traditional**
Dynamic programming		Genetic algorithms
Integer programming		Simulated annealing
Stochastic programming		Ant colony optimization
Separable programming		Particle swarm optimization
Multi-Objective programming		Neural networks
Network methods: CPM and		Fuzzy optimization
Trajectory Optimization		

Table 3-8: Methods of Operation Research [91]

A very powerful tool used in Statistics is the Design of Experiments. This is a structured set of tests of a system or process. The design of experiment is comprised of: i) a response(s), ii) a factor(s) and ii) a model.

- **A response** is a measurable result—fuel consumption, maintenance cost, NOx emissions etc.
- **A factor** is any variable that the experimenter judges may affect a response of interest. Common factor types include continuous (may take any value on an interval; e.g., climb rate), categorical (having a discrete number of levels; e.g., a specific company or brand) and blocking (categorical, but not generally reproducible; e.g., rotorcraft pilot to pilot attitude).
- **A model** is a mathematical surrogate for the system or process.

The experiment consists of exercising the model across some range of values assigned to the defined factors.

In deciding what values to use more precisely, the goal is to achieve coverage of the design space that yields maximum information about its characteristics with least experimental effort, and with condensing that the set of points sampled gives a representative picture of the entire design space. Numerous sampling methods exist to do this; which one to use depends on: i) the nature of the problem being studied, ii) the resources available time, iii) computational capacity, and iv) how much is already known about the problem.

In a helpful taxonomic discussion, Noesis Solutions [92] observes that DOE methods can be classified into two categories: i) orthogonal designs and ii) random designs. The orthogonality of a design means that the model parameters are statistically independent and that the factors in an experiment are uncorrelated and can be varied independently. Widely used orthogonal designs methods are i) fractional- and full-factorial designs, ii) central composite designs and iii) Box-Behnken designs [93]. A factorial design has some disadvantages. Initially it is usually unclear which factor is important and which is not. Since the underlying function is deterministic, there is a possibility that some of the initial design points collapse (therefore it is called a collapse problem) and one or more of the time-consuming computer experiments become useless. Most classic DOE's are only applicable to rectangular design regions and the number of experiments increases exponentially with increasing number of levels. A factorial design table is shown in Table 3-9.

A random design means that the model parameter values for the experiments are assigned based on a random process, which is another widely used DOE method. The most commonly used random DOE method is the so-called Latin Hypercube Design (LHD). A sample of a random design table is shown in Figure 3-11.

The collapse problem, which occurs at the factorial design, does not occur with LHDs. This is because if one or more factors appear not to be important, every point in the design still provides some information regarding the influence of the other factors on the response. In this way, none of the time-consuming computer experiments will turn out to be useless.

Orthogonal Array							
FACTORS							
TRIAL NUMBER	A	B	C	D	E	F	G
1	0	0	0	0	0	0	0
2	0	0	0	1	1	1	1
3	0	1	1	0	0	1	1
4	0	1	1	1	1	0	0
5	1	0	1	0	1	0	1
6	1	0	1	1	0	1	0
7	1	1	0	0	1	1	0
8	1	1	0	1	0	0	1

Table 3-9 Factorial Design Table [92]

A more detailed analysis of some principal DOE methods and the reasoning for the LHD selection is given below:

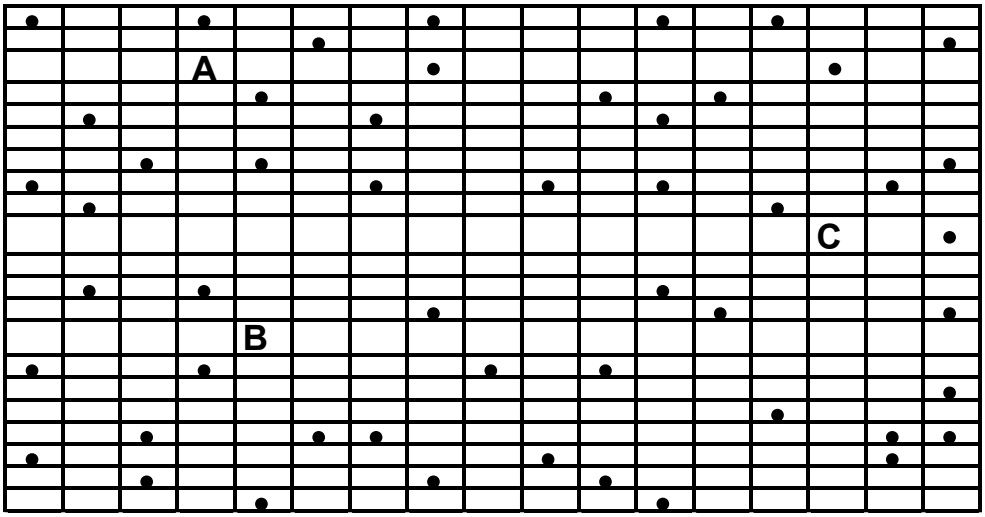

Figure 3-11: Random Design Table [92]

- **Full factorial designs:** The experiment is run on every possible combination of the factors being studied. The most conservative of all design types, yielding the highest condense results, but at the highest cost in experimental resources. The sample size is the product of the numbers of levels of the factors: a factorial experiment with a two-level factor, a three-level factor and a four-level factor requires 2 X 3 X 4 = 24 runs. Too expensive to run in many if not most cases.

- **Fractional factorial designs**: The experiment consists of a subset (fraction) of the experiments that would have been run on the equivalent full factorial design. The subset is chosen to expose information about the most important features of the problem studied, using only a fraction of the experimental runs and resources of a full factorial design. Exploits the sparsity-of-effects principle that main effects and low-order interactions usually dominate a system, and thus only a few effects in a factorial experiment will be statistically significant.

The drawback of this method is that there is no assurance that the chosen samples are independent, and the parameters has not been chosen more than once.

- **Latin hypercube designs**: Latin hypercube sampling is a statistical method for generating a sample of plausible collections of parameter values from a multidimensional distribution. In statistical sampling, a square grid containing sample positions is a Latin square if (and only if) there is only one sample in each row and each column. A Latin hypercube is the generalization of this concept to an arbitrary number of dimensions, whereby each sample is the only one in each axis-aligned hyperplane containing it. When sampling a function of N variables, the range of each variable is divided into M equally probable intervals. M sample points are then placed to satisfy the Latin hypercube requirements; this forces the number of divisions, M, to be equal for each variable. This sampling scheme does not require more samples for more dimensions (variables); this independence is one of the main advantages of this sampling scheme. Another advantage is that random samples can be taken one at a time, remembering which samples were taken so far.

The method, which is more suitable for this research, is the LHD method for the following two reasons:

a. It minimizes the computation time and

b. It enhances the independence of the parameters because it provides a sample that the chosen parameters are considered only once.

During this work, four different sample sizes with a set of operating parameters have been run to find the sample size that would provide a good population of data that will allow for an effective data analysis. The values for the samples were estimated using 2 different methods. For the first 80 samples, the factorial method was used while for the 100, 180 and 400 samples the LHS method was used. The details of the LHS

implementation and the Python code developed are explained in the flowchart at Appendix H.

3.3.1 DOE Set Up

The basic tool that was used to produce engine performance data in this research is HECTOR. HECTOR code (FORTRAN) uses a single core and has numerous settings; some of them relate to blade aeroelasticity and mission dynamic time step and it allows for different levels of accuracy. The execution time range depends on the settings that relate to the blade aeroelasticity, the mission dynamic time step, and the desired accuracy.

The execution time for a single mission with 7 segments (Idle, Hover, Climb, Cruise, Descent, Hover, and Idle) may vary from 2 to 8 hours while for other more complicated missions can be 2 to 3 days, per mission, per core. That feature makes it imperative to search for the minimum sample number of missions while trying to keep a high level of accuracy.

Due to the high number of simulations needed to conduct this DOE a code was written in Python that automates the process and allows to minimize the time for the: i) mission file administration ii) the mission settings user input and iii) the results post-processing. The automation process is divided in two parts. The first part is executed before HECTOR simulations commence. The second part is executed after all HECTOR simulations have been executed and automates the process which finally creates the lifing data population.

The scripts in the first part uses as a base the design space which relates to the flight profile operating parameters. The design space for these parameters is presented in Table 4-4. The first script implements the LHS method which estimates a set of values for the desired sample relative to the operating parameters. A representative sample of a set of values for: i) payload ii) climb rate and iii) ISA Deviation is shown in Figure E-1 in Appendix E. Then the code uses this set of values to create subfolders which will store HECTOR simulation results. For example, for a sample of 400 sets of operating parameters, 400 subfolders should be created to store HECTOR output files. The name for every subfolder is based on a mask (Payload ,climb rate, ISA deviation) that relates to the operating parameter values. For example, the subfolder

"_0.81_5.72_9.54 "means that the subfolder hosts 10 files created as HECTOR output that relate to: i) payload = 0.81 ii) climb rate=5.72 and iii) ISA Deviation=9.54.

The scripts that relate to the second part of the process run after HECTOR simulations were executed. A script alters the names of the 10 HECTOR output files so that the resulting file name includes the operating parameter values. For example, a HECTOR output file name "Engine_Performance_Vector_Data.dat" is altered to include the operating variables and is renamed to "Engine_0.81_5.72_9.54.dat". A copy of the resulting files is then transferred to a central folder which stores all the files that relate to the DOE sample.

At this point the data stored in the central folder can be used to run the 2 scripts escribed in paragraph 3.4.1. The flowchart in Appendix H shows the methodology used and Table H-1 presents the developed scripts and their input and output files.

3.3.2 LHS and DOE Results Data Analysis

The LHS method, which was addressed before, will provide a sample with life data, representative of the entire design space. The generated data can be used with one of the following methods:

a. Identify the significant inputs: The acquired data can facilitate a sensitivity analysis, which will allow the operating parameters effect assessment on the engine's life. This knowledge can prove very useful to an operator when a decision is made for the rotorcraft selection in relation to the desired missions flown and the rotorcraft capabilities.

b. Compare Alternatives: The DOE can be used for other potential engine models or types and provide data that could allow us to compare the optimum between the alternatives.

c. Reduce life data variability: The life data assessed from the DOE follow a statistical distribution with certain variability. The use of a method other than the LHS may decrease the data variability and provide a more robust model to assess the engines life. This capability can be combined with a trajectory optimization, which will allow the operator to assess the optimal values of the operational parameters in relation to the desired outcome. This outcome can relate to either NOx reduction, fuel consumption or any other parameter.

d. Optimize engine maintenance cost: The data that relates to the engine's life can be used as input to an optimizer that will assess the optimum cost concerning maintenance and the mission profiles, which has been used in the experiment.

e. Minimize, maximize or target an output: This is a potential alternative to all the other uses mentioned above. A suitable optimizer can be used which will use the operator's flight profile and relate the operating parameters with the desired output.

To exploit the component life results, which is the outcome of the experiment, a robust and appropriate method will be needed. Data analytics offer different methods and the selection should consider the data population and their nature. The selected tool to analyse the DOE results is the kriging method, which will be described, in the next paragraph. Before the model description, it is deemed necessary to discuss the reasoning for this selection. The next paragraph will address well-known methods used in data analytics provide an insight for the model selection.

3.3.3 Data Analysis Method

The requirement in this research is to construct an approximation model based on data from a computer experiment, and to use this approximation model as a surrogate for the computer model. The computer experiment is a collection of pairs of input and responses from runs of a mission simulator (HECTOR).

Data science has developed a variety of methods and tools due to the advances in computers technology and software development that can help us meet the research requirement. Data analytics, which is a part of this science, can use a variety of tools to find the connections between data and finally understand what data is really telling us. Due to the enormous need for data exploitation and effective forecasting many tools have been developed and names like: i) artificial intelligence, ii) machine learning, and neural networks, iii) fuzzy logic, and iv) spatial interpolation has gained popularity and has been introduced in the engineering field. The next paragraphs address these tools and attempt to shed light regarding their implementation.

Data analytics can be divided in the following 4 categories: i) Descriptive, ii) Diagnostic, iii) Predictive and iv) Prescriptive. Out of the four, the predictive analytics is about forecasting, and it is based on tools that exploit previous knowledge. The set of criteria that prioritize or sort this knowledge and the methods to learn from the

existing data support this process and the development of artificial intelligence (AI) tools.

Artificial intelligence (AI) which became a promising scientific field uses the increased computational power and the advances in software to simulate human intelligence behaviour. The AI's primary aim is to allow the computers learn automatically without human intervention or assistance and adjust actions accordingly and, its application cover various fields from robotics to imaging, diagnosis or engineering. Machine learning algorithms is a subfield of the artificial intelligence and can be further divided in various categories as presented in figure 3-12. The artificial neural networks are one of the machine learning tools and are very popular in engineering research.

Wikipedia explanation for artificial neural networks (ANN) is simple: "An artificial neural network is an interconnected group of nodes, like the vast network of neurons in a brain. Each circular node represents an artificial neuron and an arrow represents a connection from the output of one artificial neuron to the input of another.

The extensive usage of this tool gave the opportunity to researchers to validate its implementation in engineering, clear its boundaries and find the areas where it can be used either independently or in combination with others. As all tools, though it has advantages and disadvantages and its implementation relies to the problem specific conditions and requirements.

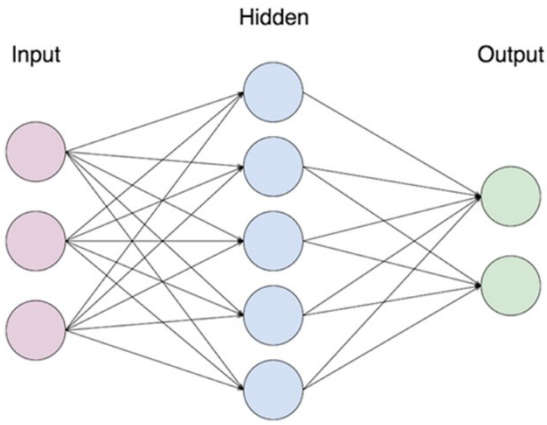

Figure 3-12 : Artificial Neural Network example

In addition to ANN, literature review showed that fuzzy logic could be used complimentary to ANN. Fuzzy logic is a methodology that developed in 1960s when Dr Zadeh [94] was working on the problem of computer understanding of natural language. Fuzzy logic seems closer to the way our brains work and as Wikipedia quotes [95], “is a form of many-valued logic in which, the truth-values of variables may be any real number between zero (0) and (1) inclusive. It is employed to handle the concept of partial truth, where the truth-value may range between completely true and false. By contrast, in Boolean logic, the truth-values of variables may only be the integer values 0 or 1”.

The inherent capability of fuzzy logic to classify the inputs according to their significance led the researchers in using it as a complimentary method to ANN. This is because neural networks capability to handle huge amount of raises an issue on how to understand which data are significant in every case. The solution to that problem is found in fuzzy logic implementation. Mathur [96] showed that artificial neuro fuzzy inference system (ANFIS) which combine both neural network and fuzzy logic principles could be used as a universal estimator and its results can be compared to kriging. Kriging, which is a preferred method for spatial interpolation, can be another good candidate in this research because it allows the estimated values to be expressed as linear combination of the known /measured values, after modelling the spatial covariance structure of the data.

Ilic [97] showed that both ANN and kriging methods can be used in this occasion, but ANN not being a non-exact interpolator it is not guaranteed to provide unbiased estimates. He evaluated ANN use in spatial interpolation and concluded that they can be used as an alternate solution, but they cannot provide the same accuracy as simple methods like Kriging. To that end, Nevtipilova [98] tested ANN’s multi-layer perception model (MLP) for spatial interpolation vs common interpolation techniques like inverse distance weighing (IDW) and ordinary kriging (OK) and evaluated the results based on the root mean square error (RSME). The evaluation concluded that the RSME resulting from ANN was higher than the one from IDW and OK and more time consuming. “The use of multilayer perceptron for spatial interpolation is an interesting option to classical methods. Bur it is requiring more knowledge of theory from the user and time consuming. The results are often uncertain and the training of MLP has to be

repeated many times to reach satisfactory results". Gumus and Sen [99] derived almost the same results while comparing ANN versus Inverse Distance Weighted (IDW), Ordinary Kriging (OK), Modified Shepard's (MS) and Multiquadric Radial Basis Function (MRBF).

D.G. Krige [100] has originally developed Kriging as a spatial interpolation method. It has later been adapted to computer experiments by Sacks et al [101]. Cranfield University researchers evaluated the Kriging method extensively in surrogate models formulation ([102], [103], [104]) and proved that it can approximate the response of the design space with sufficient accuracy.

The idea behind Kriging surrogates is to consider the output y(x) as a realization of a stochastic process Y (x) (Santner et al., 2003):

$Y(x) = \mu(x) + Z(x)$ 3-3

Where μ(x) is a deterministic function approximating the mean trend of the output. The departure from this trend is assumed to be a Gaussian process Z(x) with zero mean and auto covariance Cov [Z(x), Z(x')] = 2 R(x, x'), where σ^2 is the process variance and R(x, x¨) is the auto-correlation function providing the dependence structure.

The incorporated Kriging interpolation model in this research used a class developed in python by Pedregosa et al [105]. The next table presents the class main parameters for tuning.

The kriging method parameters tuning has a direct and influential impact on the approximating capability and the prediction accuracy of the method. It always requires numerical optimization of the nonlinear and multi-modal likelihood function to obtain the optimal kriging hyper-parameters based on the maximum likelihood estimation theory (MLE). The selected numerical optimization is the constrained optimization by linear approximation (COBYLA) which is a code developed by Powel while working for Westland Helicopters [106].

Parameter	Options
regr :	'constant', 'linear', 'quadratic'
corr	absolute_exponential', 'squared_exponential', 'generalized_exponential', 'cubic', 'linear'
theta0	The parameters in the autocorrelation Model. Default assumes isotropic autocorrelation model with theta0 = 1e-1.
optimizer	'fmin_cobyla', 'Welch'
random_start	The number of times the Maximum Likelihood Estimation should be performed from a random starting point. Default does not use random starting point (random_start = 1)
Nugget	Introduces a nugget effect to allow smooth predictions from noisy data. Default assumes a nugget close to machine precision for the sake of robustness (nugget = 10. * MACHINE_EPSILON).

Table 3-10: SciKit Kriging Model Parameters

3.3.4 Validation Method

The methodology so far showed the steps to create a population of data that relate to engine's turbine life and a surrogate model, which is based on kriging. The next step is to evaluate the model predictive performance and make sure that the prediction error and the model fitting to the observed data are acceptable. This step is important because it is not certain that a model with a good fitting based on observed data, will have the highest predictive accuracy for future data [107].

The fit of a model improves with the complexity of the model, i.e. as more predictors are included in the model the *R*2 value is expected to improve. If predictors truly capture the main features of the data, then they are retained in the model. The trick to building an accurate predictive model is not to over fit the model to the training data.

When the outcome is quantitative (as opposed to qualitative), the most common method for characterizing a model's predictive capabilities is to use the root mean squared error (RMSE). This metric is a function of the model residuals, which are the observed values minus the model predictions. The mean squared error (MSE) is calculated by squaring the residuals and summing them. The value is usually interpreted as either how far (on average) the residuals are from zero or as the average distance between the observed values and the model predictions.

If we assume that the data points are statistically independent and that the residuals have a theoretical mean of zero and a constant variance σ^2, then:

$$E(MSE) = \sigma^2 + (Model\ Bias)^2 + Model\ Variance \qquad \textbf{3-4}$$

The first term, σ^2, is the irreducible error and cannot be eliminated by modelling. The second term is the squared bias of the model. This reflects how close the functional form of the model is to the true relationship between the predictors and the outcome. If the true functional form in the population is parabolic and a linear model is used, then the model is a biased model. It is part of systematic error in the model. The third part is the 'model variance'. It quantifies the dependency of a model on the data points, which are used to create the model. If a change in a small portion of the data results in a substantial change in the estimates of the model parameters, the model is said to have high variance.

An ideal predictor is one, which will learn all the structure in the data but none of the noise. While with increasing model complexity in the training data, Prediction Error (PE) reduces monotonically, the same will not be true for test data. Bias and variance move in opposing directions and at a suitable bias-variance combination the PE is the minimum in the test data. The model that achieves this lowest possible PE is the best prediction model. The following figure is a graphical representation of that fact.

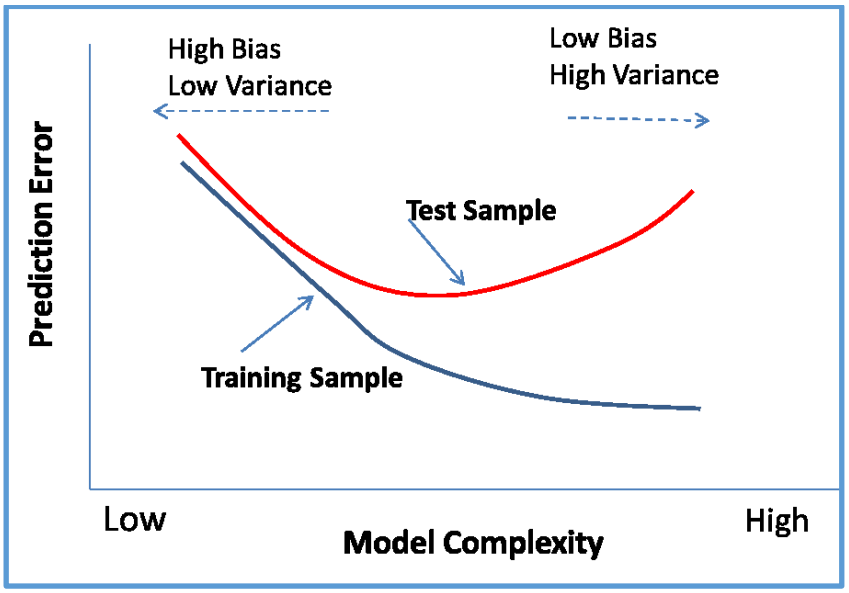

Figure 3-13: Sampling Prediction Error vs Model Complexity [107]

Cross-validation is a comprehensive set of data splitting techniques which helps to estimate the point of inflexion of PE.

In a prediction problem, the data are divided into 2 sets: i) the training data set and ii) the testing data set. The training set contains known data while the testing set contains unknown data against which the model is tested. A cross validation model needs to avoid overfitting with the known data and minimize the prediction error to unknown datasets. The cross-validation method yields meaningful results if the validation set and training set are drawn from the same population, the sample volume is big enough to allow for efficient interpolation, and only if human biases are controlled [108].

Table 3-11 shows the available methods for cross-validation. The exhaustive cross-validation methods are the ones, which learn and test on all possible ways to divide the original sample into: i) a training and ii) a validation set. Non-exhaustive cross-validation methods do not compute all ways of splitting the original sample. Those methods are based on exhaustive cross-validation methods like the “leave-p-out cross-validation” method.

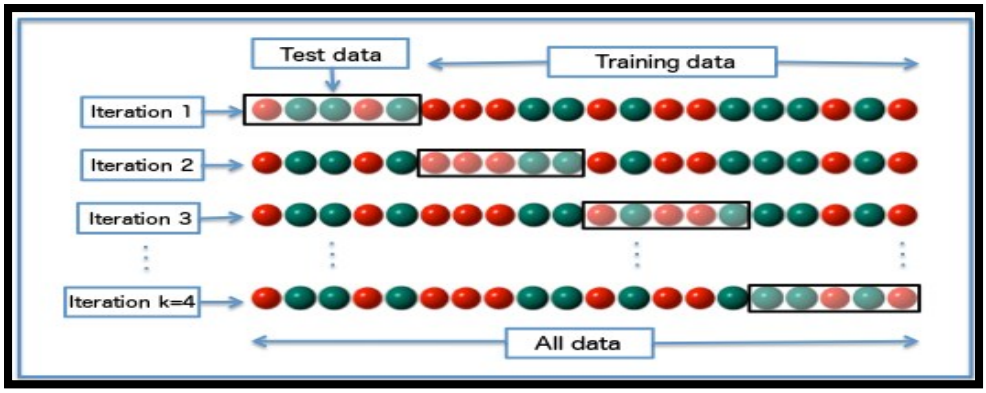

Figure 3-14: K-fold cross-validation [108]

The criteria, that can be used to choose the right method, relate to the sample size and they are i) the type predictive behaviour and ii) the required computational time iii) the data sparsity.

Exhaustive cross-validation	**Non-exhaustive cross-validation**
Leave-p-out cross-validation	*K-fold* cross-validation
Leave-one-out cross-validation	Holdout method
	Repeated random sub-sampling validation

Table 3-11: Common Types of Cross-Validation [108].

The method used in this research is the Leave p-out One because it is a least computational expensive method and its prediction capability is better in cases where we have sparse data sets.

Leave-one-out cross-validation (LOOCV) uses one observation as the validation set and considers the remaining observations as a training set. This process is repeated until all the population data have been used once. The Y-Axis has the predicted values while the X-axis represents the test values. A high level of accuracy is represented when the value scattering is around a line of 45 degrees.

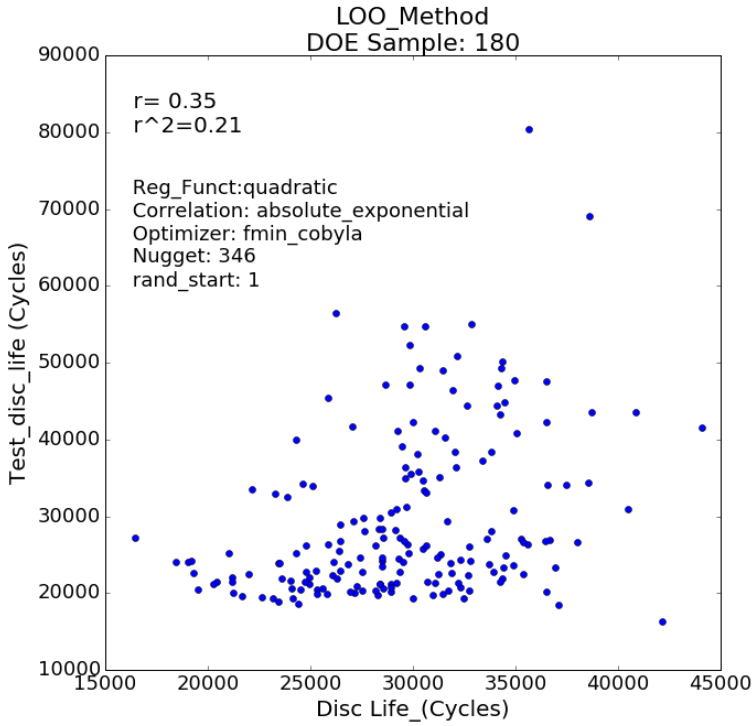

Figure 3-15: LOOCV Method Implementation (Sample Size : 180).

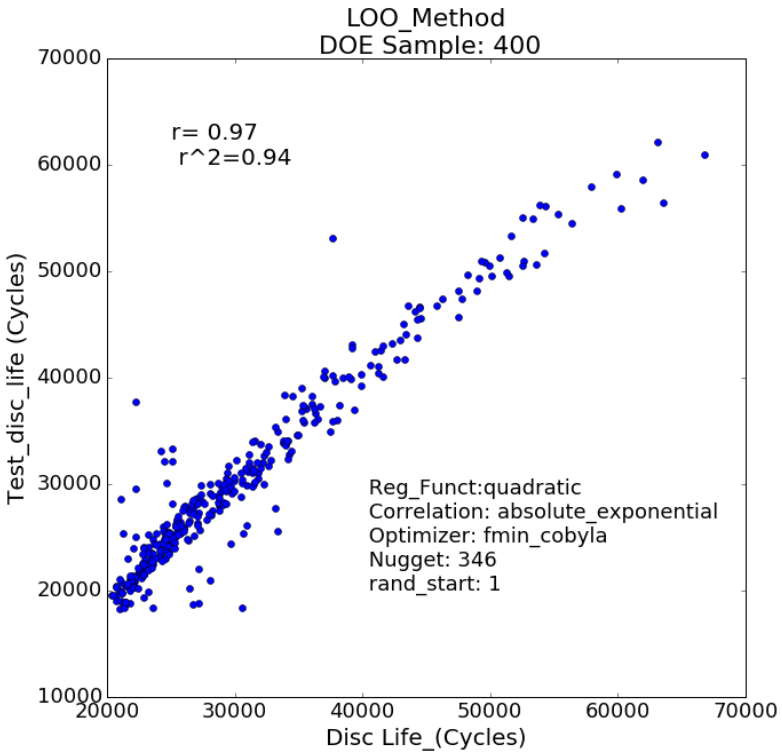

Figure 3-16: LOOCV Method Implementation (Sample Size: 400).

Figure 3-15 shows the prediction accuracy between two samples. The first sample relates to the experiment of 180 simulations out of which the 130 only converged and produced results for the turbine life. The second graph relates to the 400 simulations and shows that the calculated values shown in the X-axis are very close to the values (shown in the Y-Axis) which are estimated by the LOOCV method. A detailed analysis of how the method works with data produced by this research is shown in Appendix I.

Regarding the correlation between the predicted vs calculated value two coefficients are employed; namely the: i) Pearson correlation (r) and, ii) coefficient of determination r2. with values range (-1,0,1) and (0,1) respectively. [109], [110]

3.4 Engine Component Life Estimation Module

As mentioned in the literature review, the estimation of the engine's component life was the subject of extensive research and statistics reports from consultant companies and government agencies.

FAA accident statistics for a period of 11 years 1996-2007 revealed that the major cause for accidents in turboshaft powered helicopters was the turbine section. While other components may fail and impose maintenance actions the turbine module is the most critical due to the hostile operating environment. In addition, Spera's report [111] on experiments conducted at the Lewis research centre (NASA) revealed that the long-term failure mechanisms are the ones that dictate life. At temperatures below approximately 800^{o} C (1073 ^{o}K) mechanical fatigue is often the dominant failure mode. At higher temperatures, more than 1000 °C (1073 ^{o}K), creep, oxidation, and thermal fatigue (acting alone or together) usually cause failure.

As mentioned in paragraph 2.2.4.1, the physical method has several clear benefits compared to the other prognostic approaches. There are different physical models to implement and the criteria for the chosen solution may very well be i) the computational time, ii) the available component data and, iii) the prediction accuracy.

A framework comprised of different in-house and commercial software tools has been developed for this research. The framework parts communicate and exchange information with a code which was built in Python. A more detailed discussion follows in the next paragraphs.

3.4.1 Code description

The developed framework for this research is comprised of the following parts:

a. An in-house tool for flight dynamics simulation named Hector. The simulation computational time depends on the desired accuracy, written in FORTRAN.

b. An in-house engine performance software named Turbomatch, written in FORTRAN.

c. A 'rainflow' counting cycles algorithm, written in FORTRAN

d. A code to estimate the disc and blade stresses, built in Matlab.

e. A code, written in Python, which i) establishes the communication links between the component/module inputs and outputs, ii) uses data from the material database, iii) plots the stress, altitude and TET history vs time and finally, iv) calculates the turbine remaining life due to LCF.

The code estimates the turbine life using the strain-based method. Figure 3-17 shows a higher-level flow-chart for the code, which acts as a wrapper for the different tools and modules. The code uses two scripts, which are named "Hector_Post_Process.py" and "LCF_life.py".

First Script: Hector_Post_Process.py

The first script is comprised of two sections. The first reads HECTOR output files extracts data relative to the engine performance and flight behaviour and then creates a new file that stores the values for post-processing with the Turbomatch code. This file contains data for the engine performance and a new column that helps to filter the flight segments of the helicopter mission. This is because HECTOR pre-built bricks for the climb, cruise and descent are named "cruise" and an extra column was needed to separate the data relative to each segment. This filtering is very important because it makes easier to isolate the maximum values for each segment or sum up the values for certain variables like fuel consumption or segment duration.

More specifically the file named "hector_mission_segments_seg" includes data for i) engine power, ii) operating TET, iii) compressor rotation (PCN), iv) climb rate, v) ISA deviation, vi) flight segment and vii) mission time step.

The second section uses the values for i) altitude, ii) ISA deviation, iii) Mach number and, iv) engine's power. The output of this section is a post-calculation for bleed air, is used for the cooling temperature. This value is used later in the Matlab code to implant the effect of temperature variation in the disc stresses calculation.

This section uses a template containing "placeholders" for the values that need modification in the Turbomatch input file. Once the input file has all the needed data Turbomatch then runs the mission once again in off-design mode. The next step is to extract the TET and cooling temperature from the output file and use them to create the Matlab input file. To feed the mission input file with the appropriate values the code uses the same method used to modify the input file in Turbomatch. The first script output file is named "Hector_output.xlsx" and is used as an input to the second script.

Second Script: "LCF_life.py"

The second script is comprised of two sections. The first section reads the file "Hector_output.xlsx" and executes the Matlab code. The Matlab code used to estimate the stresses and the oxidation and creep life of the engine has been developed by Elter [13] and was oriented to estimate the life of a turbofan. To use the code for this research the code had to be altered to serve the needs of a helicopter flight and manoeuvres. The initial code used a basic profile with segments related to the aeroplane flight. These are: i) the take-off, ii) climb, iii) cruise, iv) descent and, v) taxi. The modified code assumes every time step in the flight is a small segment and enters in the code the following inputs: i) the engine rpm related to the off-design operation, ii) the TET and, iii) the cooling temperature. The output values are saved in Matlab's workspace variables and then are parsed and stored in a file named "blade/disc_stress_data.csv". Data along with the TET and altitude can be plotted and show the stress and temperature history for the duration of the flight. Figure 3-18 shows a typical flight history for an Oil & Gas mission.

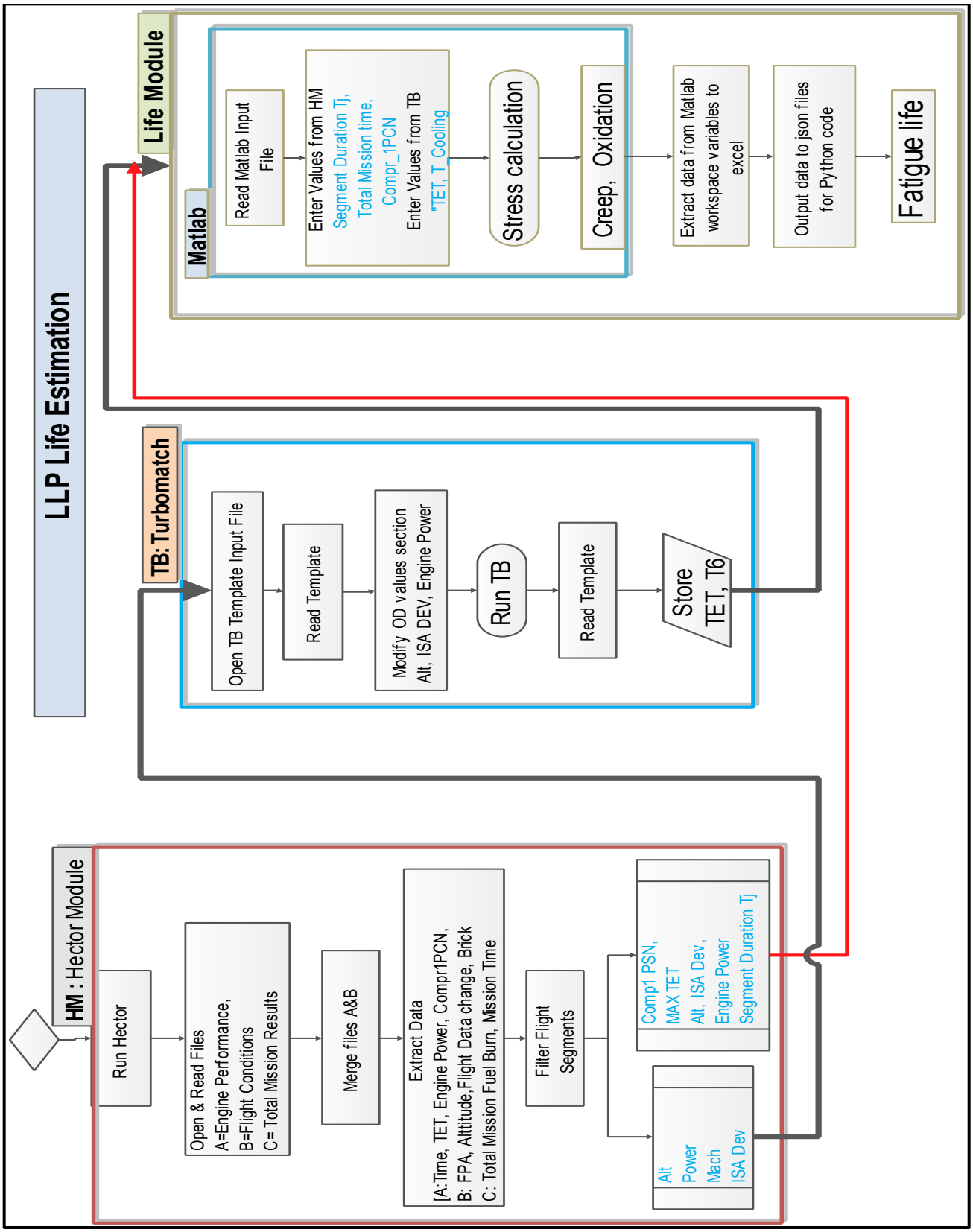

Figure 3-17: A Higher-level flow chart for the Framework.

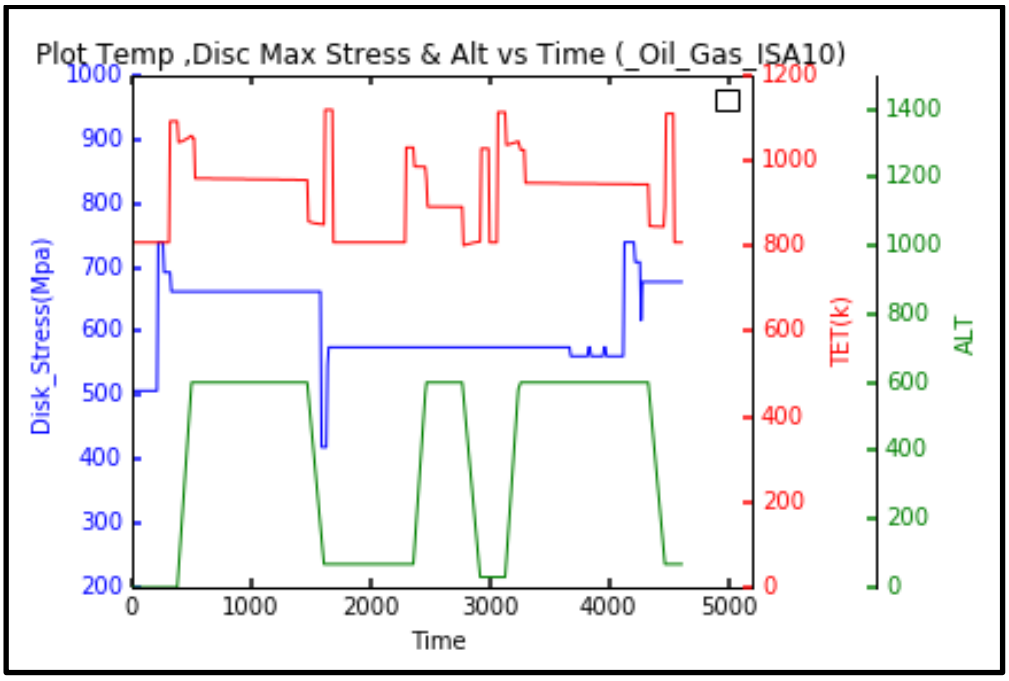

Figure 3-18: Mission Profile, TET, Disc Stress vs Time for an example Oil and Gas mission

The second section of the code estimates the turbine failure limit. This limit is the minimum value of the disc or blade failure limits.

Low Cycle Fatigue Code

Matlab produces two excel files as outputs, which store the stresses history for the turbine blade and disc. The blade and disc stresses that calculated from the Matlab code at the first section of the script comprise the mission load history and are usually of variable amplitude. To compare fatigue behaviour from variable amplitude histories to fatigue curves obtained with simple constant amplitude loading, a cycle counting method is needed. Good cycle counting methods must count a cycle with the range from the highest peak to the lowest valley and must try to count other cycles in a manner that maximizes the ranges that are counted. The ‘rainflow’ method is the most popular method of cycle counting and is the chosen method for this research.

These stress values are converted to a “.dat” file format, which is used as input to the rainflow code created by Irvine [112]. The rainflow code output is in a *.dat” file format and provides a table with stress related data. Table 3-12 presents the data.

The column “Range Limits” is created from the values in the columns “Max Peak” and “Min Valley”. The Max amplitude value relates to the amplitude created from the equations presented in Figure 2-4. This amplitude value is entered as nominal stress in the Coffin and Manson equation 2-4. Figure 3-19 shows a stress history for a passenger mission and the stress related ranges and amplitudes calculated from the “rainflow code”.

No	RANGE LIMITS (UNITS)			CYCLE COUNTS	MAX AMP	MAX MEAN	MIN VALLEY	MAX PEAK
1	218.6	to	242.9	1	121.4	622.4	418.4	738.6

Table 3-12 : Rainflow Method Results

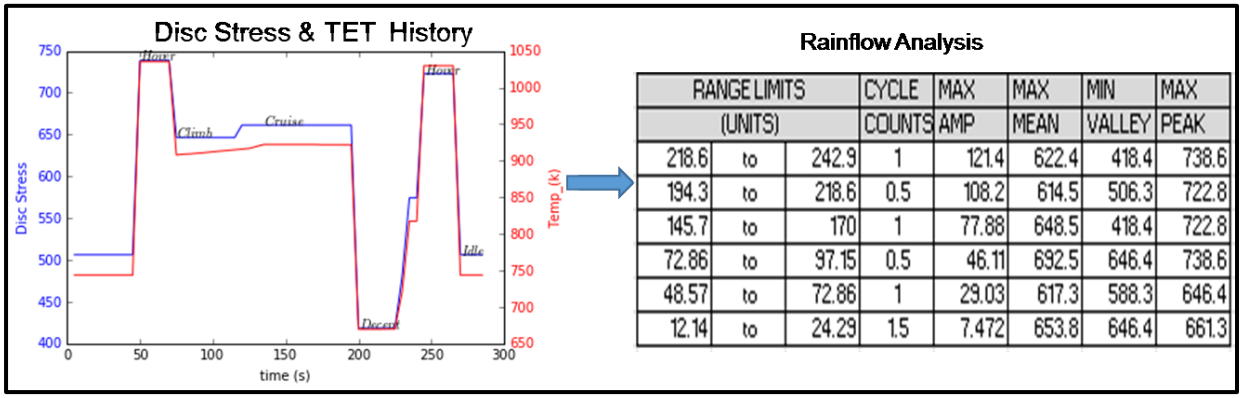

RANGE LIMITS (UNITS)			CYCLE COUNTS	MAX AMP	MAX MEAN	MIN VALLEY	MAX PEAK
218.6	to	242.9	1	121.4	622.4	418.4	738.6
194.3	to	218.6	0.5	108.2	614.5	506.3	722.8
145.7	to	170	1	77.88	648.5	418.4	722.8
72.86	to	97.15	0.5	46.11	692.5	646.4	738.6
48.57	to	72.86	1	29.03	617.3	588.3	646.4
12.14	to	24.29	1.5	7.472	653.8	646.4	661.3

Figure 3-19: Disc Stress History and ‘rainflow’ analysis

In addition, the stress value at the “Max Peak “column is used to assess the values that relate to the specific material properties: i) UTS ii) Elastic Modules (E) and III) 0.2%YS.

After this point, the code is using these values to the equations 2-4 up to 2-11 presented in paragraph 2.2.1.2. The failure limit for each range is calculated using Newton’s iteration method.

To evaluate damage from each cycle in a variable amplitude load or strain history, a quantifying measure is required. The most common measure is the life fraction or cycle ratio for crack nucleation and the crack length for crack growth. Life fraction defines the damage caused by one cycle as $D = 1/N_f$, where N, is the number of repetitions of this same cycle that equals the median fatigue life to failure. Once the damage from each cycle has been calculated, it is accumulated or summed over the entire load

history. The linear damage rule also referred to as the “Palmgren-Miner rule,” is the simplest rule and is often used. This rule assumes a linear summation of damage and predicts failure when:

$$\sum_1^i \frac{n_i}{N_{f_i}} = 1 \qquad 3\text{-}5$$

When the load levels are relatively low such that the resulting strains are mainly elastic, the strain-life and stress-life approaches usually result in similar predictions [41]. When the stress history contains large overloads, significant plastic deformation can exist, particularly at stress concentrations, and the load sequence effects can be significant. In these cases, the strain-life approach is generally superior to the stress-life approach for cumulative fatigue damage analysis. An additional advantage of the strain-life approach compared to the stress life approach is that it accounts for load sequence effects and is generally advantageous for cumulative damage analysis of notch members, in which significant plasticity usually exists. It uses the material cyclic stress-strain curve and a notch strain analysis method to obtain notch root stresses and strains, which are then used for life predictions. To that end, this research adopts the strain life approach because it covers both the elastic and plastic region of the materials used

An important capability of the developed code is that it is used to calculate the effect of the material properties and the notch sensitivity to the turbine life and help us perform a sensitivity analysis for these parameters. The effect of the case study in the next section examines the parameters effect. A flowchart at Appendix C presents the steps for the lifing code.

3.4.2 Material Safety Factors Sensitivity

The relation between notch factor (K_f) and elastic stress concentration factor (K_t) has been shown in equation 2-9 and 2-10. The lifing code developed in this research provides the capability to estimate the effect of both factors that relate to the engine’s turbine calculated life due to LCF. A sensitivity analysis will be shown in the case scenario at the next chapter.

3.5 Shop Visit Cost Prediction

The engine degradation can be classified in two categories the one being the mechanical degradation in which the components may fail and cause secondary damages and the performance degradation which can be further classified to recoverable, unrecoverable and permanent [31].

The recoverable degradation can be eliminated by maintenance actions like compressor cleaning or use of inertia separator filters to avoid air particles or sand, etc. The unrecoverable degradation can only be recovered with a major overhaul. It relates to permanent degradation caused by component ageing and can only be removed by replacing or repairing engine components.

The engine induction is compulsory at the OEM indicated time interval or during a maintenance power check flight that shows the engine inefficiency to deliver the required power according to the OEM standards.

A method to predict the time for engine induction was used by Hanumanthan [18] that related the engine TET margin consumption with the cycles to failure cumulative Weibull curve, based on degradation data which were provided in a NASA report [19] and related to JT9 engines. The graph in Figure 4-17, paragraph 2.2.2, shows an example of the TET margin consumption. Unfortunately, this degradation data found in the NASA report related to the turbofan engines flight cycles which, as analyzed in paragraph 2.2.3, are calculated based on different assumptions that the ones for turboshaft engines. Therefore, this method cannot be used to assess the engine induction service due to performance restoration. This research looked at the available data in the public domain and used the TBO values provided by the OEM.

3.6 Cost Module

The cost module built in this research estimates the costs as described in the HAI guide [5]. In addition, it will be a useful tool for the operator that will facilitate his decision on the preferred method to use concerning engine induction for service.

3.6.1 Variable Costs Estimation

The variable cost that was used is based on Harris [24] published work and operators experience and adds the engine's maintenance costs with the fuel costs. All costs are estimated on a $ / FH basis:

a. **Fuel Costs**. The basic components of the fuel calculation usually comprise the price of fuel (expressed in US$/ metric ton), the consumption rate and the fuel characteristics. The fuel costs are estimated from the equation:

$$\text{Fuel Cost} = \frac{\textbf{Gallons of fuel used}}{\textbf{Flight Hour}} * \frac{\textbf{Fuel Price}}{\textbf{Gallon}} \qquad 3\text{-}6$$

b. Engine Maintenance costs

Following the three-level maintenance system mentioned before a logical equation would combine labour and parts per level and an induction cost every time the engine should enter the MRO facility for maintenance. That is:

$$\text{Maintenance Cost} = \sum_{i=1}^{n}(\boldsymbol{MMH} + \boldsymbol{Parts})(\boldsymbol{Olevel}) + \sum_{i=1}^{m}(\text{MMH} + \text{Parts})\ (\text{I level}) + MRO_{SV} + Parts\ (LLP) + \text{MRO\_SV+ Parts (LLP)} \qquad 3\text{-}7$$

Where: (n) The inspection intervals until the engine induction for Overhaul and (m) the times that THE engine has been inducted into a repair centre.

Formula Explanation: The component named "Maintenance Repair and Overhaul _shop Visit" (MRO_SV) is a figure that is estimated from the average cost of several engines and is mostly based on the repair centre experience. It includes the labour for inspection and repairs in addition to all consumables and the test cell costs. The LLP or engine accessories replacement and the implementation of Service Bulletins that have been published from the engine OEM are added to the induction cost. An imaginary cost analysis that relates to all levels of maintenance could include the costs presented in Table 3-13.

Maintenance Action	Price	Interval	Maintenance Level
Inspections			
Per Flight Hour/ Calendar	per MMH	25 -50-75-100-125-175-200 etc Hour/30 days	O
Phase Inspections	10,000	150 -300 -450 etc Hours	I
Life limited parts			
HPT - 7000 Cycles	210,000	7000 cycles	I-D
Aft Turbine Shaft - 8000 Hour	45,000	8000 hour	D
Heavy maintenance parts			
Starter Generator	15,000	On condition	
Accessory gearbox	40,000	On condition	
Engine Heavy Maintenance			
Overhaul - 2500 Hour	500,000	2500 hour	D
MMH: Maintenance Men Hours			
O: Operator Level , I: Intermediate Level, D: Depot Level -(OEM, MRO)			

Table 3-13: Notional Table with Maintenance costs per level of maintenance [24].

- MMH for O level

Weight Class	Engine Number	MMH/FH//per engine	Total MMH/FH
Light Piston	100%	0.15	15%
Light Turbine	100%	0.15	15%
Light Turbine	200%	0.15	30%
Medium	100%	0.2	20%
Medium	100%	0.2	40%
Heavy Turbine	200%	0.3	60%
Heavy Turbine	300%	0.3	90%

Table 3-14: Engine On-Aircraft Labor Hours per Flight Hour [24]

- MMH for I Level:

The value for the MMH /FH that will be used is 0,8 MMH/FH. This value was taken from an operator [113] that owns 4 helicopters for EMV missions and comply with the value found in Harris [7] (page 624) .

- MRO_SV price:

$$\text{Engine Restoration Price} = C_{eng}\left(\frac{\$}{FH}\right) = 1.74 * SHP_{inst}^{0.67} \quad \textbf{3-8}$$

Where SHP: Shaft Horsepower installed

This estimation formula is proposed from Harris [7]. He proposes an estimation cost formula method for engine overhaul which calculates a price in $ / FH. The equation derived from regression analysis is using data from a consulting company and can be used for an initial estimate as the data used reflect prices of the latest engine configurations from three major OEM (Pratt & Whitney, Rolls Royce, and General Electric).

- LLP costs data:

In general, the LLP are high-value items and is a cost driver for the engine high maintenance. Table 3-15 shows a relative cost compared to engine value.

Module	% of Cost
LPC	5%
HPC	22%
COMB	10%
HPT	45%
LPT	13%

Table 3-15- LLP Replacement Cost per Module [114]

- Engine depreciation value:

$$D = \frac{[(P - 0.15)]}{\left[\frac{LLC_{Year}}{100}\right]} = \frac{0.85}{\frac{LLC_{Year}}{100}} \quad 3\text{-}9$$

Where P = Initial Price, 0.15 P = Residual Value, LLC $_{Year}$ = the No of years for the LLP change, e.g for an engine with LLC $_{year}$ =12 then D=7.08% per year.

- The engine initial price is estimated by using the engine restoration price (equation 3-8) and the depreciation value (equation 3-9). Thus:

$$P = C_{Eng} + x * \frac{0.85}{\frac{LLC_{Year}}{100}} \quad 3\text{-}10$$

Where X: Engine induction interval (TBO) time (years) that is estimated from EGT margin module.

The LLP value at the time of the replacement is calculated using as multipliers: i) the component value from Table 3-15, ii) the engine initial price, iii) the inflation rate, and iv) the year of induction:

$$LLP\ value = 0.45 * EIP * i^{year} \quad 3\text{-}11$$

3.6.2 Cost Module Set Up

The maintenance cost estimation as mentioned in paragraph 2.3.2.2 is a complicated task and it is imperative to make assumptions for many variables. A code in python has been developed that estimates the maintenance costs for the engine lifespan. The assumptions made in the variables used in the code and a more detailed analysis of the code is presented in the methodology in paragraph 3.5.1. A short discussion in the next lines will cover some areas so that the results can be easily understood. Table 3-16 provides a view of the variables used in the module. The user enters the values of the predefined variables in an input file and then the code estimates the values for the variables shown in Table 3-16.

All these values but one is entered by the user at a template file that creates the Python input file. The very important variable that is calculated from the life module in Python code is the LLP value. Once this value is available, the Python code calculates the variables shown in Table 3-17.

As mentioned before in paragraph 3.5 the TBO value that is used is based on public domain data but once the value has been calculated as analysed in the methodology section the value is imported through the code internally as it happens to the LLP

value. Once the code has all the data available it calculates the cost assuming the two scenarios illustrated at Ackert' [17] article: i) Maximum LLP usage and, ii) Minimum Shop Visit scenario.

User Defined Values	
Variable Name	Life Limits
TBO_R_IN	TBO Interval Scenario Initial
LLP_R_IN	Life Limited Part Interval Initial
	Maintenance Costs
FC	Fuel Cost in $/Litre
MMHLC	Maintenance Man-Hours Labour Cost
MMH_O	Maintenance Man-Hours at O level required (Table 12)
MMH_I	Maintenance Man-Hours at I level required
FHPR	Flight Hours per Year
	General Costs
SHP	Shaft Horse Power
SP	Engine Salvage Price Residual Value
ELC	Engine Life Cycle expected Years
IEP	Initial Engine Price
LLP_P_C	LLP % cost -Engine value related (Table 13)

Table 3-16: User Defined Values

The rationale for these two options is that the TBO interval is fixed from the OEM and relates to engine performance criteria while the LLP replacement time relates to the condition of the component. In relation to the LLP replacement, there are 2 scenarios that can take place. One scenario is when the time to replace an LLP is close to the TBO SV and thus it may be cost effective to replace the part at the TBO SV. The other is when this replacement action can take place at a time long after the TBO SV and the operator decide to use the maximum life of the LLP.

Calculated Values	
Variable Name	Life Limits
TBO_i	TBO value for consecutive Overhauls
LLP_i	LLP replacement time value for consecutive replacements
	Maintenance Costs
FC	Fuel Costs
MMHCO	Maintenance Man Hours cost for O Level Maintenance
MMHCI	Maintenance Man Hours cost for I level Maintenance
O_MainCost	Maintenance Cost at "O" level
I_MainCost	Maintenance Cost at "I" level
TBO_Cost	Cost of Engine inducted for Overhaul
LLP_Cost	Cost of Engine inducted for LLP Replacement
TBO_LLP	Cost of Engine inducted for Overhaul and LLP Replacement

Table 3-17: Calculated Values

The decision is mainly a trade-off between the engines variable costs and the expected availability. Each method has the pros and cons addressed in the following lines:

a. The first option implies that the operator maximizes the engine availability and avoids the extra costs incurred for the LLP induction to a repair centre later. The LLP “stub life” will be lost due to early replacement. “Stub life” is an expression used to indicate the remaining life of the component due to its replacement.

b. The second option takes advantage of the maximum life of the costly component but forces the induction of the engine more times than the first option. This affects the engine availability and increases the variable costs due to funds spent for the engine induction to a repair centre.

The LLP time for replacement is estimated through the Python wrapper and is in line with the on-condition concept. It is, therefore implied that the LLP component will fail the operator's inspection (regular O level inspections through borescope) at the wrapper-estimated time. A detailed analysis of the formulas, used in the code, exists in Appendix B.

3.6.2.1 LLP and TBO costs

The LLP replacement cost relates to the severity factor calculated for the engine's actual usage. Normally the LLP replacement time should be expected after 2 completed overhauls. An example is that a CT7 (a derivative of the military T-700-701D engine) high-pressure turbine disc has an estimated life of 7000 hours while the engine overhaul is 2500 Hours that means that the LLP expected replacement should be after the second overhaul.

The LLP replacement time will affect both the cost and engine availability.

The TBO LLP module will calculate for different LLP replacement periods.

a. 4TBO > LLP > 3 TBO
b. 3TBO > LLP > 2 TBO
c. 2TBO < LLP < TBO

The assumption in these cases is that the LLP replacement will take place after the first TBO and that the second TBO interval will be the same as the first TBO. This may seem contrary to the mature shop interval which is estimated for turbofan engines [17] but to the author's knowledge and experience so far the turboshaft engine OEM's provide the same TBO interval every time that the engine is inducted for an overhaul.

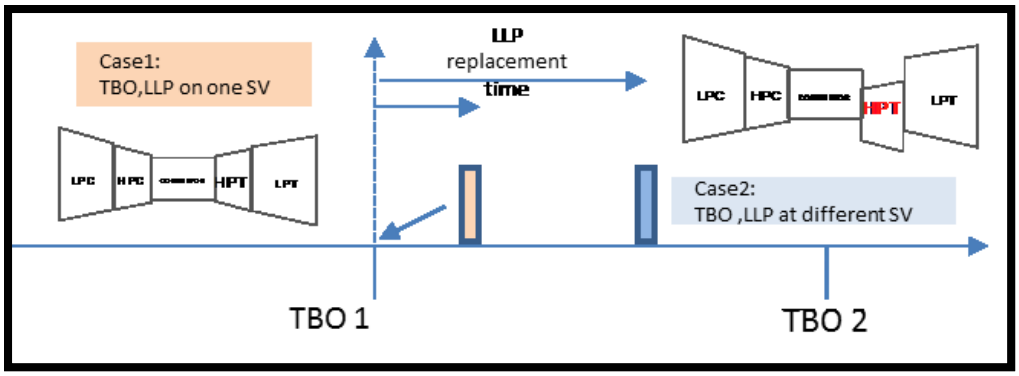

Figure 3-20: Minimum SV vs maximum LLP Usage.

3.6.2.2 Minimum Shop Visit Scenario

This scenario assumes that the operator policy is driven by his need to minimize the admin costs and maximize the engine availability. In this scenario, the LLP that needs replacement between consecutive TBO intervals is changed at the first to come TBO interval before the LLP interval. An example of three scenarios (LLP: 3200, 4200, 5600) is presented in Table 3-18 to Table 3-20. Detailed analysis of the formulas for the example scenarios exist in Appendix B.

MIN Shop Visit Concept					Equations used in the code			
No	Reason	Hours	Years in Service					
1	LLP & TBO	1800	4.5		Fuel (tbo_1)	MMH_O_I_(tbo_1)	fvcost_i	LLP_R_IN(0.45* eip_c)
2	LLP & TBO	3600	9		Fuel (tbo_1)	MMH_O_I_(tbo_1)	fvcost_i	LLP_R_IN(0.45* eip_c)

Table 3-18: Formulas for cost estimation for Min SV scenario (LLP: 3200)

MIN Shop Visit Concept					Equations used in the code			
No	Reason	Hours	Years in Service					
1	TBO	1800	4.5		Fuel (tbo_1)	MMH_O_	fvcost_i	
2	LLP & TBO	3600	9		Fuel (tbo_1)	MMH_O_	fvcost_i	LLP_R_IN(0.45* eip_c)
3	TBO	5400	13.5		Fuel (tbo_1)	MMH_O_	fvcost_i	
4	LLP & TBO	7200	18		Fuel (tbo_1)	MMH_O_	fvcost_i	LLP_R_IN(0.45* eip_c)

Table 3-19: Formulas for cost estimation for Min SV scenario (LLP: 4200)

MIN Shop Visit Concept					Equations used in the code			
No	Reason	Hours	Years in Service					
1	TBO	1800	4.5		Fuel (tbo_1)	MMH_O_	fvcost_i	
2	TBO	3600	9		Fuel (tbo_1)	MMH_O_	fvcost_i	
3	LLP & TBO	5400	13.5		Fuel (tbo_1)	MMH_O_	fvcost_i	LLP_R_IN(0.45* eip_c)

Table 3-20: Formulas for cost estimation for Min SV scenario (LLP: 5600)

3.6.2.3 Maximum LLP Usage Scenario

This scenario assumes that the engine is inducted into service following the TBO and LLP Intervals. Every time the engine is inducted for LLP replacement an admission cost is added. This cost includes the MMH for the engine disassembly, the components inspection, the test cell etc. and depends on the repair centre policy. The contracts of that kind relate the admin cost to a value of MMH (e.g. 100 MMH * MMH_cost/hr). Table 3-21 shows 3 possible scenarios that relate to a light helicopter

turboshaft engine. The scenario assumes that the LLP Interval is between the 1st-2nd, 2nd- 3rd or 3rd - 4th TBO Interval.

	Life Limited Parts Induction Scenarios (Hours)		
TBO Calendar	**3200**	**4200**	**5600**
1800.00	1800	1800	1800
3600.00	3200	3600	3600
5400.00	3600	4200	5400
5600.00	5400	5400	5600

Table 3-21: Example of Max LLP induction scenario

The formulas that the code uses for cost estimation with regard to the first scenario (LLP Interval: 3200 Hours) are shown in the following Table 3-22.

Max LLP Replacement Concept				Equations Used in the code			
No	**Reason**	**Hours**	**Years in Service**				
1	TBO	1800	4.5	Fuel (tbo_1)	MMH_O_I_(tbo_1)	fvcost_i	
2	LLP	3200	8	Fuel (LLP_1)		admin *	LLP_R_IN(0.45* eip_c)
3	TBO	3600	9	Fuel (tbo_1)	MMH_O_I_(tbo_1)	fvcost_i	
4	TBO	5400	13.5	Fuel (tbo_1)	MMH_O_I_(tbo_1)	fvcost_i	
5	LLP	6400	16	Fuel (LLP_1)		admin	LLP_R_IN(0.45* eip_c)

Table 3-22: Formulas for cost estimation for Max LLP usage scenario

The cost values will be presented in the form of present value. Present Value (PV) is a formula used in finance that calculates the present-day value of an amount that is received at a future date. The premise of the equation is that there is "time value of money". The equation that provides a quantifiable comparison between an amount today and an amount at a future time, in terms of its present-day value is the following:

$$Present\ Value(PV) = \frac{Future\ Value\ (FV)}{(1+r)^n} \qquad 3\text{-}12$$

Where: (r) is the inflation and (n) is the number of years.

3.6.3 Operators Usage Scenarios

The previous section showed many formulas that have been used to estimate the maintenance costs for the engine service life. The basic assumption could be that the helicopter flies the same flight all his life. While this approach can produce a trend for

the maintenance costs, it is not a feasible scenario. It is worth mentioning that the only available source [84] for maintenance cost estimation found in the public domain assumes that the helicopter accumulates 2 cycles per flight and bases the $/hr cost on that assumption. This method though applies to aircraft operations while, as mentioned in paragraph 2.2.1.1, the flight cycles per helicopter mission are more than two. This research will base the cycle counting on a method that will account for the helicopters different mission flight profiles on a yearly basis.

Weighted Usage Flight Profile Method (WU-FPM)

This method assumes that each flight profile relates to a certain percentage during the year. The method allows for more flexibility and can resemble real-life scenarios more accurately.

The assumptions for this method and the formulas used are shown in Table 3-26. In particular:

a. The weight factor in column (1) represents the % of the mission type flown in a year. In this scenario, the passenger mission used as reference is flown 80% of the total flights while the OAG 10% and the SAR mission 10% respectively. Table 3-23 provides a sample of the possible values for each flight profile that can be used to obtain the LLP values according to the helicopter operator yearly usage.

b. The data at column (3) stores the flight duration in hours.

c. Column (4) stores the number of cycles as calculated from the ‘rainflow counting’ method.

d. Column (5) shows the flight hours (FH) per specific mission (Ref/OAG/SAR) flown during a year time.

e. Column (6) shows the cycles flown per year per specific mission.

f. The values at column (7) which represent the calculated failure limit due to LCF for every mission were calculated using the framework developed in this research. These values represent the number of cycles to fail if the rotorcraft engine was used for the same mission all its service life (40 years).

g. The values at column (8) shows the equivalent cycles based on the weight factor for the specific mission. These cycles are based on the mission contribution that is given by the weight factors. This approach is based on the linear damage rule also referred to as the “Palmgren-Miner rule as presented with equation 3-1.

h. Column (9) shows the TBO interval proposed from the engine OEM and

i. Column (10) shows the equivalent flight hours with relation to the TBO and the total flight hours per year as shown in equation 3-13 . This value will be used for the LLP failure limit in the maintenance cost calculation:

$$\text{LLP Limit (FH)} = \left(\frac{\text{FH}}{\text{Year}}\right) * \frac{Equivalent\ Cycles/Year}{Cycles/year} \quad 3\text{-}13$$

	Weighted Factor for Missions															
Pasngr	0.8	0.7	0.6	0.5	0.4	0.3	0.2	0.1	0.8	0.7	0.6	0.5	0.4	0.3	0.2	0.1
OAG	0.1	0.2	0.3	0.4	0.5	0.6	0.7	0.8	0.1	0.1	0.1	0.1	0.1	0.1	0.1	0.1
SAR	0.1	0.1	0.1	0.1	0.1	0.1	0.1	0.1	0.1	0.2	0.3	0.4	0.5	0.6	0.7	0.8

Table 3-23: Weight Factors for Helicopter Missions

3.6.4 Cost due to Degradation

The literature addressed the mechanisms of performance degradation for the big turbofan engines. A NASA research [19] conducted for J79D engines gave enough data to researchers to address the relation between parts degradation and engine performance. Helicopter engines though have important differences than their turbofan counterparts. Apart from the obvious difference, which is their size, the operating conditions they perform are far from being similar. A small list of the differences between the turboshaft and turbofan engines may include the following:

a. Operate at different ambient temperatures range
b. Operate at harsh environmental conditions and low altitudes
c. Perform different manoeuvres and fly different segments

The literature review did not provide any data from operators or engine manufacturers so, to get a view of the performance loss due to specific parts, so simulations will be used to assess the degradation and the related costs. Turbomatch, as explained before, is a tool that is capable of simulating degradation. The performance parameters that can be altered to simulate the performance loss are the component efficiencies and air/gas path mass flow.

The turboshaft engines parts do not necessarily degrade at the same rate. Sing's [32] work provide a detailed analysis of the reasons of components degradation while Kurz

[30] provide a concise classification of components deterioration. In general, as Figure 3-21 presents, the components degrade initially following an exponential trend and beyond that point, the trend becomes more linear [29]. In this research, the simulations are used to estimate the EGT margin consumption considering: i) that the components degrade with the same rate and ii) the compressor module is degrading at a different rate than the turbine counterpart.

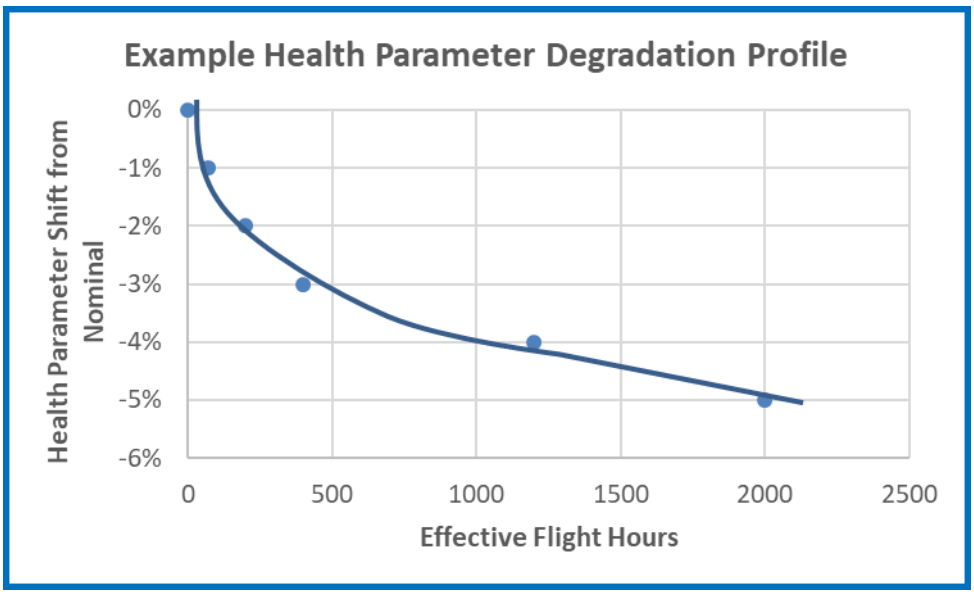

Figure 3-21: Component Degradation [29]

The assumptions for this research will be the following:

a. The performance loss is due to leakage losses, rub-in, and tip clearances. Table 3-24 presents the parameters used for the simulations.

b. The incurred fuel cost will depend on the degradation for the TBO period.

c. The engine will degrade at the same rate in every TBO interval.

d. The degradation is due to environmental conditions and is not affected from the mission profile.

e. The incurred costs are irrelevant to the ones incurred from engine induction for LLP replacement.

The total cost estimation uses the weight factor used for the WU-FPM method. This cost compares with:

a. The cost incurred without considering the degradation effect and

b. The maintenance cost for the engine performance restoration and LLP replacement.

No	Scenarios	Abreviations
A	C_eff,C_mf,T_eff,T_mf	C: Compressor
B	T_eff,T_mf	T: Turbine
C	T_mf	C_eff : Compressor Efficiency
D	T_eff	T_eff : Turbine Efficiency
E	C_eff,C_mf	C_mf : Compressor Mass Flow
F	C_mf	T_mf : Turbine Mass Flow

Table 3-24: Engine Performance Parameters

Weight Factor	Mission	Fuel Cost with Degradation	Fuel Cost per Type	Fuel Cost without Degradation	Fuel Cost per Type
(1)	(2)	(3)	(4)	(5)	(6)
0.8	Pas/nger	A	0.8* A	A*	0.8*A*
0.1	OAG	B	0.1*B	B*	0.1*B*
0.1	SAR	C	0.1*C	C*	0.1*C*
Fuel Cost for TBO (FH)			Fuel Cost $_{(TBO)}$ = 0.8*A +0.1*B+0.1*C		
Fuel Cost for Engine Life (40 years)			Total Fuel Cost = K * Fuel Cost (TBO)		

Table 3-25: Degradation Cost Estimation using Mission Profile

3.7 Summary

This chapter aimed to provide the reader with detailed information on the methodology used to assess the engines components life and the related maintenance costs. The developed code to assess the components life was analysed. The need to run a population of missions, which are representative of the rotorcraft design space within the OEM specification, was highlighted. For that reason, it was decided to perform a DOE which would provide valuable data for further analysis. The LHS sampling method has been chosen among others to set up the samples for the DOE and its capability has been explained. In addition, a validation method named LOO, which can assess the accuracy of the results calculated from the Gaussian Process implementation, has been introduced.

A significant contribution of the developed methodology is that the population generated from the DOE provides the capability to relate a baseline flight profile with a representative set of values of the operating variables. These set of values are used to run other mission profiles. This method facilitates the comparison between different mission profiles and enhances the components life results in accuracy.

The “Weighted Usage Flight Profile Method (WU-FPM)” which uses the operator flight profile named has been developed. The method uses the LLP failure cycles and a combination of missions to calculate a value for the equivalent flight hour. This value can then: i) relate the LLP failure limit to the performance restoration (TBO) limit imposed by the engine OEM, ii) be used as an input to the cost module for further post-processing. Table 3-26 presents the WU-FPM method.

The cost module which has been developed considers: i) the cost for the work performed at all levels of engine maintenance, ii) the yearly inflation, iii) the LLP replacement cost, and iv) the LLP and TBO time limits. The module uses two methods used in the civil market [17]: i) the Minimum Shop Visit and, ii) the Maximum LLP usage method, which relates the incurred cost with the engine availability.

In addition, the methodology is using the degradation effect in fuel cost to highlight the importance of the environmental conditions and compare it with the mission profile effect.

To summarize a major advantage of the methodology is that it combines life and cost analysis with real-life flight profiles and produces cost data that can facilitate both a short and long-term cost analysis regarding maintenance.

Weight Factor	Mission	FH	Cycles /mission	FH Distribution /mission	Cycles /Year	Calculated LLP Limit	Mission contribution to failure cycles	TBO (FH)	TBO Equivalent
(1)	(2)	(3)	(4)	(5) =(300*(1))	(6)= (4)*(5)	(7)	(8)=(7)*(1)	(9)	(10) = (5) * (8)/(6)
0.8	Ref	0.5	5	240	1200.00	50897.5	40718	2000	6885.66129
0.1	OAG	1.29	12	30	360.00	8109	810.9		
0.1	SAR	2.5	10	30	300.00	11622	1162.2		
Total				300	1860.00		42691.1		
				FC/FH					

Table 3-26: Weighted Usage Flight Profile Method (WU-FPM) Example

4 Chapter 4: Case Scenario

4.1 Helicopter and Powerplant Model

This research will use a version of the BO-105 helicopter which is a light, twin-engine, multi-purpose helicopter that has been initially developed by Bölkow of Ottobrunn, Germany. The helicopter type has now been in service for over 40 years, had its maiden flight in 1967. It holds the distinction of being the first light twin-engine helicopter in the world and up to today, has 27 different versions in 1976. This research will use the version BO 105CB which was developed in 1976 with more powerful Allison 250-C20B engines [49]. The helicopters specifications are shown in Table 4-1. Units' conversion for the operating parameters can be found in Appendix G.

Characteristic	Value
Crew	1 or 2 pilots
Capacity	4
Empty weight	1,276 kg (2,813 lb)
Max Take-off weight	2,500 kg (5,511 lb)
Maximum Speed	242 km/h (131 knots, 150 mph)
Cruise speed	204 km/h (110 knots, 127 mph)
Range	1,112 km (600 NM, 691 mi)
Service ceiling	5,180 m (17,000 ft)
Rate of Climb	8 m/s (1,575 ft/min)

Table 4-1: BO-105 specifications [115]

The helicopter is powered by 2 Allison 250-C20b engines. The Allison 250 series engine is featuring a free power turbine having adopted the reverse-airflow configuration. The engine consists of a multi-stage axial-centrifugal flow compressor, a single combustion chamber, a two-stage gas producer turbine, a two-stage power turbine, an exhaust collector, and an accessory gearbox as shown in Figure 4-1. A configuration of six axials and one centrifugal stage is used to compress the incoming air. The compressed air is transferred through two ducts into the combustion chamber to the end of the engine. At this point, the air flow is reversed and passes through the combustor, the two-staged gas generator turbine, and finally, the two-staged free power turbine; The gases then are exhausted through two exhaust outlets. An important design feature of the Model 250 engine is its modular

construction, which greatly simplifies maintenance and repair activity. Also, the unique reverse-flow design provides for ease of hot section maintenance.

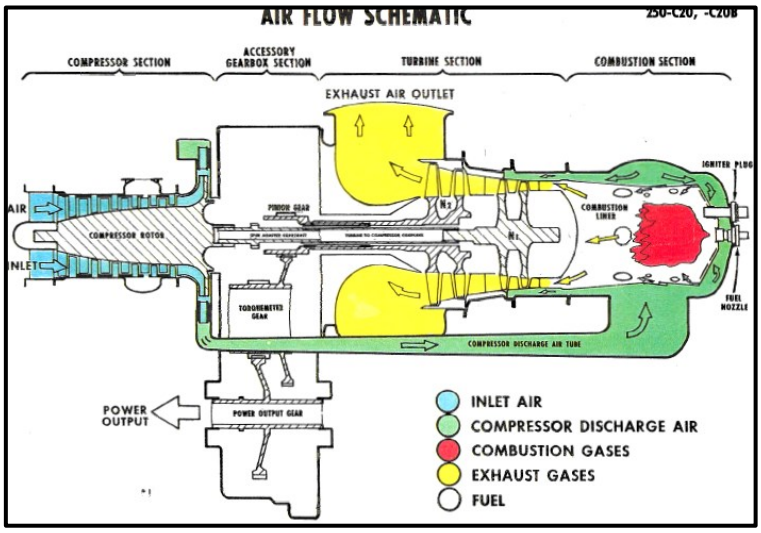

Figure 4-1: 250C20B Cutaway and Airflow Schematic

4.1.1 Component Sizing

The high-pressure turbine blade and disc geometries are measured from the gas generator area of the cutaway plot provided in

Figure 4-2. Details of the method used their approximated geometry and the material properties are shown in Appendix A

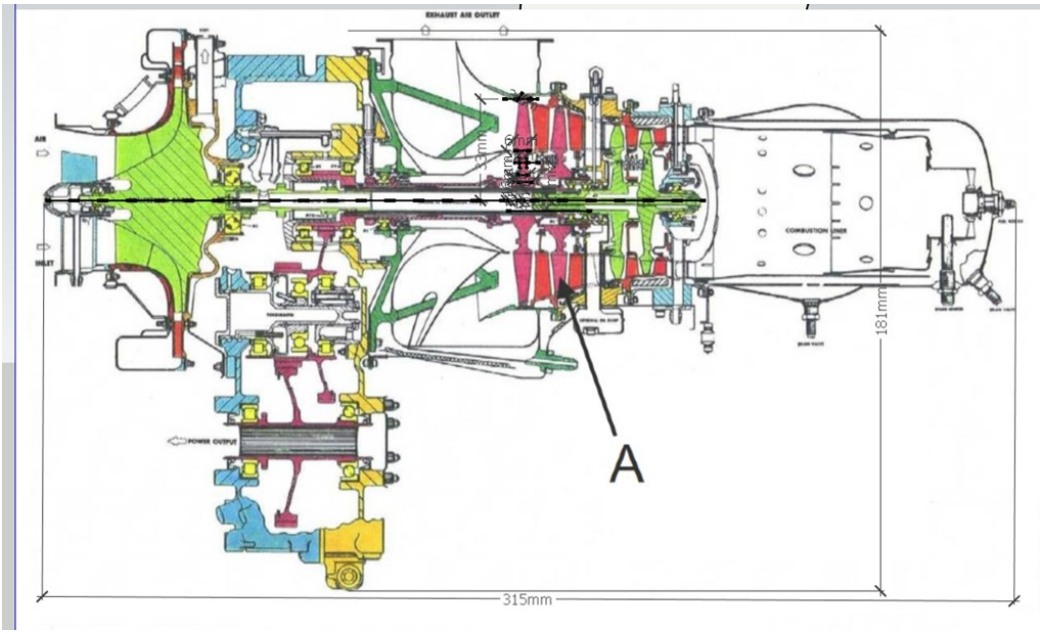

Figure 4-2-: 250C-20B Cutaway

4.1.2 Engine Design Point Selection

The design point of the Allison 250-C20B type engine was chosen at take-off conditions under ISA conditions. Several iterations were carried out to match the simulation results of TURBOMATCH with the data from the public domain. The engine details are summarized in Table 4-2. The final values used for the component efficiencies were the ones which matched the data from the public domain with regard to the engine overall performance.

The engine is sized by mass flow and overhaul pressure ratio. All the required data has been found form the public domain. The design point has been set to max continuous conditions. The engine components efficiencies presented in Table 4-3 had been configured to match the engine specification data. A variable schedule was used to avoid compressor surging. The compressor running lines are shown in the next figure.

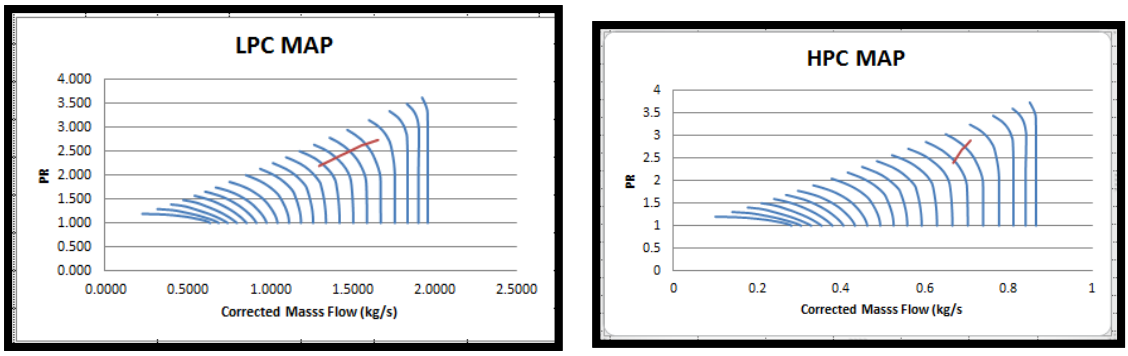

Figure 4-3: Compressor Running Lines for LPC and HPC

Parameter	Public Domain	Turbomatch
Take off Power, Max Continuous [KW]	313	313
Power at Cruise (75%) [KW]	207	
SFC at 75% [mg/l] , [lb/h/shp]	119.8 (0.709)	126
Mass Flow [kg/s],[lb/s]	1.56 (3.45)	1.56
Pressure Ratio	7.1	7.2
Gas Turbine Temperature		
30 min OEI, Take off (5 minutes), Max Continues	810 [°C], 1083.15 [°K]	1083 [°K]
Starting (1 sec duration)	927 [°C], 1200.15 [°K]	
Transient 1 (6 sec duration)	843 [°C], 1116.15 [°K]	
Transient 2(12 sec duration) & 3 occurrences	899 [°C], 1172.15 [°K]	

Parameter	Public Domain	Turbomatch
Free Turbine [rpm]	33.290	
Gas Turbine [rpm]	50970	

Table 4-2: Engine specs [116], [117]

Parameter	Value
Axial compressor pressure ratio	2.73
Axial compressor isentropic efficiency	0.8
Centrifugal compressor pressure ratio	2.6
Centrifugal compressor isentropic efficiency	0.81
Combustion pressure loss	0.5
Combustion efficiency	0.99
TET(Kelvin)	1083
High-pressure turbine cooling flow [%]	5
Compressor turbine isentropic efficiency	0.85
Power turbine isentropic efficiency	0.85
Power output [kW]	313
Mass flow [kg/s]	1.56
Overall Pressure ratio with losses	7.2

Table 4-3: Allison 250 C20B engine model, design point parameters

4.2 Component Life Estimation

It has been obvious so far that the engine rotating parts life assessment is a complex process and is based on formulas that contain statistical components. This statistical nature of the parts life assessment makes it imperative to establish a baseline flight profile that will use representative values regarding operating parameters like payload, climb rate, and ISA deviation. Furthermore, the flight profiles that will be used should be representative of realistic operator's profiles.

In this research, a passenger, a search and rescue (SAR), and an oil & gas (OAG) mission have been used. The operating parameters design space regarding: i) airspeed ii) hover and cruise altitude iii) climb/descent rates and iv) idle times was aligned with the helicopter limitations as defined from the helicopter specifications described in Table 4-1.

The missions are comprised of one to several flight sessions, while each session is divided into flight segments (idle, hover, climb, cruise, descent, hover, idle). A time-step (dt) of 15 secs is used for each individual mission segment. The turn rate used for all coordinated turns was 5^{o}/sec. An exception to that is in the case of fine-tuning the helicopter's orientation, where the turn rate calculation was based on the orientation error and the mission time-step (dt). The assumption regarding idle operation was that the overall helicopter power requirements are equal to 20% of maximum contingency engine shaft power. The methodology described in Goulos work [12] (chapter 6) was used to assess the performance of the integrated helicopter-engine system throughout the course of all missions.

The component life will be assessed using the weighted usage flight profile method. For this research, the 3 mission types mentioned above will be used.

A DOE has been performed to provide a population of estimated component lives. The following two assumptions will be used for the component estimation:

a.The operating parameters that will be used for the O&G and SAR missions will be based on these of the passenger mission.

b.The population median value is representative of the component life.

4.2.1 Passenger Mission (Reference Flight)

The research focused on the missions addressed in the previous paragraph. The mission flight profile as discussed previously influences the components life and it is important to set certain criteria when deciding on the baseline flight profile. This research assumed a simple passenger flight profile with the specification requirements as shown in Table 4-5. The main criteria for this choice have been:

a. The payload, climb rate, and ISA deviation should remain constant during the entire mission. The reasoning for that is that the results can provide a clear understanding of the impact of the specific variable in the engine life.

b. The climb rate and ISA deviation should represent missions for operators in different environments around the world.

c. The simulation time should be relatively low so that the “n” number of simulations should be performed in a logical timeframe.

Design Parameter	Min	Max	Units
Payload	0	650	Kg
Climb Rate	3	7	m/s
ISA deviation	0	15	^{o}C

Table 4-4: Operating Parameters Design Space

As mentioned in the methodology the characteristics of the reference mission will be defined from a design of experiment (DOE). The operating parameters for the mission's design space shown in Table 4-4 will be estimated by the Latin Hypercube Sampling method.
This approach will provide a population of data that allows to:

a. Understand the variables impact to lifing and
b. Choose a representative set of the operating parameters values (Median value) as a baseline.

The usage of the baseline values is considered to provide a more systematic approach that will help us when designing for the SAR and O&G missions. This approach establishes that the missions are executed within similar environmental parameters and the life estimation can be assessed in a more consistent way. A small drawback of this method is that the "payload" parameter cannot be constant during the SAR and O&G mission design while the "climb rate" and "ISA" deviation can. The passenger mission schedule assumes that the helicopter takes off from Edinburgh airport and subsequently flies to an urban area to drop off its payload.

MTE	Airspeed (m/sec)	Altitude AGL-final (m)	Climb Rate (m/sec)
Idle (2 min)	0	0	0
Hover IGE (1 min)	0	0	0
Climb	40	500	5
Cruise	60	500	0
Descent	40	0	-5
Hover IGE (1 min)	0	0	0
Idle (1 min)	0	0	0

Table 4-5: Passenger Mission Specification Requirements

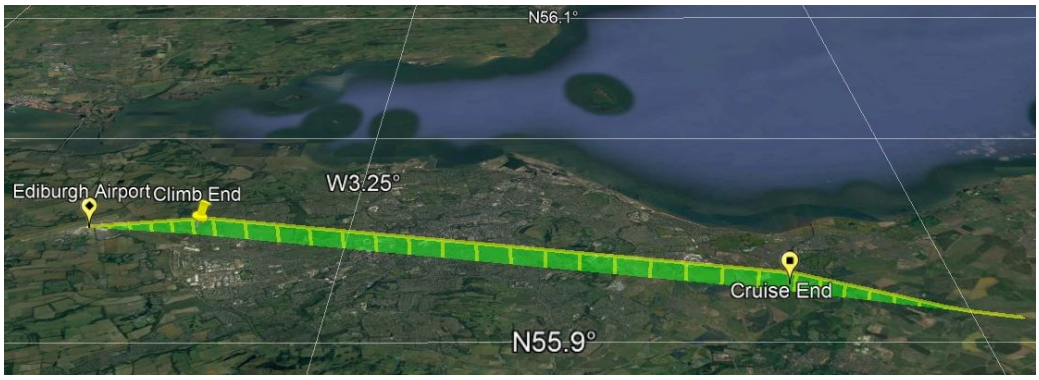

Figure 4-4: Passenger Mission

A description of the variation of the performance parameters during the flight segments, as shown in Figure 4-5, is deemed necessary:

Idle: The idle segments are located at the start and the end of each flight session. These segments relate to low values of engine shaft power, fuel flow, TET and disc stresses.

Hover: The previous trend is inverted at the hover phase. Figure 4-5 clearly shows that the TET and disc stress is increasing during the hover segments. In this segment, the induced drag is the driving component and forces the engine to provide enough power that will sustain the helicopters weight and the possible crosswinds or OGE situations.

Climb: When the helicopter enters to the climb phase, translational lift is created. This lift and the velocity gain cause a power demand decrease which happens almost linearly. At this phase, the rotor blades act like a screw in the air and the induced drag decreases. The power decreases up to the point that the helicopter enters the cruising phase.

Cruise: At this phase, the forward velocity helps the rotor produce enough lift and the demand for torque and gas generator rotational speed continues to decrease accordingly. The helicopter at this phase is considered to fly a level flight.

Descent: When the cruise segment ends, and the helicopter enters the descent phase, the power demand decreases because the induced drag is very low. The rotor exploits the incoming air due to the descent and the required power decreases. The status will change as soon as the helicopter reaches the last hover segment and it is now that the helicopter needs to sustain its weight while entering at the hover phase.

Overall, Figure 4-5 shows that the hover and the subsequent climbing forward flight are the most important in terms of engine TET and disc stresses. This phenomenon will be more profound in the succeeding SAR and AOG missions.

In general, it is known that the environment can impose restrictions into the rotorcraft flight envelope while the powerplant components life is affected considerably. An explanation with practical examples exists, either in public literature like the FAA manuals or any other commercial publication oriented to pilot preparation. This research though will focus mostly on three parameters: i) the payload, ii) the climb rate and iii) the ISA deviation. The Figure 3-7 to Figure 3-10 at paragraph 4.2.1 clearly showed how the operating environment affects the engine TET.

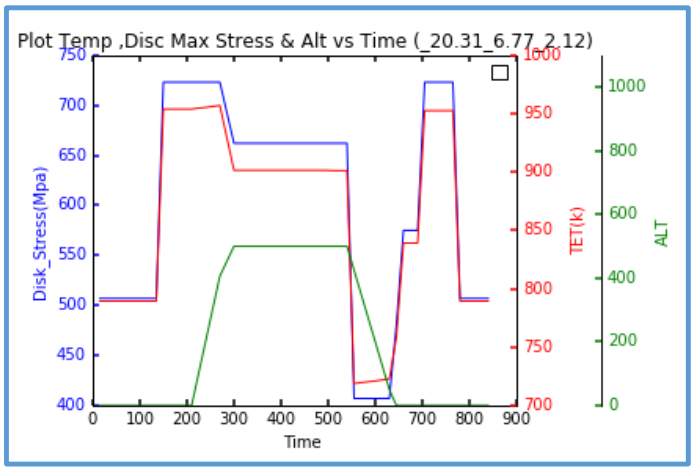

Figure 4-5: Passenger Mission Flight Profile

Figure 4-6 to Figure 4-9 show a scatter for the mission's population about the operating parameters. Using that as a base the disc life for a sample of 20 missions that relate to a certain operator's profile is superimposed. In particular, Figure 4-6 and Figure 4-7 show the impact of the payload change to engine life, while Figure 4-8 and Figure 4-9 show the effect due to ISA deviation.

	Payload (Kg)	Climb Rate (ft/min)	ISA Deviation °C
Population	0-650	3-4	0-15
Sample	20-80, 200-300, 550-650	3-4	0-15

Table 4-6: Samples design space for Load Range Change vs Disc Life

	Payload (Kg)	Climb Rate (ft/min)	ISA Deviation °C
Population	0-650	3-7	0-15
Sample	650	3-7	0-15

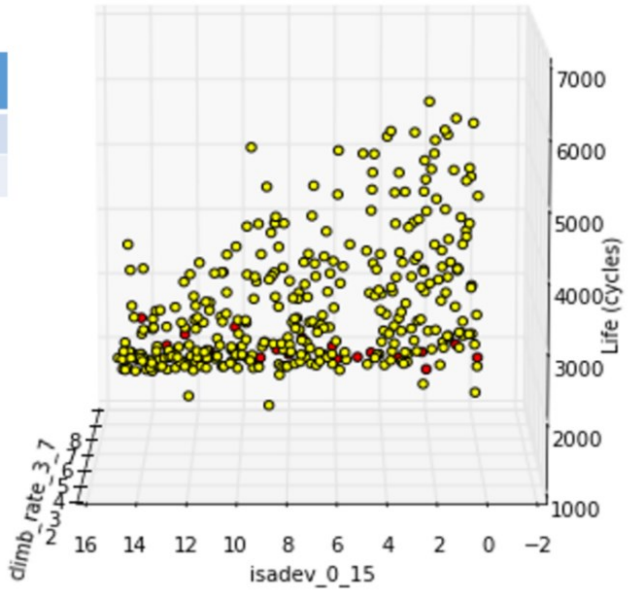

Figure 4-6: 400 Experiments (Load Sample for 650 Kg vs Disc Life)

	Payload (Kg)	Climb Rate (ft/min)	ISA Deviation °C
Population	0-650	3-7	0-15
Sample	0	3-7	0-15

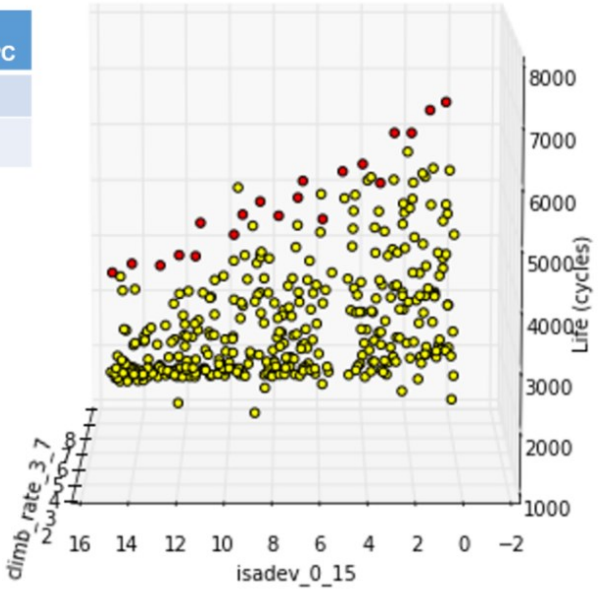

Figure 4-7:400 Experiments (Load Sample for 0 Kg vs Disc Life)

	Payload (Kg)	Climb Rate (ft/min)	ISA Deviation °C
Population	0-650	3-7	0-15
Sample	0-650	3-7	0

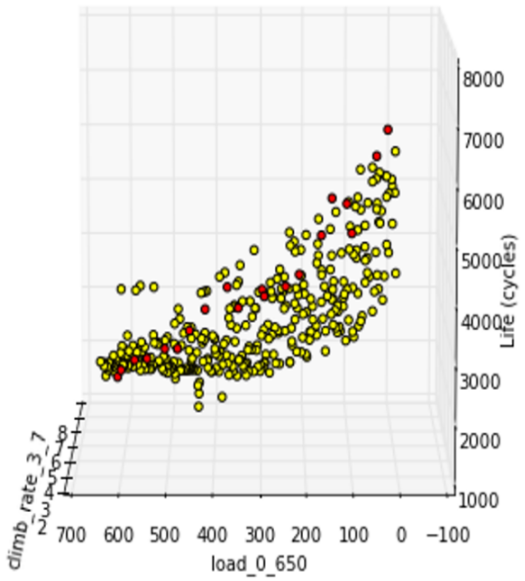

Figure 4-8: 400 Experiments (ISA deviation 0 vs Disc Life)

	Payload (Kg)	Climb Rate (ft/min)	ISA Deviation °C
Population	0-650	3-7	0-15
Sample	0-650	3-7	15

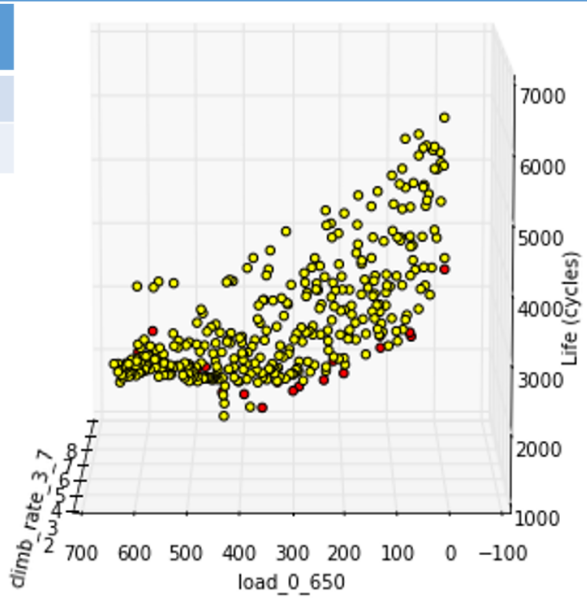

Figure 4-9: 400 Experiments (ISA deviation 15 vs Disc Life)

The turbine life results estimated from the lifing code developed in this research are presented in Appendix D. The value that will be used as a baseline for the OAG and SAR missions is presented in the next table.

Payload	Climb Rate	ISA Deviation	Turbine Disc Failure Limit
Kg	m/sec		cycles
554.94	4.89	7.03	50897

Table 4-7 : Baseline Values for Passenger Mission

4.2.1.1 Safety Factor Sensitivity Analysis for Turbine Life

The criteria and the methods, which are used in the fatigue design for the engine components, have been addressed in the literature section in paragraph 2.2.1.2. The criterion, which is mainly used for the gas turbine engines, is the safe life design criterion. This criterion uses a margin for the scatter of fatigue results and for other unknown factors. The calculations are based on stress-life, strain-life, or crack growth relations and relate to solely or partially on the field and/or simulated testing. Because inspections may not be practical or possible an allowable service life must be decided based on that calculated life.

Traditionally, components whose dominant failure mode is low cycle fatigue (LCF) have been designed based on a "crack initiation" assumption. Under this assumption, all components of a given population are considered to have failed as soon as a crack of some finite size, for example 0.031 inches, has statistically formed in the member of the population which has minimum strength properties. No attempt is made to utilize the life associated with the remaining population members who have statistically higher properties and are therefore not cracked. From a safety standpoint, this approach has been generally very successful since it contains a built-in safety factor by assuming all components life equals to the minimum value.

The U.S Air Force in their effort to find an alternative solution, have investigated [118] the retirement for cause concept and have realized that although it can be a good theoretical approach in practice it imposes a constraint to the engines operational use.

The analysis performed with the use of the lifing code used in this research assumed that the baseline values for the safety-related factor, that is: i) stress concentration factor and ii)

fatigue notch factor, are the ones shown in Table 4-8. The high and low values of the safety factors, shown in the table, are the ones within 30% range from the baseline values.

The sensitivity analysis results, which are presented in tornado graph form in Figure 4-10, show that the stress concentration factor (Kt) affects the turbine life due to LCF more than the notch sensitivity factor (q).

Factors Baseline Values	Factors	Low Factor Values	High Factor Values
0.9	Notch Sensitivity (q)	0.63	1.17
2.9	Stress Concentration (kt)	2.03	3.77

Table 4-8: Safety Factors Sensitivity Analysis Design Space Values

The q factor, which was initially introduced at the literature review, addresses the comparison between the Kf and Kt factors and it is given by the following equation:

$$q = \frac{K_f - 1}{K_t - 1} \qquad \textbf{4-1}$$

A material that experiences no reduction in fatigue due to a notch will have a notch sensitivity factor of q = 0, while one that experiences a reduction in fatigue up to the full theoretical value will have a notch sensitivity factor of q = 1. The baseline value (q=0.9) that was used in the research, assumes that the stress concentration factor value is close to the fatigue notch factor one. In practice, that means that the turbine life calculated value is strongly affected by both Kf and Kt and the stress distribution around notches or cracks that have been initiated due to amplitude variation influence the turbine life. This approach, which allows us to calculate the effect of the safety margin in the turbine life, will also provide a better view of the design methodology effect on the incurred maintenance costs.

The results, presented in Table 4-9 , show that a 30% increase in the stress concentration factor (Kt=3.77) decreases the engine life by 25% (37880) while a 30% decrease in the stress concentration factor (Kt=2.03) increases the engine life by 23% (62287). Concerning the notch sensitivity variation, a 30% decrease (q=0.63) in that factor results in 14 % increase in the turbine life (58140) while a 30% increase (q=1.17) will result in 16 % decrease in the turbine life (42061).

The component life due to LCF, presented in Table 4-20, takes into account the local stresses distribution after a crack has been developed or due to the existing notches in the turbine design. This approach is also used in a study from NASA, Lewis Research Centre [119] in which software has been developed to estimate the turbine disk weight. This study recognized the fact that actual disk lives depend upon countless details of a highly localized nature. Since any cracking in a disk is not acceptable, fatigue crack initiation is a sufficient criterion for the lifing calculations. When experimental fatigue results are unavailable, approximations of the fatigue resistance can be obtained with the aid of empirical correlations previously established between fatigue properties and corresponding tensile test properties.

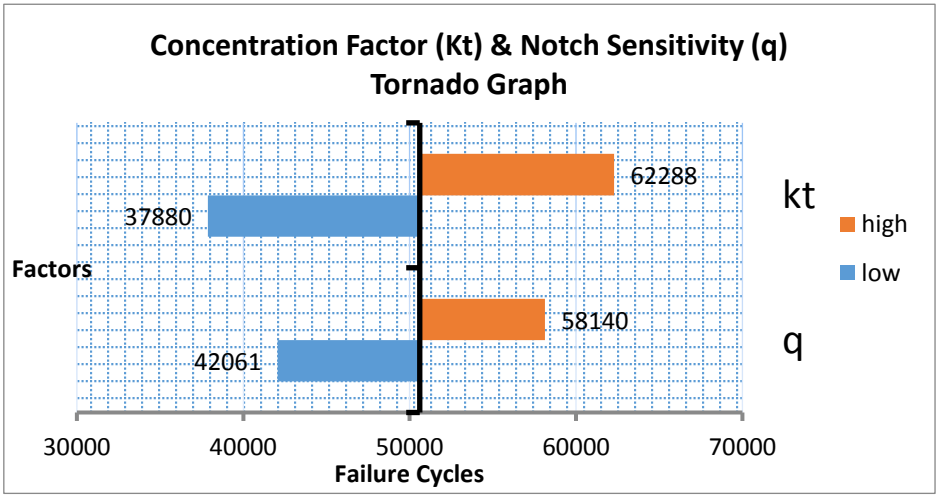

Figure 4-10: Concentration Factor (Kt) & Notch Sensitivity (q) Tornado Graph

The last 2 values in Table 4-9 will be used in the case scenario to show how the assumptions related to the safety factors affect the maintenance cost.

Notch Sensitivity (q)	Stress Concentration (Kt)	Notch Fatigue (Kf)	Life due to LCF (cycles)	% Change
0.9	2.9	2.71	50897	Baseline
0.63 (-30%)	2.9	2.2	58140	14.88313
1.17 (+30%)	2.9	3.223	42061	-16.8881
0.9	2.03 (-30%)	1.927	62287	23.07824
0.9	3.77 (+30%)	3.493	37880	-25.1497

Table 4-9 : Data for Safety Factors Sensitivity Analysis

4.2.1.2 Method Validation

As discussed in the methodology the optimum number of simulations is important when you try to implement a regression analysis or spatial interpolation. The passenger mission that has been used for the DOE has been simulated in a range of experiments (64, 180 and 400). A script in Python was built to create the design space for the operating variables.

The population that has been created from the lifing results was used as a base to find a function that can help us for the estimation of life through spatial interpolation. The DOE was designed for 400 simulations but only the 346 produced results about disc life due to LCF. There were some missions that the lifing model could not converge and the code crashed producing an error. The non-convergence was due to the material properties inability to withstand the stresses and temperature combination created during flight. The Leave one out method (LOOCV) method showed though that the 400 experiments case are capable, as shown in Figure 4-11, of creating a model that can be used for spatial interpolation and predict with accuracy the components life.

The calculated values shown in the X-axis are very close to the values (shown in the Y-Axis) which are estimated by the LOOCV method. The kriging model employed a quadratic regression function combined with absolute exponential auto-correlation, a theta parameter of one (1). The cobyla optimizer was used in combination with a number of 300 random starts to avoid being trapped in local maxima while the default nugget value (=10), which allows smooth prediction from noisy data, gave the highest coefficient values.

4.2.2 SAR Mission

The SAR mission schedule assumes that the helicopter takes-off point is the Arlanda airport in Stockholm, Sweden. After take-off it climbs and cruises towards a designated location in the Baltic Sea. Once it arrives to the control point, it follows a search pattern, which helps the crew to trace, locate, and rescue citizens in distress from a location corresponding to an assumed naval incident. Once the citizens are located, the helicopter crew hovers at 60m and picks up the citizen with a rescue hoist. At this point the helicopter weight changes until the citizens are delivered to Hogbergsgatan hospital. The helicopter hovers and lands on the hospital helipad where it drops-off the rescued citizens while the engines are running on idle. It then hovers and continues its flight to the base at Arlanda airport. Table 4-10 shows the mission specifications in more detail.

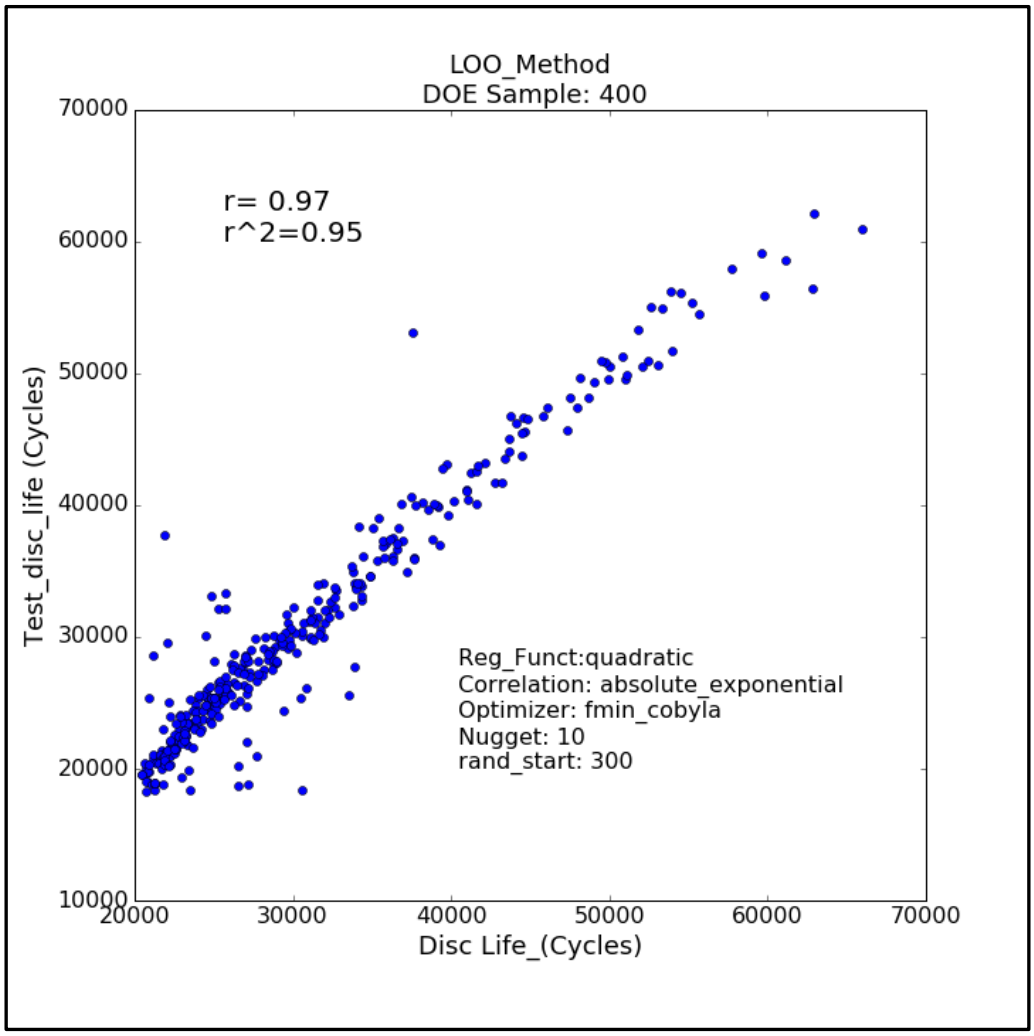

Figure 4-11: LOOCV Method (Sample Size: 400)

Figure 4-13 shows the variation for the altitude, the disc stress, and the TET. The graph shows some picks at the loiter portion of the mission at the area between 3500 to 6000 sec. This is due to the helicopter manoeuvres and the related variation in the GP turbine PCN. This variation increases the cycle's number and affects the components life due to LCF. It is also important to note that both TET and disc stress increase at the rescue phase, close to 6200 secs, due to the AUM increase.

MTE	Airspeed (m/sec)	Altitude AGL final (m)	Climb rate (m/sec)
Idle (5 min)	0	0	0
Hover IGE (1 min)	0	0	0
Climb	40	600	5
Cruise	60	600	0
Descent	50	60	-3.8
Search pattern	30	60	0
Hover IGE (2mins)	0	60	0
Climb	40	600	5
Cruise	60	600	0
Descent	50	0	-3.8
Idle (1 min)	0	0	0
Hover IGE (1 min)	0	0	0
Climb	40	600	5
Cruise	60	600	0
Descent	50	0	-3.8
Idle (1 min)	0	0	0

Table 4-10: SAR Mission Specification Requirements

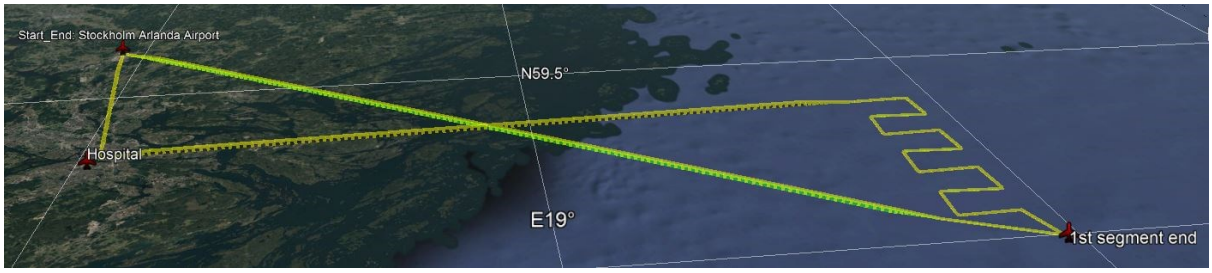

Figure 4-12: Search and Rescue Mission

. It is worth mentioning that Goulos [14] has realized the AUM significance of the flight simulation accuracy and built HECTOR code so that the changes in AUM are accounted for. The flight simulator used in this research considers both the payload variation during flight as well as the fuel consumption.

An important issue to consider is that the simulated mission used the same operating parameters for climb rate and ISA deviation except for the load parameter due to the mission requirements. The effect that the load can have at the engine TET has been discussed in

the sensitivity analysis section. In addition, the disc lifing data estimated by the DOE showed how the load variation affects the turbine disc life. Therefore, it is realized that it is important to account for the load absence. To address that a load factor should be implemented that will be multiplied by the life estimated from the lifing code. The load factor estimation will need to run a separate DOE but unfortunately, due to the research time constraints, this is not feasible at the moment. The load factor estimation will be addressed in the future work section and for the time being, the turbine life estimated by the lifing code will be used. The turbine life for the SAR mission is shown in the following Table 4-11.

Payload variation Kg	Climb Rate m/sec	ISA Deviation	Turbine Disc Failure Limit cycles	Cycles/Mission
0-200-0	4.89	7.03	11622	10

Table 4-11: Operating Values & Turbine life for SAR Mission

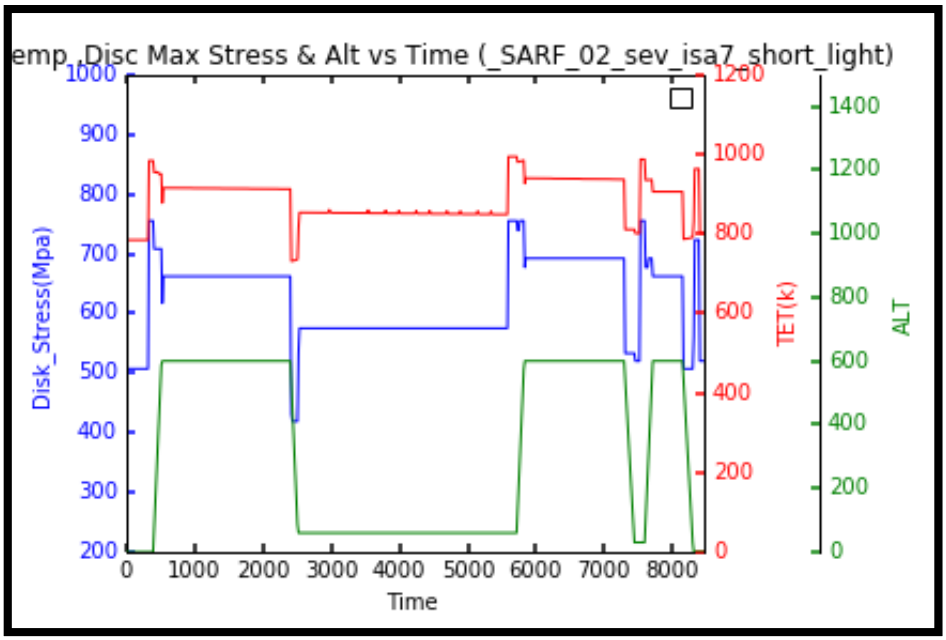

Figure 4-13: SAR Mission Flight Profile

4.2.3 Off-Shore Mission (O&G)

The O&G mission schedule uses as a take-off point the De Kooy airfield in Den Helder, Netherlands and carries a specified payload. The helicopter climbs and cruises towards a designated offshore oil/gas platform (oil rig 1) located in the North Sea where it hover, lands and drops-off the payload while the engine runs in idle mode for a certain timeframe. A similar flight pattern is used for the second offshore oil/gas platform (oil rig 2) where it picks-up another useful payload. The final segment is used to return to its base at De Kooy airfield in Den Helder. Table 4-12 and Table 4-10 shows the mission specifications.

MTE	Airspeed (m/sec)	Altitude AGL-final (m)	Climb Rate (m/sec)
Idle (5 min)	0	0	0
Hover IGE (1 min)	0	0	0
Climb	40	600	5
Cruise	60	600	0
Descent	50	0	-3.8
Hover IGE (1mins)	0	0	0
Idle (10 mins)	0	0	0
Hover IGE (1mins)	0	0	0
Climb	50	600	5
Cruise	50	600	0
Descent	40	0	-3.8
Idle (1 min)	0	0	0
Hover IGE (1 min)	0	0	0
Climb	50	600	5
Cruise	60	600	0
Descent	50	0	-3.8
Hover IGE (1 min)	0	0	0
Idle (1 min)	0	0	0

Table 4-12: Off-Shore Mission Specification Requirements

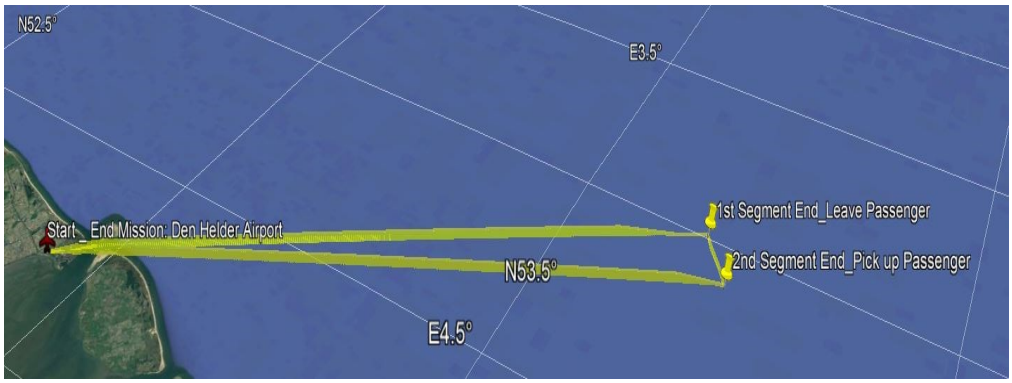

Figure 4-14: Oil and Gas Mission (OAG)

Figure 4-15 shows the variation for the altitude, the disc stress, and the TET. The graph shows that the TET and disc stress is decreasing at the second part of the mission. This is attributed to the AUM change, which is due to the passenger step down. The AUM variation will affect the estimated turbine disc life as discussed in the previous and therefore a load factor should also be implemented. The turbine life for the O&G mission is shown in the following Table 4-13.

Payload variation Kg	Climb Rate m/sec	ISA Deviation	Turbine Disc Failure Limit cycles	Cycles/Mission
0-616	4.89	7.03	8109	12

Table 4-13: Operating Values & Turbine life for O&G Mission

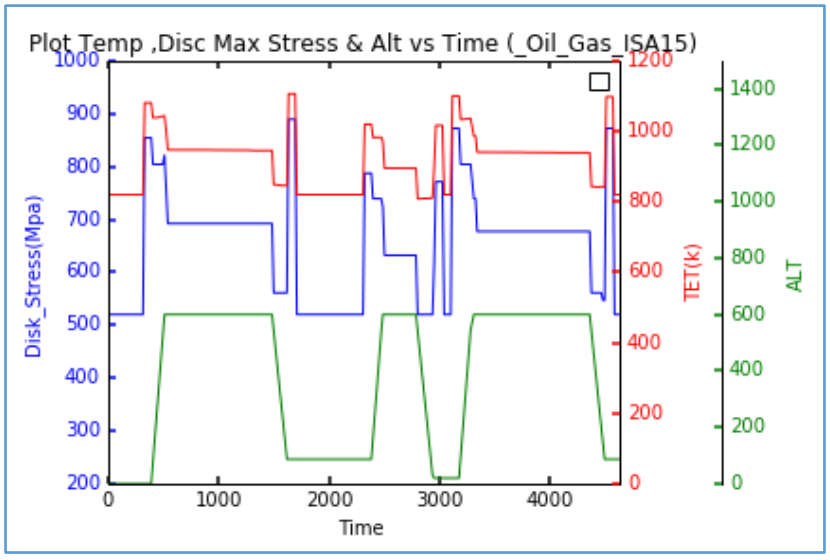

Figure 4-15: O&G Mission Flight Profile

4.2.4 Summary

The sensitivity analysis at paragraph 4.2.1 showed the effect that the operating variables have on TET. The payload contribution to the TET increase is more profound in hover and cruise and descent segments while the climb rate affects the climb segment.

The engine TET is important for the components life because it relates to the UTS and Yield stress and thus it affects the materials fatigue life. The lifing results presented in Table 4-7, Table 4-11 and, Table 4-13 show that the fatigue cycles relate to the components life and have the major contribution on it. The sensitivity analysis provides a clear view for the contribution of Payload, ISA deviation and climb rate for every segment.

The DOE that has been conducted, coupled with the LHS method, showed that a representative sample from a population of a proper number of missions selected can be used to assess the component lives for an operator once his flight profile design space is available. The results level of accuracy though highly depends on the number of the population data accuracy. Once the lifing data have been calculated with high accuracy, cost estimation for different sets of missions can now be assessed.

4.3 Fuel Cost Estimation due to Degradation

Once the design point was chosen, it is worth finding how the degradation will affect the engines EGT margin consumption. A code in Python was developed to run Turbomatch for every point in the mission profile. The code used the engine performance characteristics for the three mission profiles mentioned in the previous paragraphs. Table 4-14 shows the degradation values and the related percentages used at Turbomatch simulations.

Deg Values	0.99	0.98	0.97	0.96	0.95	0.94	0.93	0.92
% Deg	1%	2%	3%	4%	5%	6%	7%	8%

Table 4-14: Degradation Values

Once the TET was calculated, it compared to the critical TET value (1200^{o} Kelvin) and the EGT margin was calculated. The following figures show the EGT margin consumption versus the degradation value for two cases: i) when the compressor and turbine module parameters for efficiency and mass flow degrade at the same rate and ii) When the two modules degradation rate differs iii) when the efficiency parameter degrade rate differs from the mass flow rate. The next paragraphs discuss the results.

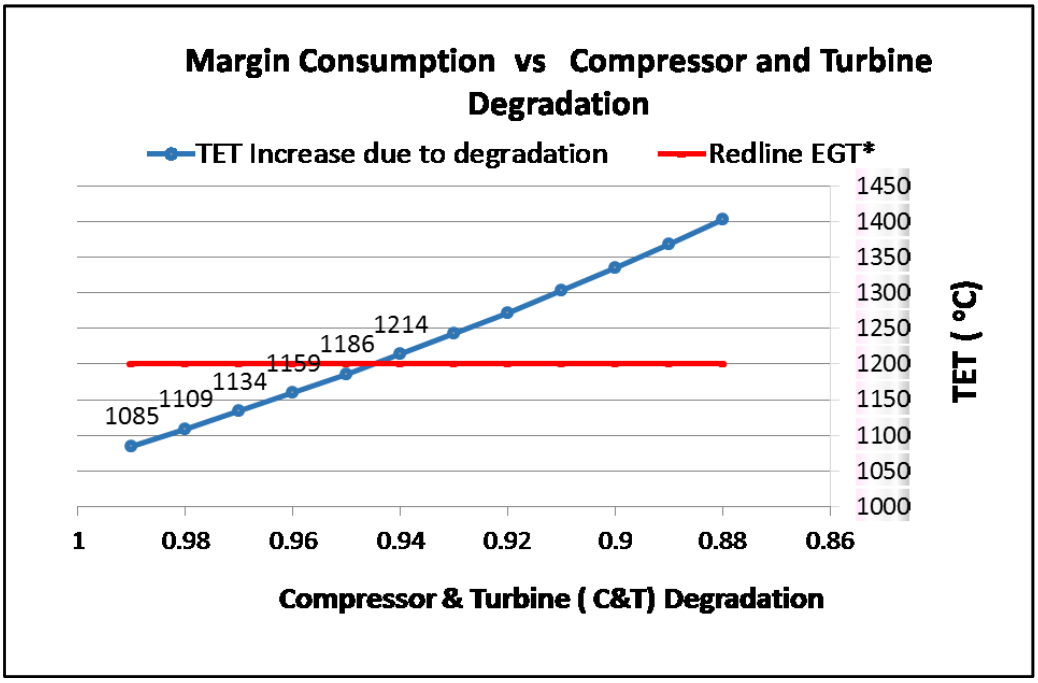

Figure 4-16 : TET increase due to degradation

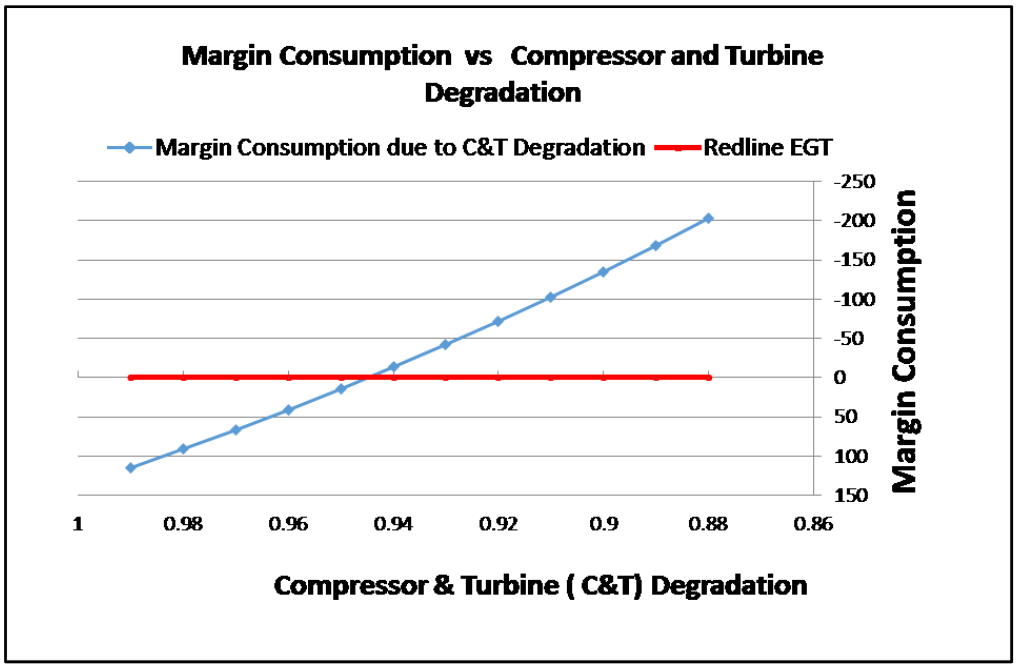

Figure 4-17: EGT Margin deterioration

Figure 4-16 and Figure 4-17 reveals that the engine consumes each safety margin when all the components and the mass flow degrade by 5.5% (0.945) of their nominal value.

The profound effect is that the turbine efficiency deterioration contributes more to the margin consumption and is the leading factor in the engine performance loss. The compressor

degradation, if acting independently, must reach a degradation level of less than a 0.88 value to force for engine removal for an overhaul. This is logical because the turbine module produces more work than the compressor and any losses to each performance have a greater effect at the engine operating temperature. Figure 4-18 provides a clearer view of the phenomenon.

Figure 4-19 and Figure 4-20 show the turbine and compressor module contribution respectively when efficiency and mass flow are decreasing separately. The interesting features in these figures are the following:

a. The component efficiency contributes more than the mass flow in both the turbine and the compressor and this is partly because the mass flow decrease is mainly a by-product of the module efficiency deterioration as very well analysed at Kurtz [29] work. As mentioned in this work the efficiency loss due to clearance losses increases the axial flow blockage, therefore, contributing to the mass flow decrease.

b. In the turbine case the EGT margin is consumed when the efficiency degrades about 10.10% (0.89).

c. In the compressor case the EGT margin is not consumed even when the efficiency degrades more than 11 % (0.88).

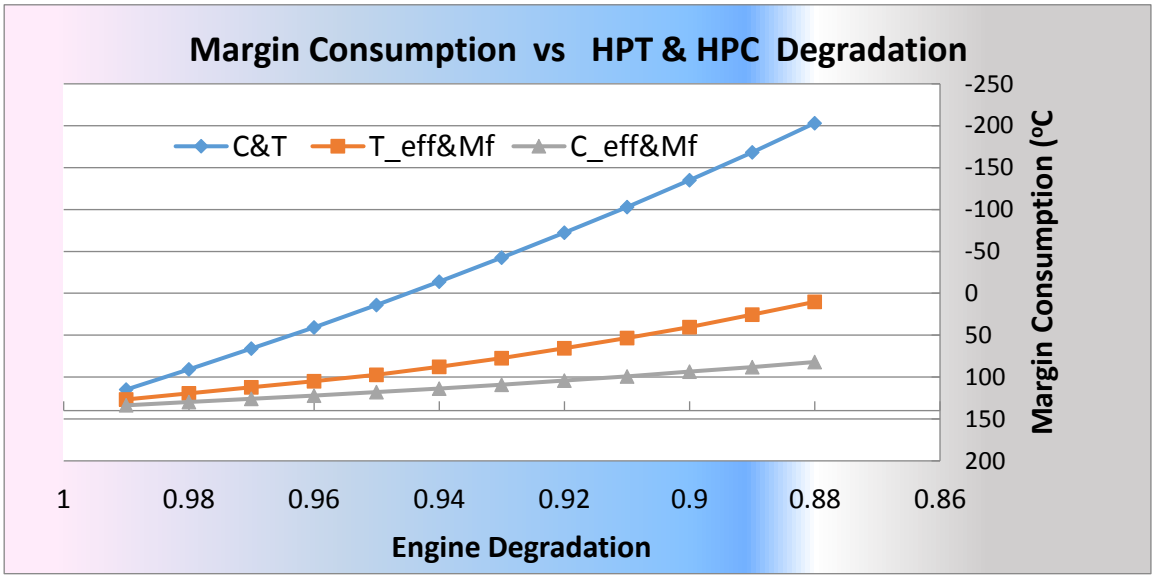

Figure 4-18: EGT Margin Consumption vs Engine Compressor/Turbine Degradation

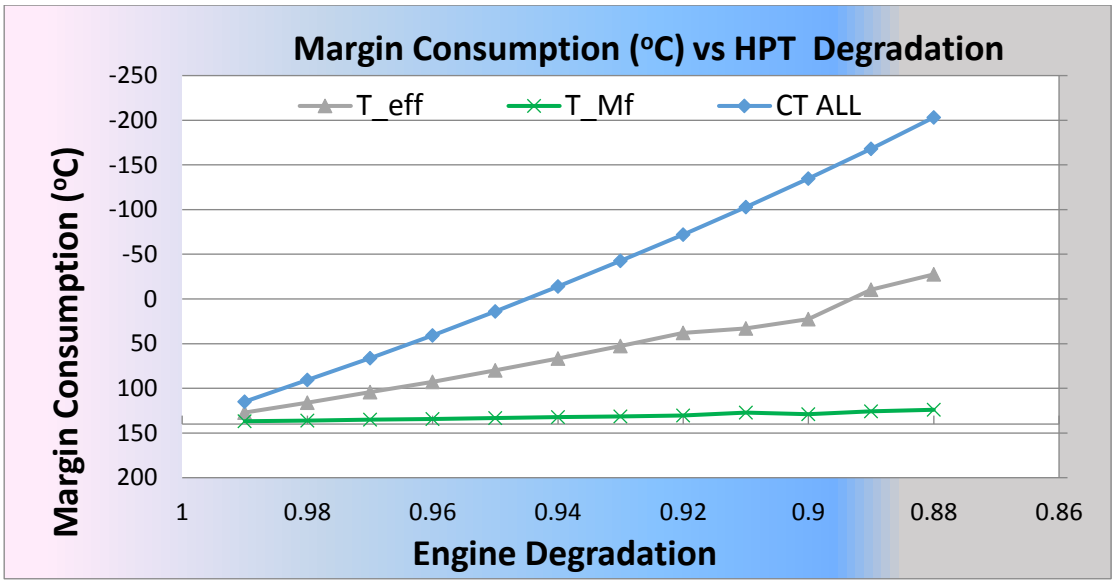

Figure 4-19: EGT Margin Consumption vs Engine Turbine Degradation

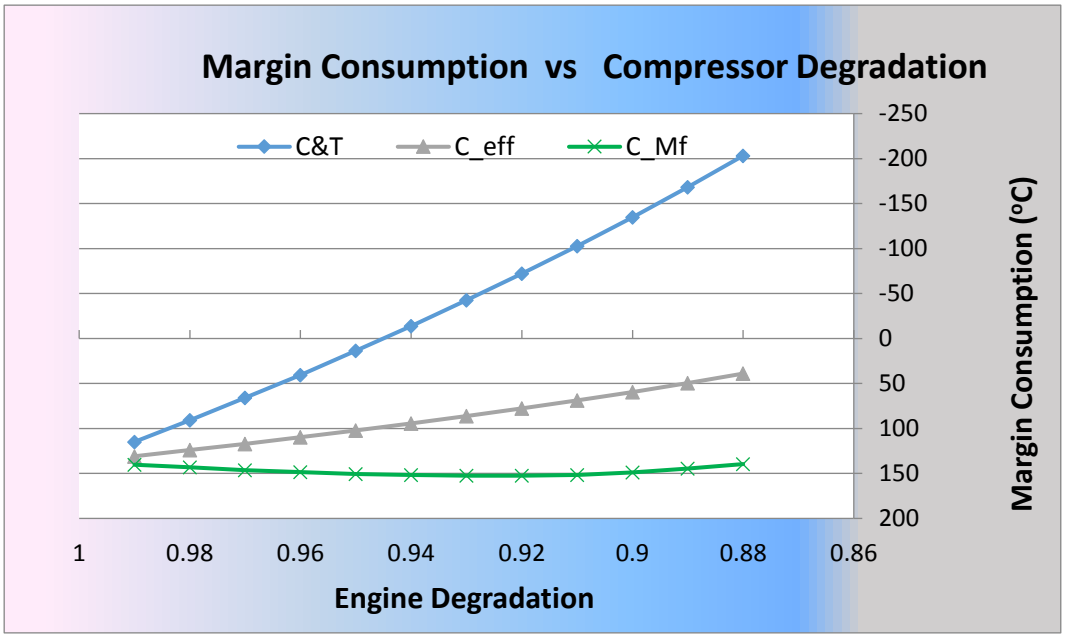

Figure 4-20 : EGT Margin Consumption vs Engine Compressor Degradation

To estimate the incurred fuel costs due to degradation we used the following assumptions:

a.The modules degrade simultaneously.

b.The parameters degradation profile is the one presented in Table 4-15.

c.The degradation value 0.945 which consumes the EGT margin is related to the flight hours that that the engine is inducted for performance restoration.

d.The rotorcraft is using the flight profile: i) 80% passenger mission, ii) 10% OAG and iii) 10% SAR.

The Following table shows the degradation vs the flight hours

Deg Value	1	0.99	0.98	0.97	0.96	0.945
% Deg	0%	-1%	-2%	-3%	-4%	-5.5%
Flight Hours	0	70	200	400	1200	2000

Table 4-15 : Degradation vs Flight Hours

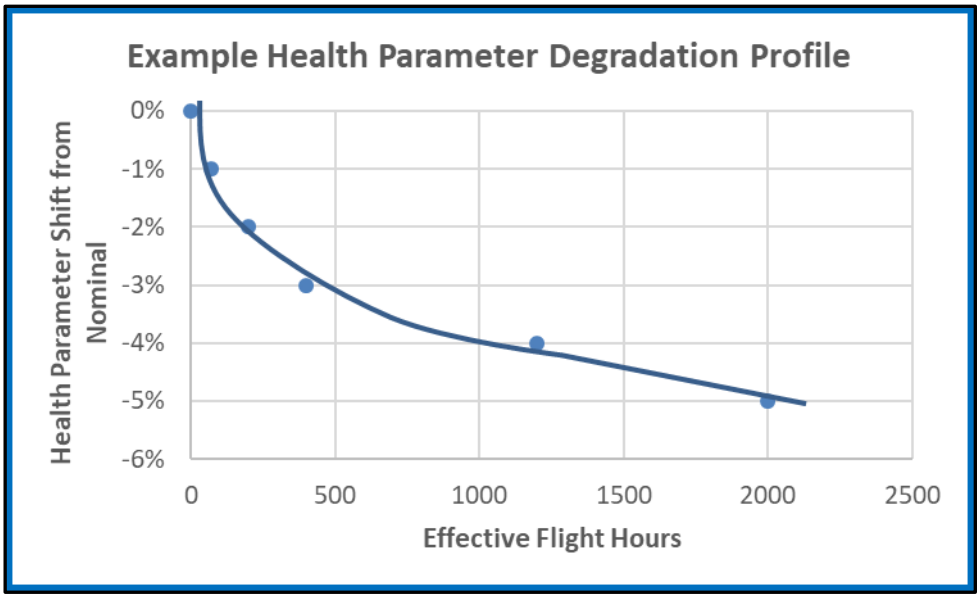

The costs incurred are presented in the next table.

Weight Factor	Mission	Fuel Cost with Degradation	Fuel Cost per Type	Fuel Cost without Degradation	Fuel Cost per Type
(1)	(2)	(3)	(4)	(5)	(6)
0.8	Pas/nger	23,395	18,716	20,759	16,607
0.1	OAG	119,258	11,926	106,591	10,659
0.1	SAR	213,653	21,365	179,705	17,970
Fuel Cost for 2000 FH *			42,629		37,146
Fuel Cost for 12000 FH *			255,772		222,875
Difference (%)				14.8	

* The value is the Net Present Value (NPV) (Eq 3.12)

Table 4-16 : Fuel Cost due to Degradation

The important finding presented in Table 4-16 is that the component degradation can increase the fuel cost by almost 15%.

4.4 Maintenance Cost Estimation

The engine used for the case scenario is an Allison 250-C20B. The value for the input variables that have been introduced in paragraph 3.5.2.1 is presented in Table 4-17.

Variable	Value
TBO_REF (FH)	2000
LLP_REF (FH)	3597 / 5566 / 6887
EIP ($)	265000
FH/YEAR	300
Fuel Cost/Lt ($)	0.43
O_int (FH)	25
I_int (FH)	100
O_MMH	0.2
I_MMH	0.8
MMH_COST ($)	102
SHP (KW)	384
ADMIN MMH ($)	101

Table 4-17: Cost Subroutine Input Values

For this case scenario, we make the following assumptions:

a. The TBO value is the same used for the OEM

b. The turbine module life (LLP) has been estimated from the lifing code for three different missions.

c. The engine retirement limit is 40 years of service [59]. Then the engine is considered scrap material and its further usage are not cost effective.

d. The cost that relates to the operator profit loss due to engine unavailability is not considered. (Future work).

e. The remaining value of the LLP is not considered in the cost estimation and the item is considered scrap material. (Future work).

The cost estimation subroutine estimates the values of the variables presented in the methodology in Table 3-17. The input values are presented in Table 4-17 and the formulas

used for each of the three scenarios are shown in Appendix B at Table B-2 and Table -3. In the following lines, graphs will be used to show the effects of the different mixture in a yearly usage in maintenance costs. The data for the graphs are presented in Appendix F. The 3 scenarios that have been used to estimate the maintenance costs are presented in Table 4-18.

Mission	Weight Factor		
	Scenarios		
	1st	2nd	3rd
Ref	0.5	0.7	0.8
OAG	0.4	0.2	0.1
SAR	0.1	0.1	0.1

Table 4-18: Mission Combination Scenarios

4.4.1 Results and Discussion

4.4.1.1 Baseline Case

The results from the estimated values are presented below. To provide a better understanding of the yearly usage effects, of all mission mixture scenarios, to the maintenance cost, the graphs will show:

a. The cumulative costs trend that relates to both methods (MSV & Max LLP usage).(Figure 4-21 &Figure 4-22

b. The maintenance cost for the MSV method for the combined missions based on a yearly usage of 300 FH.

c. The maintenance cost for the Max LLP method for the combined missions based on a yearly usage of 300 FH.

d. A combination of the estimated costs for both, MSV and Max LLP usage, methods for 3 scenarios as presented in Table 4-18.

The first three graph types can assist the helicopter operator to make an informed decision on a short-term basis while the 4th type can help on the decision with regard to budget allocation on a longer term.

The three mission mixture scenarios presented in the graphs show that when the helicopter usage for OAG mission increases, the LLP life decreases, and therefore the helicopter engine induction rate for LLP replacement increases. This, of course, increases the overall maintenance costs.

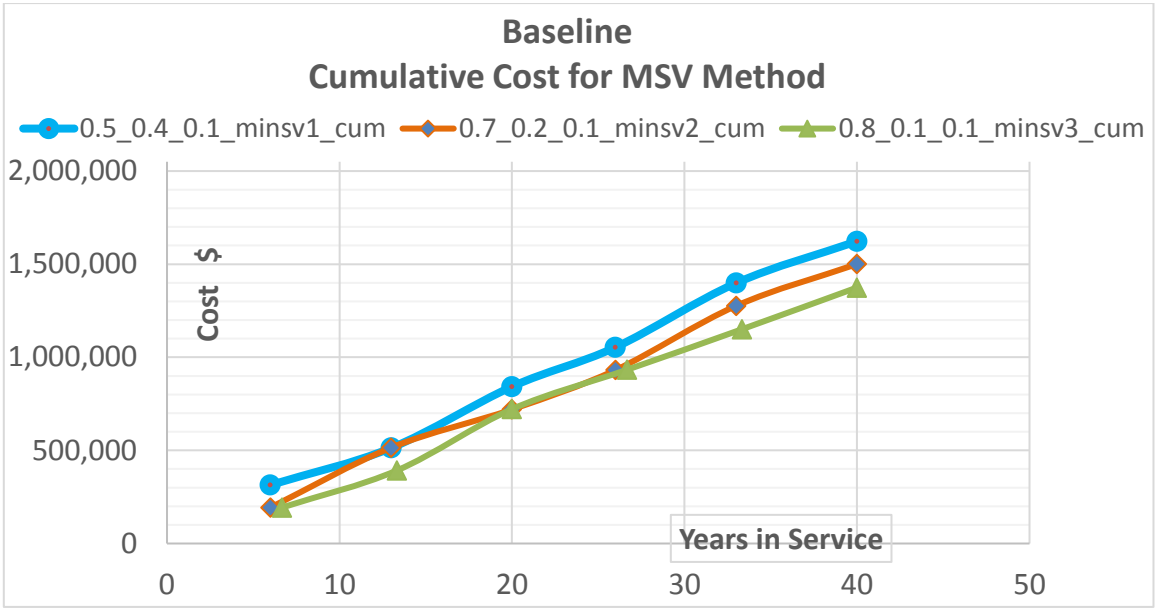

Figure 4-21: Cumulative Cost for MSV Scenarios

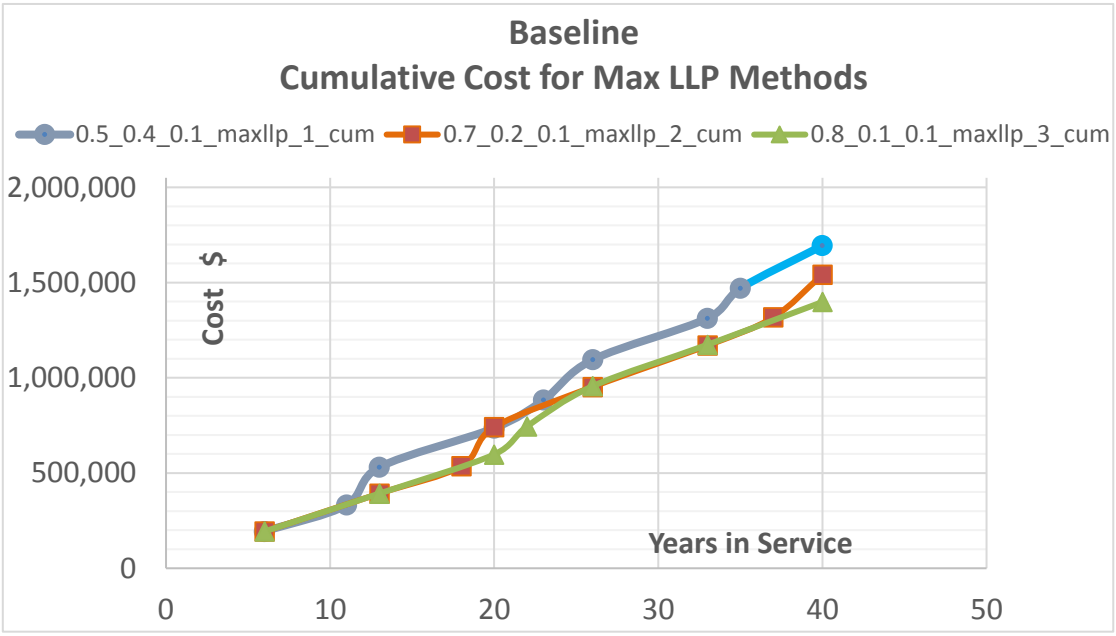

Figure 4-22: Cumulative Cost for Max LLP Scenarios

General Comments

A careful examination of the graphs in Figure 4-23 to Figure 4-25, reveals some interesting features:

a. All the graphs show that, with regard to the MinSV scenario, the engine is inducted for performance restoration 6 times, during its 40 years of service.

b. The cost for the MinSV method is presented in Figure 4-23 to Figure 4-25 with the red coloured line that forms successive peaks and troughs.

c. The Max LLP Usage line shape follows the same trend forming peaks and troughs where the peaks relate to a TBO service and the valleys to an induction just for LLP replacement. An important feature in these lines is that the induction times for a shop visit have a decreasing trend (9, 8, and 7 times) where the first scenario relates to the peak value (9 times).

d. While the engine in the MaxLLP method is inducted for service more times, thus decreasing the engine availability, the incurred service costs have a smoother distribution during the engines service time.

e. The successive peaks show a slight increase in the value due to the assumed inflation parameter is taken from the public domain. The inflation used was based on the consumer price index (CPI) and it was the average of the inflation values from 1997 to 2017 which was close to 2% per year.

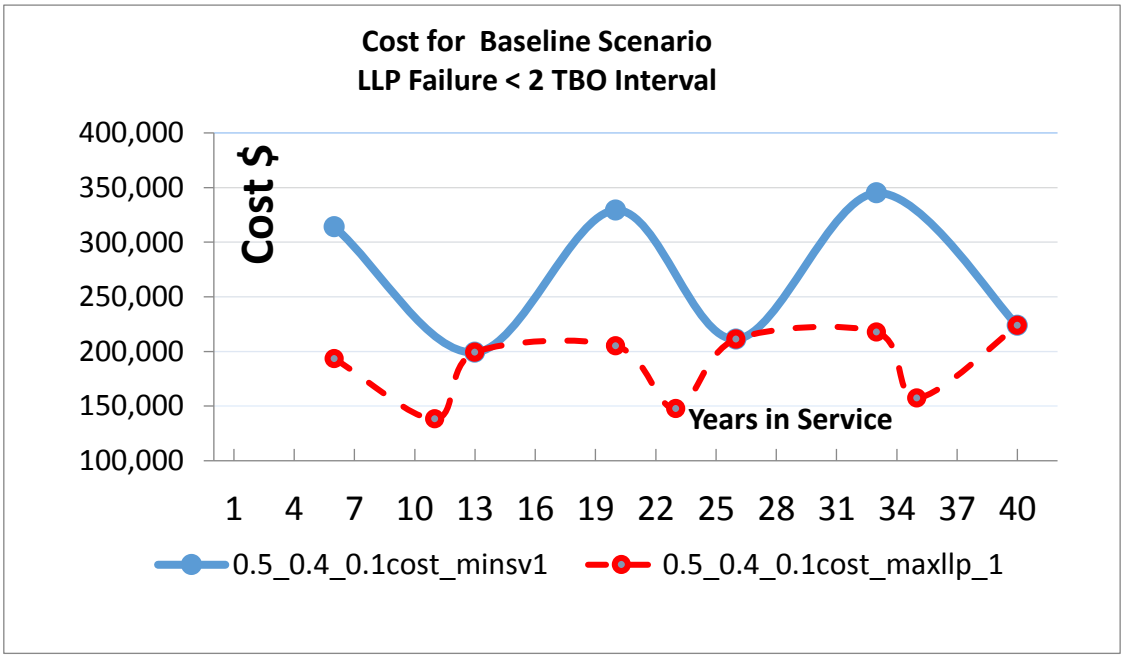

Figure 4-23: Cost for Scenario LLP Failure < 2 TBO Interval

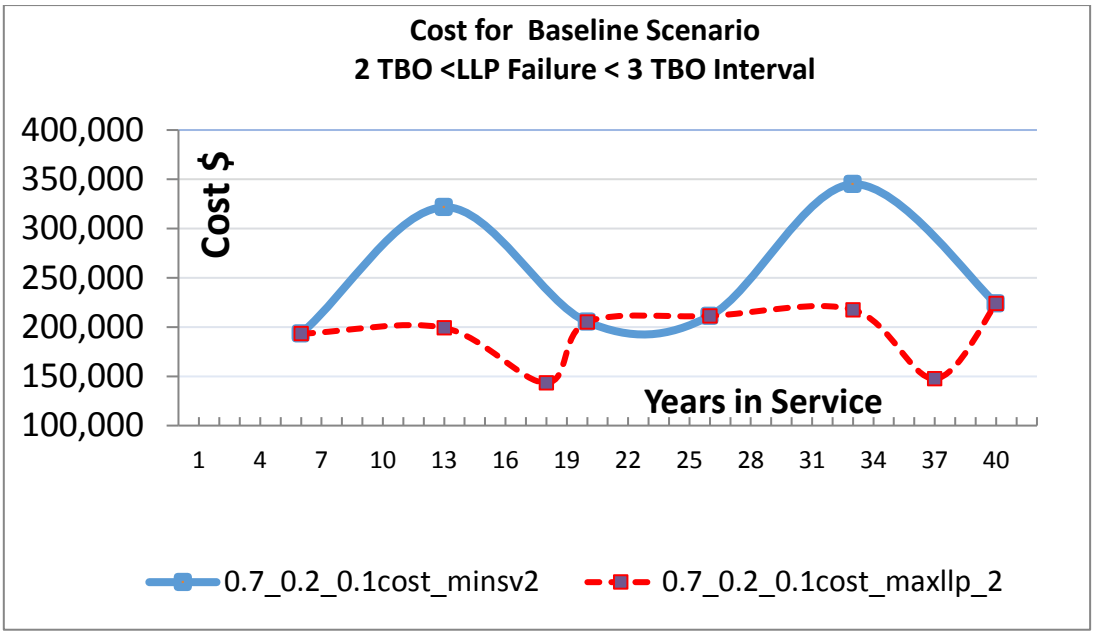

Figure 4-24: Cost for Scenario 2 TBO <LLP Failure < 3 TBO Interval

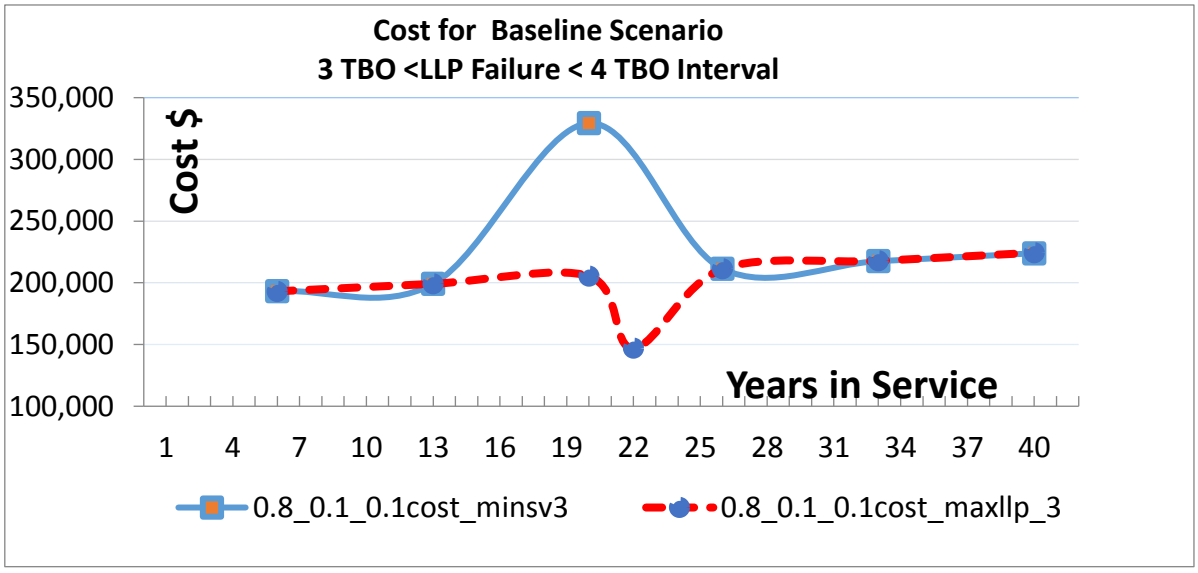

Figure 4-25: Cost for Scenario 3 TBO <LLP Failure < 4 TBO Interval

Short-Term Analysis

The reason for the features mentioned in the previous paragraph and the impact they have cost wise are discussed in the next lines:

MINSV scenario

With regard to the MinSV scenarios, shown in the graph in Figure 4-23 to Figure 4-25, the peaks are related to costs that comprise the performance restoration and the LLP

replacement while the troughs are related to induction in a repair shop only for performance restoration. This feature is interesting because it can help an operator make an informed decision for the engine maintenance cost regarding the budget available. The Min SV scenario provides more flexibility in case the operator decides to exchange the engine with another with better flight history before the peak value has been reached. The Figure 4-26 where the lines of the three scenarios are superimposed shows a better view of the incurred cost trend.

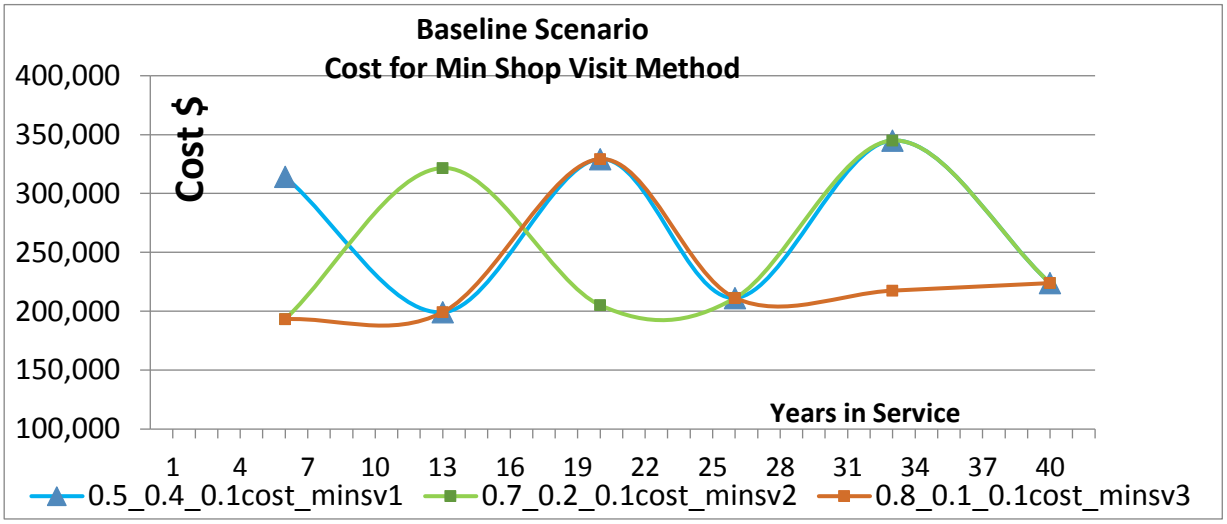

Figure 4-26: Cost for Min Shop Visit Scenarios

MaxLLP Usage Scenario

With regard to the Max LLP usage, the graph in Figure 4-27 shows the following:

a. There is a steadily increasing trend regarding the cost line, which is attributed to the assumed 2% inflation.

b. The same trend continues, and the wavelength between the peaks and troughs changes, following a pattern, which depends on the scenario.

Long-Term Analysis-Cumulative Costs

The graphs in Figure 4-23 to Figure 4-27 presented the cost trends with regard to the engine availability and in addition, the cost fluctuation for every mission combination as presented in Table 4-18 and in relation to each other.

In order to have a clearer view of the cost in the engine lifespan, a graph that represents the cumulative costs should be presented. To that end, the graphs in Figure 4-28 to Figure 4-30,

provide a clear view of the costs incurred in the engines operating life. The two interesting points are the following:

a. The costs incurred at Max LLP scenario are higher than the ones at the MINSV scenario

b. The Max LLP scenario shows cumulative costs greater than the MinSV usage scenario in the first case (LLP: 3597) while the difference decreases at the second (LLP: 5566) and is almost equal at the third case (LLP: 6856). That means that the mixture of the missions influences the engines life and the incurred cost.

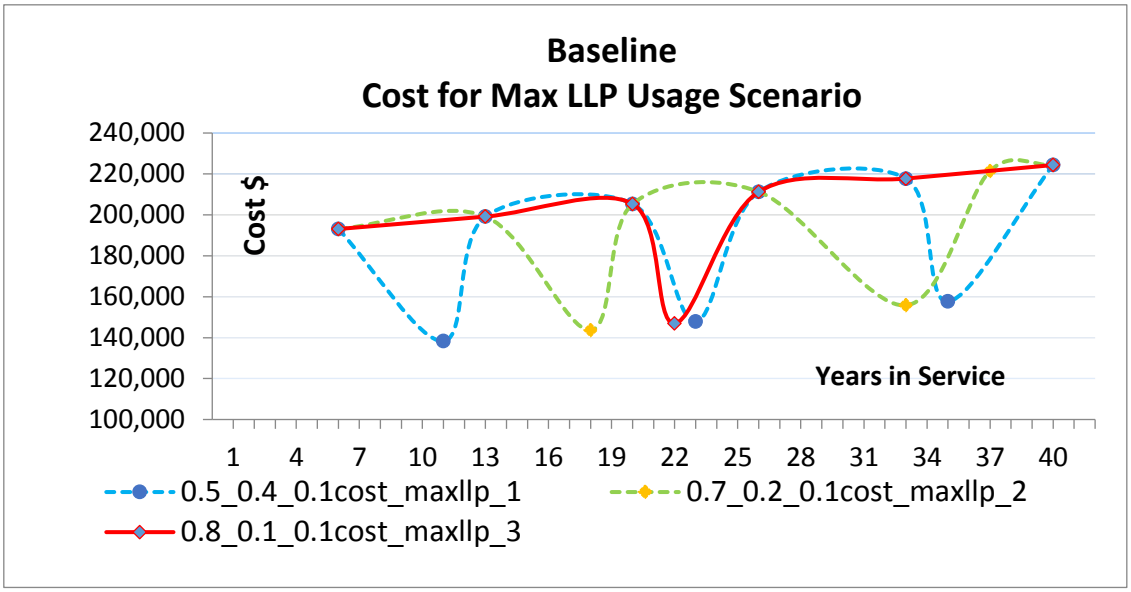

Figure 4-27: Cost for Max LLP Usage Scenario

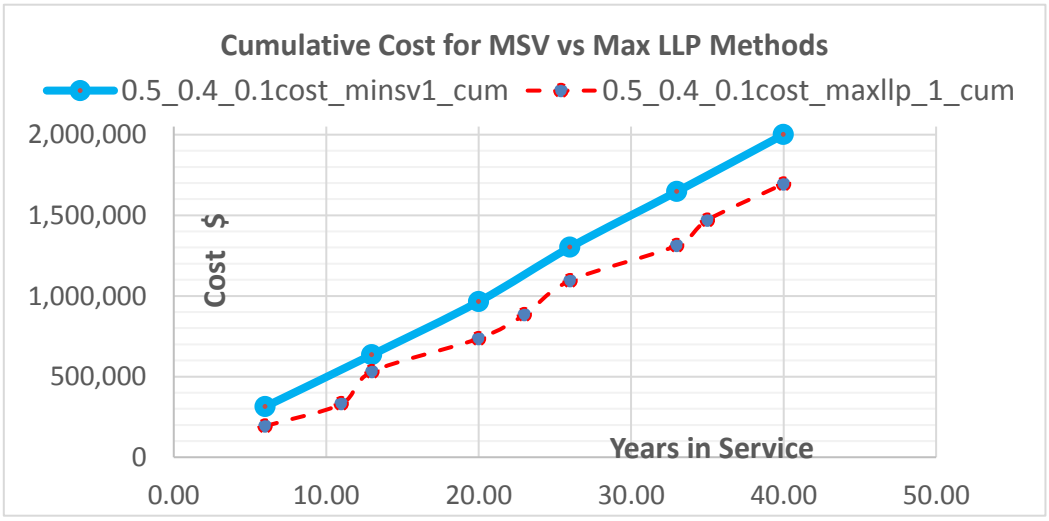

Figure 4-28: Cumulative Cost for MSV vs Max LLP for scenario 3TBO< LLP< 4 TBO

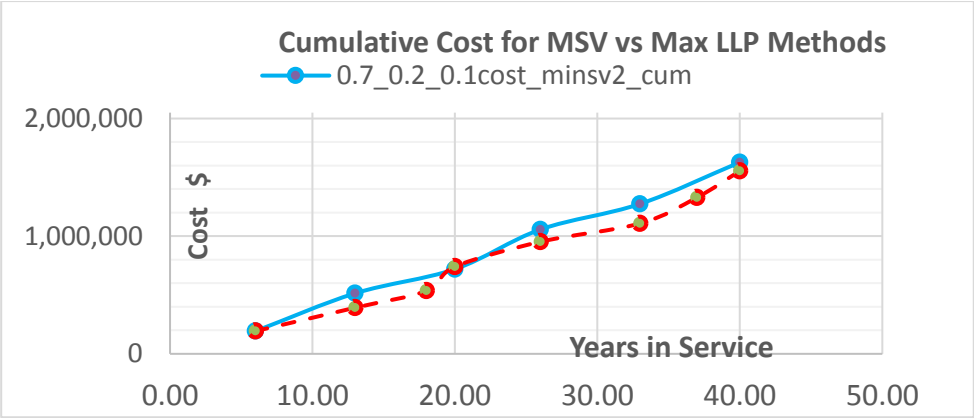

Figure 4-29: Cumulative Cost for MSV vs Max LLP for scenario 2TBO< LLP< 3 TBO

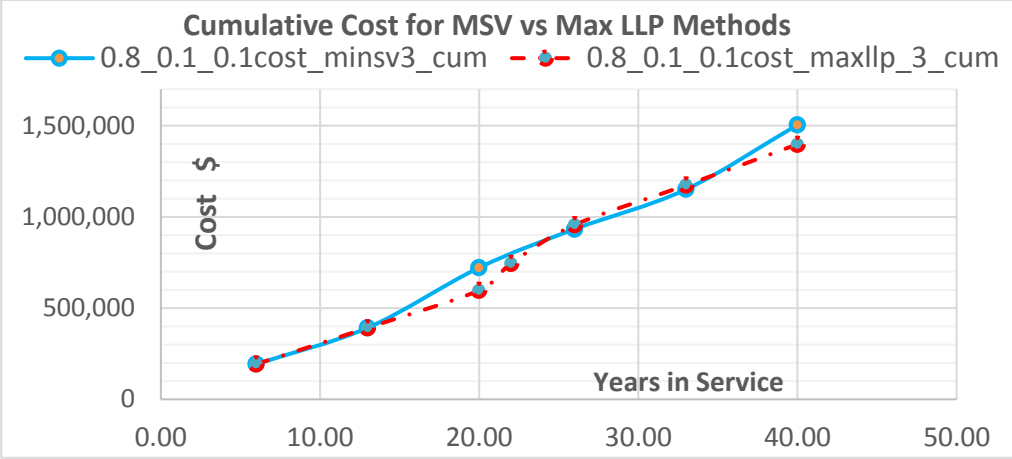

Figure 4-30: Cumulative Cost for MSV vs Max LLP for scenario TBO< LLP< 2 TBO

The representative data for the cumulative costs for the engines usage and the costs/flight hour are shown in Table 4-19 and **Table 4-20**.

Engine Initial Price		265000			
Cause	Shop Visits	Cost ($)-Present Value	Cause	Shop Visit	Cost ($)
(1)	(2)	(3)	(4)	(5)	(6)
Min SV 1	6	1,498,191	Max LLP 1	9	1,563,683
Min SV 2	6	1,385,108	Max LLP 2	8	1,423,005
Min SV 3	6	1,268,952	Max LLP 3	7	1,290,675

Table 4-19: Cumulative Cost Data for MIN SV and Max LLP Usage scenarios

Cause	Shop Visits	Cost ($/FH)	% Change	Cause	Shop Visits	Cost ($/FH)	% Change	LLP Interval (FH)
(1)	(2)	(3)	(4)	(5)	(6)	(7)	(8)	(9)
Min SV 1	6	125		Max LLP 1	9	130		3596
Min SV 2	6	115	7.5%	Max LLP 2	8	119	9.0%	5566
Min SV 3	6	106	15.3%	Max LLP 3	7	108	17.5%	6885

Table 4-20: Cumulative Cost Data for MIN SV and Max LLP Usage scenarios in $/FH.

Three important points in Table 4-20 are the following:

a. The cost values are the present values, which were estimated using the equation 3-12.

b. At the MinSV3 case, the cost per flight hour decreases close to 15 % relative to the MinSV1 case value while at the MaxLLP method the cost decreases at a higher %.

c. With regard to the engine availability, the engine in the MaxLLP3 case is inducted 2 times less than the MaxLLP31 case while for the MinSV method the engine is inducted only 6 times. That means that when the availability is of higher importance the MinSV method is the preferred one. Table 4-21 shows the results of the two methods comparisons. The data shows the following:

d. The MaxLLP method is always the one with higher incurred costs

e. The cost difference decreases and the two methods incurred costs diminish to 1.71%.

f. That means that a mission mixture that relates to higher LLP failure cycles favours the MinSV method.

Cause	Shop Visits	Cost ($/FH)	Cause	Shop Visits	Cost ($/FH)	MinSV vs MaxLLP % dif	LLP Interval (FH)
(1)	(2)	(3)	(4)	(5)	(6)	(7)	(8)
Min SV 1	6	125	Max LLP 1	9	130	4.37	3596
Min SV 2	6	115	Max LLP 2	8	119	2.74	5566
Min SV 3	6	**106**	Max LLP 3	7	108	1.71	6885

Table 4-21 : Cost comparison for MinSV vs MaxLLP methods.

4.4.1.2 Operator in Hot Climates Case

Using the same methodology, we can estimate the maintenance costs for an operator with flight profile in a hot operating environment. In this case, we assume that the operator flies to an environment where ISA Deviation is in the range 10 to 15 ie 25 to 30^0 Celsius.

Cause	Shop Visits	Cost ($/FH)	Cause	Shop Visits	Cost ($/FH)	MinSV vs MaxLLP % dif	LLP Intervals
(1)	(2)	(3)	(5)	(6)	(7)	(8)	(9)
Min SV 1	6	125	Max LLP 1	9	129	3.40	3172
Min SV 2	6	115	Max LLP 2	8	**119**	3.18	4851
Min SV 3	6	115	Max LLP 3	**8**	**118**	2.26	5975

Table 4-22: Cost comparison for MinSV vs MaxLLP methods in $/FH for Hot Climate

For this “Hot climate”, case the load and climb rate values for the baseline case were used and the ISA deviation value changed to 15. The data presented in Table 4-22 shows the following:

a. Regarding the engine induction time for performance restoration, this is kept to 6 but the LLP failure cycles as shown in column 9 decrease and the engine is inducted 8 times instead of 7 at the MaxLLP3 case.

b. The expected LLP life decrease will affect the maintenance costs for the MinSV3 and maxLLP3 cases, due to the changes in the timeframe that the engine will be inducted for LLP replacement as shown in Table 4-23. The maintenance cost at the MinSV method will be the same for the 2 first cases MinSV1 and MinSV2. In the MinSV3 case, the LLP life decreases so much as to force the engine induction for LLP replacement 2 times instead of one in the baseline case. The cost of the LLP replacement increases the cost to 115$/FH instead of 106 in the baseline case. The same applies in the case of the MaxLLP3 case because the engine is inducted 8 times instead of 7 in the baseline case. The analysis for the incurred costs for every case is shown in Appendix F.

Scenarios			
Reference		Hot Climate	
Induction Interval	Years in Service	Induction Interval	Years in Service
2,000	6	2,000	6
4,000	13	4,000	13
6,000	20	5,975	19
6,885	22	6,000	20
8,000	26	8,000	26
10,000	33	10,000	33
12,000	40	11,950	39
		12,000	40

Table 4-23: Induction Intervals for Reference and Hot Climate Scenario

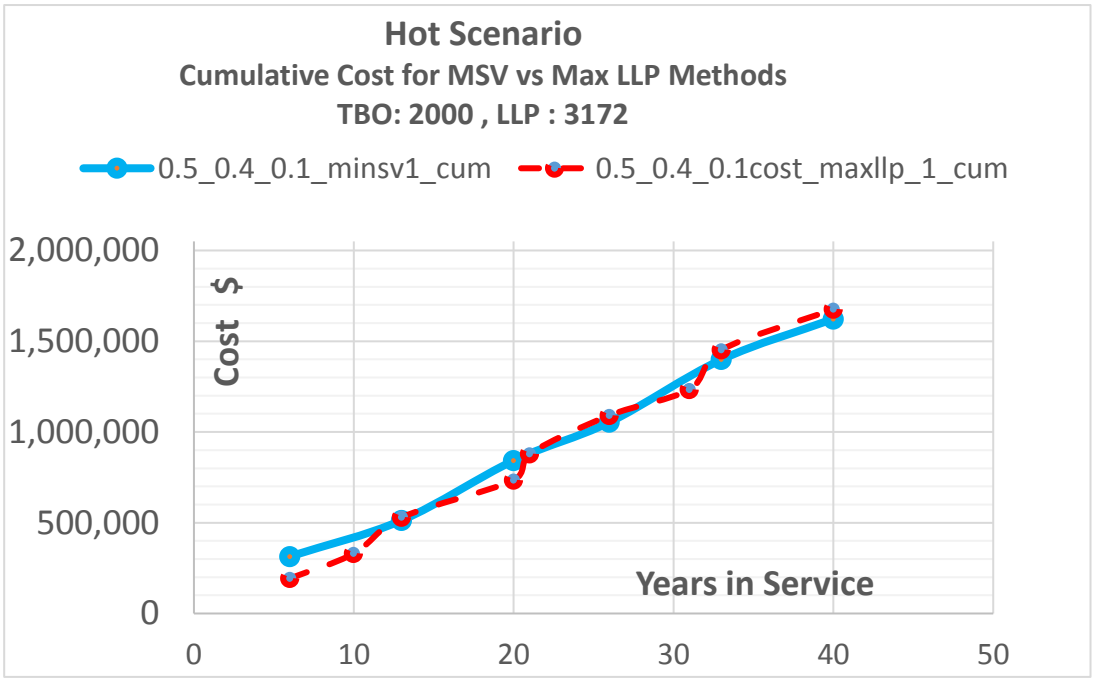

Figure 4-31: Cumulative Cost for MSV vs Max LLP for scenario 3TBO< LLP< 4 TBO

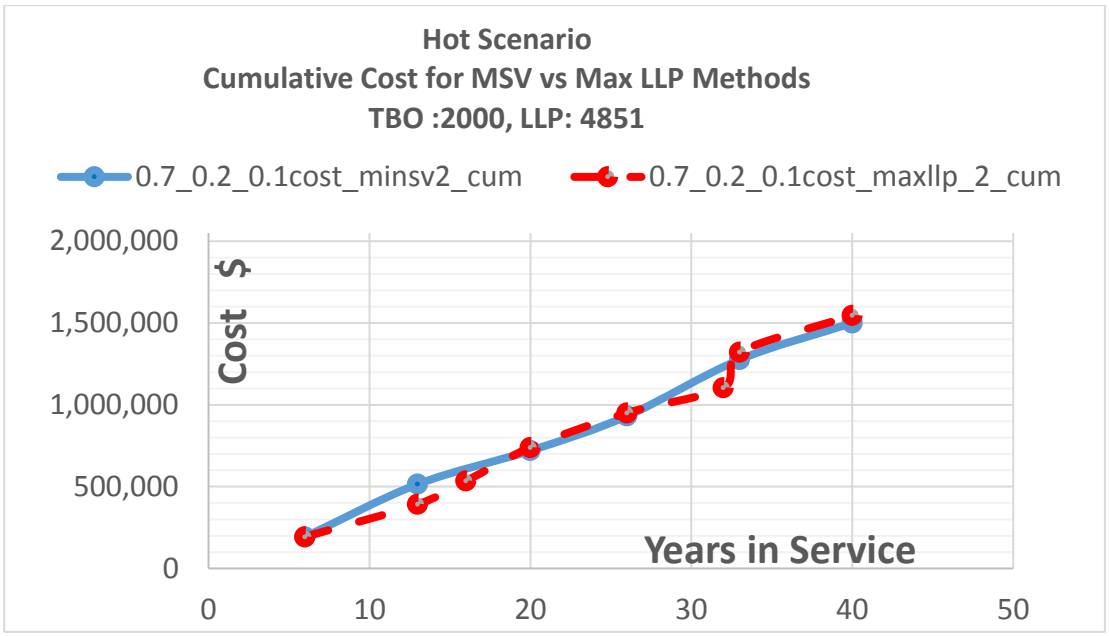

Figure 4-32: Cumulative Cost for MSV vs Max LLP for scenario 2TBO< LLP< 3 TBO

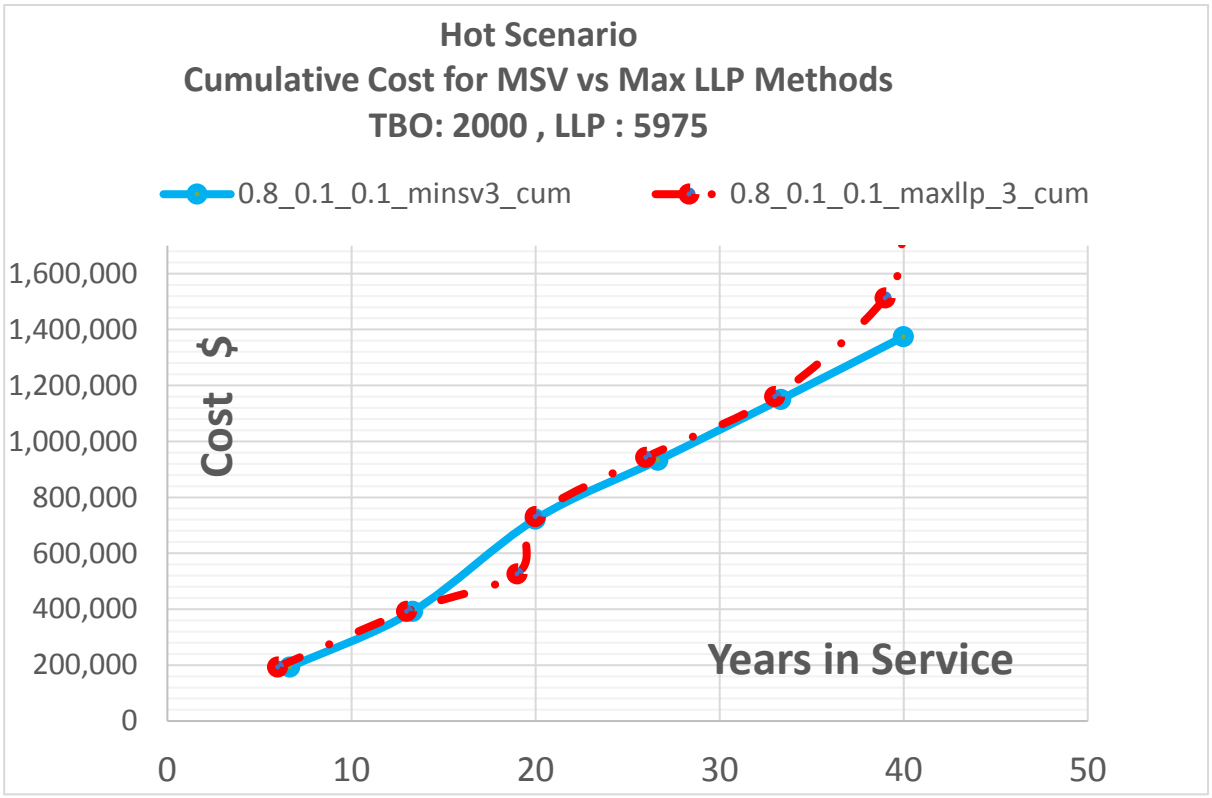

Figure 4-33: Cumulative Cost for MSV vs Max LLP for scenario TBO< LLP< 2 TBO

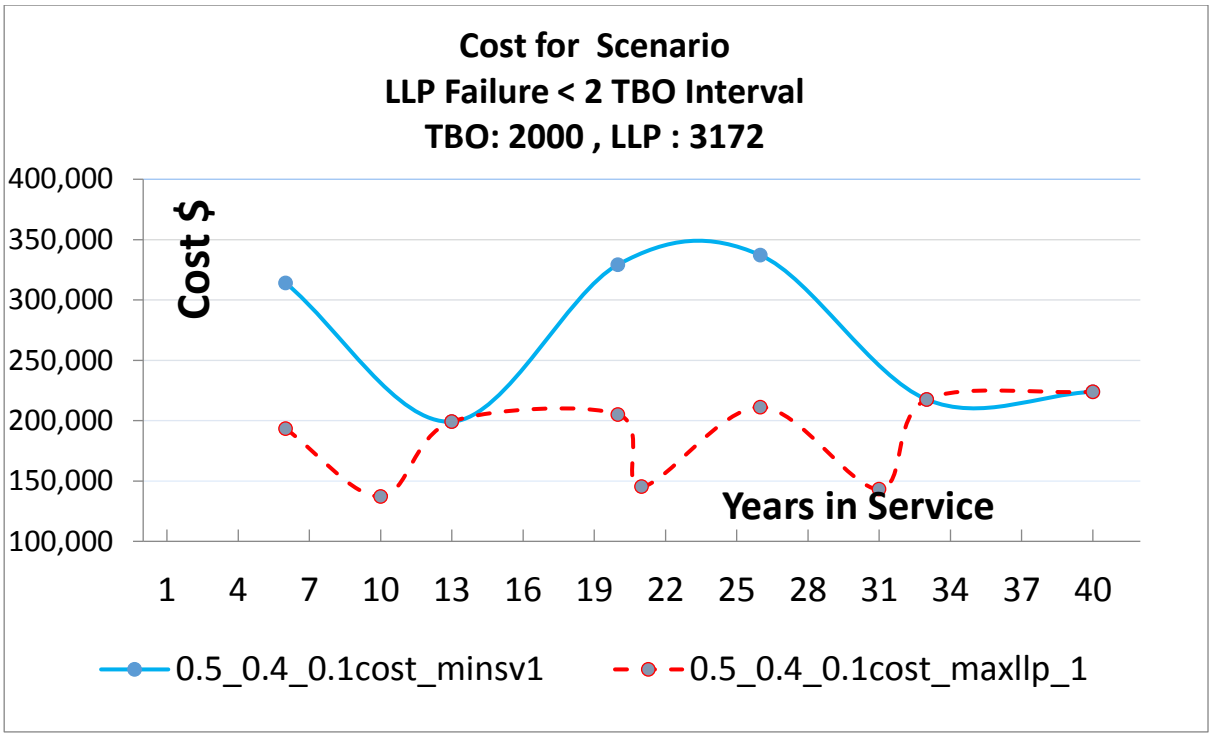

Figure 4-34: Cost for Scenario LLP Failure < 2 TBO Interval

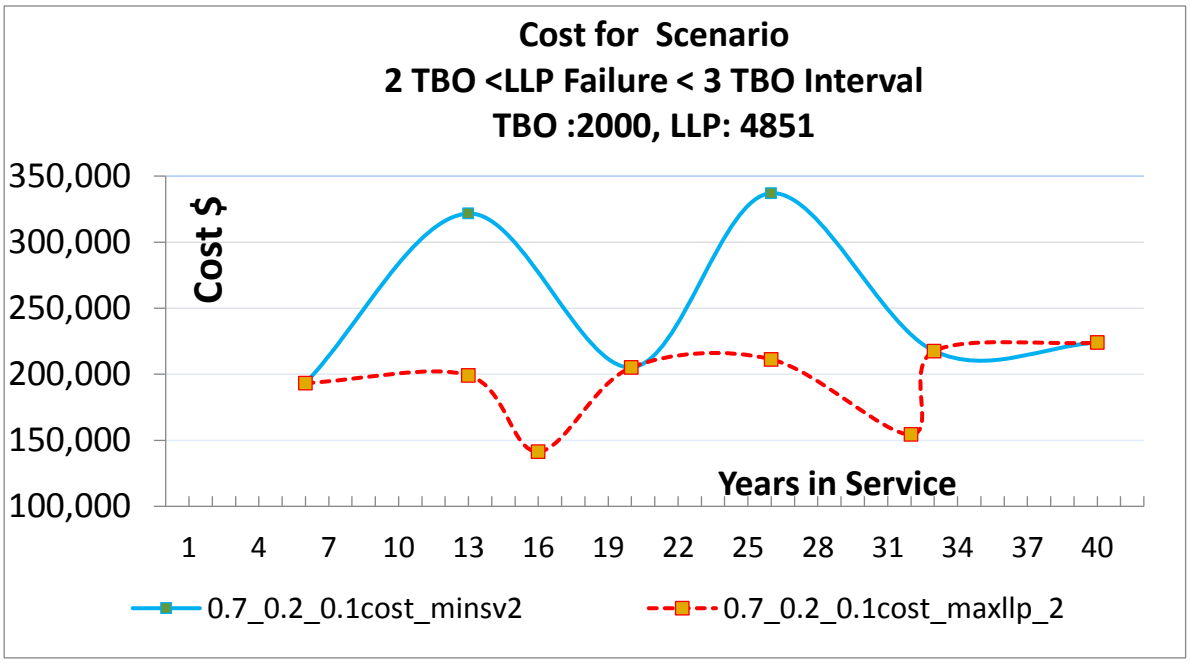

Figure 4-35: Cost for Scenario 2 TBO <LLP Failure < 3 TBO Interval

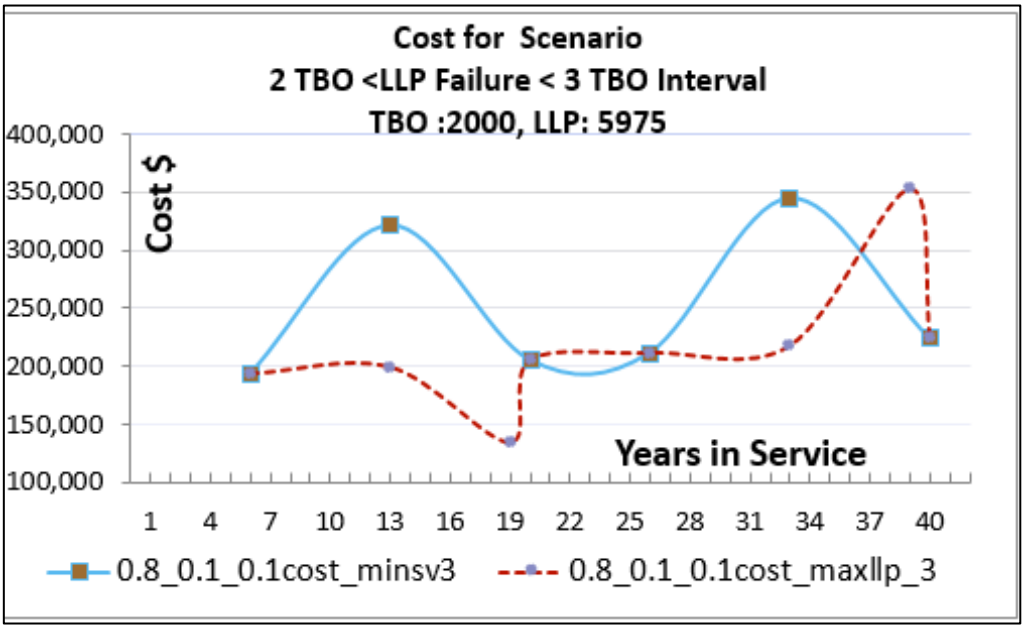

Figure 4-36: Cost for Scenario 2 TBO <LLP Failure < 3 TBO Interval

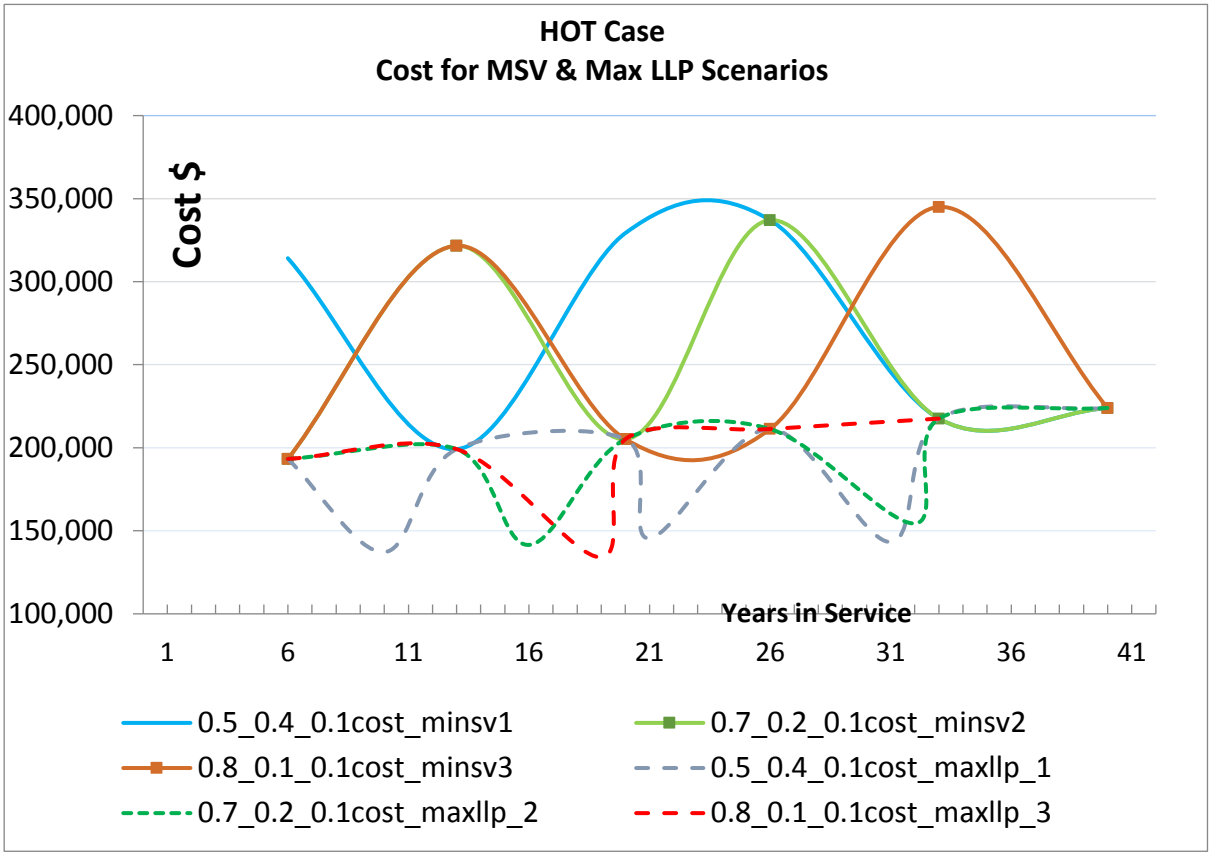

Figure 4-37: Cost for MinSV & Max LLP Usage Scenario

4.4.1.3 Safety Factors Effect on Maintenance Costs

This section will address the effect of the safety factors on the incurred maintenance costs. A question that may arise is why this research performed a sensitivity analysis and seeks their effect on component life, once the component designer does not have any means to influence the safety factors affect in components life once the component was manufactured.

While it is true that these factors values are obtained either: i) from the theory of elasticity, ii) from numerical solutions, or iii) from experimental measurements, their contribution to the component life might prove crucial when the loads that relate to rotorcraft missions help a crack nucleation to commence. At this point, it is important to mention that elastic stress concentration factors for homogeneous isotropic materials depend only on geometry (independent of material) and mode of loading. The geometry of a propagated crack which was initiated due to the imposed stresses is not known, therefore, an effort to address the safety factors affect components life and the incurred costs is deemed necessary.

Paragraph 4.2 discussed how the design for fatigue based on safety factors could alter the LLP time limits. The sensitivity analysis results presented in Table 4-9 showed that a change in the safety factors value in the range of 30% could alter the life limit up to 25 %. Using the WU-FPM method, described in paragraph 3.6.3, the equivalent LLP hour limit for the combination of missions, as shown in Table 4-18, has been estimated. The next table shows the different LLP life limits when we assume values other than the baseline for the safety factors variation:

Scenario	Safety (q=0.9)		
Mission Combination	kt = 3.77	kt = 2.03	Kt=2.9 (Baseline)
0.5/0.4/0.1	2726	4370	3596
0.7/0.2/0.1	4180	6789	5566
0.8/0.1/0.1	5152	8400	6885

Table 4-24: LLP life limits based on safety factor changes.

Table 4-25 and Table 4-26 present the differences in the costs incurred for the mission combination and the safety factors values mentioned above. A careful examination of the data in the tables raises the following questions that need to be addressed:

c. Why MAXLLP2 baseline and 3.77 cost related values are the same while the related LLP life limits are 5566 and 4180 respectively?

d. Why MinSV3 baseline and 2.03 cost related values are the same while the related LLP life limits are 6885 and 8400 respectively?

e. Why MinSV1/2/3 incurred costs have different values while the engine is inducted for performance restoration 6 times?

Cause	Shop Visits	Shop Visits	Shop Visits	Cost ($/FH)	Cost ($/FH)	Cost ($/FH)
(1)	(2)	(3)	(4)	(5)	(6)	(7)
	Kt=3.77	Kt=2.03	**Baseline**	**Baseline**	Kt=2.03	Kt=3.77
Max LLP 1	10	8	**9**	**130**	112	145
Max LLP 2	8	7	**8**	**119**	107	119
Max LLP 3	8	7	**8**	**108**	99	118

Table 4-25: Cost differences for the MaxLLP method for safety margin scenarios

Cause	Shop Visits	Shop Visits	Shop Visits	Cost ($/FH)	Cost ($/FH)	Cost ($/FH)
(1)	(2)	(3)	(4)	(5)	(6)	(7)
	Kt=3.77	Kt=2.03	Baseline	Baseline	Kt=2.03	Kt=3.77
Min SV 1	6	6	6	125	115	134
Min SV 2	6	6	6	115	106	125
Min SV 3	6	6	6	106	106	115

Table 4-26: Cost differences for the MinSV method for safety margin scenarios

The answer to these questions is based to the fact that the calculation for the engine induction cost and the LLP values use the inflation rate as a multiplier, as shown in equations 3-8 and 3-11. More specifically:

f. The answer to the 1sth question is that in both cases the engine is inducted two times just for LLP change. The one at 5566 and 11132 and the other at 4180 and 8360 respectively.

g. The answer to the 2nd question is that in the baseline case the LLP module is changed once at 6000 FH while in the second case is changed twice at 4000 (LLP : 5152) and 10000 FH (LLP: 10304 FH) .

h. The answer to the 3nd question is given from the data in Table 4-27 which shows the different number of times that the engine is inducted for performance restoration (TBO) and LLP replacement. The LLP component is replaced 3, 2 and 4 times respectively which is the reason that the incurred cost is different while the engine is inducted for 6 times in the repair shop.

	Baseline	Kt=3.77	Kt=2.03
TBO Interval	TBO and LLP Replacement		
2,000	2000 and 3596		2000 and 2726
4,000		4000 and 4370	4000 and 5452
6,000	6000 and 7192		
8,000		8000 and 8740	8000 and 8178
10,000	1000 and 10788		1000 and 10904
12,000			

Table 4-27: MinSV1 scenarios for LLP limits: i) baseline, ii) kt=2.03, iii) kt=3.77

The data in Table 4-25 and Table 4-26, which show the cost difference due to the stress-concentration factor change at a range of 30% relative to a baseline value, can be used as a basis to calculate the stress concentration factor effect on maintenance cost. The data in Table 4-28 and Table 4-29 show that the incurred costs relative to the baseline cost values lie: i) for the MinSV method in the range of -8% to 9%, and ii) for the MaxLLP method in the range of -14% to 11%.

Another important feature in the results presented in Table 4-28 and Table 4-29 that can raise a concern is that the % change does not follow a symmetrical pattern. The % change in the two first cases in the MinSV method is about 16 % (-8% to %8) while in the 3rd case it is only 9%. In addition, the % change in all MaxLLP cases is 25%, 10%, and 17% respectively.

Cause	Cost ($/FH)	Cost ($/FH)	% change	Cost ($/FH)	% change
(1)	(2)	(3)	(4)	(5)	(6)
	Baseline	Kt=2.03		Kt=3.77	
Min SV 1	125	115	-8	134	8
Min SV 2	115	106	-8	125	8
Min SV 3	106	106	0	115	9

Table 4-28: Safety factor's effect to baseline cost values in (%) change for MinSV method

Cause	Cost ($/FH)	Cost ($/FH)	% change	Cost ($/FH)	% change
(1)	(2)	(3)	(4)	(5)	(6)
	Baseline	Kt=2.03		Kt=3.77	
Max LLP 1	130	112	-14	145	11
Max LLP 2	119	107	-10	119	0
Max LLP 3	108	99	-8	118	9

Table 4-29: Safety factor's effect to baseline cost values in (%) change for a MaxLLP method

The reason for that phenomenon is that the life values that relate to these costs are flight hour values which have been calculated with the WU-FPM method, described in paragraph Operators Usage Scenarios. The cycles that have been used in this method are the median values which relate to a population of missions, therefore, the nature of the values is purely statistical. This is a fact that may explain the non-symmetrical pattern in the cost values.

The next section will discuss the conclusions drawn from this research and will recommend future work that has to be accomplished with a purpose to i) extend the scope of the research, ii) validate the results, or iii) improve the tools that have been either used or created during this 3 years' effort.

5 Chapter 5: Conclusions and Recommendations for Future Work

The proposed methodology attempted to estimate the turbine fatigue cycles for every different mission profile and assess the engine life cycle maintenance cost considering the mixture of different flight profiles for a certain timeframe instead of a single flight profile. In addition, to create a tool which will provide data to an operator, regarding turbine life limit estimation and incurred maintenance cost, considering factors like: i) fleet operating environment, ii) flight profiles used, iii) fleet number and expected availability and, iv)pilot experience and attitude.

5.1 Component Life Estimation

The literature review showed that the engines component life limits have been a favourite topic for many researchers. A part of Charkous [53] research focused on the HPT life limit and his methodology implementation on two rotorcraft types, an SA-330, and a BO-105, produced interesting results with regard to the reasons that lead to a component replacement. His findings were that creep is the prime phenomenon responsible for turbine blade damage only in long-range aeroplane missions. Hence, it is relatively rare to see such thing happening in rotorcraft, as they are mainly fly short or medium range missions. In the case of short-range missions, where relatively medium temperatures prevail, fatigue would be the main destructive phenomenon for the turbine. Therefore, this research focused on estimating the components life due to low cycle fatigue (LCF).

Variables Effect on TET

To understand the influence of the operating parameters for all the potential rotorcraft flight segments, a sensitivity analysis was carried out. The sensitivity analysis showed the effect that the operating variables have on TET. The analysis results showed that:

a. The payload firstly and the ISA deviation secondly is the most significant parameter that determines the engine TET.

b. The climb rate is more significant only in the climb segment.

A thorough review of the severity factor concept, presented in paragraph 2.3.3, revealed the importance of the reference mission flight features. The mission operating conditions should

be very carefully selected so as to relate the mission to the most representative combination of the operating design space.

Mission Segment and Flight Profile Effect on Fatigue Cycles

The results revealed that the highest stresses occur at the hover phase while the stresses decrease instantly when the rotorcraft enters the climb and the cruise segment. The 'rainflow' cycle counting method implementation showed that the high-stress amplitude values that are responsible for the life decrease relate to the stresses incurred at the hover phase. In addition, the 'rainflow' counting method coupled with the strain method implementation showed that the passenger flight mission, who was used as a reference flight experienced 4 fatigue cycles, while the SAR mission experienced 10 and the OAG 12 respectively. The main reason for the difference between the fatigue cycles is the times that the rotorcraft had to hover and the level of stress that was developed at every hover segment.

Validation Method

The validation method used for the DOE results was the LOO method. The results for 4 different sets of simulations (64, 100, 180 and 400) were validated, and the validation method showed that a population of 400 missions, whose operating parameters were estimated with the LHS sampling method, can be used to assess the component lives with a high accuracy.

The implementation of a DOE provides an interesting capability in the developed methodology. Once the lifing data for this population are available, the life for a smaller sample that relates to an operational flight profile can be easily assessed. A challenging issue with regard to this capability is that the accuracy of the estimated results depends on the population data, which relate to the simulation tool capabilities, and the method used for the interpolation. While HECTOR, the flight dynamic simulation tool, used in this research, provides the capability to set the results accuracy, the desired level regarding the power demand accuracy added a constraint to the number of simulations due to the required computational power.

Component Design Effect on Remaining Useful Life

Another important issue, brought into attention in this research, is that the component designed life is based on the assumed values of certain safety factors like i) the stress concentration, ii) the notch fatigue strength and iii) the notch sensitivity factor. The rotorcrafts missions' diversity and the incurred stresses impose an uncertainty with regard to a crack initiation and further propagation, therefore, it was deemed important to perform a sensitivity analysis to address the effect of these factors to the components life.

The sensitivity analysis results presented in Table 4-8 showed the following:

a. The effect of the stress concentration factor is more profound, compared to the notch fatigue (Kf) and the notch sensitivity factor (q).

b. A 30% increase in the stress concentration factor increases the engine life by 23% (62287) while a 30% decrease in the stress concentration factor decreases the engine life by 25% (37880).

c. With regard to the notch sensitivity variation, a 30% decrease in that factor results in 14 % decrease in the turbine life (58140) while a 30% increase will result in 16 % increase in the turbine life (42061).

5.2 Maintenance Cost Estimation

The literature review showed that there are different standardized methods available to estimate the costs of owning and operating an aircraft or rotorcraft. Roskam [75] and Jenkinson [1] proposed methods to estimate LCC costs for aircraft while the Helicopter Association International (HAI) provided a guide for rotorcraft cost estimation [4].The cost module (methodology) built in this research estimates the costs as described in HAI guide [4]. The module is based on two methods used in the aviation sector and analytically described in (Ackert article) the MinSV and MaxLLP method. The basis for both methods is the TBO and LLP replacement time limits.

An issue, which needed to be addressed in this research, was that the lifing module output provided the life limit in fatigue cycles and in order to use this life limit in the cost calculations, it had to be related to flight hours. The main difficulty in defining this relation is the inherent rotorcraft capability to perform different missions. If for example, a real-life scenario for an operator is to fly 300 hours per month with a combination of flights profiles the problem that

arises is that each one of the profiles relates to different fatigue cycle. The developed method WU-FPM, which is based on the linear damage rule, also referred to as the “Palmgren-Miner rule, was found to provide a good correlation between the flight hours and fatigue cycles.

Results from Method Implementation at Three Scenarios

The method was implemented in three case scenarios. The baseline case used a mission mixture that relates to a real-life scenario. The second case used an operator with flight profile in a hot operating environment assuming that the operator flies to an environment where ISA Deviation is in the range 10 to 15 i.e. 25 to 300 Celsius. The third scenario addressed the effect of the safety factors on the incurred maintenance costs.

The results related to the two methods showed the following features about:

a. Mission’s mixture:

1) There is no point in using one kind of mission as a reference point because it is obvious that the mission with the lowest LLP life limit will relate with the highest incurred costs. The results showed that the OAG mission is the one with the higher number of fatigue cycle, hence with the lowest LLP life limit.

2) The life limits for the three mission mixture scenarios shows that when the helicopter usage for OAG mission increases (Passenger: 0.5, OAG: 0.4, SAR: 0.1) relative to the baseline (Passenger: 0.8, OAG: 0.1, SAR: 0.1), the LLP life decreases, and, therefore, the number of times that the engine is inducted for LLP replacement increases. This shows that the WU-FPM method can relate the fatigue cycles with the TBO life limit successfully and, the results based on this method are closer to real life scenarios.

3) With regard to the baseline case, the increase in maintenance costs is close to 15,3% for the MinSV case and the increase for the MaxLLP case is 17.5%, while, for the “HOT” case scenario the increase is 7.5% and 8.5% respectively.

4) Relative to the “safety factor” scenario and the baseline case, for the Kt=3.77 case, the increase is 14,1% and 18.7% respectively while for the kt=2.03 case, the increase is 8.2% and 18.2% respectively.

b. The MinSV method:

1) The engine in all MinSV cases is inducted for performance restoration (TBO) for 6 times.

2) While the induction time for this method is the same, the cost difference between the baseline case and the all other cases is in the range of 9%.

3) The case that has the greater effect is the one that we assume a change in the safety factor which relates to the component design.

c . The MaxLLP usage

1) Relative to the MaxLLP usage method, the number of induction times for the baseline case is 9, 8 and 7 times while for the “HOT” case vs 9, 8, and 8 times respectively. The number of times that the engine is inducted for service is the same in the first two cases (MaxLLP1&2) and the highest cost difference is found at the “HOT” case, at the MaxLLP3 scenario, with a value of 10%.

2) The effect of the assumed safety factor in the design relative to the baseline case incurs higher differences in the range of -14%(for Kt=2.03) to +10 % (for Kt=3.77)

3) Like in the MinSV case, the assumptions made for safety factor in the component design phase is found to have the greater effect on maintenance cost.

In addition, the fuel cost due to component degradation presented in Table 4-16 represent only 20% of the value of the cost for overhaul. This percentage is at the range of values found in literature and presented in Table 2-3.

Method Benefits and Constraints for an Operator

Every rotorcraft delivered to an operator comes with time limits regarding the engine TBO and critical parts given from the OEM. The tool developed in this research assumes that factors like:

a. Operating environment (Humidity, sandy or salty environment, ground terrain, location elevation)
b. Flight profile (Different missions)
c. Pilot experience and attitude
d. Fleet number and expected availability
e. Data analysis capability

relate to the engine components life and degradation and dictate the need to estimate new limits based on the specific criteria.

Regarding maintenance cost, the tool provide information for:

a. The degradation effect on fuel consumption based on the environmental parameters imposed from the fleet location.

b. The appropriate maintenance approach to considering the expected fleet availability and the available budget and the best time to replace the engine avoiding high maintenance costs.

Tool constraints

The tool does not provide an optimizer to help the operator find the optimal solution based on specific criteria.

The sunk cost, which relate to the component remaining useful life value is not considered. This was due to the limited sources for price information at the public domain.

5.3 Recommendations for Future Work

The objective of this research was to create a tool that would help the operator make an informed decision with regard to the engine's maintenance costs. Even though the key objectives have been achieved, there exists scope for further development of the framework and the research.

The areas that need consideration are the following:

a. The lifing module:

The current method, which was used, for the life estimation is the strain-method due to its flexibility to cover both the elastic and plastic region of the materials. The literature review revealed that a stress-based method can be also used to assess the components life in case the where the components operating conditions lie in the elastic region. An effort to use both methods and compare the calculated life limits may reveal interesting results.

b. The DOE:

The LOO method used to validate the DOE performance showed that the sample volume is important for the method accuracy. The computational time needed for HECTOR simulations was the limiting factor for the duration of the experiment. For this research, the settings on HECTOR input files changed to reduce the computational time without sacrificing the code accuracy. The settings modification though affected HECTOR calculations and in some cases, the code was not converging. A sensitivity analysis to find the HECTOR

parameters limits for which HECTOR could not converge is highly recommended. This analysis could provide valuable results and help to decrease the number of simulations that do not converge, increase the samples useful volume and enhance the DOE accuracy.

c. The cost module:

The cost module developed for this research assumed two methods used in the aviation sector: i) the MINSV, and ii) the Max LLP usage. These two methods can provide data to perform a short and long-term cost analysis, but do not address the engine's availability issue. Engine downtime for turboshaft engines is about 2 months and is approximately the same when compared to the turbofan counterpart's downtime. This time may not influence operators with large fleets who own spare engines to avoid helicopters downtime but influences the small fleet operators.

An optimizer should be developed that will consider the rotorcraft number in the fleet, the costs associated with the engine downtime and the operators available budget.

d. The framework:

The framework developed so far uses a code to assess the failure cycles due to LCF using MATLAB, which is a commercial package. Even though engineers are not supposed to be software developers, the author's opinion is that converting the MATLAB code to Python, which is an open source language, can have long-term benefits in this type of research.

Bibliography

[1] L. R. Jenkinson, P. Simpkin and D. Rhodes, “Civil Jet Aircraft Design,” *Analysis,* 2003.

[2] F. D. Harris and G. Nag--, “An Economic Model of U . S . Airline Operating Expenses,” no. December, 2005.

[3] *Jan Roskam-Airplane Design 8 vol -ROSKAM AVIATION _ ENGINEERING (1985).pdf.*

[4] D. Rath, “Guide for the Presentation of Helicopter Operating Cost Estimates,” 2010.

[5] G. S. Org, “Rotary Aircraft,” [Online]. Available: https://www.globalsecurity.org/military/systems/aircraft/rotary.htm. [Accessed 14 Apr 2019].

[6] F. D. Harris, Introduction to Autogyros, Helicopters, and Other V/STOL Aircraft Volume II: Helicopters, vol. II, 2012.

[7] FAA, “PART 27:Airworthiness Standards:Normal Category Rotorcraft,” [Online]. Available: https://www.ecfr.gov/cgi-bin/text-idx?node=14:1.0.1.3.13#se14.1.27_11.

[8] A. Filippone, Flight Performance of Fixed and Rotary Wing Aircraft (AIAA), 2006.

[9] Federal Aviation Administration, “Helicopter Flying Handbook,” [Online]. Available: http://www.faa.gov/regulations_policies/handbooks_manuals/aviation/helicopter_flying_handbook/.

[10] F. Sullivan, *Frost and Sullivan_Global Helicopter growth to 2030.*

[11] U. Ahmed, *Two minutes on IBA,* 2016.

[12] I. Goulos, “Simulation Framework Development For The Multidisciplinary Optimisation Of Rotorcraft, Ph.D Thesis,” 2012.

[13] G. Padfield, Helicopter Flight Dynamics (AIAA Education), 2007, p. 630.

[14] I. Goulos, V. Pachidis, F. Hempert, V. Sethi, U. Kingdom, G. Geenslaan and R. Surface, “An Integrated Approach for the Multidisciplinary Optimization of Engine Cycles for Rotorcraft,” pp. 1-2.

[15] I. Goulos, V. Pachidis and P. Pilidis, “Helicopter Rotor Blade Flexibility Simulation for Aeroelasticity and Flight Dynamics Applications,” *Journal of the American Helicopter Society,* vol. 59, no. 4, pp. 1-18, 2014.

[16] P. Cantrell, *Helicopter Aviation,* 2010.

[17] B. S. Ackert, “Engine Maintenance Concepts for Financiers Elements of Turbofan Shop Maintenance Costs,” *Aircraft Monitor,* 2011.

[18] H. Hanumanthan, “Severity estimation and shop visit prediction of civil aircraft engines, Ph.D Thesis,” 2009.

[19] G. P. Sallee, “Performance Deterioration Based on Existing (Historical) Data- JT9D Jet Engine Diagnostics Program,” p. 225, 1978.

[20] K. F. Fraser, “An Overview of Health and Usage Monitoring Systems (HUMS) for Military Helicopters,” *DSTO-TR-0061,* p. 42, 1994.

[21] F. Hoffman, G. Wurzel and S. Hasbroucq, “HUMS & CBM in the Civil Helicopter Market,” *AHS 70th Annual Forum,* 2014.

[22] J. Cronkhite, “NASA_Feasibility Study of a Rotorcraft Health and Usage System,” 1996.

[23] S. Desfor, “Articles Critical Elements of Helicopter Value Part 1 of 2,” 2015. [Online]. Available: http://www.helivalues.com/index.php/2012-10-31-13-06-10/articles/60-article-4.html.

[24] F. D. Harris, Introduction to Autogyros, Helicopters, and Other V/STOL Aircraft - Volume 1 Overview and Autogyros, 2011, p. 962.

[25] Y. G. Bagul, I. Zeid and S. V. Kamatrhi, “OVERVIEW OF REMAINING USEFUL LIFE METHODOLOGIES,” in *ASME* , Brooklyn, 2008.

[26] R. Kurz and K. Brun, “Gas turbine tutorial–Maintenance and operating practices effects on degradation and life,” *Proceedings of 36th Turbomachinery,* pp. 173-185, 2007.

[27] FAA, “FAA_AC_120-113_Best Practises for Engine Time In Service Interval Extensions,” [Online]. Available: https://www.faa.gov/documentLibrary/media/Advisory_Circular/AC_120-113.pdf.

[28] J. D. MacLeod, V. Taylor and J. C. G. Laflamme, “Implanted Component Faults and Their Effects on Gas Turbine Engine Performance,” *Journal of Engineering for Gas Turbines and Power,* vol. 114, no. 2, p. 174, 1992.

[29] R. Kurz and K. Brun, “Degradation in Gas Turbine Systems,” *Journal of Engineering for Gas Turbines and Power,* vol. 123, no. 1, p. 70, 2001.

[30] J. Litt, K. Parker and S. Chatterjee, “Adaptive gas turbine engine control for deterioration compensation due to aging,” *16th International Symposium on Airbreathing Engines,* no. October, 2003.

[31] C. B. Meher-homji, M. a. Chaker and H. M. Motiwala, “Gas Turbine Performance Deterioration,” *30th Turbomachinery Symposium, Texas A&M University, Texas,* pp. 139-176, 2001.

[32] M. Sing, “Gas turbine engine performance deterioration modelling and analysis ,Ph . D THESIS,” no. February, 1988.

[33] R. 1. Stephens, A. Fatemi, R. R. Stephens and H. 0. Fuchs, “METAL FATIGUE IN ENGINEERING Second Edition,” 2001.

[34] J. Collins, “Wiley: Failure of Materials in Mechanical Design: Analysis, Prediction, Prevention, 2nd Edition - Jack A. Collins,” 1993. [Online]. Available: http://eu.wiley.com/WileyCDA/WileyTitle/productCd-0471558915.html.

[35] G. R. Halford, T. G. Meyer, R. S. Nelson, D. M. Nissley and G. A. Swanson, “Fatigue Life Prediction Modeling for Turbine Hot Section Materials,” *Journal of Engineering for Gas Turbines and Power,* vol. 111, no. 2, p. 279, 1 4 1989.

[36] Y. O. H. Liu, “Literature survey on oxidations and fatigue lives at elevated temperatures,” New York, 1984.

[37] S. Mahadevan, H. Mao and D. Ghiocel, “Probabilistic Simulation of Engine Blade Creep-fatigue Life,” in *43rd AIAA/ASME/ASCE/AHS/ASC Structures, Structural Dynamics, and Materials Conference*, Reston, Virigina, 2002.

[38] A. Mahashabde, “Assessing selected technologies and operational strategies for improving the environmental performance of future aircraft, MSc Thesis,” Massachusetts Institute of Technology, 2006.

[39] S. S. Manson and T. J. Dolan, “Thermal Stress and Low Cycle Fatigue,” *Journal of Applied Mechanics,* vol. 33, no. 4, p. 957, 1 12 1966.

[40] G. Dieter, “Mechanical metallurgy,” [Online]. Available: https://archive.org/details/mechanicalmetall00diet.

[41] A. Fatemi, “Fatigue from Variable Amplitude Loading,” *University of Toledo,* pp. 1-73.

[42] H. Boyer, “Fatigue Testing,” *Atlas of Fatigue Curves,* vol. 11, pp. 1-25, 1986.

[43] R. Stone, “Fatigue life estimates using Goodman Diagrams,,” 2012.

[44] R. Stephens, R. R. Stephens and H. Fuchs, METAL FATIGUE Second Edition, 2001, p. 452.

[45] R. A. Cookson and A. Haslam, “Mechanical Design of Turbomachinery,” *Thermal Power MSc Course Notes, Cranfield University, Bedfordshire, UK,* 2011.

[46] Efunda, “Low-Cycle Fatigue,” [Online]. Available: http://www.efunda.com/formulae/solid_mechanics/fatigue/fatigue_lowcycle.cfm.

[47] ASME, “Elements of Metallurgy and Engineering Alloys,” *ASM International 2008,* pp. 1-70, 2008.

[48] E. Zaretsky, R. C. Hendricks and . S. Soditus, “Weibull-Based Design Methodology for Rotating Aircraft Engine Structures”.

[49] ASM, Fatigue and Fracture Volume 19, ASM International Handbook Committee, Ed., 1996.

[50] R. Viswanathan and J. Stringer, “Failure Mechanisms of High Temperature Components in Power Plants,” *Journal of Engineering Materials and Technology,* vol. 122, no. 3, p. 246, 1 7 2000.

[51] V. Suria, “A Flexible Lifing Model For Gas Turbines creep and low cycle fatigue approach,” 2006.

[52] Mars-G-Fontana, *Corrosion Engineering Mars G Fontana McGraw Hill 3rd Edition,* 1987, p. 576.

[53] K. Charkous, “Rotorcraft Trajectory, Component Lifing And Operating Cost, MSc Thesis,” 2013.

[54] S. Pascovici, “Thermo Economic and Risk Analysis for Advanced Long Range Aero Engines, Ph.D Thesis,” 2008.

[55] K. Ramsden, Turbomachinery. MSc Course notes, Cranfield, 2005.

[56] M. Elter, “Development of a Probabilistic Weibull Based Life Prediction and Reliability Model for Standard Turbomachinery Components. Msc. Thesis,” 2016.

[57] EASA AD No : 2008-0211 and EASA, *Easa Emergency Airworthiness Directive,* vol. 201609, 2012, pp. 3-4.

[58] FAA, *AC 33.70-1 Guidance Material for Aircraft Engine Life Limited Parts Requirements,* 2017.

[59] ASTM, “E1049-85: Standard Practices for Cycle Counting in Fatigue Analysis,” *E1049 - 85,* vol. 85, no. Reapproved 2011, pp. 1-10, 2011.

[60] P. Fernandes, J. Hesselbach and C. Herrmann, “An Overview on Degradation Modelling for Service Cost Estimation,” 2011.

[61] M. Thurston, “An open standard for Web-based condition-based maintenance systems,” *2001 IEEE Autotestcon Proceedings. IEEE Systems Readiness Technology Conference,* no. 814, pp. 401-415, 2001.

[62] T. Tinga, “Application of physical failure models to enable usage and load based maintenance,” *Reliability Engineering and System Safety,* vol. 95, no. 10, pp. 1061-1075, 2010.

[63] N. C. Cavoli, “Commercial Engine Logistics Cost Projections—A Dynamic and Flexible Approach,” vol. 114, pp. 1-10, 2015.

[64] R. a. T. Stabrylla, *Effects of aircraft power plant usage on turbine engine relative durability life,* vol. 16th, 1980.

[65] R. Donaldson, D. Fischer, J. Gough and M. Rysz, “Economic Impact of Derated Climb on Large Commercial Engines,” *2007 Boeing Performance and Flight Operations Engineering Conference,* pp. 8.1 - 8.11, 2007.

[66] D. Nalianda, “Impact of environmental taxation policies on civil aviation a techno-economic environmental risk assessment, PhD Thesis,” 2012.

[67] U. Zuazo, “Investigation into Combined Severity by means of Lifing and Degradation Calculations, MSc Thesis,” 2014.

[68] V. Lejona, “Thermomechanical Fatigue Lifing Study of Aero Engine,MSc Thesis,” Cranfield, University, UK, 2014.

[69] E. Maqueda, “Engine Overall Severity, MSc Thesis,” 2014.

[70] B. S. Dhillon, Life cycle costing for engineers., Taylor & Francis Group, 2010, pp. Chapter1, P1.

[71] B. S. Dhillon, Life cycle costing: Techniques, models, and applications, New York: Gordon and Breach Science Publishers, 1989.

[72] R. Scott, “Development of a Rotorcraft Lifecycle Cost Model Incorporating Reliability and Maintainability with Application to Rotorcraft Preliminary Design,” 2013.

[73] Y. Zhao, A. Harrison, R. Roy and J. Mehnen, “Aircraft Engine Component Deterioration and Life Cycle Cost Estimation,” *Proceedings of the 18th CIRP International 657 Conference on Life Cycle Engineering,\May 2nd - 4th, 2011,* 2011.

[74] S. Isakowitz, “NASA Cost Estimating Handbook,” *NASA HQ, Washington DC, spring,* 2015.

[75] Office of Acquisition and Project Management, Life Cycle Cost Handbook-Guidance for Life Cycle Cost Estimation and Analysis, 2014, p. 89.

[76] J. Roskam, Airplane Design Airplane Cost Estimation_ Design, Development, Manufacturing and Operating, vol. 8, Ottawa, 1990.

[77] B. Roberson, “Fuel conservation strategies: cost index explained,” 2007. [Online]. Available: http://www.boeing.com/commercial/.

[78] Airbus, “Getting to grips with cost index, Flight operations support and line assistance,” 1998.

[79] F. D. Harris and M. P. Scully, “Rotorcraft cost too much,” *Journal of the American Helicopter Society,* vol. 43, no. 1, pp. 3-13, 1998.

[80] R. Scott, “Historical Trends in Turboshaft Engine Procurement Cost,” *Journal of the American Helicopter Society,* vol. 62, no. 3, pp. 1-9, 2017.

[81] R. Seemann, S. Langhans, T. Schilling and V. Gollnick, “Modeling the Life Cycle Cost of Jet Engine Maintenance,” *Deutscher Luft- und Raumfahrtkongress,* no. SEPTEMBER, pp. 663-672, 2011.

[82] L. Marinai, D. Probert and R. Singh, “Prospects for aero gas-turbine diagnostics: A review,” *Applied Energy,* vol. 79, pp. 109-126, 2004.

[83] B. o. T. Statistics, “Form 41 Financial Data,” [Online]. Available: http://www.transtats.bts.gov/Tables.asp?DB_ID=135.

[84] D. E. Kowalski, “A Cost Analysis Of The Decision To Cannibalize Major Components Of The Navy’s H-60 Helicopters At The Operational Level, MSc Thesis,” 2000.

[85] Conklin & De Decker, “Product life cycle cost.,” [Online]. Available: https://site.conklindd.com/s/product-life-cycle-cost.

[86] W. L. MacMillan, “Development of a modular-type computer program for the calculation of gas turbine off-design performance, Ph.D Thesis,” 1974.

[87] P. C. Austin and E. W. Steyerberg, “The number of subjects per variable required in linear regression analyses,” *Journal of Clinical Epidemiology,* vol. 68, no. 6, pp. 627-636, 2015.

[88] G. C. R. Montgomery, Douglas C., Applied Statistics and Probability for Engineers.

[89] J. Frost, “How to Interpret P-values and Coefficients in Regression Analysis - Statistics By Jim,” [Online].

[90] S. G. Powell, “Spreadsheet Modeling for Insight,” no. October, 2004.

[91] Wikipedia, *Data analysis - Wikipedia,* 2016.

[92] S. S. Rao, Engineering Optimization: Theory and Practice, 2009, p. 813.

[93] N. Solutions, *Design of Experiments _ Noesis Solutions _ Noesis Solutions.*

[94] ReliaSoft Corporation, “Box-Behnken Designs for Optimizing Product Performance,” [Online]. Available: http://www.weibull.com/hotwire/issue130/hottopics130.htm.

[95] C. A. Kumar, “A Tribute to Prof. Lotfi A. Zadeh,” *Journal of Information & Knowledge Management,* vol. 16, no. 04, 2017.

[96] Wikipedia, “Fuzzy logic,” [Online]. Available: https://en.wikipedia.org/wiki/Fuzzy_logic. [Accessed 3 4 2019].

[97] N. Mathur, I. Glesk and A. Buis, “Comparison of adaptive neuro-fuzzy inference system (ANFIS) and Gaussian processes for machine learning (GPML) algorithms for the prediction of skin temperature in lower limb prostheses,” *Medical Engineering and Physics,* vol. 38, pp. 1083-1089, 2016.

[98] V. Ilić, J. M. Tadić and A. Imširagić, “Kriging with Machine Learning Covariates in Environmental Sciences: A Hybrid Approach,” *GeoMLA, Geostatistics and Machine Learning Applications in Climate and Environmental Sciences,* 2016.

[99] V. Nevtipilova, *Testing Artificial Neural Network (ANN) for Spatial Interpolation,* vol. 03, 2014.

[100] K. Gumus, “Comparison of spatial interpolation methods and multi-layer neural networks for different point distributions on a digital elevation model,” *Geodetski vestnik,* pp. 523-543, 2013.

[101] D. G. Krige, *Journal of the Chemical Metallu , Rgical {\&} Mining Society of South Africa,* Vols. 119--139, no. 6, pp. 119--139, 1951.

[102] J. Sacks, “Design and analysis of computer experiments.,” *Statistical Science,* vol. 4, no. 01, 1989.

[103] I. Goulos, “Design Optimisation of Separate-Jet Exhausts for the Next Generation of Civil,” pp. 1-13, 2017.

[104] V. Pachidis, “Design Space Exploration and Optimization of Conceptual Rotorcraft Powerplants,” *Journal of Engineering for Gas Turbines and Power,* vol. 12, p. 137, 2015.

[105] F. Ali, K. Tzanidakis, I. Goulos, V. Pachidis and R. D'Ippolito, “Multidisciplinary design and optimisation of conceptual rotorcraft powerplants for operational performance and environmental impact,” *Aeronautical Journal,* vol. 119, pp. 891-914, 2015.

[106] F. Pedregosa, G. Varoquaux, A. Gramfort, V. Michel, B. Thirion, O. Grisel, M. Blondel, P. Prettenhofer, R. Weiss, V. Dubourg, J. Vanderplas, A. Passos, D. Cournapeau, M. Brucher, M. Perrot and E. Duchesnay, “Scikit-learn: Machine Learning in Python,” *Journal of Machine Learning Research,* vol. 12, pp. 2825----2830, 2011.

[107] A. Conn, “On the Convergence of Derivative-Free Methods for Unconstrained Optimization,” 1997.

[108] P. E. College, “Applied Data Mining and Statistical Learning,” [Online]. Available: https://onlinecourses.science.psu.edu/stat857/node/160.

[109] F. Wikipedia, “Cross-validation (statistics) - Wikipedia,” [Online].

[110] Wikipedia, “Pearson correlation coefficient,” 2019. [Online]. Available: https://en.wikipedia.org/wiki/Pearson_correlation_coefficient.

[111] Wikipedia, “Coefficient of determination,” [Online]. Available: https://en.wikipedia.org/wiki/Coefficient_of_determination. [Accessed 30 March 2019].

[112] A. Spera, David, “Life Prediction of Turbine Components : On_going studies at NASA Lewis Research Center,” 1973.

[113] T. Irvine. [Online]. Available: http://www.vibrationdata.com/.

[114] “InterSalonica,” [Online]. Available: https://www.airintersalonica.gr/index.php/ourfleetgr.

[115] H. K. Reddick, “Army Helicopter Cost Drivers turbine costs vs compressor costs,” 1975.

[116] WIKIPEDIA, “MBB Bo 105,” 2009. [Online].

[117] EASA, “250C20B Certificate Data Sheet,” 2012.

[118] Janes, *Rolls-Royce Model 250 (M250).*

[119] R. J. Hill, W. H. Reimann and J. S. Ogg, “A Retirement for Cause Study of an Engine Turbine Disk,” US Airforce, Ohio, 1981.

[120] S. Loewenthal, “Factors that affect the Fatigue strength of Power Transmission Shafting and their Impact on Design,” NASA, Cleveland, Ohio, 1984.

[121] R. Corporation, Life Data Analysis Reference.

Appendix A Component Sizing

The high-pressure turbine blade and disc geometries are measured from the cutaway plot provided in Figure A-1.The data for the ratio between the dimensions in the real engine and the ones at the sketch is given in Table A-1. The sketch dimensions are estimated using the Google sketch tool and depend on the image canvas used. The important value here is the ratio which is used to estimate the real dimensions with reference to the ones measured with the tool. The blade cross-sectional area at the root is estimated assuming that all blades are covering 60 % of the disc rim area [56] The high-pressure turbine is equipped with 38 blades. Its absolute rotational speed equivalent to 100 % relative rotational speed is 50970 rpm [116]. The materials are assumed to be for the blade René 95 and for the disc Inconel 718. The material properties are shown in Table A-2

Sketch		Real	Ratio
Length (mm)	22638	1037	0.04568

Table A-1: 250C-20B Gas Turbine Cutaway[105]

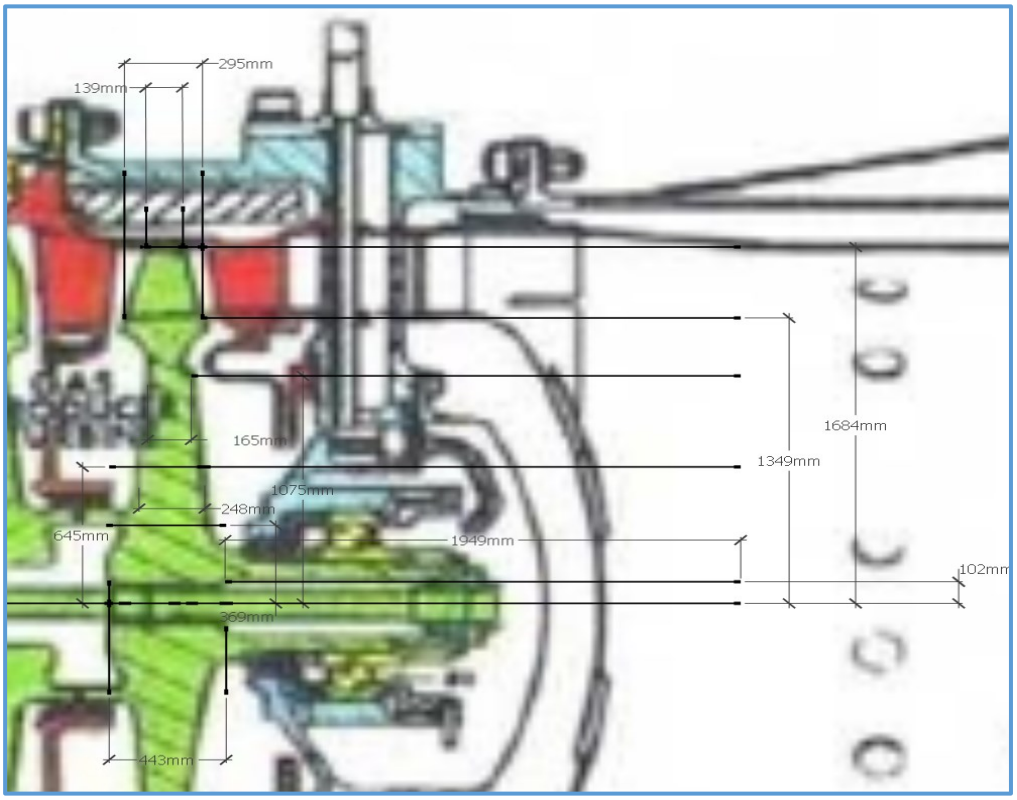

Figure A-1:250C-20B Gas Turbine Cutaway

Figure A-2 : 250-C20B Hot Section Turbines 1st

Property	**Inconel 718**		**Rene 95**	
LM curve (stress in (MPa))	36	50	30	50.0
	34	100	28.4	100.0
	32	172	26.3	300.0
	30	303	25	500.0
	28	400	23	620.0
	26	500	21	850.0
Material density (kg/m^3)	8220.96		8248.64	
Data in yield stress (ys) curve	300.00	1122.64	300.00	1274.99
	355.79	1111.46	375.71	1237.62
	411.58	1100.28	451.43	1216.74
	467.37	1089.25	527.14	1198.43
	523.16	1078.41	602.86	1179.76
	578.95	1067.23	678.57	1164.42
	634.74	1055.24	754.29	1153.27
	690.53	1044.05	830.00	1134.86
	746.32	1035.11	905.71	1122.70
	802.11	1023.09	981.43	1105.43
	857.89	1001.11	1057.14	999.82
	913.68	970.32	1132.86	604.57
	969.47	927.68	1208.57	355.34
	1025.26	823.38	1284.29	229.69
	1081.05	610.08	1360.00	27.96
	1136.84	366.97		

Property	Inconel 718		Rene 95	
	1192.63	203.49		
	1248.42	122.62		
	1304.21	87.84		
	1360.00	62.59		
The elastic modulus of the material(MPa)	205000.0		209000.0	
Fatigue ductility coefficient (mm)	0.35		0.15	
Fatigue strength coefficient (MPa)	1736.0		1785.0	
Fatigue strength exponent	-0.08		-0.08	
Fatigue ductility exponent	-0.59		-0.59	
The linear coefficient of thermal expansion (mm/°C)	11.5E-6		11.3E-6	
Poisson's ratio	0.29		0.3	
Larson Miller (LM) constant	25.0		20	

Table A-2: Material Properties [56]

	Blade Geometry	
	Radius	Cross-sectional area
Blade root	0.0376 m	0.132 10^{-3} mm²
Blade tip	0.078 m	0.117 10^{-3} mm²
Disc Geometry		
	Radius	Thickness
Ring 1	0.015 m	0.05220 m
Ring 2	0.024 m	0.046519252 m
Ring 3	0.0328 m	0.02241925 m
Ring 4	0.051 m	0.0222952 m
Rim	0.0600 m	0.0222298 m

Table A-3: 250-C20B-Gas Producer Disc Blade and Disc Geometry

Appendix B Maintenance Scenarios & Formulas

Table B-1 shows an example of three different scenarios with regard to the LLP and TBO interval periods that relate to the cost scenario of Maximum LLP. Table B-2 and Table B-3 show the formulas used in the code to estimate the cost in every scenario.

	Life Limited Parts Induction Scenarios (Hours)		
TBO Calendar	**3200**	**4200**	**5600**
1800.00	1800	1800	1800
3600.00	3200	3600	3600
5400.00	3600	4200	5400
5600.00	5400	5400	5600
7200.00	6400	7200	7200
9000.00	7200	8400	9000
10800.00	9000	9000	10800
11200.00	9600	10800	11200
12600.00	10800	12600	12600
14400.00	12600	12600	14400
16200.00	12800	14400	16200
16800.00	14400	16200	16800
18000.00	16000	16800	18000
22400.00	16200	18000	22400

Table B-1: Scenarios for LLP and TBO intervals

TBO	LLP	FH/Year
1800	3200/4200/5600	400

Max LLP Replacement Concept				Equations used in the code		
No	Reason	Hours	Years in Service			
1	TBO	1800	4.5	MMH_O_I_(tbo_1)	fvcost_i	
2	LLP	3200	8		admin *	LLP Cost
3	TBO	3600	9	MMH_O_I_(tbo_1)	fvcost_i	
4	TBO	5400	13.5	MMH_O_I_(tbo_1)	fvcost_i	
5	LLP	6400	16		admin	LLP Cost
6	TBO	7200	18	MMH_O_I_(tbo_1)	fvcost_i	
7	TBO	9000	22.5	MMH_O_I_(tbo_1)	fvcost_i	
8	LLP	9600	24		admin	LLP Cost
9	TBO	10800	27	MMH_O_I_(tbo_1)	fvcost_i	
10	TBO	12600	31.5	MMH_O_I_(tbo_1)	fvcost_i	
11	LLP	12800	32		admin	LLP Cost
12	TBO	14400	36	MMH_O_I_(tbo_1)	fvcost_i	
13	LLP	16000	40		admin	LLP Cost
14	TBO	16200	40.5	MMH_O_I_(tbo_1)	fvcost_i	
15	TBO	18000	45	MMH_O_I_(tbo_1)	fvcost_i	
16	LLP	19600	49		admin	LLP Cost
17	TBO	19800	49.5	MMH_O_I_(tbo_1)	fvcost_i	

Table B-2: Formulas used for the Max LLP Usage Scenario

NOTE : The concept is that the operator will decide to induct the engine for Overhaul						
MIN Shop Visit Concept						
No	**Reason**	**Hours**	**Years in Service**			
1	LLP & TBO	1800	4.5	MMH_O_I_(tbo_1)	fvcost_i	LLP Cost
2	LLP & TBO	3600	9	MMH_O_I_(tbo_1)	fvcost_i	LLP Cost
3	LLP & TBO	5400	13.5	MMH_O_I_(tbo_1)	fvcost_i	LLP Cost
4	LLP & TBO	7200	18	MMH_O_I_(tbo_1)	fvcost_i	LLP Cost
5	LLP & TBO	9000	22.5	MMH_O_I_(tbo_1)	fvcost_i	LLP Cost
6	LLP & TBO	10800	27	MMH_O_I_(tbo_1)	fvcost_i	LLP Cost
7	LLP & TBO	12600	31.5	MMH_O_I_(tbo_1)	fvcost_i	LLP Cost
8	LLP & TBO	14400	36	MMH_O_I_(tbo_1)	fvcost_i	LLP Cost
9	LLP & TBO	16200	40.5	MMH_O_I_(tbo_1)	fvcost_i	LLP Cost
10	LLP & TBO	18000	45	MMH_O_I_(tbo_1)	fvcost_i	LLP Cost
11	LLP & TBO	19800	49.5	MMH_O_I_(tbo_1)	fvcost_i	LLP Cost
12	LLP & TBO	19600	49	MMH_O_I_(tbo_1)	fvcost_i	LLP Cost
1	TBO	1800	4.5	MMH_O_I_(tbo_1)	fvcost_i	
2	LLP & TBO	3600	9	MMH_O_I_(tbo_1)	admin	LLP Cost
3	TBO	5400	13.5	MMH_O_I_(tbo_1)	fvcost_i	
4	LLP & TBO	7200	18	MMH_O_I_(tbo_1)	admin	LLP Cost
5	TBO	9000	22.5	MMH_O_I_(tbo_1)	fvcost_i	
6	LLP & TBO	10800	27	MMH_O_I_(tbo_1)	admin	LLP Cost
7	TBO	12600	31.5	MMH_O_I_(tbo_1)	fvcost_i	
8	LLP & TBO	14400	36	MMH_O_I_(tbo_1)	admin	LLP Cost
9	TBO	16200	40.5	MMH_O_I_(tbo_1)	fvcost_i	
10	LLP & TBO	18000	45	MMH_O_I_(tbo_1)	admin	LLP Cost
11	TBO	19800	49.5	MMH_O_I_(tbo_1)	fvcost_i	
12	LLP & TBO	19600	49	MMH_O_I_(tbo_1)	admin	LLP Cost
No	Reason	Hours	Years in Service	LLP Cost =(0.45* eip_c)		
1	TBO	1800	4.5	MMH_O_I_(tbo_1)	fvcost_i	
2	TBO	3600	9	MMH_O_I_(tbo_1)	fvcost_i	
3	LLP & TBO	5400	13.5	MMH_O_I_(tbo_1)	admin	LLP Cost
4	TBO	7200	18	MMH_O_I_(tbo_1)	fvcost_i	
5	TBO	9000	22.5	MMH_O_I_(tbo_1)	fvcost_i	
6	LLP & TBO	10800	27	MMH_O_I_(tbo_1)	admin	LLP Cost
7	TBO	12600	31.5	MMH_O_I_(tbo_1)	fvcost_i	
8	TBO	14400	36	MMH_O_I_(tbo_1)	fvcost_i	
9	LLP & TBO	16200	40.5	MMH_O_I_(tbo_1)	admin	LLP Cost
10	TBO	18000	45	MMH_O_I_(tbo_1)	fvcost_i	
11	TBO	19800	49.5	MMH_O_I_(tbo_1)	fvcost_i	
12	LLP & TBO	19600	49			

Table B-3: Formulas used for the Min SV Scenario

Appendix C Lifing Code Analysis

This appendix is a supplement to paragraph 3.2.1 which describes the code that estimates the blade and disc failure limit.

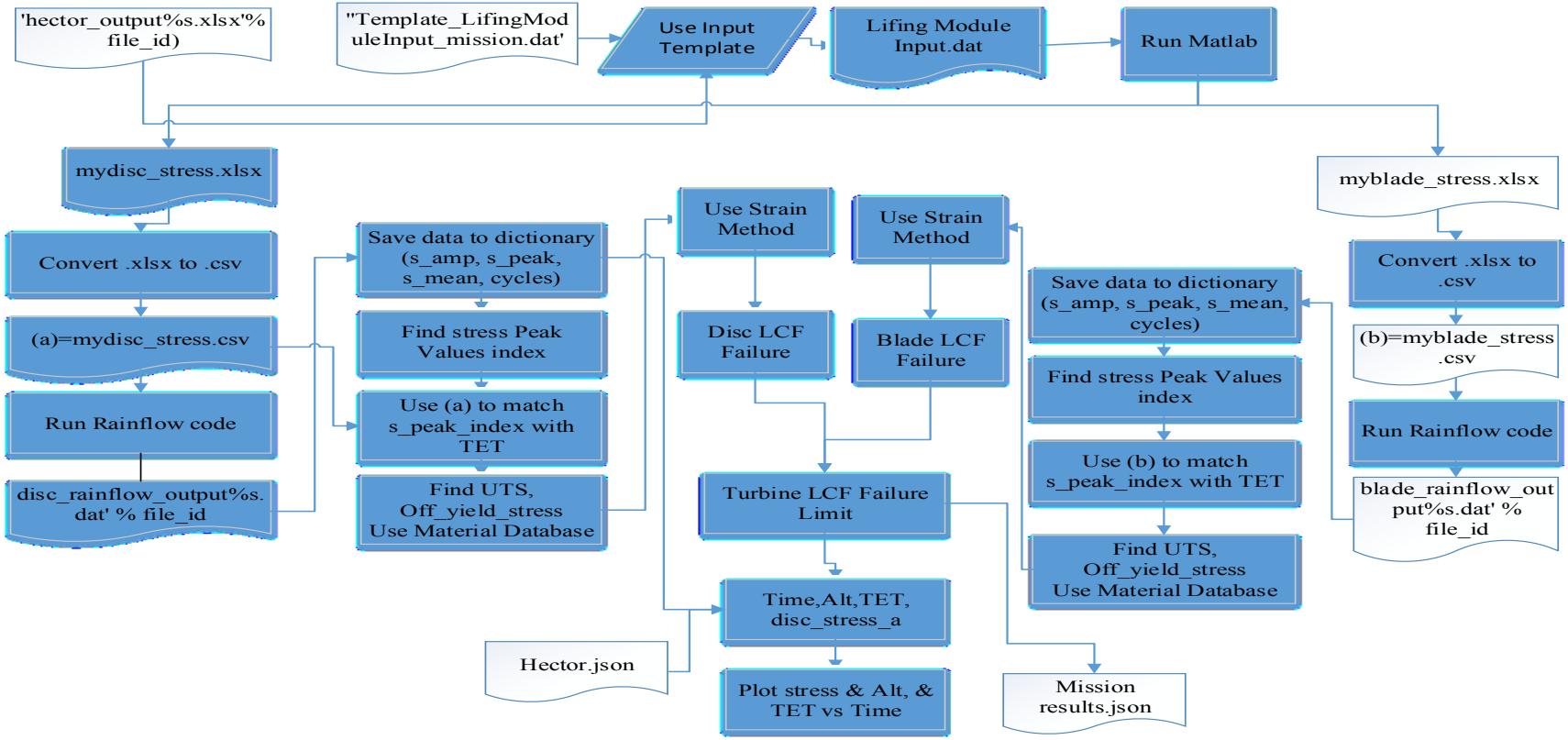

Figure C-1: Flowchart for the script LCF_life.py

Appendix D : Results for Operating Parameters Sensitivity Analysis

Load	Climb_Rate	ISA	hover_max_tet	climb_max_tet	cruise_max_tet	descent_max_tet
200	3	0	1242.84	1132.77	1137.09	930.34
200	4	0	1242.84	1162.95	1137.27	930.36
200	5	0	1242.84	1197.8385	1137.27	930.36
200	6	0	1242.84	1220.49	1137.47	930.38
200	3	5	1262.96	1150.18	1152.32	943.88
200	4	5	1262.96	1180.58	1152.47	943.91
200	5	5	1262.96	1209.78	1152.53	943.93
200	6	5	1262.96	1237.95	1152.54	943.91
200	3	10	1283.06	1167.67	1167.5	958.15
200	4	10	1283.06	1198.27	1167.67	958.18
200	5	10	1283.06	1226.97	1167.77	958.2
200	6	10	1283.06	1255.44	1167.76	958.19
200	3	15	1303.19	1185.25	1182.62	972.67
200	4	15	1303.19	1215.66	1182.7	972.66
200	5	15	1303.19	1244.2	1183	972.71
200	6	15	1303.19	1272.99	1183.23	972.69
350	3	0	1276.29	1155.1	1151.68	942.28
350	4	0	1276.29	1222.4555	1151.88	942.3
350	5	0	1276.29	1186.85	1151.88	942.3
350	6	0	1276.29	1245.4	1152.26	942.31
350	3	5	1297.11	1173	1167.04	957.15
350	4	5	1297.11	1204.52	1167.21	957.16
350	5	5	1297.11	1233.35	1167.23	957.2
350	6	5	1297.11	1263.32	1167.36	957.19
350	3	10	1317.96	1190.96	1182.5	972.25
350	4	10	1317.96	1221.86	1182.75	972.27
350	5	10	1317.96	1251.12	1182.75	972.3
350	6	10	1317.96	1281.29	1182.83	972.29
350	3	15	1338.99	1209.01	1198.02	987.67
350	4	15	1338.99	1239.39	1198.37	987.69
350	5	15	1338.99	1268.94	1198.38	987.73
350	6	15	1338.99	1299.3	1198.45	987.72
500	3	0	1311.99	1178.52	1167.73	955.97
500	4	0	1312.45	1246.3103	1168.22	956.18
500	5	0	1312.45	1210.01	1168.22	956.18
500	6	0	1312.39	1272.16	1168.41	956.18
500	3	5	1334.3	1197.29	1184.12	972
500	4	5	1334.25	1228.05	1184.3	972
500	5	5	1334.29	1258.53	1184.4	972.05
500	6	5	1334.19	1290.56	1184.52	972.02
500	3	10	1356.17	1215.07	1200.84	988.04
500	4	10	1356.11	1246.12	1201.16	988.03
500	5	10	1356.14	1276.82	1201.24	988.08
500	6	10	1356.05	1309	1201.32	988.03
500	3	15	1378.1	1232.61	1218.23	1004.19
500	4	15	1378.03	1264.28	1218.81	1004.2
500	5	15	1378.07	1295.17	1218.71	1004.25
500	6	15	1377.38	1327.09	1218.44	1003.94
650	3	0	1349.63	1201.37	1189.4	971.48
650	4	0	1350.51	1271.1539	1190.4	971.89
650	5	0	1350.51	1234.13	1190.4	971.89
650	6	0	1350.46	1300.38	1190.85	971.88
650	3	5	1373.21	1220.31	1209.59	988.38
650	4	5	1373.15	1252.67	1209.98	988.37
650	5	5	1373.2	1284.99	1210.25	988.44
650	6	5	1373.1	1319.4	1210.36	988.38
650	3	10	1396.04	1238.92	1232.64	1004.92
650	4	10	1395.99	1271.11	1233.45	1004.92
650	5	10	1396.03	1303.77	1233.14	1005
650	6	10	1395.94	1338.66	1233.33	1004.93
650	3	15	1418.97	1257.27	1258.4	1022.18
650	4	15	1418.91	1289.9	1258.35	1022.19
650	5	15	1418.96	1322.7	1259.22	1022.23
650	6	15	1418.86	1357.98	1259.32	1022.18

Figure D-1: Experiment Results for TET at all flight segments

Load	Climb_Rate	ISA	hover_max_pcn	climb_max_pcn	cruise_max_pcn	descent_max_pcn
200	3	0	0.93	0.88	0.88	0.75
200	4	0	0.93	0.89	0.88	0.75
200	5	0	0.93	0.91	0.88	0.75
200	6	0	0.93	0.92	0.88	0.75
200	3	5	0.93	0.88	0.88	0.76
200	4	5	0.93	0.89	0.88	0.76
200	5	5	0.93	0.91	0.88	0.76
200	6	5	0.93	0.92	0.88	0.76
200	3	10	0.94	0.88	0.88	0.76
200	4	10	0.94	0.9	0.88	0.76
200	5	10	0.94	0.91	0.88	0.76
200	6	10	0.94	0.93	0.88	0.76
200	3	15	0.95	0.89	0.89	0.76
200	4	15	0.95	0.9	0.89	0.76
200	5	15	0.95	0.92	0.89	0.76
200	6	15	0.95	0.94	0.89	0.76
350	3	0	0.94	0.89	0.88	0.76
350	4	0	0.94	0.92	0.88	0.76
350	5	0	0.94	0.9	0.88	0.76
350	6	0	0.94	0.93	0.88	0.76
350	3	5	0.95	0.89	0.89	0.77
350	4	5	0.95	0.9	0.89	0.77
350	5	5	0.95	0.92	0.89	0.77
350	6	5	0.95	0.93	0.89	0.77
350	3	10	0.96	0.89	0.89	0.77
350	4	10	0.96	0.91	0.89	0.77
350	5	10	0.96	0.93	0.89	0.77
350	6	10	0.96	0.94	0.89	0.77
350	3	15	0.96	0.9	0.89	0.77
350	4	15	0.96	0.92	0.9	0.77
350	5	15	0.96	0.93	0.9	0.77
350	6	15	0.96	0.95	0.9	0.77
500	3	0	0.95	0.9	0.89	0.77
500	4	0	0.95	0.93	0.89	0.77
500	5	0	0.95	0.91	0.89	0.77
500	6	0	0.95	0.94	0.89	0.77
500	3	5	0.96	0.9	0.9	0.78
500	4	5	0.96	0.92	0.9	0.78
500	5	5	0.96	0.93	0.9	0.78
500	6	5	0.96	0.95	0.9	0.78
500	3	10	0.97	0.91	0.9	0.78
500	4	10	0.97	0.92	0.9	0.78
500	5	10	0.97	0.94	0.9	0.78
500	6	10	0.97	0.95	0.9	0.78
500	3	15	0.98	0.91	0.91	0.78
500	4	15	0.98	0.93	0.91	0.78
500	5	15	0.98	0.95	0.91	0.78
500	6	15	0.98	0.96	0.91	0.78
650	3	0	0.97	0.91	0.9	0.78
650	4	0	0.97	0.94	0.9	0.78
650	5	0	0.97	0.92	0.9	0.78
650	6	0	0.97	0.95	0.9	0.78
650	3	5	0.98	0.91	0.91	0.79
650	4	5	0.98	0.93	0.91	0.79
650	5	5	0.98	0.94	0.91	0.79
650	6	5	0.98	0.96	0.91	0.79
650	3	10	0.99	0.92	0.92	0.79
650	4	10	0.99	0.94	0.92	0.79
650	5	10	0.99	0.95	0.92	0.79
650	6	10	0.99	0.96	0.92	0.79
650	3	15	0.99	0.93	0.93	0.79
650	4	15	0.99	0.94	0.93	0.79
650	5	15	0.99	0.96	0.93	0.79
650	6	15	0.99	0.97	0.93	0.79

Figure D-2: Experiment Results for TET at all flight segments

Appendix E Estimated Turbine Life Results

The results at the next table are based on the DOE for 400 Simulations. They present the results for different values of the b exponent in Coffin Manson formula (equation 2-8). The value of 50897.5 cycles is the one used for the reference flight.

Operating Parameters			Material Properties : (b_disc values)							
Payload	Climb Rate	ISA Deviation	(-0.058)	(-0.06)	(-0.062)	(-0.064)	(-0.07)	(-0.073)	(-0.075)	(-0.077)
0.81	5.72	9.54	80670.19	57229.62	41686.87	31089.89	14517.16	10482.44	8581.95	7112.682
2.44	4.19	2.19	181792.2	121097.2	83283.84	58960.2	24247.65	16664.44	13257.34	10708.3
4.06	3.98	5.91	149687	100863.7	70111.02	50124.47	21133.63	14673.68	11745.57	9541.234
463.94	6.29	10.18	30202.82	23854.97	19185.28	15675.98	9237.664	7342.919	6367.204	5562.172
465.56	5.46	10.78	41392.61	31756.75	24895.2	19888.06	11113.05	8655.823	7417.643	6411.472
467.19	4.35	2.49	71234.97	51361.58	38007.21	28781.71	14017.96	10312.75	8540.32	7153.853
468.81	6.45	8.27	28743.23	22902.29	18549.89	15241.68	13064	7225.852	6270.584	5479.857
470.44	5.38	8.08	19003.8	14603.62	11477.43	9199.98	5215.237	4099.61	3536.92	3079.091
546.81	3.25	12.81	44063.62	32962.54	25270.32	19794.69	10565.67	8091.724	6869.092	5889.083
548.44	6.41	2.87	23016.63	17849.52	14126.21	11380.46	6494.312	5105.585	4401.919	3828.055
550.06	4.04	13.93	85404.69	63765.29	48753.76	38059.11	20024.9	15195.64	12812.61	10905.66
551.69	4.21	7.48	24987.77	18518.42	14069.06	10925.81	5701.655	4327.307	3654.661	3119.448
553.31	3.9	14.04	39068.89	29709.64	23127.26	18374.96	10172.43	7909.055	6774.662	5855.826
554.94	4.89	7.03	50897.5	37112.86	27740.69	21196.2	10549.59	7829.596	6518.894	5488.526
556.56	4.13	12.77	84834.66	63002.48	47920.43	37221.11	19320.95	14579.07	12252.68	10399.45
559.81	5.96	2.53	39093.67	30009.71	23495.17	18718.3	10323.9	7982.592	6808.974	5860.071
618.31	6.97	11.19	96357.93	69075.5	50887.64	38406.03	18601.17	13666.37	11310.21	9468.688
619.94	4.36	3.99	26070.8	20508.71	16402.09	13310.61	7652.096	6004.077	5162.874	6628
621.56	3.5	14.38	36930.99	27129.13	20436.29	15740.6	8026.201	6025.652	5053.378	4283.84
623.19	3.92	7.86	32235.19	24520.05	19064.83	15108.98	8248.607	6353.743	5406.337	4641.392
624.81	4.96	9.58	42503.42	31653.01	24166.3	18859.51	9981.097	7622.575	6461.814	5534.089
626.44	4.45	6.36	76233.99	55954.68	42078.55	32329.33	16299.96	12148.31	10134.09	8542.739
628.06	4.05	10.89	67550.91	49849.98	37758.54	29261.85	15218.8	11532.13	9725.627	8285.896
629.69	3.81	6.17	80916.65	59633.33	44988.02	34645.01	17509.45	13039.62	10866.64	9148.403
631.31	4.42	7.44	73165.51	53789.84	40580.67	31320.65	16094.1	12127.14	10191.49	8653.951
632.94	6.82	2.98	66575.74	48719.78	36553.21	28036.01	14102.63	10511.63	8772.668	7400.434
636.19	3.42	11.38	18655.3	14825.04	12003.52	9878.505	5957.145	4792.136	4188.683	3688.341
637.81	4.61	14.34	20059.1	15247.97	11874.41	9445.224	5268.347	4119.782	3544.658	3078.941
641.06	5.78	12.39	27153.73	21404.73	17216.44	14092.15	8404.184	6734.886	5873.82	5161.629
642.69	4.67	4.37	22845.19	18029.6	14475.37	11796.91	6869.058	5419.708	4675.434	4063.356
644.31	6	3.09	70627.8	51882.51	39129.6	30202.16	15540.66	11722.09	9858.329	8377.389
645.94	5.05	3.69	26150.96	20179.89	15915.03	12792.85	7287.456	5732.667	4945.494	4303.342
647.56	4	5.64	31862.71	24156.95	18762.6	14883.96	8229.287	6403.696	5490.585	4751.839

Table E-1: Lifing Results for different values for the b exponent in Manson equation

Appendix F Calculated Results for Maintenance Cost Analysis

Cost Analysis for the Baseline Scenario

Min SV 1

	Engine Induction (FH) (**)	Interval	years	FV	O_main	I_maint	LLP value	Total	Cum
1	2000 and 3596	2,000	7	190,049	1,621	1,621	120,849	314,141	314,141
2		4,000	13	192,598	3,286	3,286		199,170	513,311
3	6000 and 7192	6,000	20	195,180	4,996	4,996	124,112	329,283	842,595
4		8,000	27	197,797	6,750	6,750		211,298	1,053,893
5	10000 and 10788	10,000	33	200,450	8,551	8,551	127,463	345,014	1,398,907
6		12,000	40	203,137	10,399	10,399		223,935	1,622,841

Table F-1: Cost for MINSV Method and Mission Mixture 0.5_0.4_0.1

(**): The first value (2000) relates to the TBO Interval and the second (e.g 3596) to the LLP failure limit. The cost of this item increases the cost for a normal TBO.

Min SV 2

	Engine Induction (FH) (**)	Interval	years	FV	O_main	I_maint	LLP value	Total	Cum
1		2,000	7	190,049	1,621	1,621		193,292	193,292
2	4000 and 5566	4,000	13	192,598	3,286	3,286	122,470	321,640	514,932
3		6,000	20	195,180	4,996	4,996		205,172	720,103
4		8,000	27	197,797	6,750	6,750		211,298	931,401
5	10000 and 11132	10,000	33	200,450	8,551	8,551	127,463	345,014	1,276,415
6		12,000	40	203,137	10,399	10,399		223,935	1,500,350

Table F-2: Cost for MINSV Method and Mission Mixture 0.7_0.2_0.1

Min SV 3

	Engine Induction (FH)	Interval	years	FV	O_main	I_maint	LLP value	Total	Cum
1		2,000	7	190,049	1,621	1,621		193,292	193,292
2		4,000	13	192,598	3,286	3,286		199,170	392,462
3	6000 and 6885	6,000	20	195,180	4,996	4,996	124,112	329,283	721,746
4		8,000	27	197,797	6,750	6,750		211,298	933,043
5		10,000	33	200,450	8,551	8,551		217,551	1,150,595
6		12,000	40	203,137	10,399	10,399		223,935	1,374,530

Table F-3: Cost for MINSV Method and Mission Mixture 0.8_0.1_0.1

	Engine Induction (FH)	Years	FV	O_main	I_maint	admin	LLP value	Total	Cum Max 1
0	2,000	7	190,049	1,621	1,621			193,292	193,292
1	3,596	12		2,947	2,947	10,242	122,140	138,276	331,568
2	4,000	13	192,598	3,286	3,286			199,170	530,738
3	6,000	20	195,180	4,996	4,996			205,172	735,910
4	7,192	24		6,036	6,036	10,491	125,101	147,663	883,573
5	8,000	27	197,797	6,750	6,750			211,298	1,094,871
6	10,000	33	200,450	8,551	8,551			217,551	1,312,422
7	10,788	36		9,273	9,273	10,745	128,133	157,425	1,469,847
8	12,000	40	203,137	10,399	10,399			223,935	1,693,782

Table F-4: Cost for MaxLLP Method and Mission Mixture 0.5_0.4_0.1

	Engine Induction (FH)	years	FV	O_main	I_maint	admin	LLP value	Total	Cum Max 2
0	2,000	7	190,049	1,621	1,621			193,292	193,292
1	4,000	13	192,598	3,286	3,286			199,170	392,462
2	5,566	19		4,621	4,621	10,378	123,754	143,373	535,836
3	6,000	20	195,180	4,996	4,996			205,172	741,007
4	8,000	27	197,797	6,750	6,750			211,298	952,305
5	10,000	33	200,450	8,551	8,551			217,551	1,169,856
6	11,132	37		9,591	9,591	10,770	128,427	147,609	1,317,465
7	12,000	40	203,137	10,399	10,399			223,935	1,541,400

Table F-5: Cost for MAXLLP Method and Mission Mixture 0.7_0.2_0.1

	Engine Induction (FH)	years	FV	O_main	I_maint	admin	LLP value	Total	Cum Max 3
0	2,000	7	190,049	1,621	1,621			193,292	193,292
1	4,000	13	192,598	3,286	3,286			199,170	392,462
2	6,000	20	195,180	4,996	4,996			205,172	597,634
3	6,885	23		5,766	5,766	10,469	124,845	146,848	744,481
4	8,000	27	197,797	6,750	6,750			211,298	955,779
5	10,000	33	200,450	8,551	8,551			217,551	1,173,331
6	12,000	40	203,137	10,399	10,399			223,935	1,397,266

Table F-6: Cost for MAXLLP Method and Mission Mixture 0.8_0.1_0.1

Cost Analysis for Hot Climate "Scenario" for the MINSV Method

Min SV 1

	Engine Induction (FH)	Interval	years	FV	O_main	I_maint	LLP value	Total	Cum
1	2000 and 3172	2000	7	190049.2	1621.455	1621.455	120849	314141.1	314141
2		4000	13	192597.6	3286.394	3286.394		199170.3	513311
3	6000 and 6344	6000	20	195180.1	4995.692	4995.692	124111.7	329283.2	842595
4	8000 and 9516	8000	27	197797.3	6750.24	6750.24	125776	337073.8	1179668
5		10000	33	200449.6	8550.944	8550.944		217551.5	1397220
6		12000	40	203137.5	10398.73	10398.73		223934.9	1621155

Table F-7: Cost for MINSV Method and Mission Mixture 0.5_0.4_0.1

Min SV 2

	Engine Induction	Interval	years	FV	O_main	I_maint	LLP value	Total	Cum
1		2000	7	190049.2	1621.455	1621.455		193292.1	193292
2	4000 and 4851	4000	13	192597.6	3286.394	3286.394	122469.5	321639.9	514932
3		6000	20	195180.1	4995.692	4995.692		205171.5	720103
4	8000 and 9702	8000	27	197797.3	6750.24	6750.24	125776	337073.8	1057177
5		10000	33	200449.6	8550.944	8550.944		217551.5	1274729
6		12000	40	203137.5	10398.73	10398.73		223934.9	1498664

Table F-8: Cost for MINSV Method and Mission Mixture 0.7_0.2_0.1

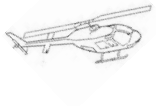

	Engine Induction (FH) (**)	Interval	years	FV	O_main	I_maint	LLP value	Total	Cum
1		2000	7		190049.2	1621.455	1621.455		193292.1
2	4000 and 5975	4000	13		192597.6	3286.394	3286.394	122469.5	321639.9
3		6000	20		195180.1	4995.692	4995.692		205171.5
4		8000	27		197797.3	6750.24	6750.24		211297.8
5	10000 and 11950	10000	33	200449.6	8550.944	8550.944	127462.5	345014	1276415
6		12000	40	203137.5	10398.73	10398.73		223934.9	1500350

Table F-9: Cost for MINSV Method and Mission Mixture 0.8_0.1_0.1

Cost Analysis for Hot Climate "Scenario" for the Max LLP Method

	Engine Induction	Years	FV	O_main	I_maint	admin	LLP value	Total	Cum Max 1
0	2000	6.666667	190049	1621.455	1621.455			193292.1	193292.08
1	3,172	10.57333		2591.778	2591.778	10213.5	121796	137193.1	330485.16
2	4000	13.33333	192598	3286.394	3286.394			199170.3	529655.51
3	6000	20	195180	4995.692	4995.692			205171.5	734827.02
4	6,344	21.14667		5294.227	5294.227	10431.56	124396.4	145416.4	880243.43
5	8000	26.66667	197797	6750.24	6750.24			211297.8	1091541.2
6	9,516	31.72		8110.891	8110.891	10654.28	127052.3	143274.1	1234815.3
7	10000	33.33333	200450	8550.944	8550.944			217551.5	1452366.8
8	12000	40	203137	10398.73	10398.73			223934.9	1676301.7

Table F-10:Cost for MaxLLP Method and Mission Mixture 0.5_0.4_0.1

	Engine Induction	Years	FV	O_main	I_maint	admin	LLP value	Total	Cum Max 1
0	2000	6.666667	190049	1621.455	1621.455			193292.1	193292.08
1	4000	13.33333	192598	3286.394	3286.394			199170.3	392462.43
2	4,851	16.17		4008.227	4008.227	10328.35	123165.6	141510.4	533972.84
3	6000	20	195180	4995.692	4995.692			205171.5	739144.35
4	8000	26.66667	197797	6750.24	6750.24			211297.8	950442.15
5	9,702	32.34		8279.677	8279.677	10667.49	127209.8	154436.6	1104878.8
6	10000	33.33333	200450	8550.944	8550.944			217551.5	1322430.3
7	12000	40	203137	10398.73	10398.73			223934.9	1546365.2

Table F-11: Cost for MAXLLP Method and Mission Mixture 0.7_0.2_0.1

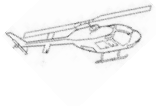

	Engine Induction (FH)	Years	FV	O_main	I_maint	admin	LLP value	Total	Cum Max 1
0	2000	6.666667	190049	1621.455	1621.455			193292.1	193292.08
1	4000	13.33333	192598	3286.394	3286.394			199170.3	392462.43
2	5,975	19.91667		4974.049	4974.049	10405.96	124091.1	134039.2	526501.59
3	6000	20	195180	4995.692	4995.692			205171.5	731673.1
4	8000	26.66667	197797	6750.24	6750.24			211297.8	942970.9
5	10000	33.33333	200450	8550.944	8550.944			217551.5	1160522.4
6	11,950	39.83333		10351.95	10351.95	10828.4	129128.7	149832.6	1310355
7	12000	40	203137	10398.73	10398.73			223934.9	1534289.9

Table F-12: Cost for MAXLLP Method and Mission Mixture 0.8_0.1_0.1

Appendix G Conversion Tables Used

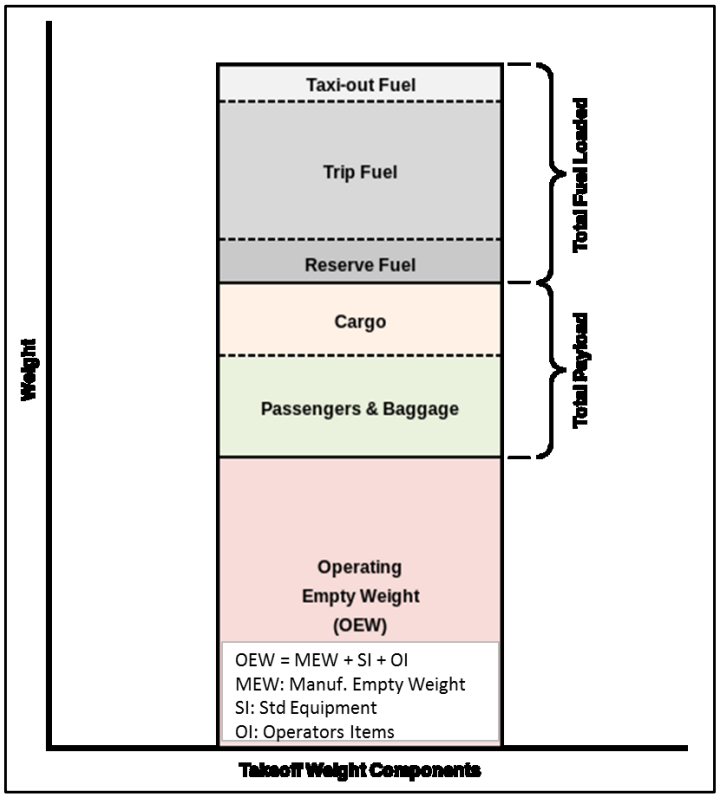

Figure G-1: Take-off weight components

kts	m/sec	mph	km/hr	ft/min
10	5.14443	11.53092784	18.52	1012.69
20	10.28886	23.06185567	37.04	2025.38
30	15.43329	34.59278351	55.56	3038.07
40	20.57772	46.12371134	74.08	4050.76
50	25.72215	57.65463918	92.6	5063.45
60	30.86658	69.18556701	111.1	6076.14
70	36.01101	80.71649485	129.6	7088.83
80	41.15544	92.24742268	148.2	8101.52
90	46.29987	103.7783505	166.7	9114.21

Table G-1: Velocity Conversion

	m/s	km/h	mph	knot	ft/s
1 m/s =	1	3.6	2,236,936	1,943,844	3,280,840
1 km/h =	0.277778	1	0.621371	0.539957	0.911344
1 mph =	0.44704	1,609,344	1	0.868976	1,466,667
1 knot =	0.514444	1,852	1,150,779	1	1,687,810
1 ft/s =	0.3048	109,728	0.681818	0.592484	1

Table G-2 : Conversions between common units of speed

Direction	Formula	H*	B*
0 to 90	abs(H-90)	57.65	32.35
90 to 360	(360-H) +90	172.88	277.12
H*: Enter Google Earth Heading Value. This is the value taken from Google distance measurement tool			
B*: Value for HECTOR			

Table G-3: Heading Calculations for HECTOR mission input file

A tutorial for bearing calculation can be found on the following website:

http://www.mathsteacher.com.au/year7/ch08_angles/07_bear/bearing.htm

Appendix H Design of Experiment Set Up

The experiment design is performed in several steps. The flowchart in figure H-1 shows the process in more detail.

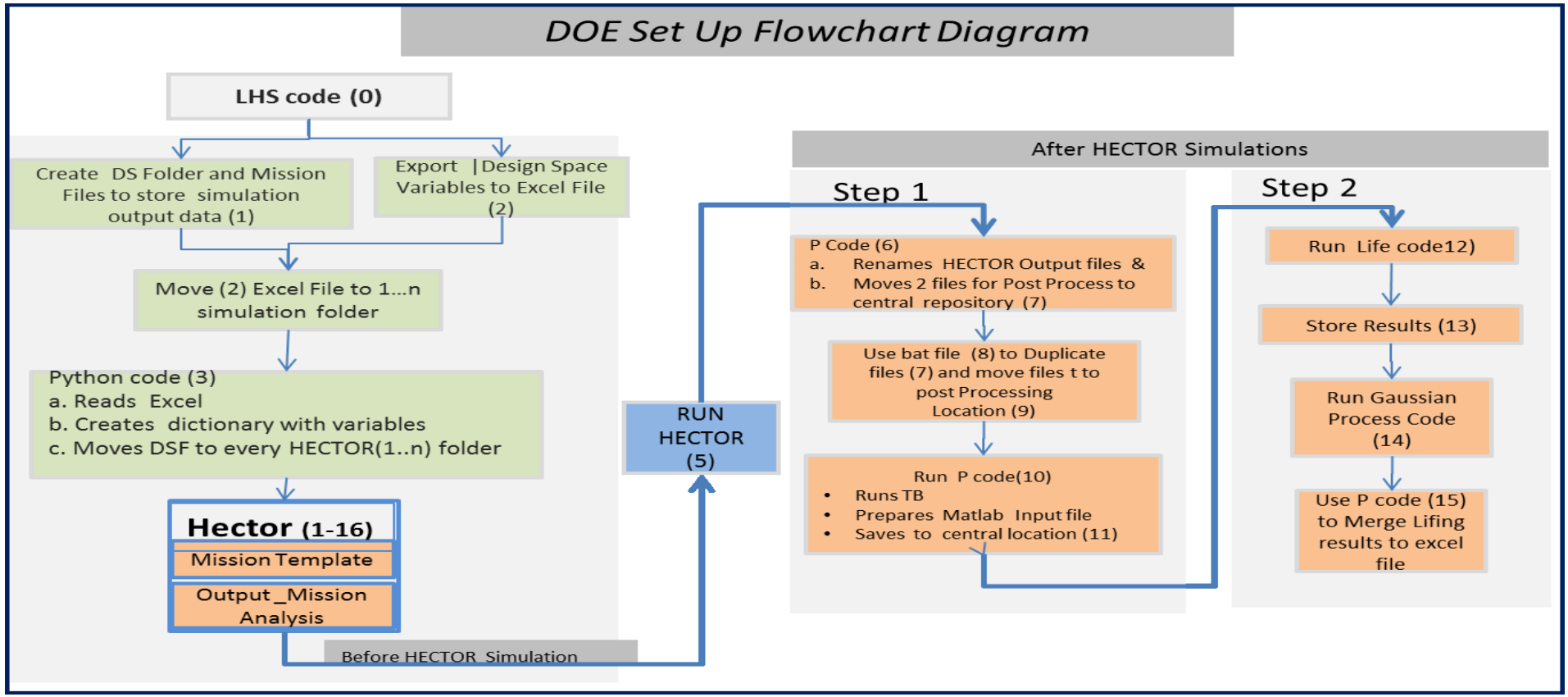

Figure H-1: DOE Set up Flowchart Diagram

Appendix I Leave one out (LOOCV) Cross Validation Method Implementation

To implement the LOO method, a code has been developed in Python. The code uses the following steps:

- It creates two lists values. The one list named “doe list “keeps the values related to i) the payload, ii) ISA deviation, and iii) the climb rate while the other is named “disc life” and stores the values that represent the disc failure cycles.
- The code uses one combination of the operation variables for testing while keeps the others as a training set. The disc life for the test set is assessed using the Gaussian process.
- A for loop is used to run the LOO method steps “N” times where N is the population created from the DOE. These estimated values can compare to the initially calculated value.
- The estimated values are stored and then plotted against the calculated values. The figures in paragraph 3.3.4 show the importance of the sample population.

index	doe_list	disc life
0	200,3,0	5000
1	200,4,0	4500
2	200,5,0	4000
3	200,6,0	3500
4	350,3,0	3400
5	350,4,0	3200

train_index	test_index
0,1,2,3,5	4

X_train	X_test
200,3,0	
200,4,0	
200,5,0	
200,6,0	
	350,3,0
350,4,0	

Y_train	Y_test
5000	
4500	
4000	
3500	
	3300
3200	

Actual	Predicted
3400	3300